Uley South groundwater model

Department for Environment and Water
July 2020

DEW Technical report 2020/37

Government of South Australia
Department for Environment and Water

Department for Environment and Water
Government of South Australia
July 2020

81-95 Waymouth St, ADELAIDE SA 5000
Telephone +61 (8) 8463 6946
Facsimile +61 (8) 8463 6999
ABN 36702093234

www.environment.sa.gov.au

Disclaimer

The Department for Environment and Water and its employees do not warrant or make any representation regarding the use, or results of the use, of the information contained herein as regards to its correctness, accuracy, reliability, currency or otherwise. The Department for Environment and Water and its employees expressly disclaims all liability or responsibility to any person using the information or advice. Information contained in this document is correct at the time of writing.



With the exception of the Piping Shrike emblem, other material or devices protected by Aboriginal rights or a trademark, and subject to review by the Government of South Australia at all times, the content of this document is licensed under the Creative Commons Attribution 4.0 Licence. All other rights are reserved.

© Crown in right of the State of South Australia, through the Department for Environment and Water 2019

ISBN 978-1-925964-88-2

Report prepared by:

Cameron Wood and Chris Li
Water Science Unit
Science, Information and Technology Branch
Strategy, Science and Corporate Services Division
Department for Environment and Water

Preferred way to cite this publication

Department for Environment and Water (DEW) 2020. *Uley South groundwater model*, DEW Technical report 2020/37, Government of South Australia, Department for Environment and Water, Adelaide.

Foreword

The Department for Environment and Water (DEW) is responsible for the management of the State's natural resources, ranging from policy leadership to on-ground delivery in consultation with government, industry and communities.

High-quality science and effective monitoring provides the foundation for the successful management of our environment and natural resources. This is achieved through undertaking appropriate research, investigations, assessments, monitoring and evaluation.

DEW's strong partnerships with educational and research institutions, industries, government agencies, Landscape Boards and the community ensures that there is continual capacity building across the sector, and that the best skills and expertise are used to inform decision making.

John Schutz
CHIEF EXECUTIVE
DEPARTMENT FOR ENVIRONMENT AND WATER

Acknowledgements

The authors would like to thank the following people:

- SA Water staff, in particular Michelle Irvine, Glyn Ashman, Nara Somaratne, Daniel Hoefel and Nardine Habner who provided the opportunity to work on this project and took part in helpful discussions throughout the course of the work.
- DEW staff who assisted in discussing the development of the model, in particular Juliette Woods for reviewing this report.
- Hugh Middlemis (HydroGeoLogic Pty Ltd) for providing external peer review.
- John Liddle for copy editing the report.

Contents

Foreword ii

Acknowledgements iii

Summary x

1 Introduction 1

1.1 Background 1

1.2 Aims 2

2 Conceptual model 3

2.1 Location and topography 3

2.2 Climate 3

2.3 Soil, vegetation and land use 5

2.4 Geology 7

2.4.1 Regional geology 7

2.4.2 Coastal geology and bathymetry 10

2.5 Hydrogeology 10

2.5.1 Aquifers 10

2.5.2 Groundwater flow and trends 11

2.5.3 Groundwater flow between aquifers 16

2.5.4 Aquifer properties 17

2.5.5 Groundwater recharge to the QL aquifer 19

2.5.6 Recharge to the TS aquifer 22

2.5.7 Evapotranspiration 22

2.5.8 Groundwater extraction 22

2.5.9 Groundwater salinity 25

2.5.10 Coastal groundwater processes 27

2.6 Conceptual model and water balance 31

2.6.1 Inflows 31

2.6.2 Outflows 31

2.6.3 Summary 32

2.7 Conceptual model uncertainty 33

3 Previous groundwater models 34

3.1 Finite element groundwater model (1980) 34

3.2 One-layer MODFLOW model (2002) 34

3.3 Spreadsheet water balance model (2006; 2009) 34

3.4 Three-layer MODFLOW model (2007) 36

3.5 Two and four-layer MODFLOW model (2010) 37

3.6 MODHMS seawater intrusion model (2013) 37

3.7 Two-layer highly parameterised MODFLOW model (2015) 38

3.8 SEAWAT model (2017) 39

3.9 Summary of previous models 40

4 Model construction 42
4.1 Model approach, platform, domain and grid 42
4.2 Model layer elevations 44
4.2.1 Surface elevation 44
4.2.2 Aquifer layer elevations 45
4.2.3 Layering to simulate connection between TS and QL layers 45
4.3 Domain boundary conditions 46
4.3.1 Northern boundary 46
4.3.2 Coastal boundary 48
4.3.3 Inactive cells 49
4.4 Groundwater recharge and evapotranspiration 49
4.5 Groundwater extraction 52
4.6 Aquifer parameters 53
4.7 Observation data and time discretisation 61
4.7.1 Steady state model 61
4.7.2 Transient model 61
4.7.3 Initial conditions 63

5 Model calibration 64
5.1 Calibration approach 64
5.2 Steady state calibration 64
5.3 Transient calibration 64
5.4 Mass balances 74
5.5 Seawater interface simulations 77
5.6 Summary of transient models 80

6 Model uncertainty and limitations 81
6.1 Uncertainty analysis 81
6.2 Model capability, limitations and uncertainty 87

7 Model scenarios 90
7.1 Overview 90
7.2 Climate change impacts on rainfall and recharge 90
7.3 Scenario results 94
7.3.1 Scenarios 1A and 1B – pumping 3.8 GL/y 94
7.3.2 Scenarios 2A and 2B – pumping 5 GL/y 94
7.3.3 Scenario 3A and 3B – pumping up to 6.8 GL/y 95
7.3.4 Seawater intrusion 96
7.4 Predictive parameter uncertainty 98

8 Conclusions and recommendations 102
8.1 Conclusions 102
8.2 Recommendations 102

9 Appendices 105

10 References 146

List of figures

Figure 1.1.	History of water use per year in the Eyre Peninsula (EPNRMB, 2016)	1
Figure 2.1.	The Uley South Basin study area	4
Figure 2.2.	Long-term rainfall data at Big Swamp (BoM station 18017)	5
Figure 2.3.	Soil type and land cover in the Uley South Basin	6
Figure 2.4.	Shallow soil over calcrete and exposed calcrete near a sinkhole in the Uley South Basin	7
Figure 2.5.	Cross section through the Uley South Basin	9
Figure 2.6.	Interpreted AEM data at elevation -23 m AHD, and estimated basement surface with areas where the QL is likely to be dry (figures from Fitzpatrick et al., 2009).	10
Figure 2.7.	Observation wells and potentiometric surfaces	13
Figure 2.8.	Long-term groundwater trends in the Quaternary Limestone aquifer, western portion of Uley South	14
Figure 2.9.	Long-term groundwater trends in the Quaternary Limestone aquifer, central portion of Uley South	14
Figure 2.10.	Long-term groundwater trends in the Quaternary Limestone aquifer, eastern portion of Uley South	15
Figure 2.11.	Groundwater levels in the northern part of the TS aquifer	15
Figure 2.12.	Long-term groundwater trends in the TS aquifer within the Uley South Basin	16
Figure 2.13.	Groundwater levels in nested wells ULE109 (TS aquifer) and ULE197 (QL aquifer)	16
Figure 2.14.	Hydraulic conductivity (a) and specific yield (b) data for the QL aquifer	18
Figure 2.15.	Potential changes in recharge in response to changes in average annual rainfall based on four global climate models in the Southern Basins Prescribed Wells Area, dashed lines show the upper and lower 95% confidence intervals (from Green et al., 2012)	20
Figure 2.16.	Average annual water balance (mm/y) for the Southern Basins (Swaffer 2017).	21
Figure 2.17.	Yearly groundwater extraction rates from the QL aquifer in Uley South (SA Water)	23
Figure 2.18.	Location of SA Water TWS wells	24
Figure 2.19.	Estimated extraction and metered extraction (when data is available) from TWS 11	25
Figure 2.20.	Groundwater salinity in the Uley South Basin	26
Figure 2.21.	Example groundwater salinity trends in TWS wells (see Figure 2.18 for location of TWS wells)	27
Figure 2.22.	Groundwater salinity in TWS 3 and groundwater level in adjacent observation well ULE190	27
Figure 2.23.	Salinity with depth in SLE010, samples taken during drilling in 1962	30
Figure 2.24.	Salinity profiles from sonding in SLE069 (well is screened from 14 to -22 m AHD)	30
Figure 2.25.	Salinity profiles from sonding in ULE205 (well is screened from 28 to -32 m AHD)	31
Figure 2.26.	Conceptual model (not to scale) of groundwater flow processes in the Uley South Basin	32
Figure 3.1.	A modelled groundwater level hydrograph from Harrington et al. (2006) for observation well ULE114 (SWL = standing water level)	35
Figure 3.2.	A modelled groundwater level hydrograph from Alcoe (2009) for observation well ULE134	36
Figure 3.3.	Simulated extent of seawater intrusion in the bottom of the QL aquifer in 2007 (from Werner and Dang, 2013)	37
Figure 3.4.	Simulated salinographs (fraction of seawater concentration) in SLE069 from Werner and Dang, 2013	38
Figure 3.5.	Simulated (red lines) and observed (black lines) contemporary (2005–2009) QL groundwater levels in Uley South Basin	39
Figure 3.6.	Simulated salt content at SLE069 assuming no pumping (blue line) and actual pumping (red line) from TWS wells (Badaruddin, 2017)	39
Figure 4.1.	Model domain and top elevation of Layer 1	43
Figure 4.2.	Correlation between satellite-based digital elevation model products ASTER and SRTM	44
Figure 4.3.	Cross section of model grid for model versions 1 and 2	46
Figure 4.4.	Model boundary conditions and inactive cells	47
Figure 4.5.	Groundwater levels in ULE175 and water levels assigned to simulate flow from Uley Wanilla	48

Figure 4.6. Transient recharge estimates from eight wells using the water table fluctuation method (gaps in the time series reflect gaps in observation records) 50
Figure 4.7. Recharge zones and average recharge rates 51
Figure 4.8. Layer 1 horizontal hydraulic conductivity values for the six models 55
Figure 4.9. Layer 2 horizontal hydraulic conductivity values for the six models 56
Figure 4.10. Layer 2 vertical hydraulic conductivity for the six models 57
Figure 4.11. Layer 3 horizontal hydraulic conductivity for all six models 58
Figure 4.12. Layer 1 specific yield for the six models 59
Figure 4.13. Layer 3 specific storage for the six models 60
Figure 4.14. Location of observation wells 62
Figure 5.1. Steady state modelled vs measured groundwater levels 66
Figure 5.2. Transient modelled vs measured groundwater levels 67
Figure 5.3. Measured and modelled potentiometric surfaces in the QL aquifer in December 2017 68
Figure 5.4. Transient modelled and measured groundwater levels at well ULE114 (QL) for all six models 69
Figure 5.5. Transient modelled and measured groundwater levels at well ULE092 (QL) for all six models 70
Figure 5.6. Transient modelled and measured groundwater levels at well ULE096 (QL) for all six models 70
Figure 5.7. Transient modelled and measured groundwater levels at well ULE097 (QL) for all six models 70
Figure 5.8. Transient modelled and measured groundwater levels at well ULE098 (QL) for all six models 70
Figure 5.9. Transient modelled and measured groundwater levels at well ULE099 (QL) for all six models 70
Figure 5.10. Transient modelled and measured groundwater levels at well ULE101 (QL) for all six models 70
Figure 5.11. Transient modelled and measured groundwater levels at well ULE102 (QL) for all six models 71
Figure 5.12. Transient modelled and measured groundwater levels at well ULE109 (TS) for all six models 71
Figure 5.13. Transient modelled and measured groundwater levels at well ULE114 (QL) for all six models 71
Figure 5.14. Transient modelled and measured groundwater levels at well ULE127 (TS) for all six models 71
Figure 5.15. Transient modelled and measured groundwater levels at well ULE134 (QL) for all six models 71
Figure 5.16. Transient modelled and measured groundwater levels at well ULE135 (QL) for all six models 71
Figure 5.17. Transient modelled and measured groundwater levels at well ULE139 (QL) for all six models 72
Figure 5.18. Transient modelled and measured groundwater levels at well ULE145 (QL) for all six models 72
Figure 5.19. Transient modelled and measured groundwater levels at well ULE147 (QL) for all six models 72
Figure 5.20. Transient modelled and measured groundwater levels at well LKW034 (TS) for all six models 72
Figure 5.21. Transient modelled and measured groundwater levels at well SLE006 (QL) for all six models 72
Figure 5.22. Mass balance area and long-term observation wells for the QL aquifer 73
Figure 5.23. Simulated groundwater levels at ULE190 for the calibrated model (solid orange line) and with no pumping (dashed orange line) 76
Figure 5.24. Modelled net inflow from Layer 2 (TS) to Layer 1 (QL) (positive values are net inflow, negative values are net outflow) in the TWS area in all six models, with measured salinity in TWS 3 and TWS 20 76
Figure 5.25. Simulated seawater interface toe locations in the QL aquifer, December 2017 78
Figure 5.26. Simulated and measured elevation of the seawater interface in SLE010 (1962) and SLE069 for all six models 79
Figure 5.27. Simulated inland extent of the seawater interface parallel to coast (transect running through SLE069) 80
Figure 6.1. Range of objective function values for models generated for the null space Monte Carlo simulations 82
Figure 6.2. Mean (solid blue line) and range (blue cloud) of modelled groundwater levels at ULE114, based on 1000 model runs with different parameter sets 83
Figure 6.3. Weighted mean (solid blue line) and 95% confidence interval (blue cloud) of modelled groundwater levels at ULE114, based on 355 models with phi <20% of original model (left figure) and modelled range of groundwater levels from all six calibrated conceptual models (right figure) 83

Figure 6.4. Weighted mean (solid blue line) and 95% confidence interval (blue cloud) of modelled groundwater levels (SLE006–ULE102), based on 355 models with phi <20% of original model 84
Figure 6.5. Weighted mean (solid blue line) and 95% confidence interval (blue cloud) of modelled groundwater levels (ULE114–ULE109), based on 355 models with phi <20% of original model 85
Figure 6.6. Weighted mean (solid blue line) and 95% confidence interval (blue cloud) of modelled groundwater levels (ULE127–ULE188), based on 355 models with phi <20% of original model 86
Figure 6.7. Weighted mean (solid blue line) and 95% confidence interval (blue cloud) of modelled groundwater levels (ULE190–ULE189), based on 355 models with phi <20% of original model 87
Figure 7.1. Projected changes in mean annual rainfall for the Eyre Peninsula, based on RCP 4.5 (blue) and RCP 8.5 (red), taken from Charles and Fu (2015b). 91
Figure 7.2. Simulated change in average annual recharge for given changes in average annual rainfall based on unsaturated zone modelling, dashed lines represent 95% confidence intervals (figure taken from Green et al., 2012) 92
Figure 7.3. Example of scenario recharge time series for model areas where the average recharge from 1986 to 2005 was 95 mm/y 93
Figure 7.4. Measured and synthetic water levels used as TS boundary inflow from Uley Wanilla 93
Figure 7.5. Scenarios 1A and 1B: Historic and projected modelled groundwater levels in ULE190 (adjacent to TWS 3/20) with pumping reduced to 3.8 GL/y from 2018 onwards 94
Figure 7.6. Historic and projected modelled groundwater levels in ULE190 (adjacent to TWS 3/20) with pumping continued at 5 GL/y from 2018 onwards 95
Figure 7.7. Historic and projected modelled groundwater levels in ULE190 (adjacent to TWS 3/20) with pumping increased up to 6.8 GL/y from 2018 onwards 96
Figure 7.8. Historic and projected modelled seawater interface position at SLE069 for model version 1c 97
Figure 7.9. Historic and projected modelled seawater interface position at SLE069 for model version 2b 98
Figure 7.10. Historic and projected groundwater levels for predictive uncertainty model scenario 1b (3.8 GL/y) 99
Figure 7.11. Historic and projected groundwater levels for predictive uncertainty scenario 2b (5 GL/y) 100
Figure 7.12. Historic and projected groundwater levels for predictive uncertainty scenario 3b (6.8 GL/y) 101
Figure 9.1. Average hydraulic conductivity values and their range, for wells with multiple pumping tests 106
Figure 9.2. Drawdown curves for the step drawdown test in 6028-2160 (TWS 14), T = 484 m2/d (Q = flow rate) 107
Figure 9.3. Drawdown curves for the step drawdown test in 6028-2164 (TWS 16), T = 13,000 m2/d (Q = flow rate) 107
Figure 9.4. Simulated seawater interface depth at SLE069 for model version 1c with different tip/toe slope parameters 108
Figure 9.5. Pilot point locations in Layer 1 110
Figure 9.6. Pilot point locations in Layer 2 111
Figure 9.7. Pilot point locations in Layer 3 112

List of tables

Table 2.1. Tertiary sand depths, water cuts and water levels in the area where the QL aquifer is dry (m bgl = metres below ground level) 11
Table 2.2. Summary of recharge rates in the Uley South Basin 22
Table 2.3. Estimates of groundwater discharge to the coast from previous studies 28
Table 2.4. Estimates of the inland location of the seawater interface toe in the QL aquifer from previous studies 29
Table 2.5. Preliminary conceptual model water balance for the QL aquifer in the Uley South Basin 32
Table 3.1. Summary of parameter values used in previous groundwater models of the Uley South Basin 41
Table 4.1. Parameters used in the SWI2 package 49

Table 4.2.	Summary of model versions calibrated	52
Table 4.3.	Aquifer parameter ranges used in model calibration	54
Table 4.4.	Aquifer parameter ranges in calibrated models (see Figures 4.8 to 4.13 for spatial distributions)	54
Table 5.1.	Average pre-development (1961–75) mass balance for all six versions of the model	74
Table 5.2.	Average long-term post development (1976–2017) mass balance for all six versions of the model	75
Table 5.3.	Average contemporary (2008–2017) mass balance for all six versions of the model	75
Table 5.4.	Simulated maximum inland extent of the 50% seawater-freshwater interface toe in the QL aquifer in December 2017	77
Table 7.1.	Summary of model scenarios	90
Table 9.1.	Aquifer test data for the Uley South Basin, all values are for the QL aquifer unless specified	105

Summary

Groundwater from the Quaternary Limestone (QL) aquifer in the Uley South Basin has been an important resource for the Eyre Peninsula since the 1970s, currently meeting approximately 70 percent of water demand through the South Australian Water Corporation (SA Water) supply network. However, this groundwater resource is sensitive to extraction and variation in rainfall recharge. It may be prone to risks from over-exploitation such as seawater intrusion, and increased salinity via inflow from the underlying Tertiary Sand (TS) aquifer. Therefore, it is important to understand the impact of various extraction and climate scenarios on groundwater resources in Uley South.

In this report, a multi-model approach has been taken to simulating groundwater flow and seawater intrusion in the Uley South Basin. The work was commissioned by SA Water to help it assess future supply options. The model draws on the many field and modelling studies that have been conducted in Uley South in the past, as well as new data and information collected through the course of the study. The multi-model approach addresses both conceptual and parameter uncertainty. However, areas of uncertainty remain, so the limitations of the model have been identified and recommendations for further studies are made.

Model scenarios were developed in consultation with SA Water to assess the potential impact of extraction and climate on groundwater levels in town water supply (TWS) wells and position of the seawater interface at the coast. Pumping regimes are: reduced pumping (3.8 GL/y), continued pumping at the current rate (5 GL/y), and increased pumping (up to 6.8 GL/y). Climate regimes are: based on the last 10 years of recharge data, or reduced rainfall recharge based on climate change projections. Scenario results show that:

- Reduced groundwater extraction (3.8 GL/y) is likely to lead to some recovery in groundwater levels. However, longer-term declines may occur as a result of reduced rainfall recharge based on climate change projections, and ongoing monitoring of groundwater level and salinity will be needed. The seawater interface is likely to be relatively stable in the short-term. However, a small amount of seawater intrusion may occur in future as recharge reduces based on climate change projections, and ongoing monitoring will be required.
- Continued pumping at current rates (5 GL/y) shows relatively stable groundwater levels in the short term. However, longer-term declines are predicted. Groundwater levels do not reach the minimum level recorded in the late 1990s but they may reach the same level as recorded in the mid-2000s, when groundwater salinity in one of the TWS wells was higher. Thus, adverse impacts to the resource may be anticipated and careful monitoring of groundwater level and salinity will be required for continued pumping at current rates. The seawater interface is likely to be relatively stable in the short-term. However, seawater intrusion is likely to occur in future as recharge reduces, and ongoing monitoring will be required.
- Increased extraction to meet projected demand (up to 6.8 GL/y by 2040) shows groundwater levels are likely to decline, potentially to the same level as the late 1990s, when salinity in one of the TWS wells increased. Close and careful monitoring would be essential to detecting adverse impacts of increased pumping. The combination of an increase in extraction with decreases in recharge is also likely to result in enhanced seawater intrusion, which is undesirable.

These results can help SA Water plan future supply options for the Eyre Peninsula, while understanding the assumptions and limitations in the modelling approach. It should be emphasised that scenarios are based on the last 10 years rainfall/recharge, which includes an even mix of above and below average rainfall years. Further work should be done to assess the potential impact of successive years of below average rainfall. While improvements to the model could be made, it may be necessary to collect more data related to parameters and processes to constrain model calibration before further refining the model. Areas in which more information could be collected relate to measurement and monitoring of the seawater–freshwater interface and understanding of the connection between the TS and QL aquifers.

1 Introduction

1.1 Background

Since the 1970s groundwater has been the main source of water for municipal supply, irrigation and stock and domestic use in the Eyre Peninsula region, supplementing and eventually replacing surface water supply from the Tod Reservoir (Figure 1.1). Water supply is provided by the South Australian Water Corporation (SA Water). Groundwater extraction has predominantly been from Quaternary Limestone (QL) aquifers in discrete groundwater lenses and basins. In the Southern Basins Prescribed Wells Area (SBPWA) these include the Uley Wanilla lens, the Coffin Bay lens, the Lincoln Basin, and the Uley South Basin (Figure 2.1). Aquifers in these areas are typically responsive to annual rainfall and groundwater extraction, with residence times of 35 years or less (Evans, 1997).

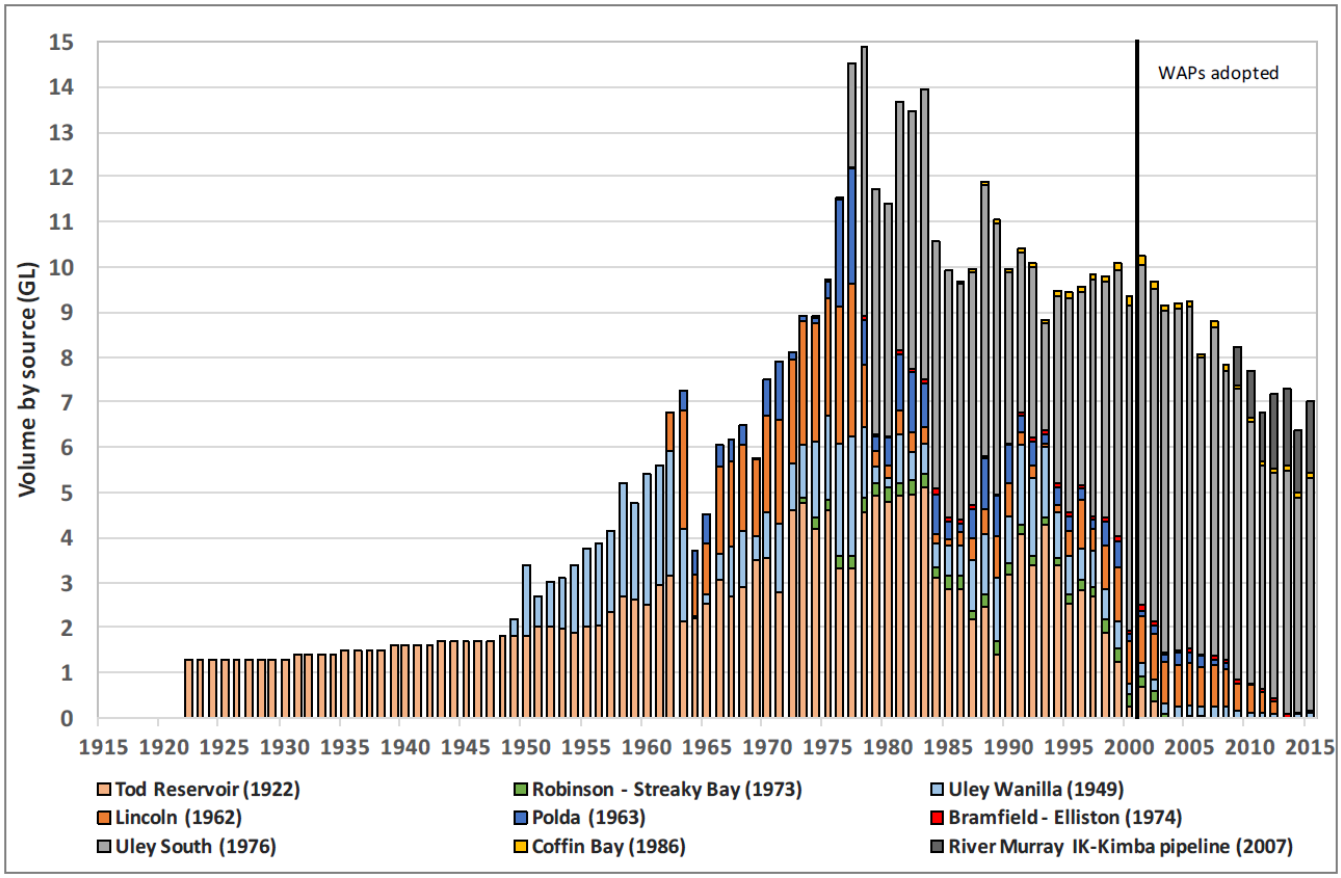


Figure 1.1. History of water use per year in the Eyre Peninsula (EPNRMB, 2016)

Over time, groundwater extraction from some of these basins has reduced or ceased completely, due to issues with yield and salinisation from seawater intrusion (Somaratne and Ashman, 2018). The majority of SA Water's supply to the Eyre Peninsula now relies on groundwater in the Uley South Basin with current extraction around 5 GL/y (Figure 1.1). Other smaller lenses occur within the SBPWA, but they have smaller groundwater resource capacities (e.g. the Coffin Bay lenses) or there is no groundwater extraction from them due to low capacity and issues such as seawater intrusion (e.g. the Lincoln lenses). The increasing reliance on Uley South has led to several technical investigations and intensive monitoring and management, with groundwater allocations being determined annually through the Water Allocation Plan (WAP) for the Southern Basins and Musgrave Prescribed Wells Areas (EPNRMB, 2016).

There is currently no alternative supply that could replace Uley South groundwater if allocation or extraction were significantly reduced. Augmentation schemes such as desalination have been discussed in previous investigations (South Australian Water Corporation, 2008). Given the importance of the resource, it is essential that SA Water has access to modelling tools to understand the impact of various extraction and climate scenarios on groundwater resources in the Eyre Peninsula. This led SA Water to engage DEW to develop a groundwater model of the Uley South Basin.

1.2 Aims

The aim of this study is to investigate the potential impact of various groundwater pumping and climate scenarios on groundwater resources in the Uley South Basin, using groundwater modelling. Many groundwater models have been developed for the Uley South Basin previously (Shepherd, 1980; James-Smith and Brown, 2002; Zulfic et al., 2007; Werner, 2010; Knowling et al., 2015). Ongoing investigations and monitoring have continued to build understanding of groundwater resources in the basin, leading to the new groundwater models developed in this study. Specifically, the project aims are to:

- Develop a groundwater flow model for the QL aquifer in the Uley South Basin.
- Use the model to assess the potential impact of future groundwater extraction and climate scenarios on groundwater resources.

2 Conceptual model

2.1 Location and topography

The Uley South Basin occupies 112 km^2 within the Southern Basins Prescribed Wells Area, on the south-western edge of the Eyre Peninsula, South Australia (Figure 2.1). For the purposes of this study, the extent of the Uley South Basin approximates the saturated extent of Quaternary limestone sediments (hydrogeology is discussed further below) with the ocean bounding the basin to the south.

The Uley South Basin is topographically enclosed, being bounded to the east by exposed basement sediments and to the west by basement highs and sand dunes (Evans, 1997). Elevation in the central basin ranges from 2 to 35 m AHD (Australian Height Datum, which has sea level as zero). However, elevations up to 200 m AHD occur in the western dunes, and up to 140 m AHD in the coastal cliffs which meet the ocean boundary (Figure 2.1).

2.2 Climate

The climate in the study area is characterized by hot, dry summers and cool, wet winters (BoM, 2017). Long-term average rainfall varies from 557 mm/y at Big Swamp (BoM station 18017) to 575 mm/y at Westmere (BoM station 18137, Figure 2.1). Cumulative deviation from mean rainfall shows that rainfall was generally above average from the mid-1960s to the early 1990s (rising trend in Figure 2.2), followed by a period of below average rainfall until 2009. Since 2009, a mixture of above and below average rainfall years have been observed.



Figure 2.1 The Uley South Basin study area

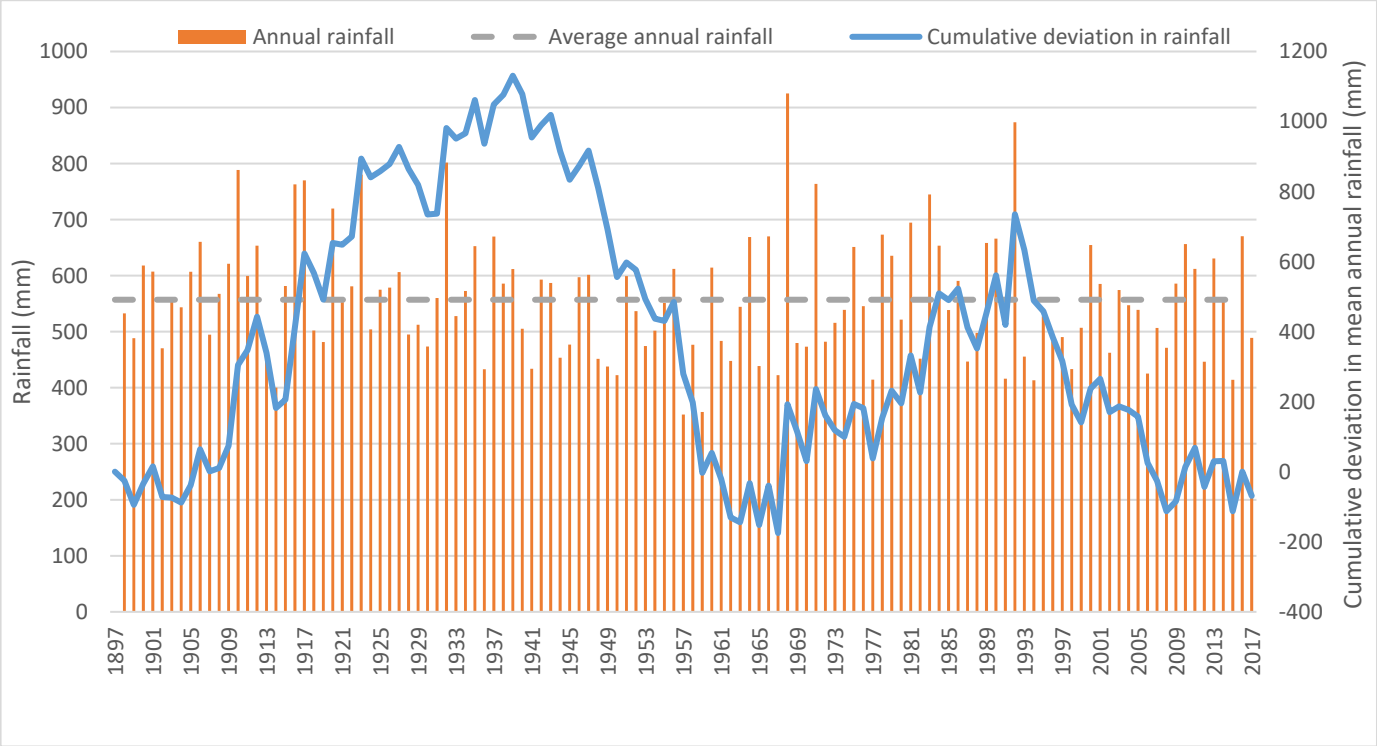


Figure 2.2. Long-term rainfall data at Big Swamp (BoM station 18017)

2.3 Soil, vegetation and land use

Soils are typically thin, calcareous loams overlying calcrete, with the exception of the deep sands in the western sand dunes (Figure 2.3, Hall et al., 2009). In many locations surface soils are absent and sheet limestone or calcrete is exposed at the surface (Harrington et al., 2006). The lack of soil and exposed calcrete surfaces (Figure 2.4) leads to rapid surface runoff following rainfall, which can be channelled to karst sinkholes where it directly recharges the aquifer (Ordens et al., 2012).

The central Uley South Basin was once dominated by drooping sheoak (*Allocasuarina verticillata)*. However, grazing pressure and rabbit plagues following European settlement resulted in the loss of much of this vegetation (Swaffer, 2014). The central basin is now typified by sparse grasslands, and dense vegetation is typically found in more elevated areas (Figure 2.3). The dominant tree species in the more densely vegetated areas are coastal white mallee (*Eucalyptus diversifolia*) and drooping sheoak (Swaffer, 2014).

The basin is a reserve, with no farmed agriculture occurring within it. A network of gravel roads connects the various pumping stations used by SA Water for groundwater extraction. Along the south-eastern coastal margin, a series of wind turbines are positioned as part of the Cathedral Rocks Wind Farm, taking advantage of strong offshore winds.

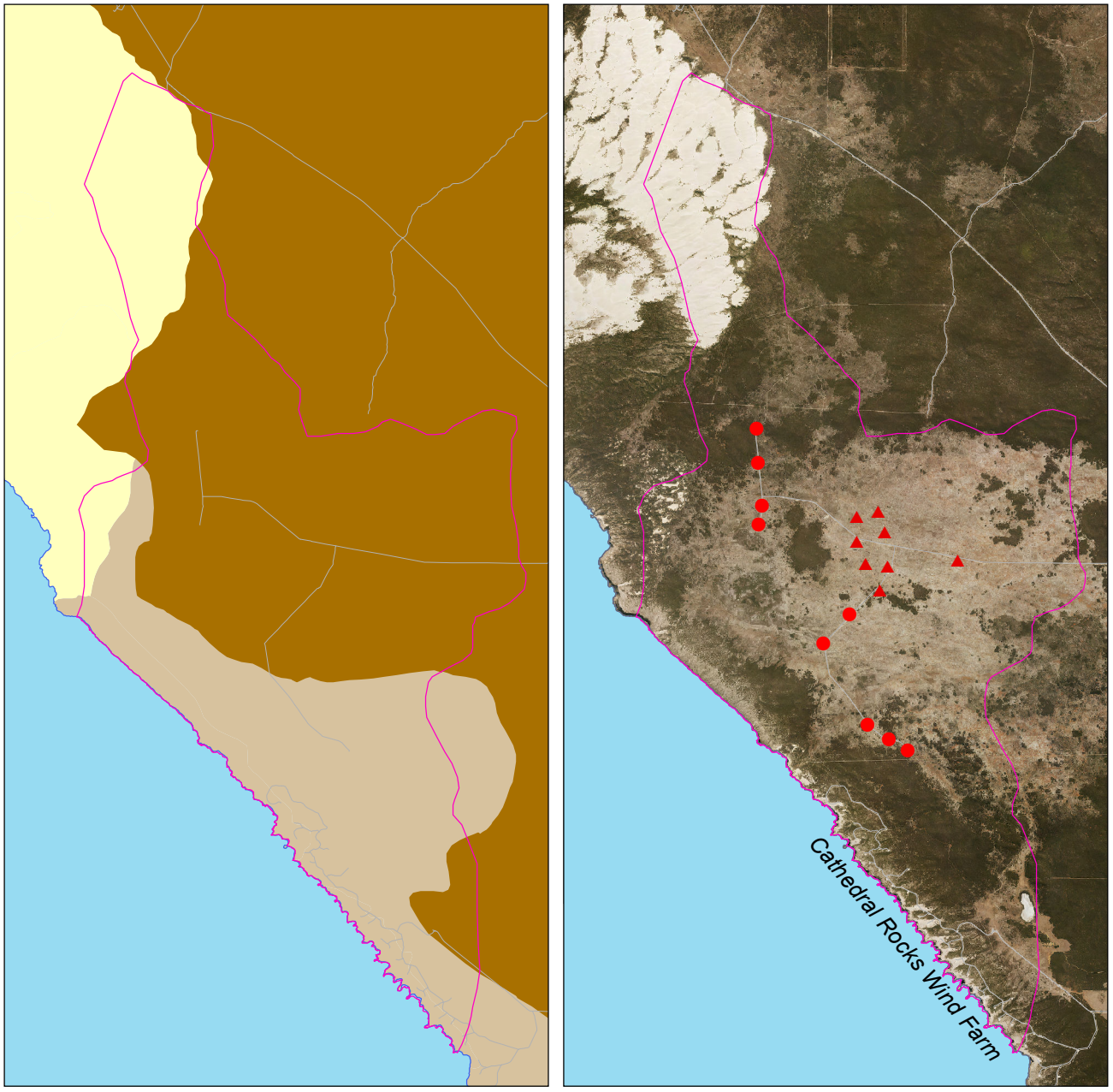


Figure 2.3 Soil type and land cover in the Uley South Basin

2.4 Geology

2.4.1 Regional geology

Surface geology in the Uley South Basin is dominated by the Pleistocene Bridgewater Formation, with areas of Holocene sand dune deposits associated with deep sand soils on the western margin of the basin (Figure 2.3). The Bridgewater Formation is also commonly referred to as the Quaternary aquifer or Quaternary Limestone (QL) aquifer in the region (Evans, 1997; Harrington et al., 2006; Knowling et al., 2015). The QL unit ranges in thickness from less than 5 m near the basin margins, to 90 m thick in the uplifted coastal areas. Lithological descriptions of the QL aquifer vary. Morton and Steel (1968) describe the QL as a weakly to moderately cemented aeolianite, with very well cemented limestone and calcrete present in some areas. Sibenaler (1976) describes the QL as a moderately to well cemented calcareous sandstone, with well cemented, cavernous areas in the vicinity of town water supply wells. Evans (1997) describes the QL sediments as fine sands and shell fragments, which are unconsolidated or loosely aggregated, with some secondary cementation and secondary porosity (solution features). Bestland (2010) surveyed outcrops along the coastal cliffs of Uley South Basin and described an upper and lower Bridgewater Formation, where the upper section is dominated by calcrete layers, fossil soil horizons and thin dune sand sheets, while the lower section consists of dune sand sheets and calcareous fossil soil interbeds.

The cavernous, secondary porosity described above can be seen in the surface geology as karst sinkholes (Figure 2.4). These features may act as preferential conduits for groundwater recharge (Ordens et al., 2012; Somaratne et al., 2018). Karst features are also likely to be present in the aquifer, based on high transmissivity values reported for QL aquifer tests (Sibenaler, 1976; Watkins et al., 2015).



Figure 2.4. Shallow soil over calcrete and exposed calcrete near a sinkhole in the Uley South Basin

The QL is underlain by a discontinuous clay layer, the Tertiary Uley Formation. Often referred to as the Tertiary Clay (TC) Aquitard, the unit is up to 25 m thick and comprised of sandy clay with minor laterite (Zulfic et al., 2007). The TC is absent in several areas of the basin, most notably the north-east and north-west margins of the basin, and in the south-eastern coastal region (Figure 2.5). The TC is underlain by the Tertiary Wanilla Formation, comprised of fluvial sand and clay, with some lignite (Zulfic et al., 2007). The Wanilla Formation is often referred to as the Tertiary Sand (TS) Aquifer, which is a confined to semi-confined aquifer. Where the TC is absent, the QL formation directly overlies the TS (Figure 2.5).

The Tertiary Sand unit is underlain by Archaean basement, consisting of gneiss and quartzite (Zulfic et al., 2007). Aquifer units within the basement have not been investigated or described, and there is no known interaction with the overlying units. However, the structure of the basement exhibits some influence on the architecture of the Uley South Basin. Figure 2.6 from Fitzpatrick et al. (2009) shows the interpreted elevation based on aerial electromagnetic (AEM) data at -23 m AHD of the basement (bedrock). A series of north-south trending basement highs and troughs occur through the basin, which control thickness of the overlying aquifer units. The basement outcrops at two locations along the coast (Figure 2.5) where it is directly overlain by the QL formation (Bestland, 2010). Drilling conducted in July 2018 found the QL to be dry above basement on the western margin of the basement, confirming the western extent of the basin mapped by Fitzpatrick et al. (2009) (Figure 2.6). Drilling in 2018 also confirmed the presence of dry limestone in the north-western arm of the basin, again confirming the work of Fitzpatrick. It should be noted that a new drillhole (6028-3073) was dry despite being logged as sandy limestone to a depth of 72 m below ground, with no shallow basement present (see section 4.1). It is possible that shallow basement may occur just south of drillhole 6028-3073, and that the drillhole is dry owing to some localised heterogeneity related to this.

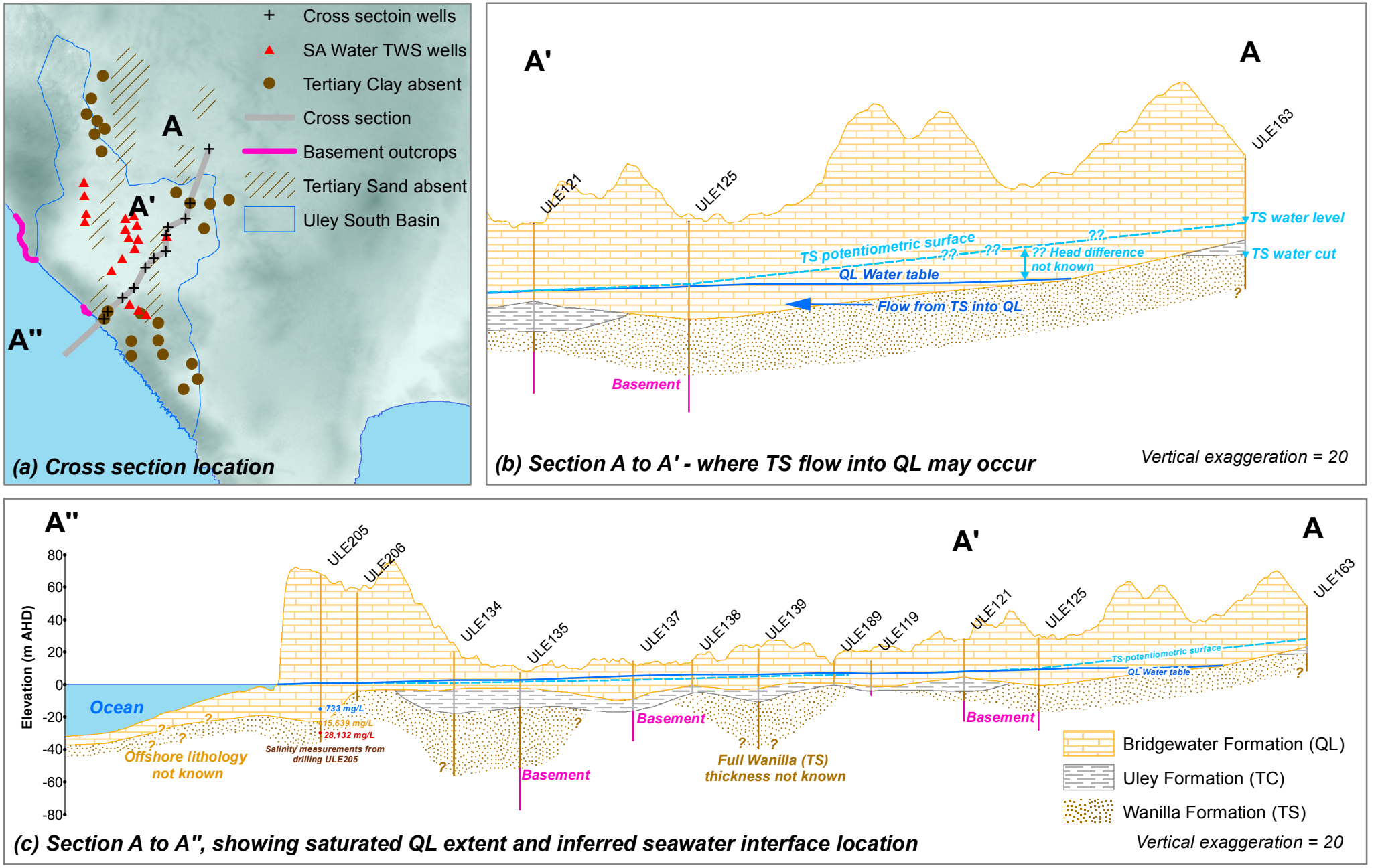


Figure 2.5 Cross section through the Uley South Basin

Government of South Australia
Department for Environment and Water

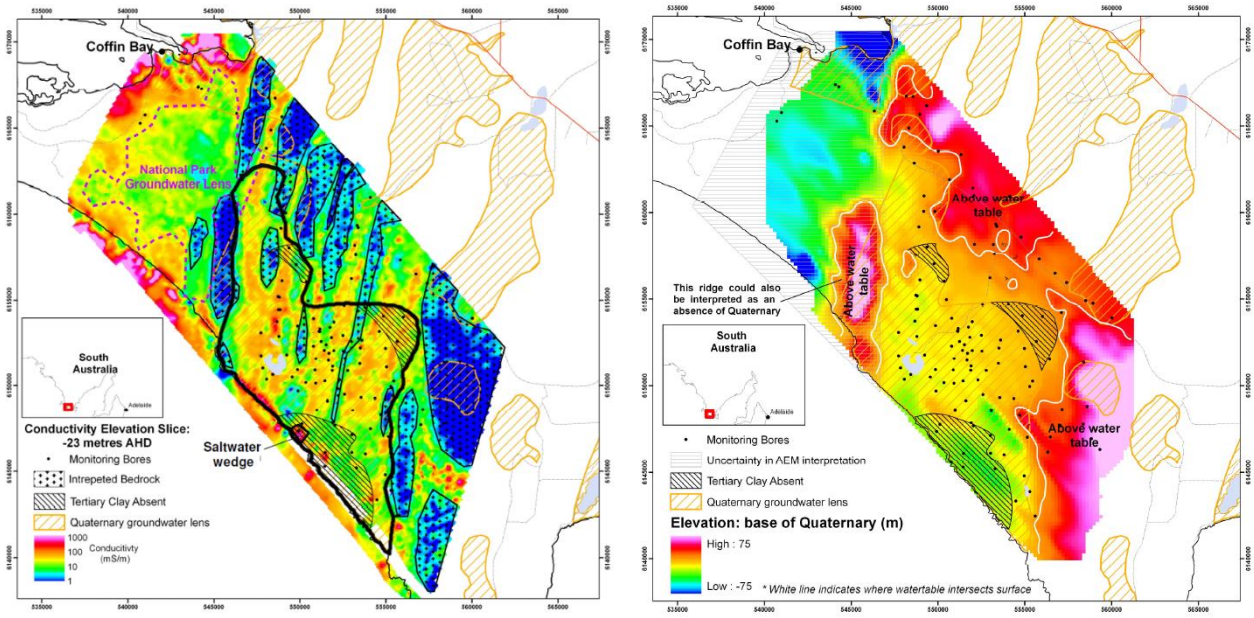


Figure 2.6. Interpreted AEM data at elevation -23 m AHD, and estimated basement surface with areas where the QL is likely to be dry (figures from Fitzpatrick et al., 2009).

2.4.2 Coastal geology and bathymetry

The cliffs which mark the southern boundary of the Uley South Basin meet the ocean in a 'high-energy' coastal environment which receives persistent south-westerly winds (Bourman et al., 2016). With the exception of the basement outcrops along the coast, only the QL is present in the coastal cliffs (no outcrops of TC or TS were identified by Bestland, 2010). Bestland (2010) identified a series of wave cut platforms at the base of the cliffs in the vicinity of the basement outcrops. However, these were likely to comprise layers of resistant limestone or rock debris, rather than basement alone. With the exception of these wave cut platforms, bathymetry data shows that the ocean floor generally slopes offshore to reach a depth of -40 m AHD at 4 km offshore (Geoscience Australia, 2017). The extent of the QL, TC and TS layers and their thicknesses in the offshore environment is not currently known.

2.5 Hydrogeology

2.5.1 Aquifers

The QL forms the main unconfined aquifer in the Uley South Basin. The outline of the basin (Figure 2.5) is based on the saturated extent of the QL aquifer, as determined by assessing 'water cut' elevations (the depth at which saturation is encountered when drilling) from drilling records (Somaratne et al. 2018). However, within the QL boundary, areas where the aquifer is dry may occur, due to the undulating topography and elevated basement areas (Werner 2010; Knowling et al., 2015). Groundwater extraction for town water supply occurs exclusively from the QL aquifer, and hence groundwater processes in the QL aquifer are the main focus of this study.

The TC formation, where present (Figure 2.5), serves as an aquitard separating the QL from the underlying TS aquifer. Morton and Steel (1970) describe the TC as a semi-permeable confining bed, and thus the TS aquifer is a leaky type confined aquifer. There is no groundwater extraction from the TS aquifer in the Uley South Basin. Nested wells screened in both aquifers are only found at one location in the study area (see Figure 2.13 and accompanying discussion). However, across the basin the difference in groundwater levels in both aquifers appears to be small (Knowling et al., 2015).

The TS extends further north where the QL is dry (Figure 2.6), to the Uley East and Uley Wanilla lenses (where the QL is again saturated), however there are areas where the TS is absent (Figure 2.5). Harrington et al. (2006) describe the TS as the water table aquifer in this zone where the QL is dry, and drilling information from this area shows that the water cut elevation may occur in the TS sediments (i.e. the TC is not saturated above it). In some locations where the QL is dry, TS water levels are above the top elevation of the formation, suggesting confined conditions, while in other areas this is not the case, confirming that the aquifer may be unconfined in parts of this area (Table 2.1).

Table 2.1. Tertiary sand depths, water cuts and water levels in the area where the QL aquifer is dry (m bgl = metres below ground level)

Observation well	TC thickness (m)	Depth to TS (m bgl)	Depth to first water cut (m bgl)	TS water level (m bgl)
ULE 128	3.65	26.21	26.21	21.47
ULE 175	5.4	15	15	12 to 17
LKW 13	13.72	44.2	48.77	39.5
ULE 170	1	26	26	25 to 25.7
ULE 169	4.5	18	17.5	13.6 to 16.6
ULE 163	4	28	29	19 to 19.5
ULE 174	2	24	29	21.6 to 22.23
LKW 12	9.15	36.58	32	24.8 to 25.75
ULE 129	9.75	21.64	29.57	15
ULE 165	6	34	no info	24.2 to 24.5
ULE 90	1.52	27.43	no info	
ULE 89	0	25.91	37.49	24.5 to 27.1
ULE 130	6.1	15.85	15.85	11 to 11.8
LKW 10	0	46.6	33.22	26.1 to 26.6
ULE 162	2	7	no info – water yield referred to as seepage	12 to 17.7
ULE 164	2	22	24.5	21 to 22
ULE 77	12.5	TS absent	27.13	
ULE 168	18	TS absent		
LKW 28	8.51	TS absent		
ULE 78	2.74	TS absent		
ULE 172	12.5	TS absent		
LKW 29	10.06	TS absent		
LKW 14	7.9	TS absent		

2.5.2 Groundwater flow and trends

Many observation wells in the basin have screened sections which straddle both the QL and TS aquifers, which can make hydrogeological interpretation difficult. In this report, the focus will be on wells screened exclusively in the QL or TS aquifer. Groundwater flow in the QL aquifer in Uley South is from the northern parts of the basin towards the coast (Figure 2.7). Long-term records of groundwater level in the QL show that groundwater levels generally rose in the late 1960s (Figure 2.8, 2.9 and 2.10), in response to above average rainfall (Figure 2.2). Declines were observed in the late 1970s, most likely due to the commencement of groundwater extraction for town water supply from the basin in 1976, at a rate of 5000 to 6000 ML/y. Groundwater levels further declined from the early 1990s through to the mid to late 2000s, as rainfall declined and groundwater extraction increased up to 7500

ML/y. Groundwater levels were stable in the mid to late 2000s, and started rising in 2010. During this period extraction declined from 7300 ML in 2007 to 5790 ML in 2010, and rainfall was above average in 2010, 2011 and 2013. Groundwater extraction has been relatively stable at 4741 to 5410 ML/y since 2011, and rainfall has fluctuated. However, most groundwater levels in the QL have been declining since 2014. In 2017, 91% of observation wells in the QL aquifer were showing declining trends, with two wells showing their lowest groundwater levels on records (Department for Environment and Water, 2018a).

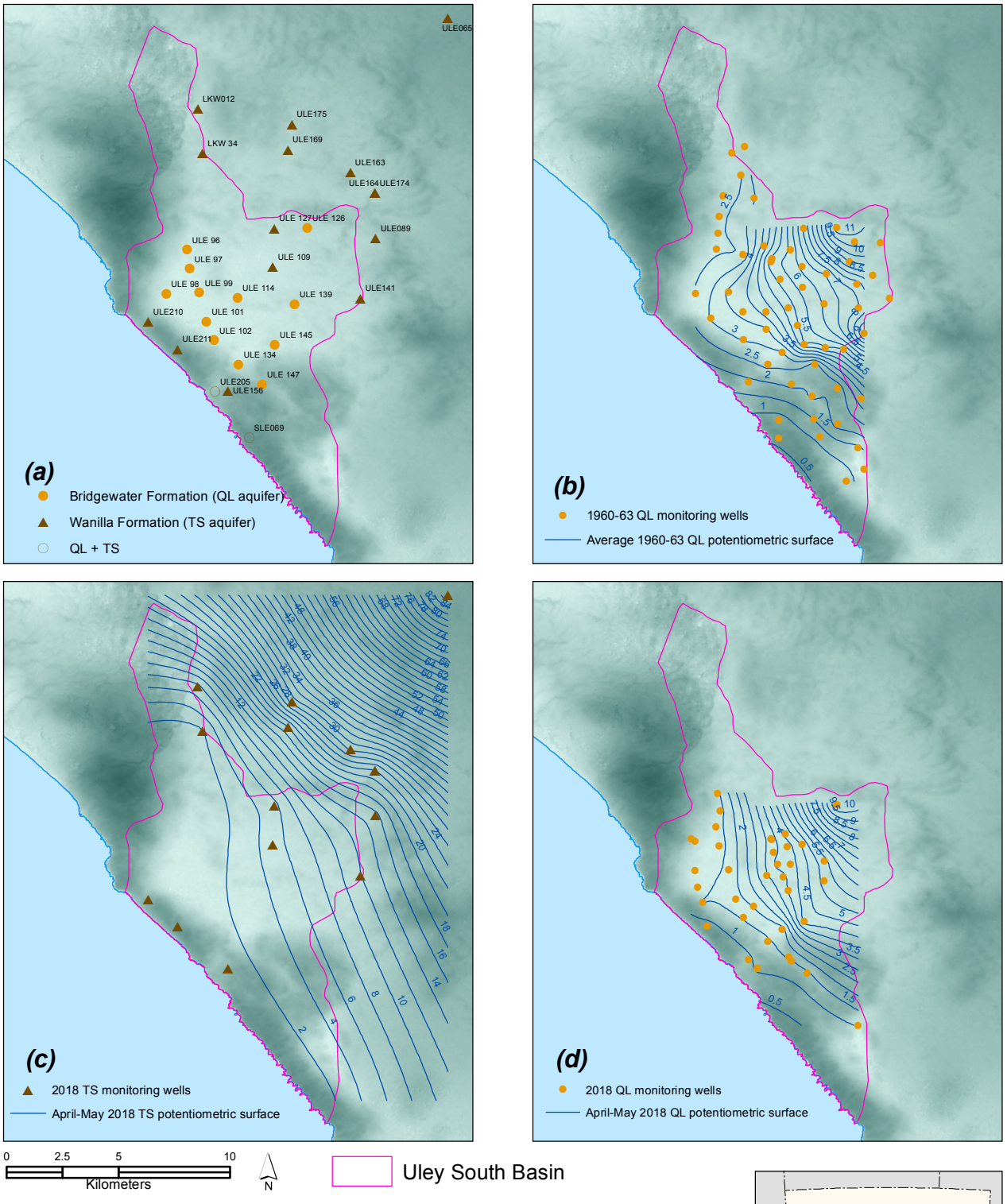


Figure 2.7. Observation wells and potentiometric surfaces; (a) long term observation wells and coastal wells; (b) average 1960-63 (pre-development) potentiometric surface in the QL aquifer; (c) 2018 potentiometric surface in the TS aquifer; (d) 2018 potentiometric surface in the QL aquifer

Government of South Australia
Department for Environment and Water

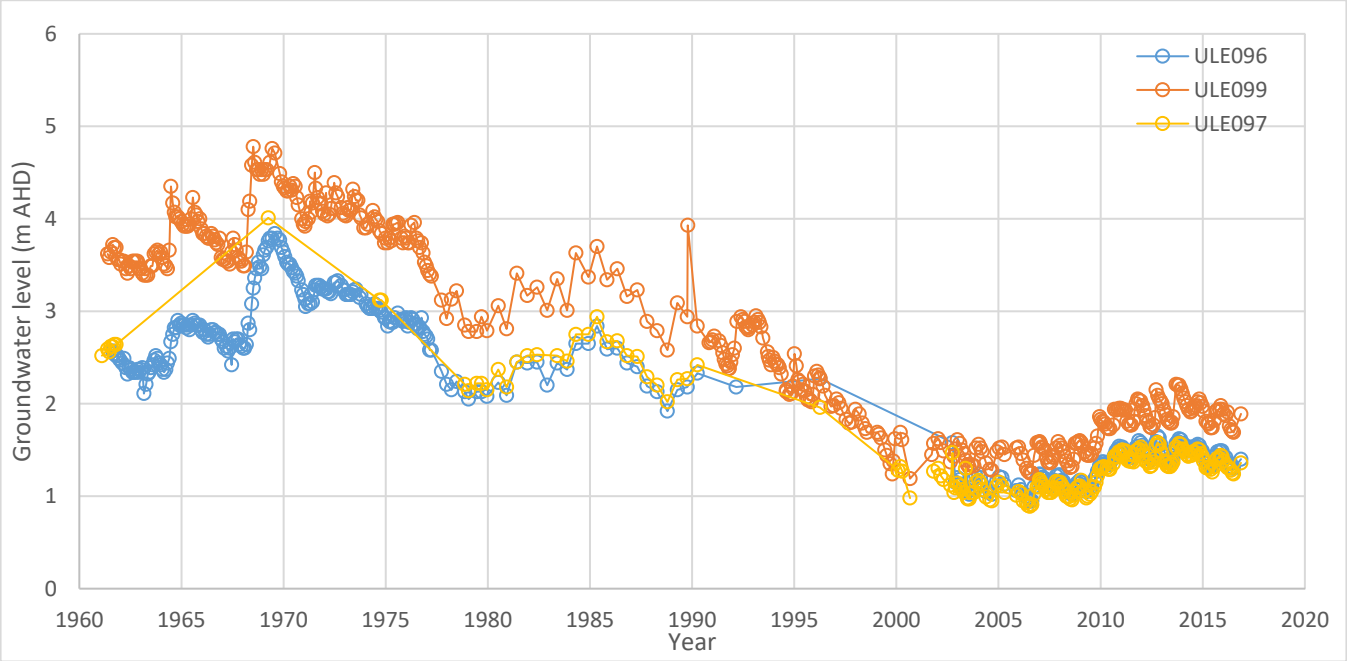


Figure 2.8. Long-term groundwater trends in the Quaternary Limestone aquifer, western portion of Uley South

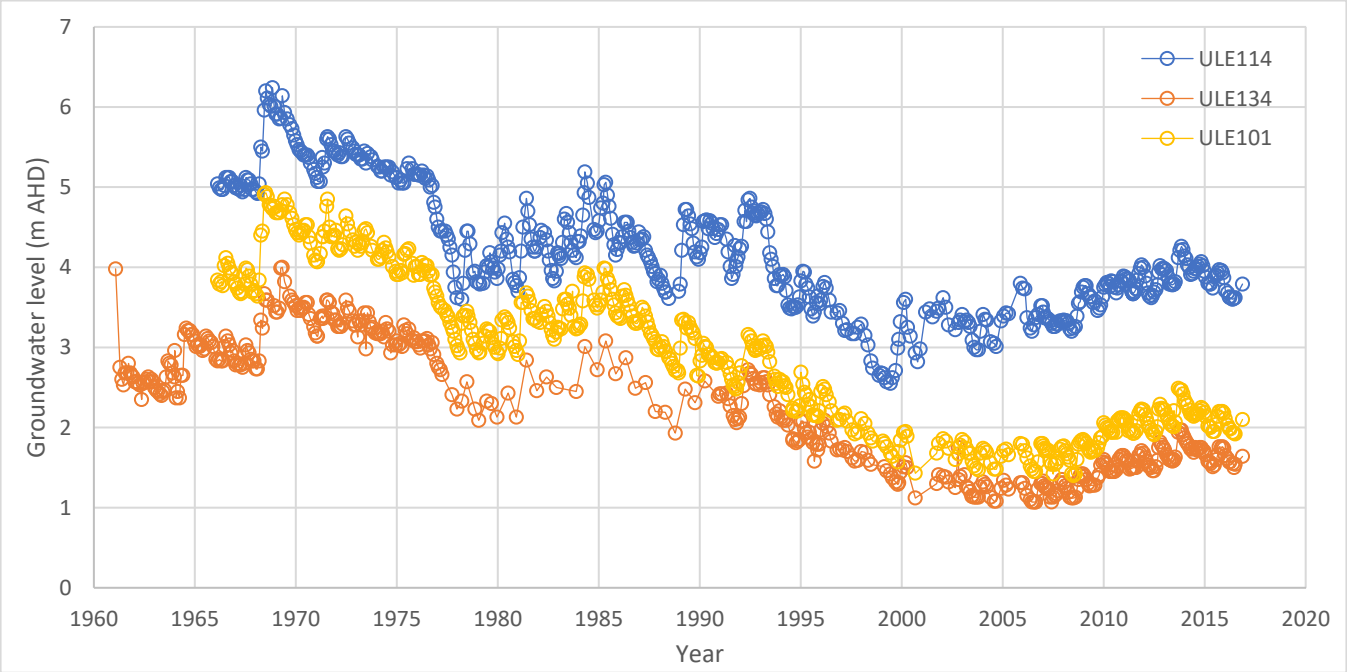


Figure 2.9. Long-term groundwater trends in the Quaternary Limestone aquifer, central portion of Uley South

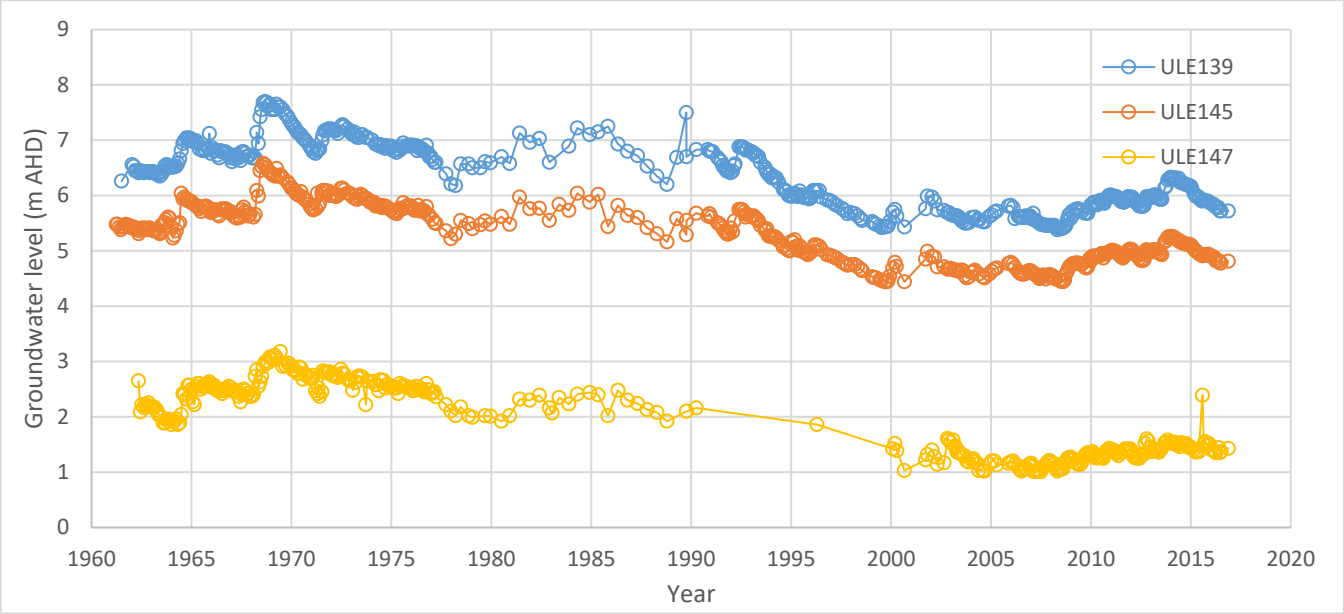


Figure 2.10. Long-term groundwater trends in the Quaternary Limestone aquifer, eastern portion of Uley South

Groundwater in the TS aquifer flows from the northern part of the study area towards the coast (Figure 2.7). However, there are far fewer monitoring wells in the TS aquifer, and there is no groundwater extraction from this formation. North of the saturated QL aquifer area, groundwater levels in the TS are influenced by processes occurring upgradient. In the western part of the aquifer, groundwater levels have shown declines since the late 1980s, which reflect declining trends in the Uley Wanilla lens to the north. However, in the eastern part of the aquifer, groundwater levels have been relatively stable over the past 30 years (Figure 2.11).

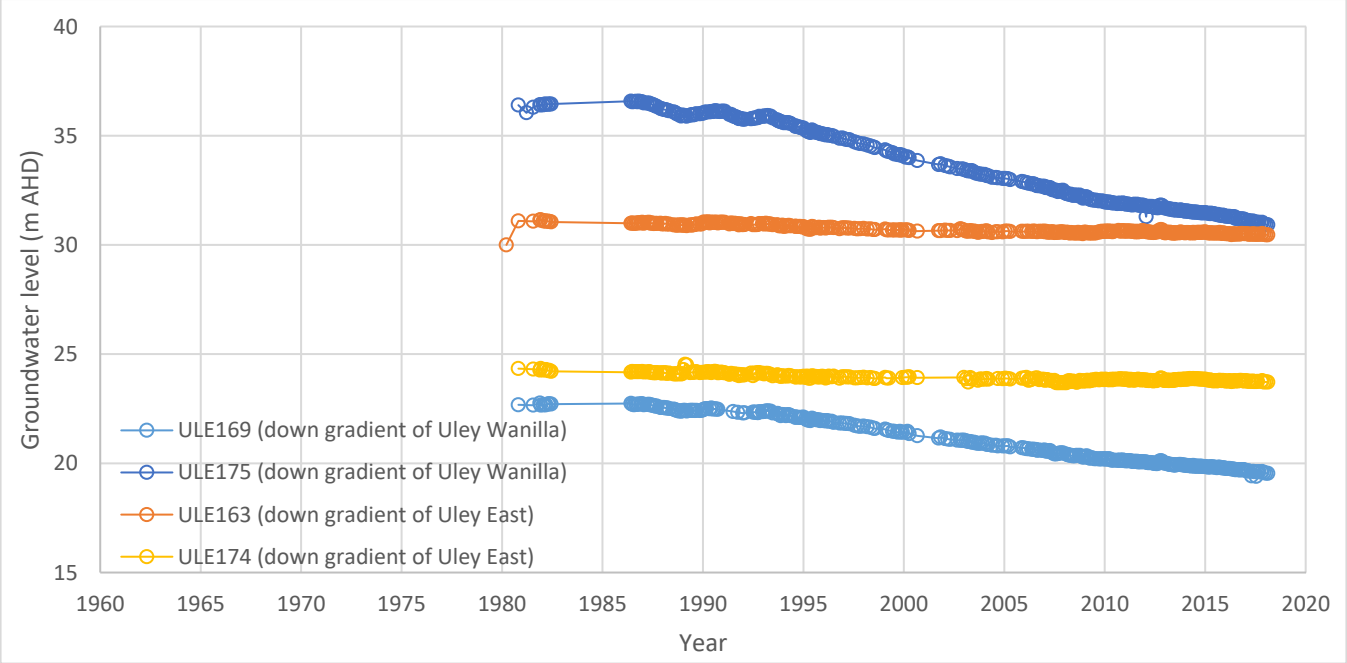


Figure 2.11. Groundwater levels in the northern part of the TS aquifer

Within the Uley South Basin, groundwater levels in the TS aquifer have shown similar trends over time to levels in the QL aquifer, with rises observed in the late 1960s, and declines in the late 1970s and 1990s (Figure 2.12). As there is no direct extraction from the TS aquifer, the trend may be in part a pressure response to trends in the QL aquifer (Evans, 1997), as the TS is generally confined. However, in some areas the TS and QL aquifers are likely to

be in equilibrium. Nested wells in both aquifers can only be found at one location in the northern part of the QL aquifer (see Figure 2.8a for location of ULE109), and they show very similar trends since the early 1990s, despite the TC layer being 10 m thick at this location (Figure 2.13).

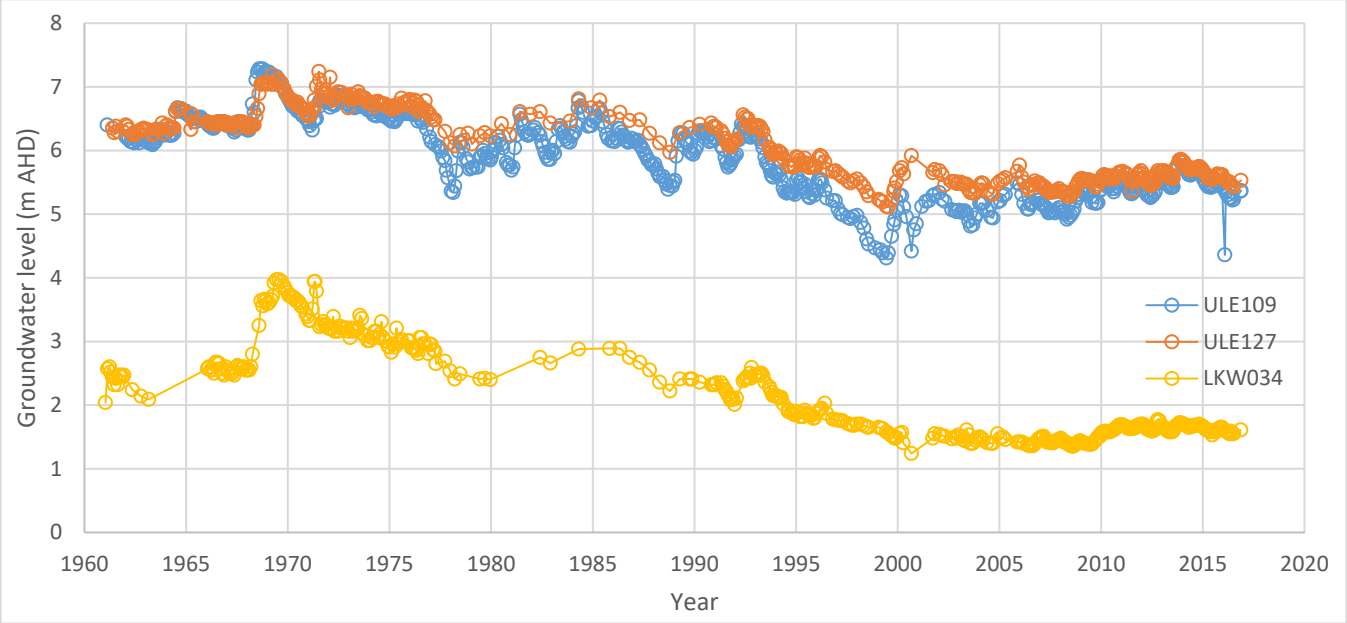


Figure 2.12. Long-term groundwater trends in the TS aquifer within the Uley South Basin

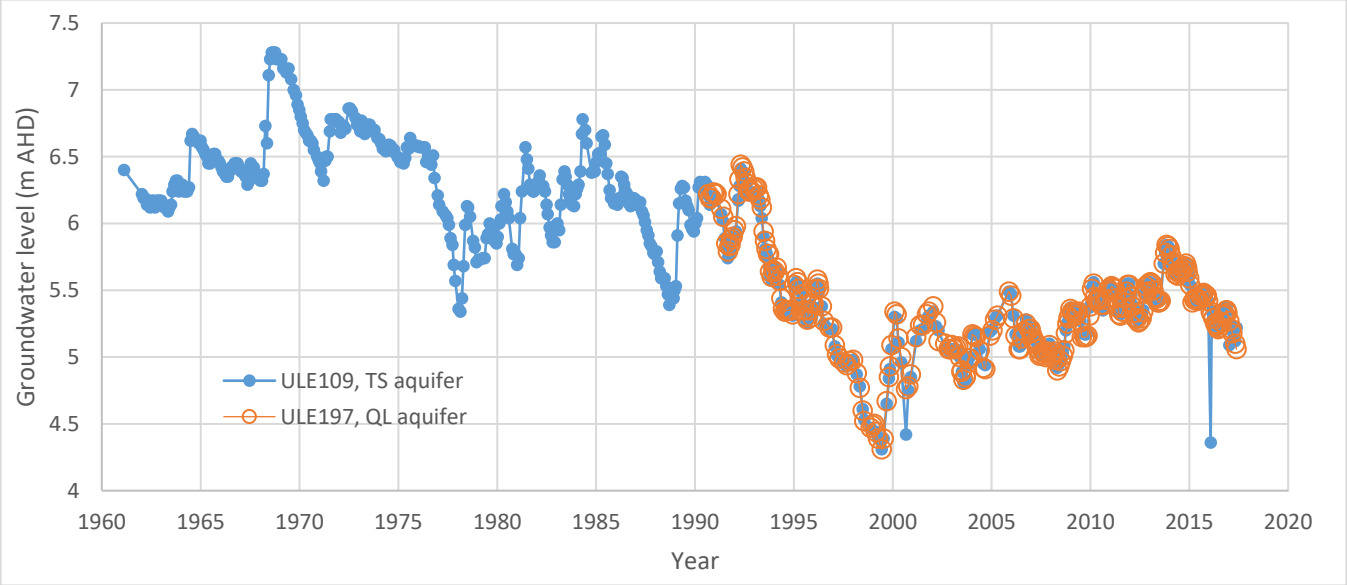


Figure 2.13. Groundwater levels in nested wells ULE109 (TS aquifer) and ULE197 (QL aquifer)

2.5.3 Groundwater flow between aquifers

In the northern part of the Uley South area where the TC is absent, the QL and TS aquifers are in direct connection (Figure 2.5). While there are limited 'nested' observations of groundwater levels in both the QL and TS, analysis of potentiometric surfaces shows that there is the potential for flow from the TS to the QL aquifer near the boundary of the QL aquifer (Figure 2.6). Conceptually, flow from the TS to the QL may occur as horizontal or lateral inflow where the aquifers connect (Harrington et al., 2006), or as vertical or upwards flow. The conceptualisation of TS flow into QL at the Uley South Basin margin is supported by groundwater salinity data (Section 2.5.9) which shows that QL groundwater resembles TS water closer to the margin of the QL aquifer, while in the central part of the

basin QL groundwater is less saline than the TS, as a result of a higher proportion of rainfall recharge. There is thought to be additional upwards leakage from the TS to QL aquifer in parts of the basin where the TC is absent, such as the south-eastern coastal area (Zulfic et al., 2007).

2.5.4 Aquifer properties

Hydraulic properties for the QL aquifer derived from aquifer test analysis in Uley South have been reported by Morton and Steel (1968), Painter (1968), Sibenaler (1976) and Barnett (1978). Further values have been obtained from unpublished reports to SA Water by Watkins et al. (2015), analysis of unpublished aquifer test data for town water supply wells 14, 16 and 21 (data found in the DEW and SA Water internal databases), and values determined by borehole nuclear magnetic resonance (NMR) reported by Davis et al. (2012). This gives 50 hydraulic conductivity values for the QL aquifer, ranging from 1 to 4848 m/d. However, in some cases, multiple values are provided at individual locations, due to both step drawdown and constant rate pumping tests being conducted, and follow up tests being conducted when replacement wells were drilled. Thus the 50 hydraulic conductivity values relate to 30 well locations (Figure 2.14).

The values of hydraulic conductivity derived from borehole NMR (0.2 to >360 m/d) are generally lower than those given by aquifer tests. As noted by Davis et al. (2012), the estimation of hydraulic conductivity from borehole NMR requires input of lithology-based coefficients, which in the Uley South study were based on Gulf of Mexico sandstones. Thus, the authors state that the estimates are likely to represent lower limits of aquifer conductivity. Nevertheless, they provide useful lower bounds for parameter estimation, as well as information on the relative spatial distribution of aquifer properties.

Specific yield (S_y) estimates for the QL aquifer range from 0.007 to 0.72. The high hydraulic conductivity and very high specific yield values are derived from aquifer tests in areas where the QL is 'well cemented and cavernous' (Sibenaler, 1976). In many reported cases there is very little water table drawdown recorded during pumping tests, which gives rise to the high estimates of hydraulic conductivity and specific yield. For example, Watkins et al. (2015) report less than 10 cm drawdown in response to a 10-hour constant rate aquifer test at rates of 25–30 L/s. Davis et al. (2012) also report high 'mobile' porosity values based on borehole NMR of up to 80%. Davis et al. (2012) do state that these values should be considered as upper limits and may be influenced by borehole construction. Nevertheless, they suggest high effective porosity may be present in the QL, consistent with high S_y values derived from aquifer tests.

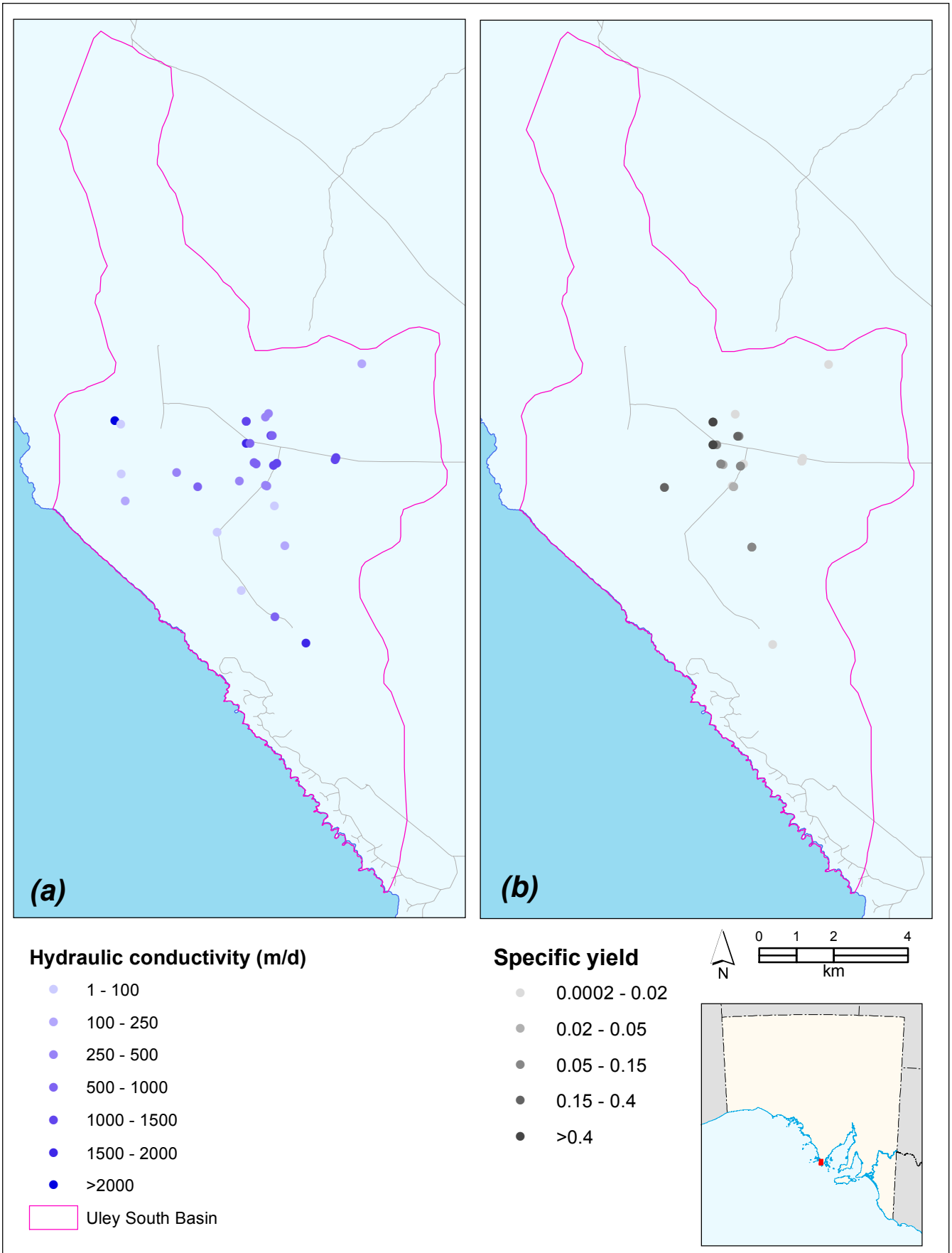


Figure 2.14 Hydraulic conductivity (a) and specific yield (b) data for the QL aquifer

Only one value of hydraulic conductivity for the TS aquifer, 22 m/d, has been reported by Morton and Steel (1968), who also reported a storage value of 0.007 for the TS. Morton and Steel (1968) also report one value of vertical conductivity for the TC aquifer of 6.8 x 10^{-4} m/d. Appendix A gives the hydraulic conductivity values and their sources, as well as interpretation of unpublished aquifer test data.

2.5.5 Groundwater recharge to the QL aquifer

Groundwater recharge has been extensively investigated in the Uley South Basin. Sibenaler (1976) estimated recharge to be 55 mm/y, by assuming that 10% of annual rainfall equates to recharge. Barnett (1978) reviewed groundwater level fluctuations and winter rainfall from 1962 to 1978, and derived an average recharge rate of 105 mm/y for years in which average rainfall occurs. Based on groundwater level fluctuations, Barnett also concluded that recharge was unlikely to occur in years when winter rainfall was less than 217 mm.

Evans (1997) estimated recharge to the Uley South Basin using multiple methods. A flow net analysis yielded a recharge rate of 157 mm/y, while a water balance analysis yielded a recharge rate of 78 mm/y. Evans also used the water table fluctuation method to estimate recharge. The water table fluctuation method estimates recharge based on changes in groundwater level (Healy & Cook, 2002) by:

$$R = \frac{\Delta h}{\Delta t} S_y \qquad (1)$$

Where R is the recharge rate, Δh is the rise in the water table over a specified time (Δt), and S_y is the specific yield. Using this method, Evans calculated a recharge rate of 46 mm/y, using a specific yield of 0.15.

Evans (1997) applied the chloride mass balance method to derive recharge rates. Assuming there is no run-off and no chloride contributed to groundwater by leaching from aquifer materials, recharge can be estimated by:

$$R = \frac{PC_p}{C_{gw}} \qquad (2)$$

Where R is the annual recharge rate, P is annual precipitation, C_p is the chloride concentration in rainfall (typically estimated based on distance from the coast), and C_{gw} is the chloride concentration in groundwater. Based on this method, Evans estimated recharge to range from 63.6 to 70.5 mm/y.

Evans (1997) also used chlorofluorocarbon (CFC)-based groundwater ages to estimate recharge. The groundwater age method relies on samples being collected from short well screens (Solomon et al., 2006), where recharge is given by:

$$R = \frac{z\theta}{t} \qquad (3)$$

Where R is the annual recharge rate, z is the depth from which the sample was collected, θ is porosity, and t is the apparent, tracer-derived age of the groundwater sample. Evans found CFC-based apparent ages ranging from 5 – 17 years in the QL aquifer Uley South Basin, and calculated recharge rates ranging from 25 to 200 mm/y (using a porosity of 15%). Summarizing all the various recharge estimation techniques, Evans reported an average recharge rate of 160 mm/y for the QL aquifer in Uley South.

Green et al. (2012) used the unsaturated zone model LEACHM to simulate recharge to the Uley South Basin and other basins in the southern Eyre Peninsula. LEACHM uses the Richards equation to simulate one-dimensional flux through the unsaturated zone (Hutson, 2005). Green et al. (2012) developed models for the dominant unsaturated zone lithologies in the Eyre Peninsula, and compared simulated recharge to recharge estimated from the water table fluctuation method at observation wells where the same lithology was present. Model parameters were varied in order to achieve a good fit to measured estimates of recharge. The models used daily climate data, and individual recharge events were summed to give annual recharge. The calibrated LEACHM models yielded average annual recharge rates varying from 57 to 153 mm/y for soil types in the Uley South Basin. Green et al. (2012) then used these unsaturated zone models to assess the impact of future climate scenarios, generated from 'low' and 'high' emissions scenarios from four global climate models. The results give guidance on the potential impacts of

climate change on groundwater recharge in the Uley South Basin (Figure 2.15). The different symbols in Figure 2.15 represent different GCMS, where multiple points for each GCM represent different emission scenarios.

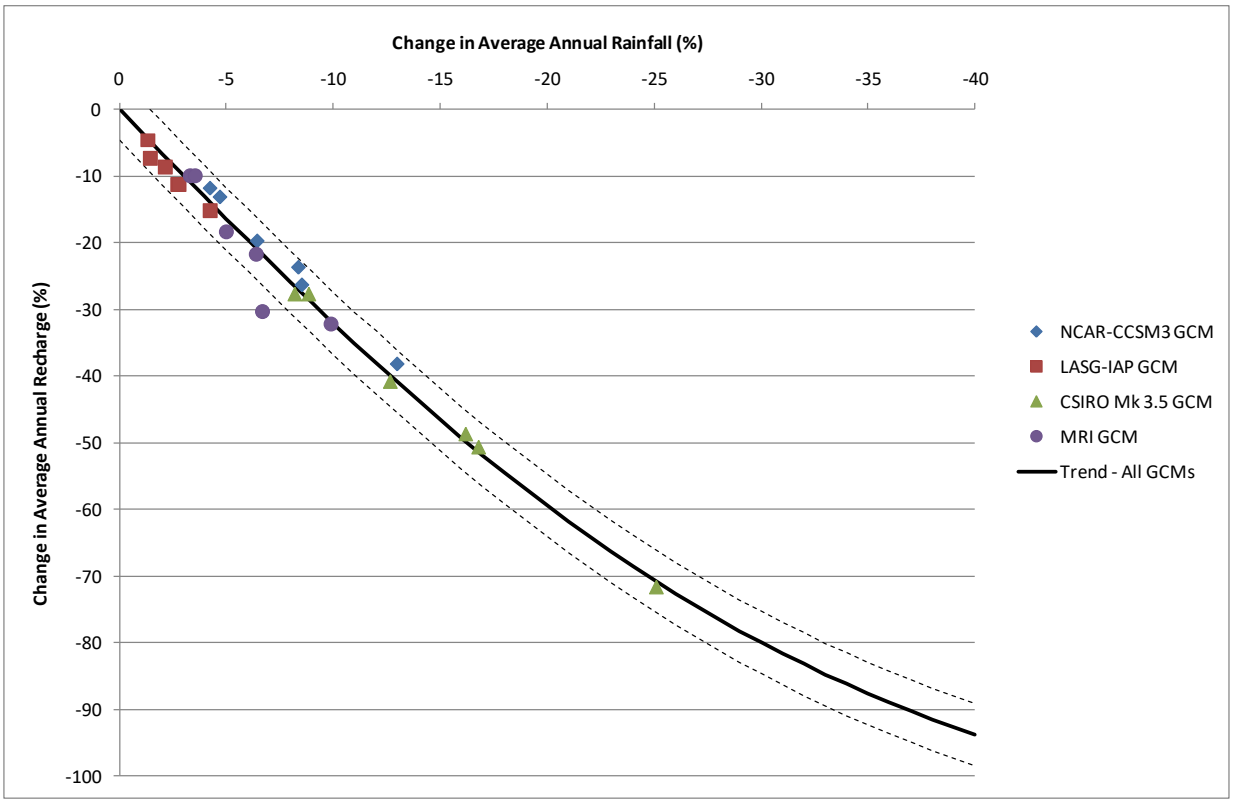


Figure 2.15. Potential changes in recharge in response to changes in average annual rainfall based on four global climate models in the Southern Basins Prescribed Wells Area, dashed lines show the upper and lower 95% confidence intervals (from Green et al., 2012)

Ordens et al. (2012) estimated recharge in Uley South using the water table fluctuation and chloride mass balance methods. A correction was applied to the water table fluctuation method to account for the potential influence of groundwater pumping on groundwater level declines, and hence impacts on recharge estimated from water table trends. Using data from 15 wells, this approach estimated the mean annual recharge rate to range from 47 to 129 mm/y. The range reflects the range of S_y values (0.1 to 0.25) used. Ordens et al. (2012) also applied the chloride mass balance method to estimate average basin-wide recharge ranging from 52 to 63 mm/y, with maximum and minimum values from individual wells ranging from 35 to 114 mm/y.

Ordens et al. (2014) also used LEACHM to evaluate the impact of unsaturated zone conceptualization (e.g. root depth and lithology) on simulated recharge in the Uley South Basin, reporting a range of recharge rates for different land use and lithology across the basin. Knowling et al. (2015) cited Ordens et al. (2014) in using a spatially and temporally averaged recharge rate of 84 mm/y for the Uley South Basin, with a range from 0 to 240 mm/y.

Bresciani et al. (2014) extended the chloride mass balance work of Ordens et al. (2012) to account for the influence of vegetation and distance from the coast on chloride deposition in Uley South Basin. Rainfall and chloride deposition were measured at three vegetated and three 'open field' sites, and a Geographic Information System approach was used to develop spatial maps of chloride deposition. This method yielded recharge estimates of 69 to 73 mm/y.

Swaffer (2017) investigated spatial variability in groundwater recharge using a water balance approach based on remote sensing data. Satellite derived evapotranspiration (ET) data (Guerschman et al., 2009) was subtracted from precipitation data across the Southern Basins to yield annual water balances at 250 m pixels for the period 2001 to

2010 (Figure 2.16). Following Crosbie et al. (2015), Swaffer corrected bias in the recharge estimates derived from this approach by comparing them with estimates from the water table fluctuation method. While Swaffer acknowledges that the accuracy of water balance values on the pixel scale is uncertain, the data still provides important information on broad spatial and temporal trends. For example, the results show that a deficit between ET and rainfall consistently occurs in areas of mallee woodland, indicating that no recharge occurs under this vegetation. This conclusion is consistent with studies of recharge under mallee vegetation in similar calcrete environments (Allison et al., 1985).

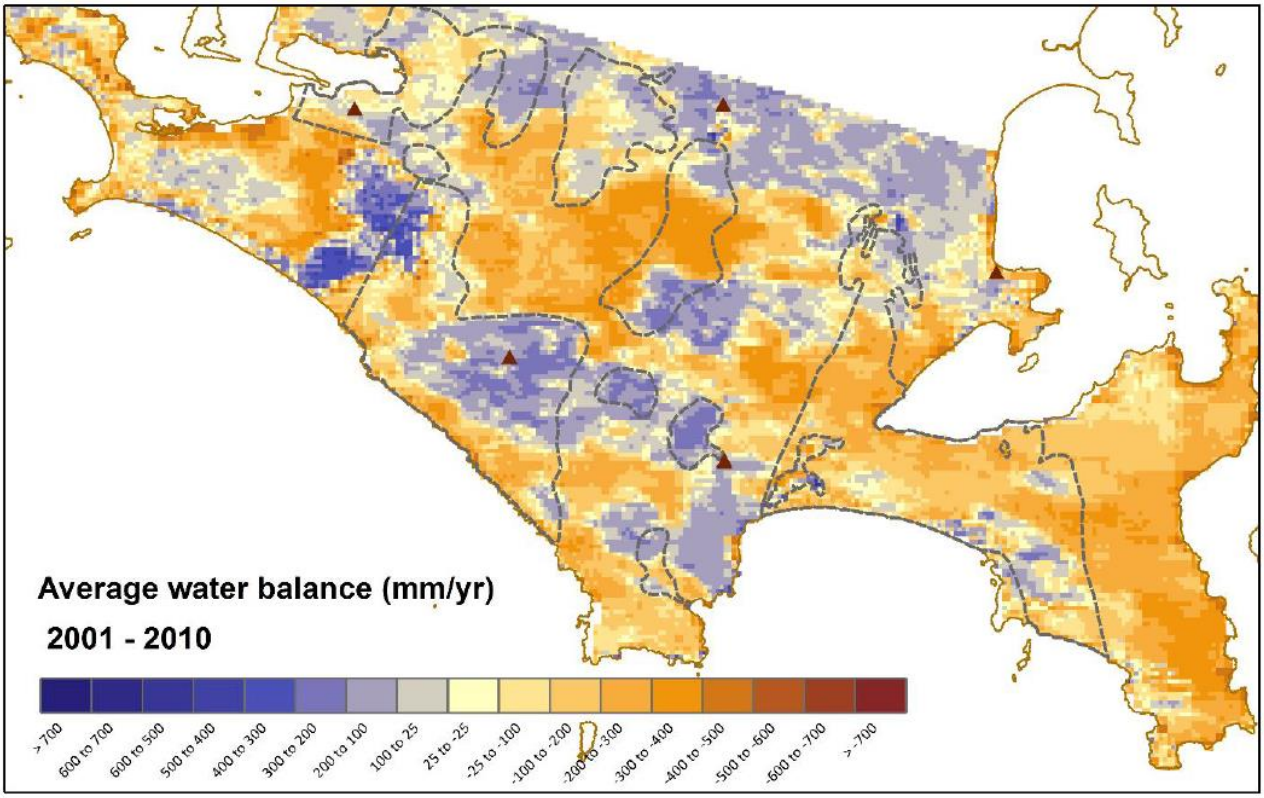


Figure 2.16. Average annual water balance (mm/y) for the Southern Basins (Swaffer 2017).

The examples above highlight the variability in estimated recharge rates in the Uley South Basin (Table 2.2). Much of this variability is due to the natural spatial and temporal variability in recharge. However, the method applied to estimate recharge is also likely to influence the result. In summarizing recharge in the Uley South Basin, the Water Allocation Plan for the Southern Basins and Musgrave Prescribed Wells Area (EPNRMB, 2016) gives a recharge rate of 129 mm/y based on the work of Ordens et al. (2012), noting that the then-stable groundwater levels could not be sustained with lower recharge rates and the extraction rate of ~5700 ML/y (Stewart, 2013).

Table 2.2. Summary of recharge rates in the Uley South Basin

Study	Method	Recharge rate (mm/y)
Sibenaler (1976)	Recharge is 10% of rainfall	55
Barnett (1978)	Hydrograph analysis	105
Evans (1997)	Chloride mass balance	63.6 to 70.5
Evans (1997)	Water table fluctuation	46
Evans (1997)	Water balance	78
Evans (1997)	Flow net analysis	157
Evans (1997)	CFC	25 to 200
Ordens et al. (2012)	Chloride mass balance	52 to 63
Ordens et al. (2012)	Water table fluctuation	47 to 129
Green et al. (2012)	Unsaturated zone modelling	57 to 153
Ordens et al. (2014)	Unsaturated zone modelling	0 to 240
Bresciani et al. (2014)	Chloride mass balance (accounting for chloride deposition)	69 to 73
EPNRMB (2016)	Summary of existing methods	129

2.5.6 Recharge to the TS aquifer

The potentiometric surface in Figure 2.7 shows that groundwater in the TS aquifer flows into the Uley South region from upgradient. Based on groundwater isotope and chemistry evidence, groundwater recharge to the TS aquifer is thought to occur in the Big Swamp area in the Uley East lens, and via downward leakage from the QL aquifer in the Uley Wanilla lens (Evans, 1997; Harrington et al., 2006). Groundwater levels in the TS aquifer downgradient of the Uley East lens have shown generally stable trends over time (Figure 2.11). However, groundwater levels in the TS aquifer downgradient of the Uley Wanilla lens have shown declining trends since the mid-1980s. These declines correlate with declines in the QL aquifer level in the Uley Wanilla lens, suggesting recharge to the TS from the QL in Uley Wanilla has declined with time. This impacts groundwater levels in the TS aquifer in the part of the study area where the QL aquifer is dry, with groundwater levels in ULE175 showing a declining trend since the early 1990s (Figure 2.11).

2.5.7 Evapotranspiration

Swaffer at al. (2014) measured evapotranspiration (ET) and tree water use of coastal white mallee and drooping sheoak in the Uley South Basin, and found it was unlikely that groundwater was being used by these species. Thus, ET of groundwater by vegetation in the Uley South Basin is not considered to be a significant component of the water balance. There are small, swampy low-lying areas of the basin where ET of shallow groundwater may occur (Harrington et al., 2006). These areas may have been intermittent recharge/discharge features prior to groundwater development, when groundwater levels were higher (Morton and Steel, 1970). However, groundwater modelling by Knowling et al. (2015) found that shallow groundwater ET is likely to represent a minor component of the water balance (assuming an extinction depth of 2 m).

2.5.8 Groundwater extraction

Annual groundwater extraction rates from the Uley South Basin have been reported since extraction commenced in 1976 (Figure 2.17). Groundwater extraction is from the QL aquifer, and was initially from eight wells drilled in the central part of the basin in 1976 (Figure 2.18). An additional nine wells were drilled in 1999, and the 1976 wells were replaced at the same locations in 2014 (Figure 2.3). The master meter collates flow from all extraction wells in the basin. Monthly master meter data has been collected since 1996, while monthly flow data from meters on individual extraction wells has been collected since 2013. Extraction has varied over time, ranging from

approximately 4000 to 6000 ML/y during the 1980s. Extraction increased to more than 7000 ML/y in the early-2000s. However, extraction has decreased since then to the current rate of approximately 5000 ML/y.

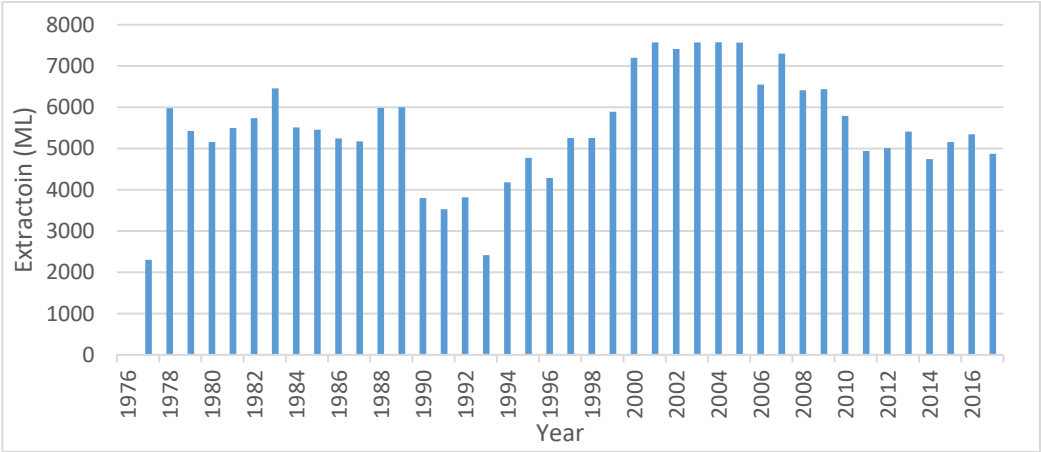


Figure 2.17. Yearly groundwater extraction rates from the QL aquifer in Uley South (SA Water)

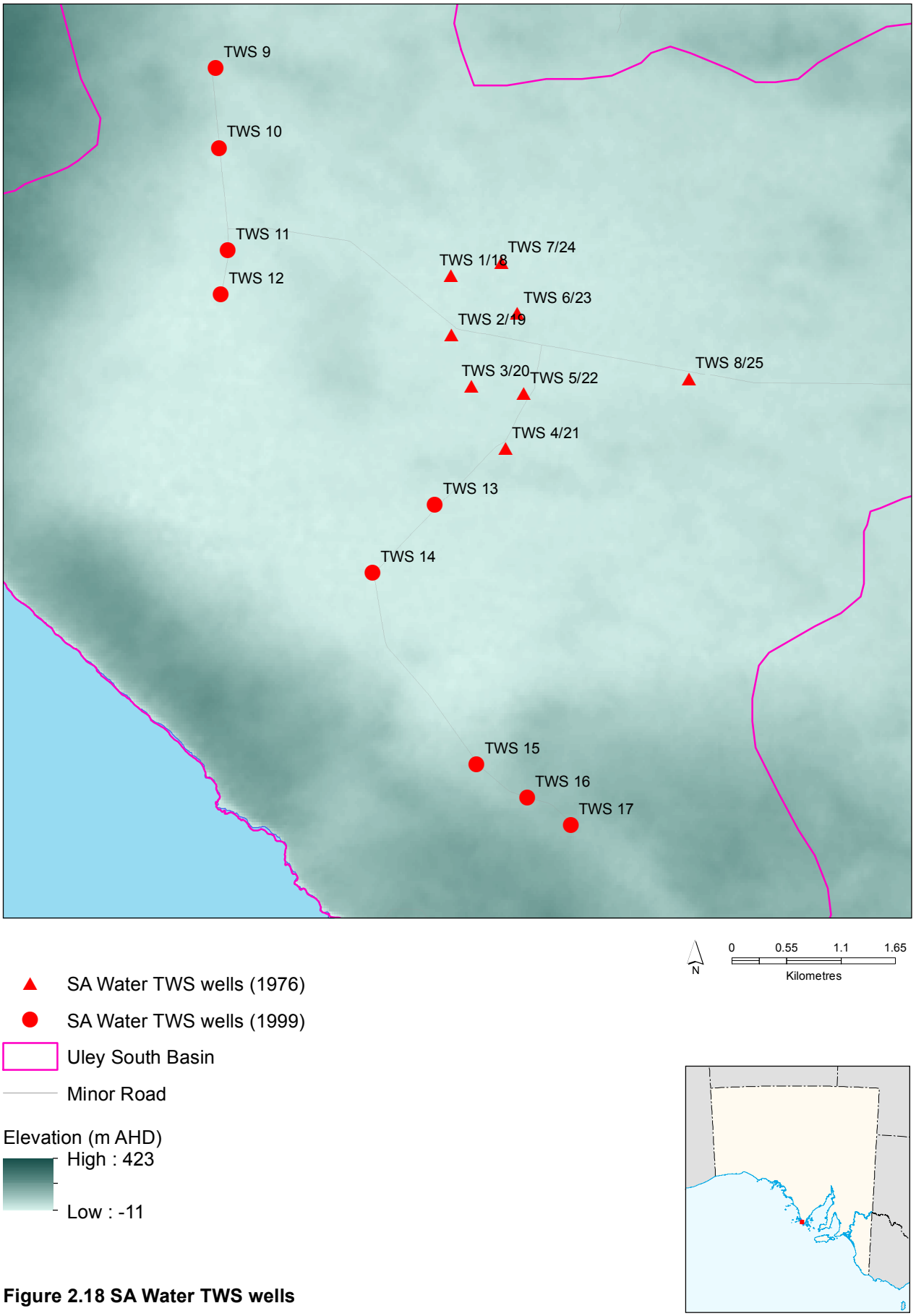


Figure 2.18 SA Water TWS wells

The metered data from individual bores does not give a complete data record for 2013 to 2017, as there are periods of missing data due to meters being replaced or gaps in monitoring. However, monthly individual bore extractions can be estimated from monthly master meter data, based on knowledge of how extraction is distributed in the basin, which was provided by SA Water. This estimated individual bore extraction, when compared with available metered bore extractions, generally shows good agreement (Figure 2.19).

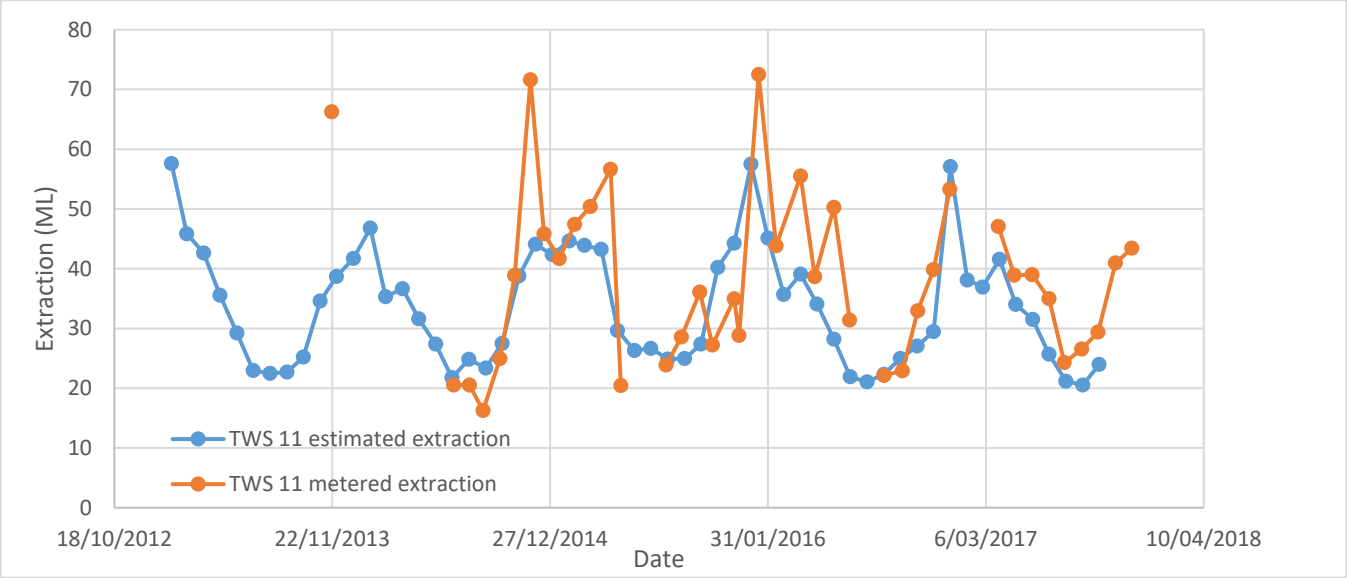
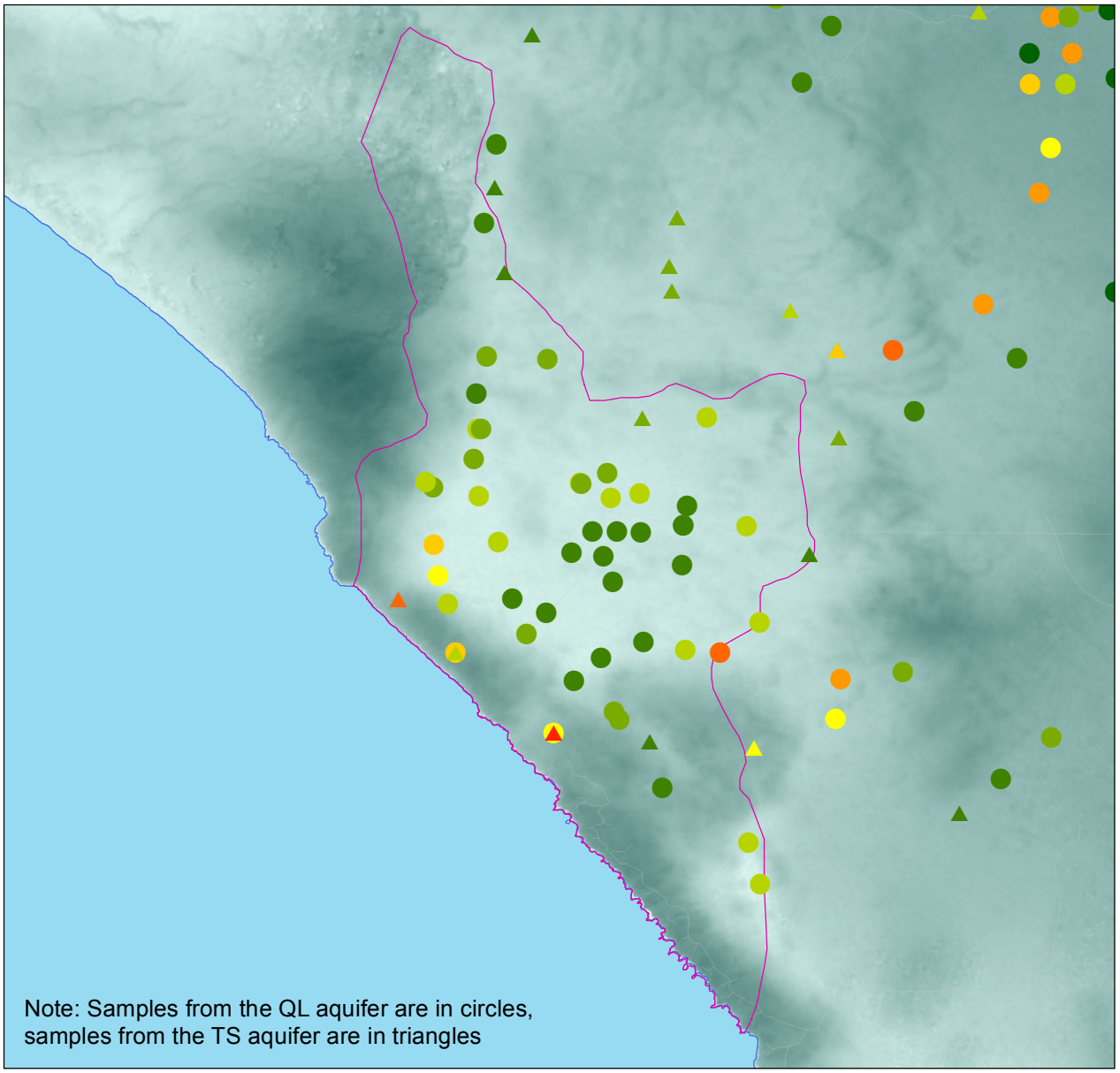


Figure 2.19. Estimated extraction and metered extraction (when data is available) from TWS 11

2.5.9 Groundwater salinity

Groundwater salinity in the QL aquifer ranges from 300 mg/L to 1010 mg/L, with the majority of values ranging from 500 to 700 mg/L. This is based on spot measurements of salinity (Figure 2.20), as well as long term salinity monitoring in TWS wells. Groundwater salinity in the TS aquifer ranges from 400 to 1550 mg/L. Closer to the margins of the QL aquifer, groundwater chemistry resembles that of the underlying TS aquifer, supporting the notion that TS water may flow into the QL aquifer where the TC is absent. Salinity in the nested wells ULE109 (TS) and ULE197 (QL) are very similar (673 and 677 mg/L respectively). However, within the central portion of the Uley South Basin, QL salinity is lower (<500 mg/L), indicating dilution of groundwater through rainfall recharge within the basin (Figure 2.20).



Total dissolved solids (mg/L) - QL in circles, TS in triangles

- 200 - 400
- 400 - 500
- 500 - 600
- 600 - 700
- 700 - 800
- 800 - 900
- 900 - 1000
- 1000 - 1500
- 1500 - 2000

Uley South Basin

Towns

Minor Road

N

0 1.5 3 4.5

Kilometres

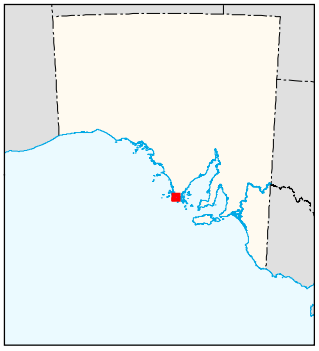


Figure 2.20 Groundwater salinity in the Uley South Basin

Groundwater salinity in TWS wells has shown stable trends over the period of monitoring, with the exception of 6028-2169 (TWS 12) which has shown a trend of rising salinity since the mid-2000s (Figure 2.21). Groundwater salinity in TWS 3 (6028-701) showed an increase in the late 1990s of between from less than 500 to more than 600 mg/L, as groundwater extraction increased and groundwater levels declined (Figure 2.22). Salinity decreased again in 2010 as groundwater extraction decreased, and a period of above average rainfall was observed. As TWS 3 is located 4.6 km inland, this isolated trend is unlikely to relate to seawater intrusion. It is more likely that reduced groundwater levels in the QL and increased pumping resulted in increased flow from the TS aquifer in this area (note TWS 20 replaced well 3 in 2016).

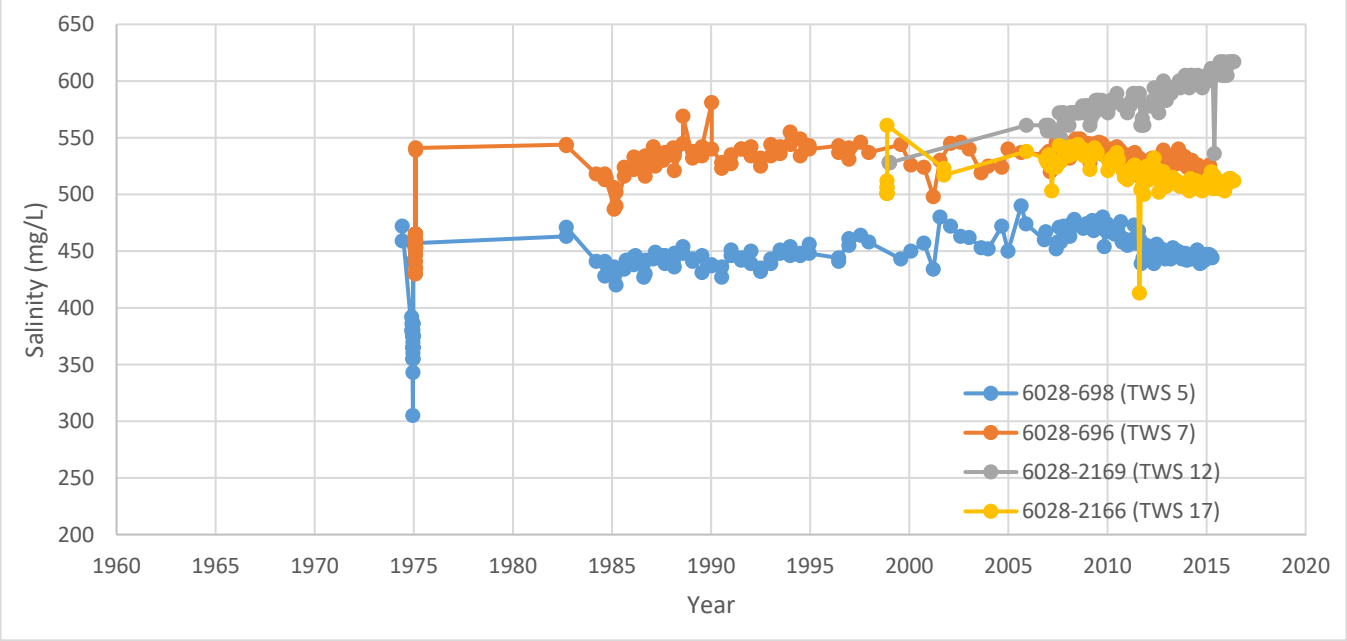


Figure 2.21. Example groundwater salinity trends in TWS wells (see Figure 2.18 for location of TWS wells)

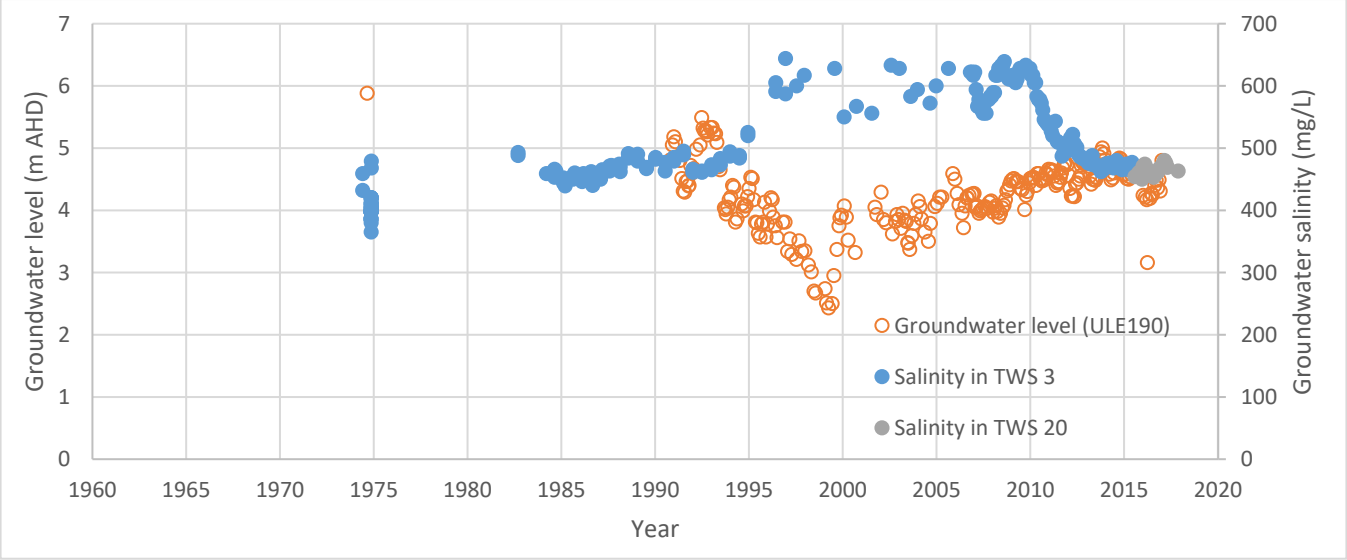


Figure 2.22. Groundwater salinity in TWS 3 and groundwater level in adjacent observation well ULE190

2.5.10 Coastal groundwater processes

Groundwater is thought to discharge at the coast from the QL aquifer, however rates of coastal groundwater discharge have not been measured. Various authors have estimated rates of groundwater discharge to the sea

using both analytical and numerical methods with rates ranging from 5280 to 30,000 ML/y (Table 2.3). The variation in estimates can be attributed to the different methods applied. Evans (1997) noted that the TS was likely to be hydraulically connected to the coast, as TS levels near the coast display the influence of a tidal signal. However, there have been no studies of groundwater discharge from the TS aquifer.

Table 2.3. Estimates of groundwater discharge to the coast from previous studies

Discharge to the coast	Method	Author
15,185 ML/y (QL pre-development) 2675 ML/y (TS pre-development)	Darcy's Law	Morton and Steel (1970)
30,000 ML/y (pre-development)	Darcy's Law	Barnett (1978)
10,700 ML/y (pre-development)	Darcy flow analysis	Evans (1997)
5280 ML/y (pre-development)	Flow analysis accounting for seawater interface	Evans (1997)
18,658 ML/y (pre-development)	Numerical model	Zulfic et al. (2007)
18,000 ML/y (average 1967–2007)	Analytical model	Alcoe (2009)
29,200 ML/y (pre-development) 14,100 ML/y (post-development)	Numerical model	Werner (2010)
16,425 ML/y (pre-development) 6570 ML/y (post-development)	Numerical model	Knowling et al. (2015)
10,800 ML/y (post-development)	Analytical model	Somaratne (2019)

Given the importance of the QL aquifer for water supply, numerous studies have investigated the inland extent of the seawater-freshwater interface in the aquifer and potential for seawater intrusion, using analytical and numerical methods (Table 2.4). Analytical studies have been used to estimate where the interface intersects the base of the aquifer – also referred to as the 'toe' of the seawater wedge. These studies have estimated the toe in the QL to occur at 150 to 600 m inland under pre-development conditions (prior to pumping), and 450 to 1800 m for post-development conditions. Further numerical modelling has estimated the seawater wedge to extend 500 m to 1645 m inland (see Table 2.4 for references).

Table 2.4. Estimates of the inland location of the seawater interface toe in the QL aquifer from previous studies

Location of interface toe	Method	Author
220 m (pre-development) 450 m (post development)	Analytical model	Seidel (2008)
440 m (post-development, western part of basin) 900 m (post development, eastern part of basin)	Analytical model	Ward et al. (2009)
100 to 600 m (pre-development) 650 to 1800 m (post-development)	Analytical model	Alcoe (2009)
500 m (pre-development)	Numerical model	Werner and Dang (2013)
600 m (pre-development) 1645 m (post-development*)	Numerical modelling with SEAWAT, where * is the inland extent of the 0.05 relative salt content contour	Badaruddin (2017)
158 m (pre-development) 490 m (post development)	Analytical model	Somaratne (2019)

Monitoring of the seawater-freshwater interface is limited to wells of sufficient depth in the coastal zone. Well SLE010 was drilled in 1962 in the cliffs 500 m from the coast. Salinity sampling conducted during drilling showed a transition from brackish to saline water between -22 and -25 m AHD, coinciding with the base of the QL aquifer (Figure 2.23). While SLE010 has been abandoned, a replacement well SLE069 was drilled 15 m away in 2003. SLE069 has a 36 m long-screened section (from 14 to -22 m AHD) which straddles both the QL and TS aquifers (the TC is absent in this area). Salinity profiling in this well with a sonde salinity meter has shown salinity increases from -15 to -25 m AHD, showing the interface within the QL aquifer (Figure 2.24). While this gives some indication of the transition zone, sonde profiles in long-screened wells should be interpreted with caution, as long-screened wells may 'short circuit' vertical gradients across the interface, giving the appearance of the interface being at a higher elevation than it really is (Shalev et al., 2009).

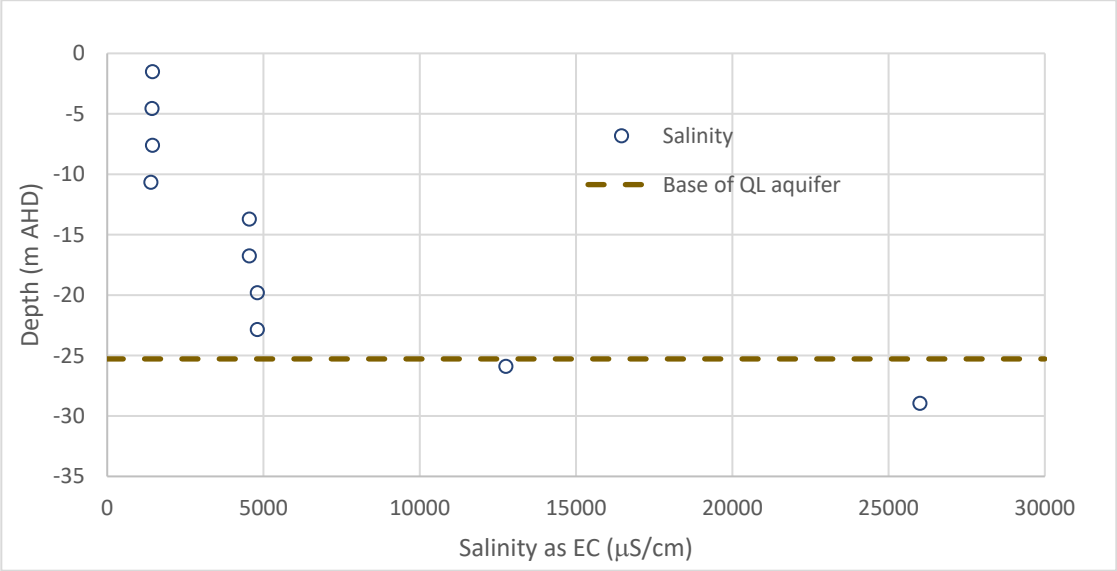


Figure 2.23. Salinity with depth in SLE010, samples taken during drilling in 1962

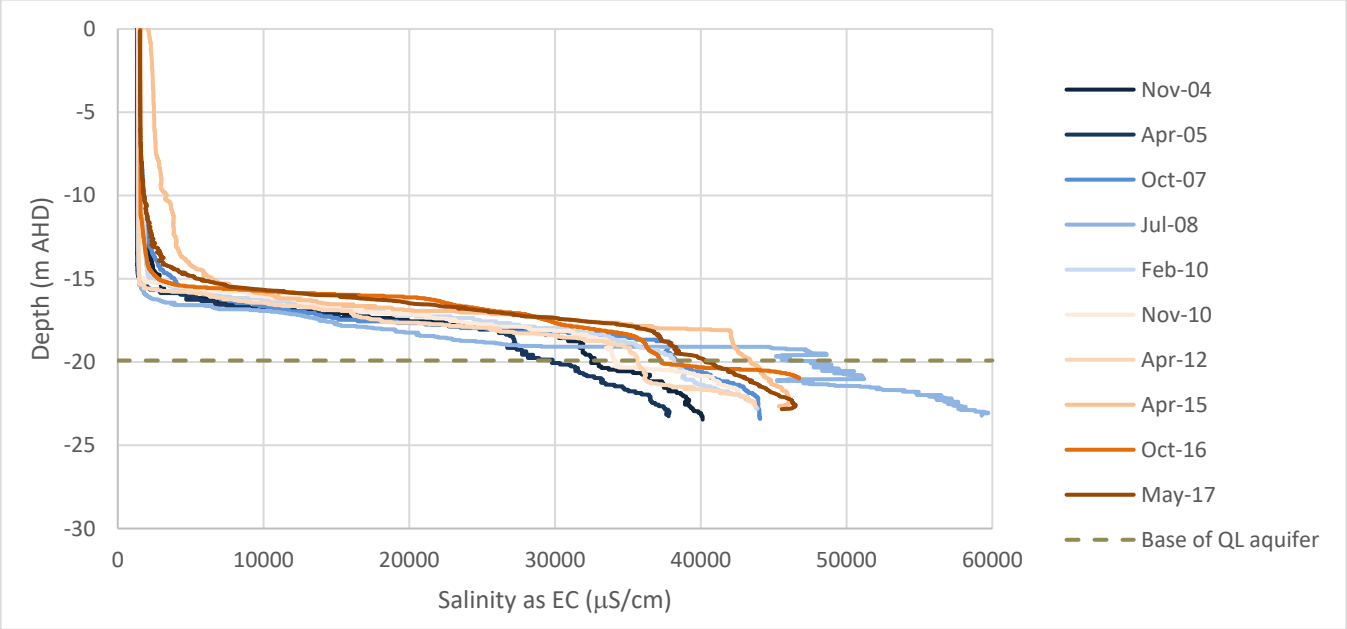


Figure 2.24. Salinity profiles from sonding in SLE069 (well is screened from 14 to -22 m AHD)

Salinity profiles in ULE205, which is located 400 m from the coast, show brackish water in the QL aquifer, with the transition to saline water occurring in the TS aquifer. As with SLE069, it is important to note that the long screen in this well (from 28 to -32 m AHD) may influence salinity readings. For example, sonde measurements show elevated salinity up to 7800 µS/cm in the QL aquifer between -5 and -10 m AHD in May 2017. However, well ULE223, drilled 40 m north of ULE205 in June 2018 and screened exclusively in the QL aquifer, showed lower salinity (~2700 µS/cm) in the QL over this interval.

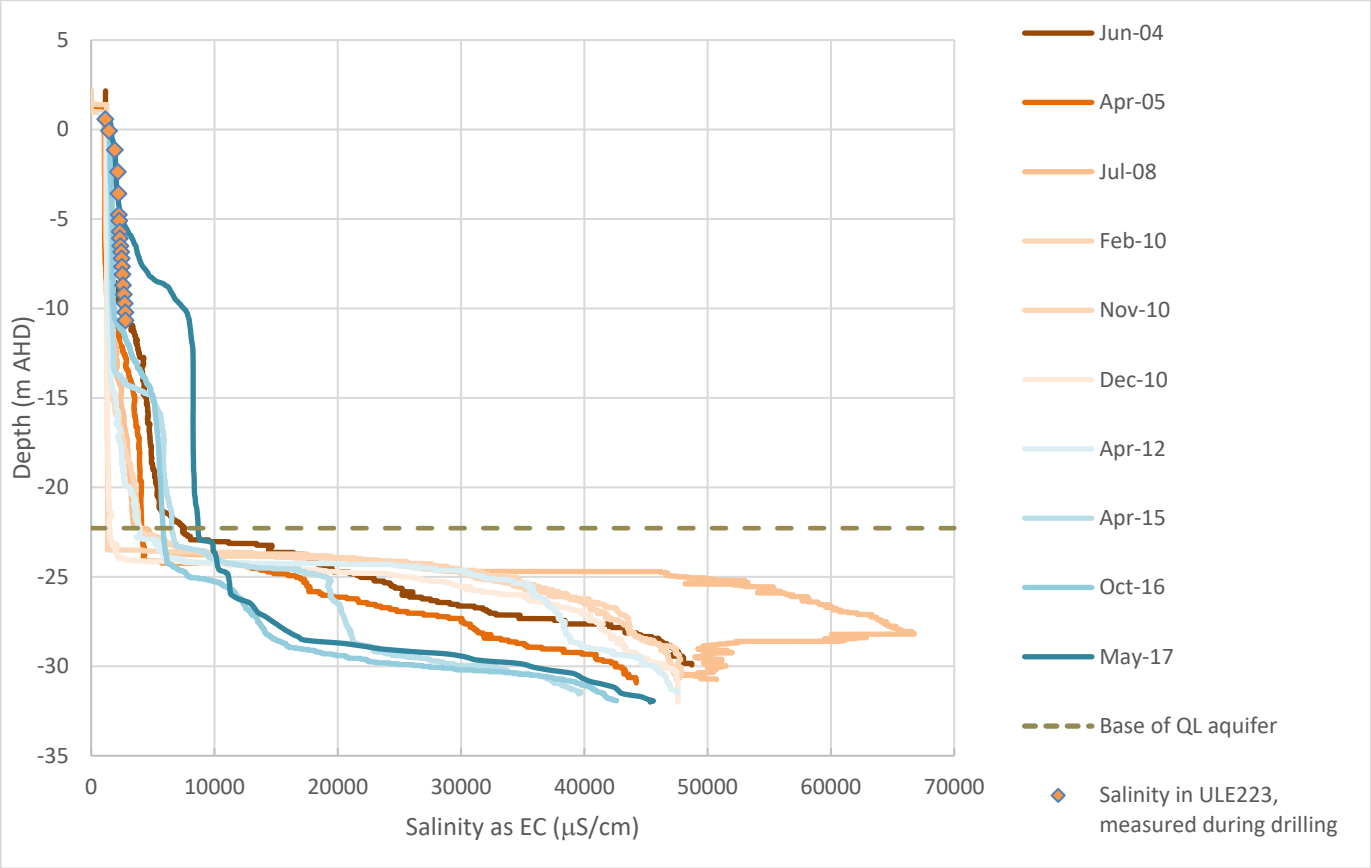


Figure 2.25. Salinity profiles from sonding in ULE205 (well is screened from 28 to -32 m AHD)

2.6 Conceptual model and water balance

Based on available data and the significant number of investigations that have previously been conducted, a preliminary water balance for the QL aquifer in the Uley South Basin can be constructed. Conceptually the QL aquifer in the Uley South Basin is unconfined, with groundwater flow southwards from the basin boundary to the coast. Inflow sources are predominantly rainfall recharge (diffuse and point source) and TS aquifer inflow. Discharge occurs at the coast and via pumping within the basin (Figure 2.26). Evapotranspiration of shallow groundwater is not thought to be significant. The following section summarizes the key processes and estimated flux rates.

2.6.1 Inflows

The QL aquifer is sensitive to annual rainfall recharge, and a wide range of studies have estimated recharge to vary from 25 to 200 mm/y. Based on a saturated extent of the QL aquifer of 112 km^2, recharge volumes may vary from 2800 to 22,405 ML/y. The TS aquifer is also thought to contribute to the QL aquifer. However, there have been few studies that have quantified this flux. Zulfic et al. (2007) developed a groundwater flow model for Uley South Basin (see Section 3.4), and the steady state mass balance showed upward leakage into the QL aquifer from the TS to be 5101 ML/y.

2.6.2 Outflows

Groundwater discharge to the coast occurs from the QL aquifer. However, estimates of discharge vary from 5280 to 30,000 ML/y depending on the method used to estimate discharge. Groundwater extraction for town water supply commenced in 1976, and extraction rates have ranged from 2415 to 7576 ML/y. However, since 2010 the average extraction rate has been 5158 ML/y.

2.6.3 Summary

Given the transient nature of processes such as recharge in the Uley South Basin, the water balance for the QL will show large variation from year to year. This is reflected in groundwater level observations, including pre-development periods (Figure 2.8). Rather than attempt to describe an 'average' water balance, the range in values derived from previous studies and models is presented in Table 2.5. As demonstrated in Table 2.5, the water balance may be in surplus or deficit in any given year, depending largely on the volume of rainfall recharge, as well as pumping and discharge to the coast.

Table 2.5. Preliminary conceptual model water balance for the QL aquifer in the Uley South Basin

Inflows	**Volume (ML/y)**
Recharge	2800 to 22,400
Inflow from TS aquifer	5100
Outflows	**Volume (ML/y)**
Pumping	2415 to 7576
Discharge to the coast	5280 to 30,000
Outflow to the TS aquifer	-
Total inflows	*7900 to 27,500*
Total outflows	*7695 to 37,576*

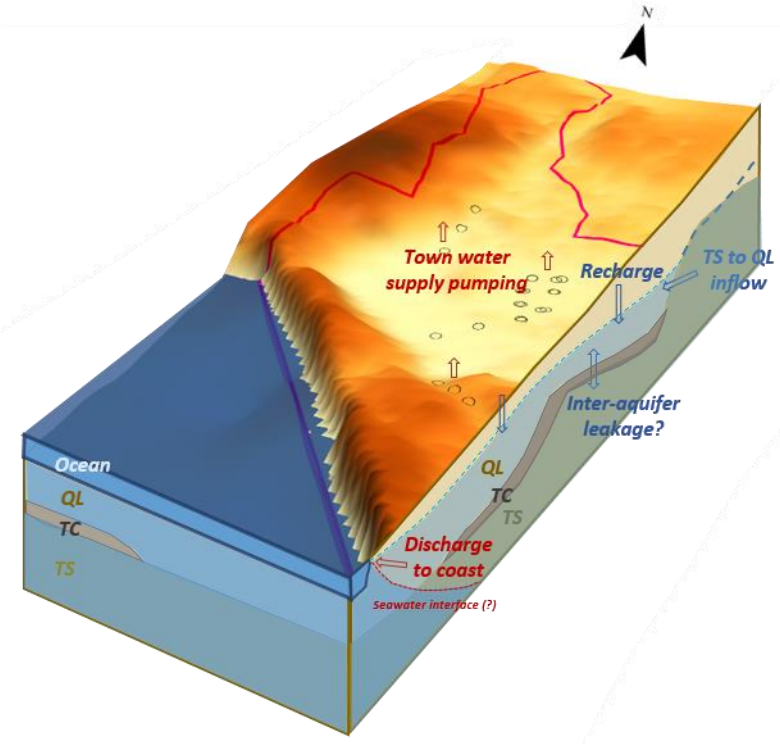


Figure 2.26. Conceptual model (not to scale) of groundwater flow processes in the Uley South Basin

2.7 Conceptual model uncertainty

The QL aquifer in the Uley South Basin is very responsive to changes in rainfall recharge and extraction, and this is represented in the ranges of values given in the water balance. However, these ranges are also due to uncertainty in some of the key processes. Areas of uncertainty include:

- Discharge to the coast: Previous estimates of groundwater discharge to the coast have been derived from analytical and numerical methods and show large variation. Estimates of discharge from numerical groundwater models in particular depend on modelled recharge rates and aquifer parameterisation. There are no field-based estimates of coastal discharge using methods such as seepage meters or chemistry (Burnett et al., 2006) and such methods would be difficult to apply in the high-energy coastal cliff environment of Uley South. Hence, in this study simulated rates of discharge to the coast will be a result from the model, rather than being used as a pre-determined flux to calibrate the model. To reduce uncertainty in modelled rates of groundwater discharge in future, it may be useful to further apply techniques such as NMR to improve confidence in coastal aquifer parameter values for modelling. Further analysis of the AEM data described by Fitzpatrick et al. (2009) may also be useful in determining the position of the seawater-freshwater interface and constraining modelled seawater interface results.
- Recharge variability and sinkhole location: Previous studies of recharge have produced a wide range of estimates. This is in part due to the variety of methods employed to estimate recharge, but also because recharge is spatially and temporally variable. For example, recharge is thought to be enhanced in areas where sinkholes are located. However, simulation of enhanced recharge through sinkholes can only be done where sinkholes have been surveyed.
- TS flow into QL: Flow from the TS aquifer into the QL in the northern part of the basin is conceptualised to occur based on variation in water chemistry in the QL aquifer. However, rates of inflow have not been quantified. Further work could be done, potentially with environmental tracers and mixing models to refine estimates of TS flow into the QL aquifer.
- Interaction between aquifers and sensitivity to vertical hydraulic conductivity: The TC is conceptualised as a leaky aquitard with low vertical hydraulic conductivity, which is absent in some areas in the Uley South Basin. Rates of inter-aquifer leakage are difficult to quantify because of similarity in water levels (Figure 2.13) and chemistry (Section 2.5.9) in both aquifers. Hence rates of inter-aquifer leakage have only been determined by numerical modelling studies, which depend on aquifer parameterisation. As with discharge to the coast, simulated inter-aquifer leakage will be a result of the model, rather than a flux which is used to calibrate it.
- Uncertainty in hydraulic parameters: In reviewing conceptual uncertainty, uncertainty in hydraulic parameters is evident, as it is with every model. Given the karst nature of the QL aquifer, it is unlikely this uncertainty can be significantly reduced; rather, efforts could be made to determine its impact on model results through further conceptual and parameter uncertainty analyses.

3 Previous groundwater models

The importance of groundwater resources in the Uley South Basin has led to several projects in the past which have simulated groundwater flow and pumping. This chapter provides a summary overview of previous groundwater models for the study area. Table 3.1 gives a summary of the parameters used in each model, while sections 3.1 to 3.7 briefly describe the models and their results.

3.1 Finite element groundwater model (1980)

The earliest groundwater modelling study of the Uley South Basin is a three–dimensional finite element model of the QL aquifer developed using the Aquifer Flow through Porous Media package by Golder Associates (Shepherd, 1980). The model was based on the conceptualization given by Barnett (1978). The model domain was discretised into 93 elements with 114 nodes.

The model simulated the impact of groundwater extraction at 1980 rates of 5 GL/y, as well as increases in pumping to rates of 7.5 GL/y, 10 GL/y and 12.6 GL/y. It was found that pumping 5 GL/y produced a 1 to 2 m decline in the water table in parts of the model domain. Increased pumping to 7.5 GL/y showed little change in the water table. However, further increases in pumping to 10 GL/y and 12 GL/y resulted in a significant loss of storage from the aquifer. The author recommended further investigations into the thickness of the QL aquifer, the potential for leakage through the Tertiary Clay unit, and the spatial variability of aquifer permeability.

3.2 One-layer MODFLOW model (2002)

A one-layer model of the QL aquifer in the Uley South Basin was constructed in 2002 by James–Smith and Brown (2002) using the MODFLOW code (Harbaugh, 2005). Its purpose was to collate existing data and assess the impact of various recharge and pumping scenarios on groundwater resources in the Basin. The model domain was based on the extent of saturated Quaternary Limestone sediments, and divided into 500 m by 500 m cells.

The north-western and south-eastern boundaries of the model were set as no-flow boundaries, while the coast was simulated as a constant head boundary, with a hydraulic head value of 0 m representing sea level. A small part of the north-eastern boundary was assigned a general head boundary to allow for groundwater inflow. James-Smith and Brown (2002) stated that understanding of recharge in this north-eastern part of the model domain was limited, and described the groundwater inflow at this boundary as representing either lateral groundwater inflow or enhanced recharge from surface run-off. Ten aquifer parameter zones were used to assign hydraulic conductivity and recharge was specified using a winter recharge period in the transient model (April to October) with a value of 225 mm/y for the main town water supply area of the basin, and 60 mm/y elsewhere (Table 3.1).

The transient model was run from 1977 to 2020, with extraction of 5.1 GL/y from 1977 to 2000, and 9.8 GL/y (the maximum capacity of all town water supply pumping wells) from 2000 to 2020. The model was calibrated by trial and error and reproduced a good match with measured groundwater levels. More importantly the model helped identify key uncertainties in the conceptual understanding of the Uley South Basin. In particular, the authors recommended further work to estimate recharge to the basin and to investigate aquifer properties in high hydraulic conductivity zones.

3.3 Spreadsheet water balance model (2006; 2009)

Harrington et al. (2006) developed a spreadsheet water balance model for groundwater in the Uley South Basin. The water balance calculated an annual change in storage based on groundwater inflows and outflows. The

inflows were recharge estimated from winter rainfall using the approach of Barnett (1978), groundwater inflow and leakage. The outflows were pumping extraction, leakage and groundwater discharge at boundaries. The change in storage (ΔS) given by the water balance was converted to a change in groundwater level (Δh) using:

$$\Delta h = \frac{\Delta S}{A_{US} \cdot S_y} \qquad (4)$$

Where A_{US} is the area of the Uley South Lens, and S_y is the specific yield of the Quaternary Limestone aquifer. Despite the relatively simple approach, the annual water balance model showed a reasonable match to measured groundwater levels at ULE114 (Figure 3.1). The model was used to simulate the impact of extracting 10GL/y and 20 GL/y. The simulations showed that extracting 10 GL/y resulted in groundwater level declining to within 2 to 4 m of the base of the aquifer, while extracting 20 GL/y resulted in groundwater levels declining beyond the base of the aquifer.

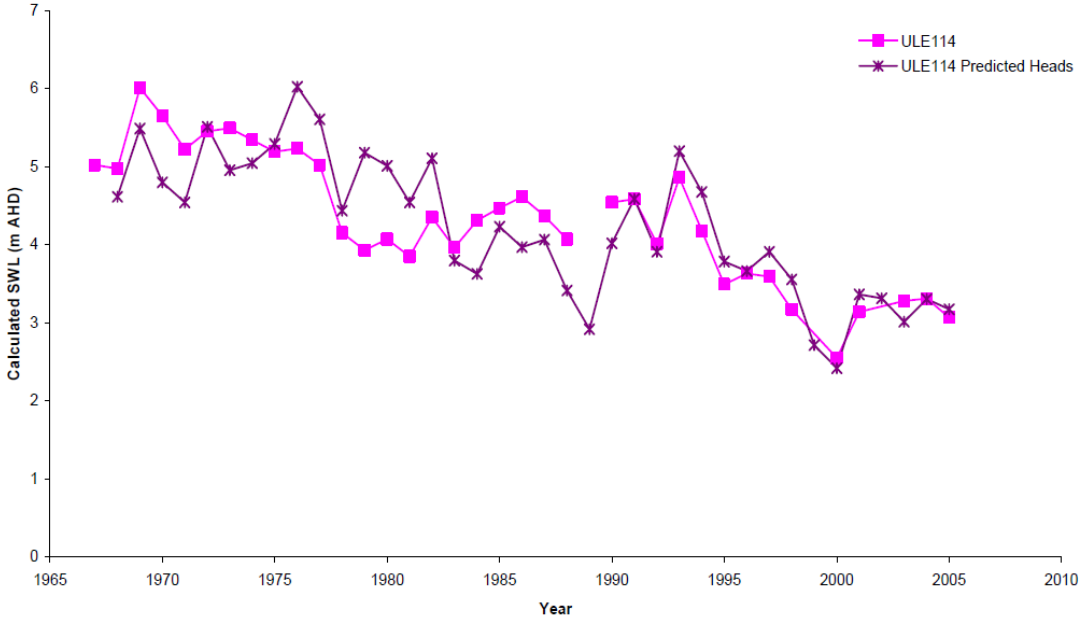


Figure 3.1. A modelled groundwater level hydrograph from Harrington et al. (2006) for observation well ULE114 (SWL = standing water level)

Alcoe (2009) further developed a transient water balance model for the Quaternary Limestone aquifer, calibrated to groundwater levels at six observation wells, for assessing volumetric fluxes in Uley South. The water balance approach calculated a change in aquifer storage at monthly time steps, based on the difference between aquifer inflows and outflows. Inflows included recharge (based on unsaturated zone modelling with the LEACHM code (Wagenet and Hutson, 1989)) and groundwater inflows from surrounding basins (based on Darcy's Law calculations). Outflows included groundwater pumping and discharge to the sea. The model of Alcoe (2009) also included a component of seawater intrusion (positive or negative), based on an analytical approximation of the coastal salt water interface toe location and salt-water wedge volume, and how it changes with time.

Calculated water levels were compared to measurements from six observation wells, and the model calibrated by varying specific yield (S_y, Equation 1) and horizontal hydraulic conductivity values (K_h) used in the groundwater inflow and coastal interface calculations. The model was able to simulate groundwater levels in Uley South quite well (Figure 3.2), with calibrated values of K_h ranging from 255 to 467 m/d, and S_y of 0.2 to 0.3 for the six wells.

The calibrated water balance fluxes showed that groundwater discharge to the sea had decreased proportionately from the 1980s to the 2000s, as groundwater pumping had increased. The model was further used to define a management 'trigger' level to prevent seawater intrusion. In this approach, the aim was to define a management

target/trigger level that identifies when the toe of the salt-water wedge may encroach more than 2100 m inland from the coast. The specific distance was based on the location of SA Water production bores 15, 16 and 17, situated 2100 m from the coast. Alcoe (2009) found that seawater encroachment could occur if groundwater levels fell below 1.27 to 1.29 m AHD at observation well ULE134 (one of the six wells used to calibrate the water balance model, located close to the coast). Hence a recommended management target to prevent seawater intrusion was maintaining groundwater levels above 1.29 m AHD at observation well ULE134.

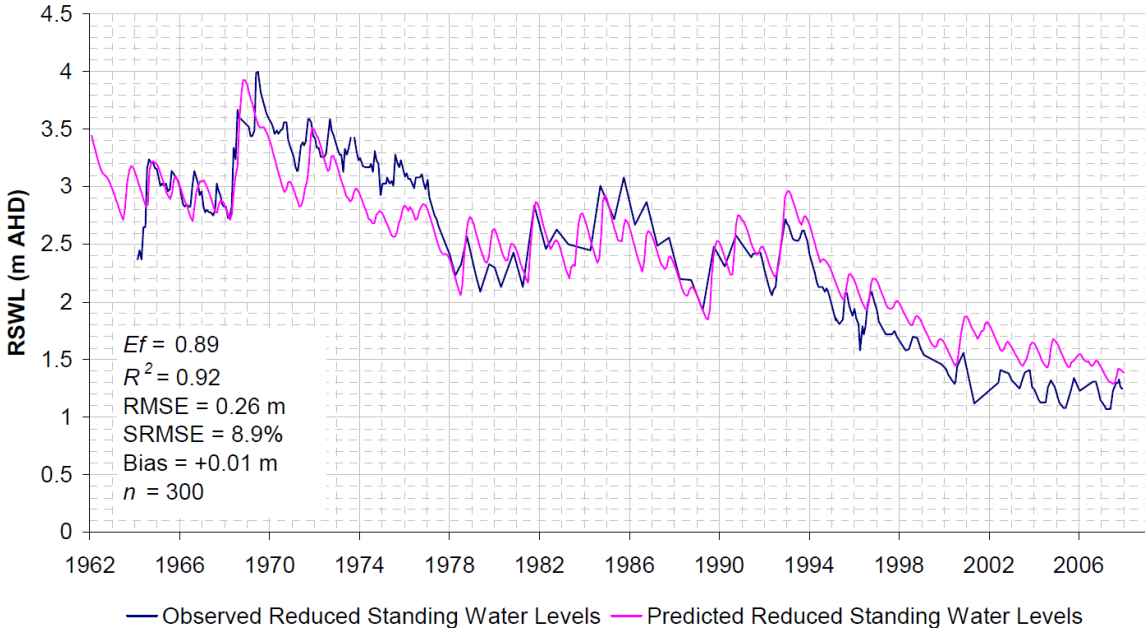


Figure 3.2. A modelled groundwater level hydrograph from Alcoe (2009) for observation well ULE134

The study of Alcoe (2009) gives an important 'first order approximation' of the risks and potential management approaches to seawater intrusion in Uley South. Alcoe recommended that the results could be compared to future numerical modelling of seawater intrusion processes, to identify when an analytical approach may be suitable for assessing management options.

3.4 Three-layer MODFLOW model (2007)

Following the spreadsheet modelling and conceptualisation work of Harrington et al. (2006), Zulfic et al. (2007) developed a three-layer numerical model of the Uley South, Uley Wanilla and Uley East lenses using the MODFLOW code. The three layers represented the QL, TC and TS formations, with flow from the Uley East and Uley Wanilla lenses to the Uley South lens occurring in the TC and TS layers. The model also simulated interaction between the three layers, with recharge to the TS occurring in the Uley East and Uley Wanilla lenses as downwards flow from the QL. Conversely in the Uley South Basin, the model simulated upwards leakage into the QL aquifer.

The transient model was calibrated for the 1949 to 2005 period, with scenarios run from 2005 to 2020. Scenarios differed by pumping rate and recharge. Pumping rates were: 7.5 GL/y (the rate at 2005), 8.5 GL/y or 10 GL/y. Recharge was 1990-2005 rates repeated or a 50% reduction in 1990-2005 recharge. While all scenarios predicted increased drawdown from increased pumping, recovery was observed in winter assuming the 1990-2005 recharge was repeated. However, when recharge was reduced by 50%, drawdown persisted with no winter recovery. The results highlighted the dynamic role of both pumping and recharge on groundwater levels in the Uley South Basin. The authors also made several important recommendations regarding further required work in areas such as inter-aquifer leakage, monitoring and modelling of the seawater-fresh water interface and measurement of evapotranspiration, which had not yet been studied.

3.5 Two and four-layer MODFLOW model (2010)

Following the AEM survey of Uley South (Fitzpatrick et al., 2009) and work by Alcoe (2009) and Ward et al. (2009), as well as preliminary research on recharge and evapotranspiration later documented in Ordens et al. (2012) and Swaffer (2014), a new model was developed to accommodate new conceptual understanding of the basin (Werner, 2010). Steady state and transient models were calibrated to observed data, and PEST (Doherty, 2010) was used to optimise parameter values in zones based on observed ranges. Steady state versions of the model were setup with four layers to simulate the QL, TC, TS and weathered basement. However, due to model run times and the calibration approach with PEST, the transient model was setup as a two-layer model representing the QL and TS formations, with the TC simulated implicitly with vertical hydraulic conductivity.

The model was used to run scenarios on future extraction and potential impact of climate change on reduced recharge. The model projected pumping at the average 2005–07 rate of 6.4 GL/y for 48 years from 2007. Two recharge scenarios were considered, one assuming average recharge and another assuming recharge decreases by 30%. Under the reduced recharge scenario, groundwater levels continued to decline. Werner (2010) also made many recommendations, such as re-interpretation of the AEM data collected by Fitzpatrick et al. (2009) to accommodate knowledge gained from additional drilling and to confirm the location of dry QL areas that became apparent during modelling. Further recommendations included more analysis of metered pumping data, improved conceptualisation of groundwater processes in the north-west of the basin, and conversion of the model to a seawater intrusion model.

3.6 MODHMS seawater intrusion model (2013)

Following the recommendations of Werner (2010), Werner and Dang (2013) developed a three-dimensional seawater intrusion model of Uley South using MODHMS. An 11-layer model was developed and calibrated to groundwater levels from 1960–2007. The simulated extent of seawater intrusion showed good agreement with salinity depth profiles in wells (SLE069 and ULE205) as well as the spatial location of interpreted seawater from Fitzpatrick et al. (2009, see Figure 2.6, Figure 3.3). The results also demonstrated the influence of complex coastal geology on the extent of seawater intrusion, with the basement outcrops at the coast essentially dividing the basin into two sections where seawater intrusion may occur (Figure 3.3).

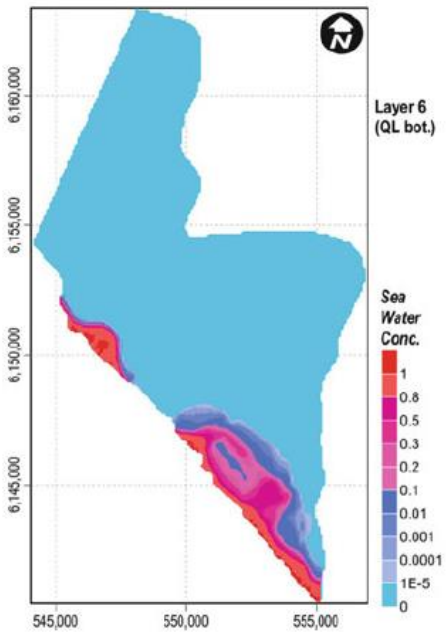


Figure 3.3. Simulated extent of seawater intrusion in the bottom of the QL aquifer in 2007 (from Werner and Dang, 2013)

Simulated transient salinity trends in observation wells showed that the seawater interface had shifted position over time in response to recharge and pumping, with a general increasing trend from the mid-1990s to 2007 (Figure 3.4 where the orange line is from the model using time-averaged recharge and the blue line is using seasonally-variable recharge). Werner and Dang also noted variable salinity trends at the end of the simulation, when groundwater levels were stable, demonstrating that salinity had not reached equilibrium in the basin. Werner and Dang simulated the potential for seawater intrusion to 'reverse' by running a scenario for 48 years from 2007 with no pumping. The results showed that high salinity contours retreated to pre-development levels. However, a dispersed plume of lower concentration seawater remained in the aquifer. Based on this, Werner and Dang concluded that further seawater intrusion should ideally be avoided, rather than treated as a problem that can be remediated.

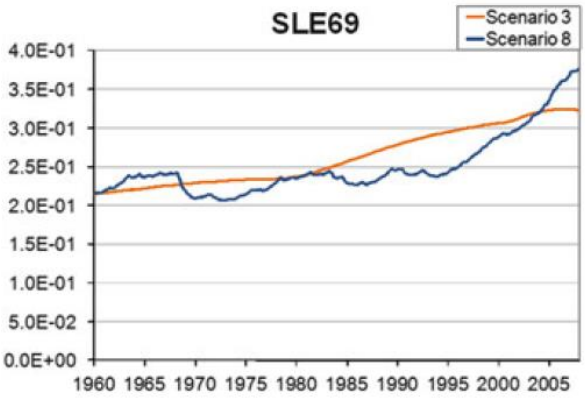


Figure 3.4. Simulated salinographs (fraction of seawater concentration) in SLE069 from Werner and Dang, 2013

3.7 Two-layer highly parameterised MODFLOW model (2015)

Uncertainty in the relative impact of climate and pumping on groundwater resource condition in the Uley South Basin was raised by a Natural Resources Committee investigation into water resources on Eyre Peninsula (Natural Resources Commission, 2013). Consequently Knowling et al. (2015) developed a two-layer numerical flow model of the Uley South Basin, with the TC simulated implicitly by varying vertical hydraulic conductivity. Model layer elevations were based on the AEM data described by Fitzpatrick et al. (2009) as well as drill logs and geological descriptions of the coastal cliffs (Bestland, 2010). Transient recharge was based on the modelling of Ordens (2014). Steady state and transient (1960–2012) models were calibrated using the pilot point method with parameter estimation software PEST (Doherty, 2010). The pilot point approach yielded spatially variable estimates of hydraulic conductivity and specific yield in the QL aquifer, with values of up to 10,000 m/d and 0.41 respectively.

The transient model yielded new insight into groundwater flow in the QL aquifer, showing further areas likely to be dry due to high basement elevations (Figure 3.5). The model also showed a likely disconnect between saturated QL in the north–west and saturated QL in the main town water supply area, with separation due to high basement areas previously identified as above the water table by Fitzpatrick et al. (2009) (Figure 2.6, Figure 3.5).

Knowling et al. (2015) used the transient model to assess relative pumping and climate impacts by running the model with and without town water supply pumping from 1976–2012. It was concluded that pumping contributed to aquifer depletion 1.4 to 2.9 times more than climate. A linear uncertainty analysis was conducted, which showed that the impact of model uncertainty was less than the impact of pumping or climate on simulated groundwater levels, which improves confidence in the model results.

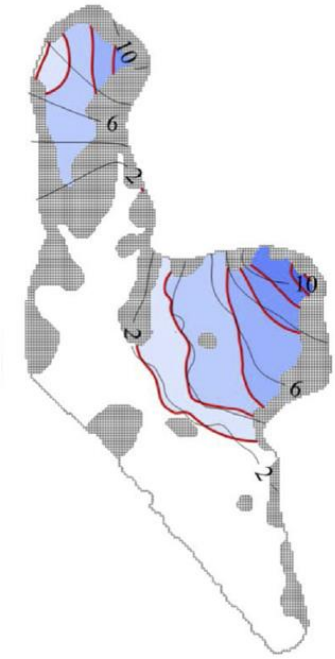


Figure 3.5. Simulated (red lines) and observed (black lines) contemporary (2005–2009) QL groundwater levels in Uley South Basin

3.8 SEAWAT model (2017)

Badaruddin (2017) developed the model of Knowling et al. (2015) into a seawater intrusion model with SEAWAT (Langevin et al., 2008), to assess the relative impact of climate and pumping on movement of the seawater interface. The model was divided into 10 layers, and the QL treated as a confined aquifer to avoid dry cell issues with SEAWAT. The model was used to simulate the transient movement of the seawater interface from 1960–2012 under conditions of both historical pumping and no pumping. The results showed that pumping increased the inland extent of seawater intrusion in the QL aquifer by 5.8 times compared to climate (Figure 3.6). From the perspective of total salt mass in the aquifer, pumping resulted in 2.4 times the amount of salt coming into the aquifer from seawater intrusion compared to impacts from climate.

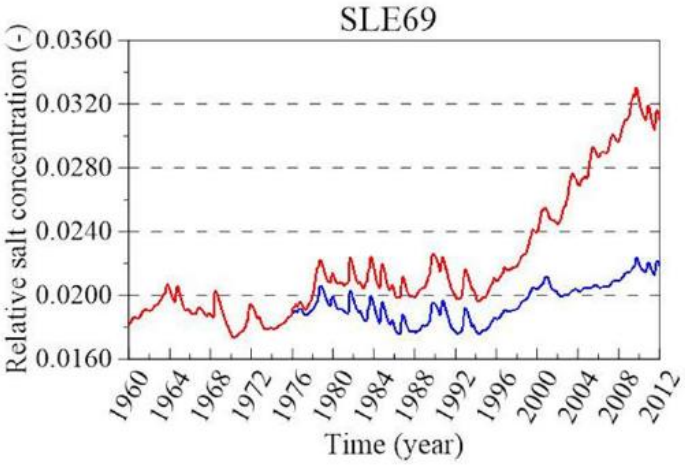


Figure 3.6. Simulated salt content at SLE069 assuming no pumping (blue line) and actual pumping (red line) from TWS wells (Badaruddin, 2017)

3.9 Summary of previous models

The models described in this section of the report provide a wealth of information on groundwater flow processes in the Uley South Basin. The models also plot the development of conceptual understanding in the basin over time, and how recommendations from modelling studies have guided ongoing investigations. They demonstrate that pumping strongly influences both groundwater levels and seawater intrusion, and that future scenarios are dependent upon both pumping and climate change assumptions. Parameter sets associated with these models (Table 3.1) provide an invaluable guide to any further modelling of the Basin.

The conceptual model of the basin has not changed significantly since the modelling of Knowling et al. (2015). However, additional data sets are available including aquifer parameters from pump tests and geophysics, new drilling information including areas where the QL is dry and basement is encountered, new survey elevations on some wells and geophysical and survey information on the location of sinkholes. With this new data available, SA Water commissioned the construction of a new groundwater flow model.

Table 3.1. Summary of parameter values used in previous groundwater models of the Uley South Basin

Parameter values	Shepherd (1980)	James–Smith and Brown (2002)	Harrington et al. (2006)	Zulfic et al. (2007)	Alcoe (2009)	Werner (2010)	Werner and Dang (2013)	Knowling et al. (2015)
Horizontal hydraulic conductivity QL (m/d)	200 to 600	30 to 2000	Not cited	5 to 1500	255 to 467	4.2 to 1100	2 to 910	2 to 10,000
Horizontal and vertical hydraulic conductivity TC (m/d)	-	-	-	$4.8x10^{-3}$ to 10 (horizontal) $4.8x10^{-5}$ to 5 (vertical)	-	1.4×10^{-2} (vertical)	0.1 to 2 (horizontal)	Modelled implicitly with a vertical conductivity varying from $10^{-3.6}$ to 1
Horizontal hydraulic conductivity TS (m/d)	-	-	-	0.01 to 150	-	1 to 13	1 to 8.9	0.1 to 1320
Specific yield QL	0.3	0.1	0.15	0.2 to 0.3	0.2 to 0.3	0.15 to 0.33	0.15 to 0.32	0.007 to 0.41
Specific storage TS (m^{-1})	-	-	-	10^{-3} to 10^{-4}	-	$2.9x10^{-6}$	$3x10^{-6}$	$2.4x10^{-6}$ to $3.2x10^{-6}$
Recharge (mm/y)	106	225 (TWS area) 60 (rest of basin)	61 to 338	Average = 100	Average = 160 (1960 to 2007); 122 (1993 to 2007)	Average from 1960 to 2007 ranges from 132 to 159	112	Average = 84 (range from 0 to 240)
Model type	Finite element (114 nodes)	MODFLOW based numerical model (cells 500m x 500m)	Spreadsheet based analytical model	MODFLOW based numerical model (cells 500m x 500m, 115m x 125m in places)	Spreadsheet based analytical model	MODFLOW based numerical model (cells 100m x 100m)	MODHMS based flow and seawater intrusion model (based on Werner 2010).	MODFLOW based numerical model (cells 100m x 100m)

4 Model construction

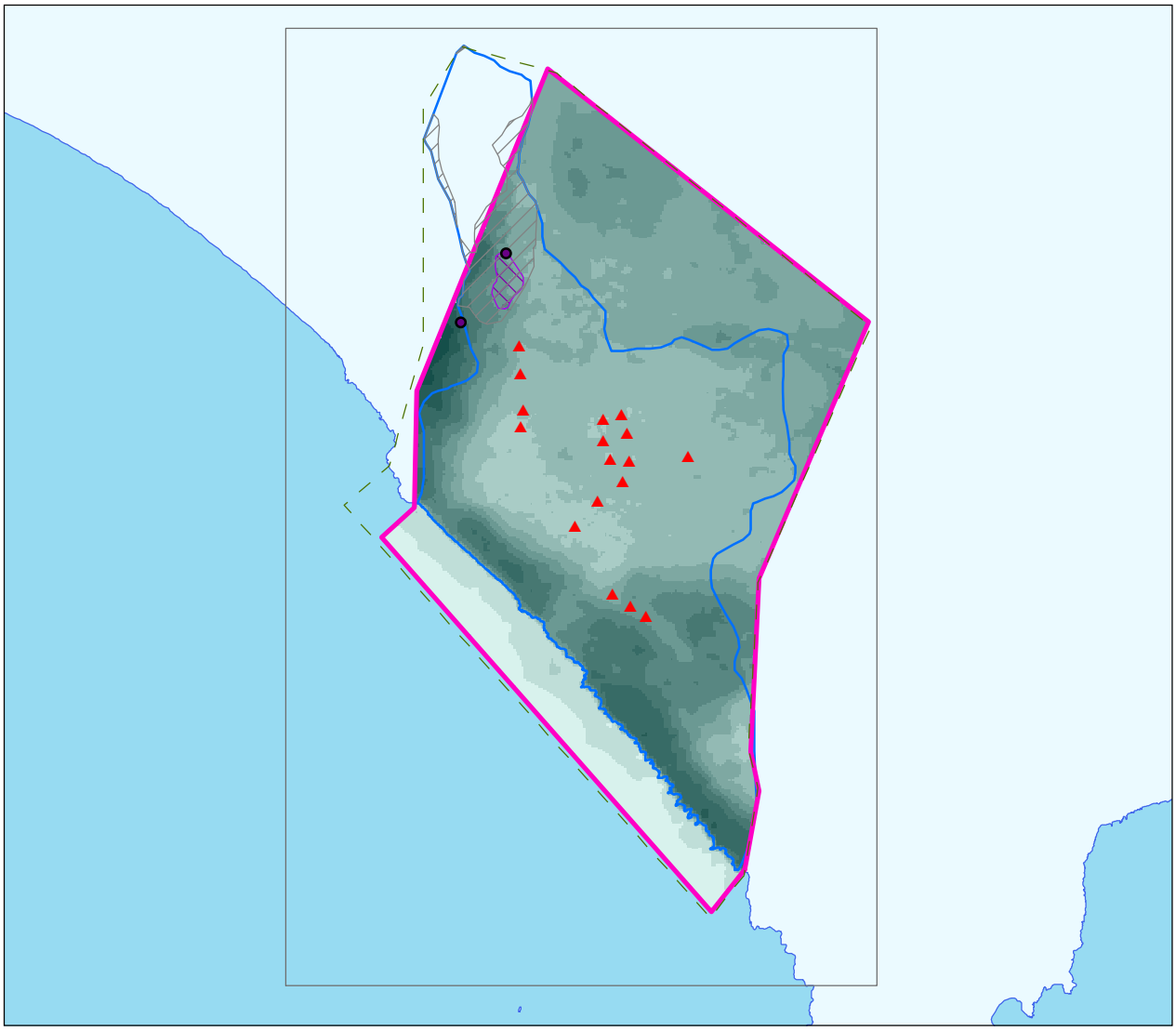
4.1 Model approach, platform, domain and grid

The main focus of this study is groundwater resources in the QL aquifer in Uley South Basin, as described in Section 2. A multi-model approach is taken, in which two domains were constructed to accommodate conceptual uncertainty in flow from the TS to QL aquifer (Section 4.2.3), and each of these models is calibrated with three different sets of recharge values (Section 4.4), resulting in six models in total (Table 4.2).

The model is constructed in MODFLOW 2005 (Harbaugh, 2005) using the Groundwater Vistas software interface (Rumbaugh and Rumbaugh, 2017). MODFLOW 2005 is used as it is compatible with the SWI2 package (Bakker et al., 2013) in Groundwater Vistas, which is used to simulate movement of the seawater-freshwater interface at the coast (discussed further in section 4.3.2).

The model domain covers the QL and TS areas which influence the TWS wells and the coast. As discussed in Section 2.6, flow in the QL aquifer may be supplemented by flow from the TS aquifer to the north, hence the model domain extends north of the saturated QL aquifer to where the water table is in the TS aquifer. A preliminary model domain covered the full saturated extent of the QL aquifer. However, drilling conducted during this study found dry QL in the north-west of the basin, in the vicinity of the dry QL area mapped by Fitzpatrick et al. (2009) and the area simulated as dry (QL aquifer) by Knowling et al. (2015) (Figure 4.1). Furthermore, mass balance analysis during model calibration showed that this north-west part of the basin was not impacting significantly on the mass balance of the QL or TS in the rest of the domain. Hence to reduce model size and run times for the SWI2 simulations, the domain was reduced to cover the main saturated extent of the QL aquifer and TS aquifer to the north (Figure 4.1). This domain matches early delineations of the basin by Morton and Steel (1968). The domain also extends offshore by 2 km, so that the coastal boundary may be simulated using the SWI2 package (Bakker et al., 2013).

The origin coordinate for the grid (the south-western corner of the domain) is E542174 N6137200, and the grid at its maximum is 16.68 km in width (east-west) and 26.98 km in length (north-south). Grid cells are 60 m x 60 m, and the model consists of three layers. However, model cells are inactive outside the domain area (Figure 4.1). Within each layer there are also inactive cells, relating to dry QL areas in Layer 1, and areas where the TS aquifer is absent in Layer 3. Thus, the model domain consists of 118,490 or 127,651 active cells, depending on the conceptualisation of the flow between the TS and QL aquifers.



Dry QL wells (June 2018)
QL dry (Fitzpatrick et al., 2009)
North-west QL dry (Knowling et al., 2015)
Domain_square
Preliminary domain
Final model domain
Uley South Basin
SA Water suply wells

N

0 2 4 6
Kilometres

Top elevation (m AHD)

-33 to -11
-11 to 0
0 to 11
11 to 33
33 to 55
55 to 77
77 to 99
99 to 121
121 to 143
143 to 165
165 to 187



Figure 4.1 Model domain and top elevation of Layer 1

4.2 Model layer elevations

4.2.1 Surface elevation

Surface elevation for the land-based part of the domain is based on Shuttle Radar Tomography Mission (SRTM) 1 Arc-Second Global elevation data, developed by the National Aeronautics and Space Administration (NASA) and National Geospatial-Intelligence Agency, and accessed via the United States Geological Survey, 2017). The SRTM elevation data has a horizontal resolution of 30 m and a vertical resolution of <16m. The Advanced Spaceborne Thermal Emission and Reflection Radiometer (ASTER) digital elevation model, developed by the Ministry of Economy, Trade and Industry of Japan and NASA (JPL, 2017), was also assessed for use in the model. However, the SRTM elevation data showed overall better correlation with existing ground level elevations based on surveyed data at 126 groundwater wells in Uley South (root mean squared error 5.15 m) compared to the ASTER data (root mean squared error 7.63 m) (Figure 4.2). Note there is still some error between satellite-based surface elevations and bore elevations. However, given that evapotranspiration is not thought to be a significant part of the groundwater balance (Knowling et al., 2015), the error is not considered significant. If more refined surface elevation data becomes available in the future, then it is recommended that it be re-incorporated in the model.

The model domain extends offshore, and sea floor elevations are based on the Australian bathymetry and topography grid, June 2009 (Huang et al. 2013; Geoscience Australia, 2017). The Australian bathymetry grid has a horizontal resolution of 250 m, while the model has a cell size of 60 m, and many bathymetry cells along the coast overlap both ocean and land, picking up high elevation values from the coastal cliffs in Uley South. To avoid having model cells assigned erroneously high elevations offshore, all bathymetry cells with elevations above sea level (> 0 m AHD) that overlapped the coast were deleted from the bathymetry data set. Contact points were then created at the base of the cliff, with elevations equal to sea level (0 m AHD). Following this, the SRTM ground surface elevation, manually-created sea level contact points, and the bathymetry grid were blended by interpolation with kriging, to create a continuous surface elevation grid for the entire onshore and offshore domain (Figure 4.1).

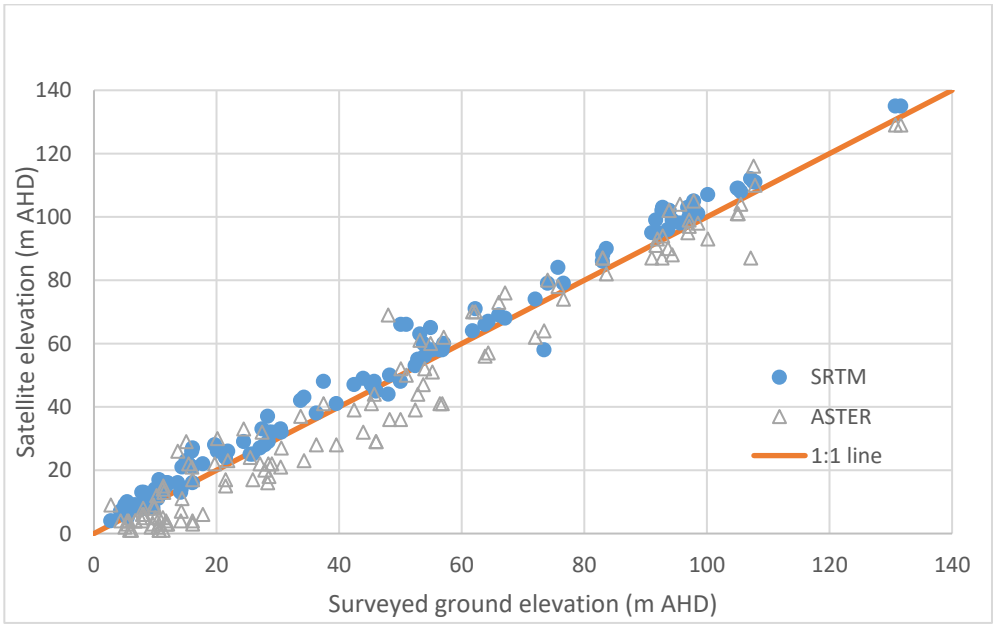


Figure 4.2. Correlation between satellite-based digital elevation model products ASTER and SRTM

4.2.2 Aquifer layer elevations

The elevations of aquifer layers are based primarily on drillhole data. Geophysical data, in particular the AEM data described by Fitzpatrick et al. (2009), was used to constrain layer elevations along the western boundary of the basin, after drilling in July 2018 confirmed the presence of dry limestone and shallow basement (Figure 4.1).

4.2.3 Layering to simulate connection between TS and QL layers

Groundwater flow from the TS into the QL formation is conceptualised to occur where the two units are in contact along the northern, inland boundary of the Uley South lens, where the TC is absent (Figure 2.5). This inflow has previously been simulated as upwards leakage from the TS into the QL model layer where the TC is absent (Zulfic et al., 2007; Werner, 2010). However, based on the conceptualisation of Somaratne et al. (2018) which used geophysics to identify further areas where the TC is absent, SA Water proposed the process could be simulated as horizontal inflow in areas where the TC is absent.

In order to deal with conceptual uncertainty regarding the flow of water from the TS into QL in the northern part of the basin, two models were set up. The inclusion of multiple models is considered useful in engaging stakeholders and informing decision making (Ferré, 2017). The first model (herein model version 1) follows the conceptualisation of Zulfic et al. (2007), where flux between the QL and underlying layers is vertical. It simulates the basin as a three-layer system, with all layer elevations based on drillhole data and geophysics. In the middle layer, zones of higher horizontal and vertical hydraulic conductivity (K_h and K_v) represent areas where the TC is absent, and thus connection with the other layers is vertical.

The second model (herein model version 2) follows the conceptualisation of Somaratne et al. (2018). Layer 1 simulates both the QL aquifer in the Uley South Basin area and the TS aquifer in the north. The bottom elevation of Layer 1 in this second model is lowered so that it remains saturated in the north, so that flow from TS to QL occurs directly through Layer 1 (Figure 4.3). Thus, in this second version of the model, the TS is simulated as an unconfined aquifer in the northern part of the domain, which connects directly to the QL. This conceptualisation may be accurate for some parts of the northern TS area, where variably unconfined and confined conditions are present (Table 2.1). It should be emphasized though that the TS is not exclusively unconfined in this area; hence it may not be an exclusively accurate representation of connection between the TS and QL.

An alternative to simulating flow from the TS into the QL in the model would be to connect flow between the layers using MODFLOW-USG (Panday et al. 2013). However, at the time of writing, the software package used (Groundwater Vistas) did not support the SWI2 package with the MODFLOW-USG version of MODFLOW; hence MODFLOW-2005 was used instead of MODFLOW-USG. Furthermore, early examples of density-dependent modelling with MODFLOW-USG demonstrate potential difficulties with model convergence (Panday at al. 2017); hence a simplified approach to simulating coastal processes with SWI2 was adopted.

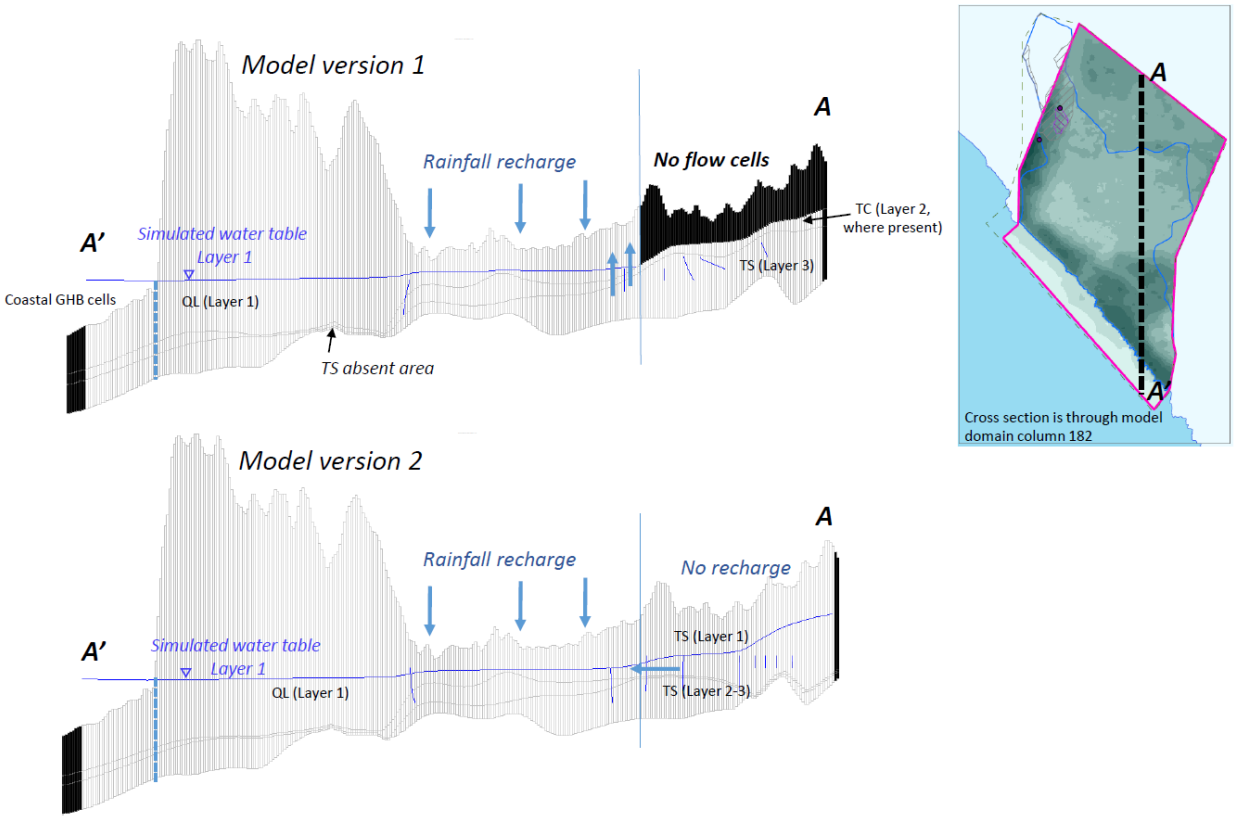
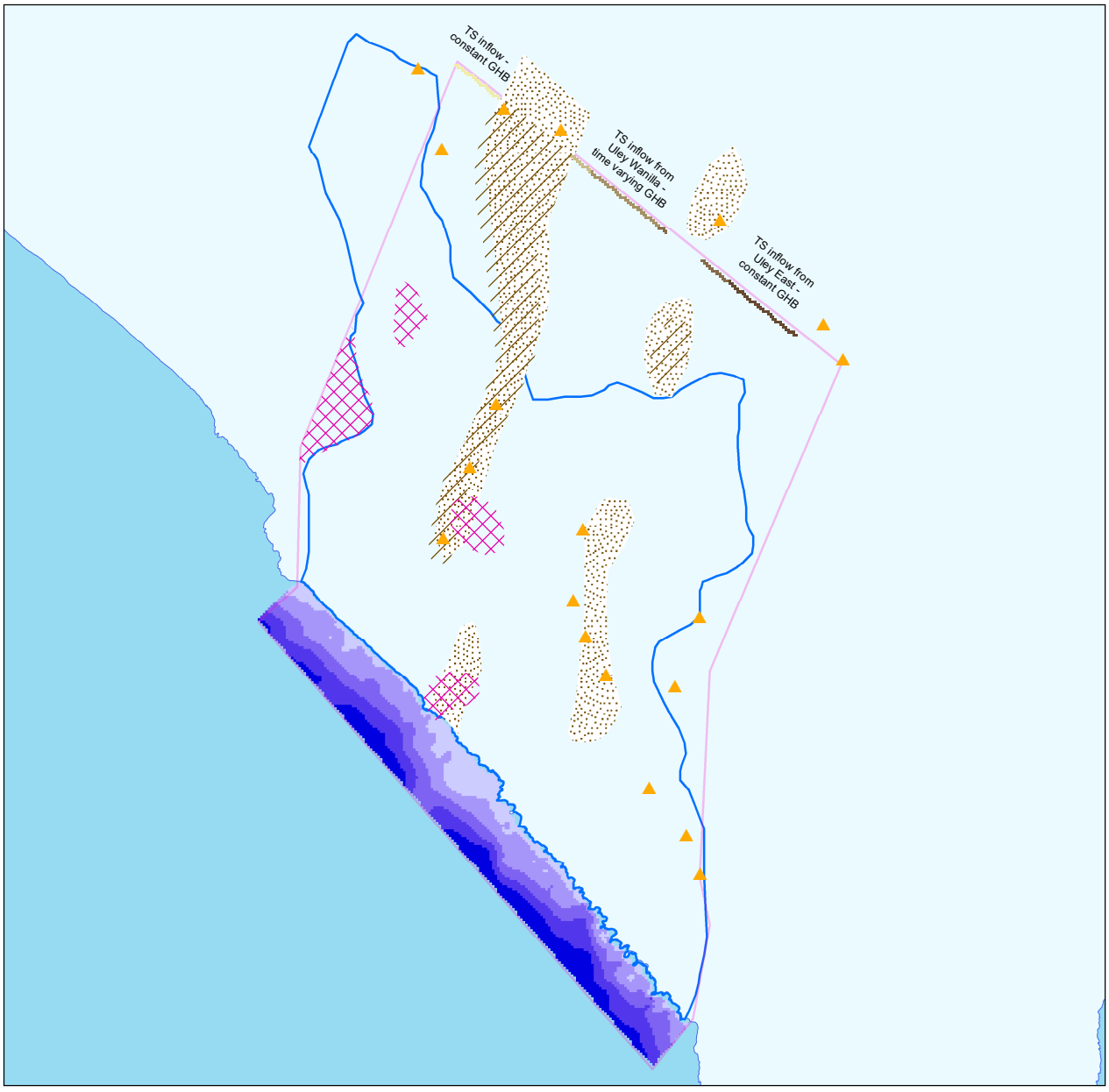


Figure 4.3. Cross section of model grid for model versions 1 and 2

4.3 Domain boundary conditions

4.3.1 Northern boundary

The northern boundary of the model represents the region where only the TS aquifer is saturated. Groundwater levels in the TS aquifer both inside and outside the domain vary along this boundary. In the north-eastern part of the domain, groundwater levels are generally stable (Figure 2.11) and, as discussed in Section 2.5.5, are likely fed by groundwater inflow from the Big Swamp area in the Uley East lens. However, in the central part of the domain, groundwater levels in the TS have declined since the mid-1980s, influenced by declining trends in the Uley Wanilla lens (see Section 2.5.5). The boundary for flow into the TS aquifer is thus assigned as a head dependent flux boundary using the MODFLOW General Head Boundary (GHB) package (Harbaugh, 2005). The boundary is divided into sections, separated by areas where the TS is absent (Figure 4.4). The central GHB (flow from Uley Wanilla) is set as a time-varying GHB, with a trend based on groundwater levels in ULE175 (Figure 4.5). Elsewhere the GHB values are constant in time, with head values based on the potentiometric surface of the TS (Figure 4.4). Boundary conductance values are calculated based on aquifer conductivity and thickness along the northern boundary, varying from 80 to 140 m^2/d. In model version 1, this boundary applies to Layer 3 only, while in model version 2, the boundary applies to all layers, as Layers 1 and 2 also simulate the TS aquifer in the north.



GHB cells coastal (m AHD)

- 0 - 0.10
- 0.10 - 0.25
- 0.25 - 0.40
- 0.40 - 0.55
- 0.55 - 0.76

GHB cells TS inflow (m AHD)

- 24.76 - 27.84
- 27.84 - 30.92
- 30.92 - 34.00
- 34.00 - 37.08
- 37.08 - 40.16

N

0 1.5 3 4.5

Kilometres

- No flow cells (basement)
- No flow cells (TS absent)
- TS absent (Harrington et al., 2006)
- Model domain
- QL saturated
- TS absent



Figure 4.4 Model boundary conditions and no flow cells

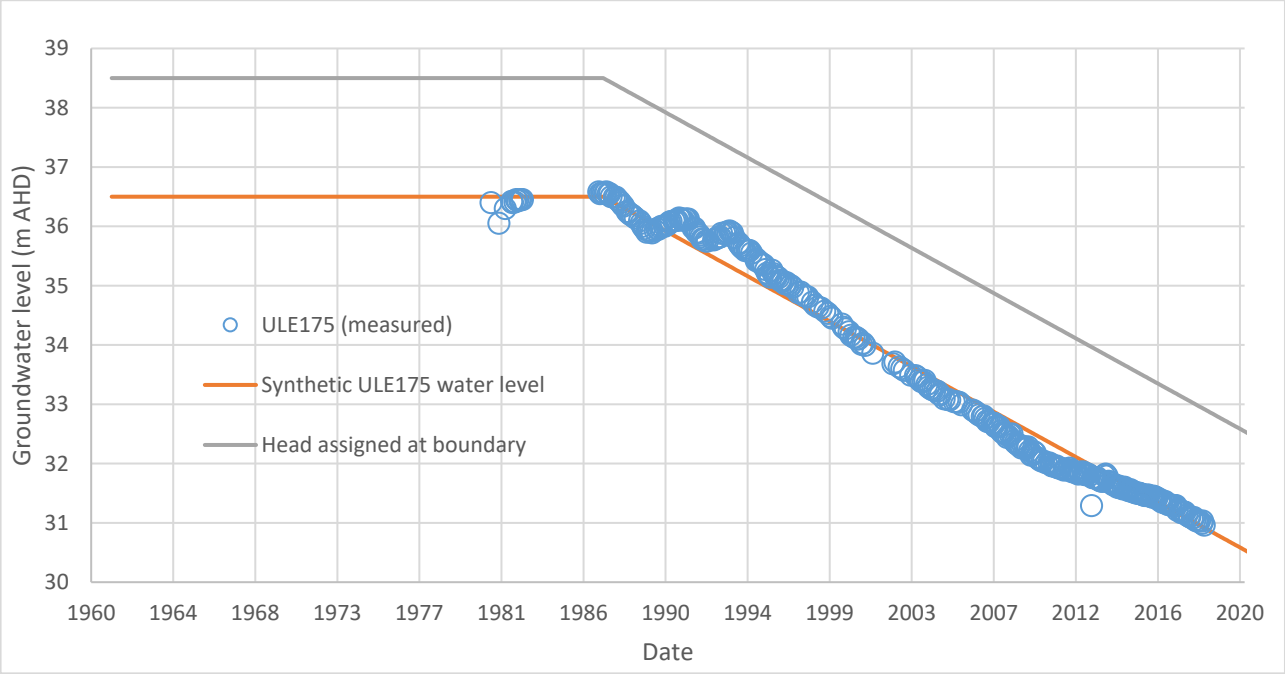


Figure 4.5. Groundwater levels in ULE175 and water levels assigned to simulate flow from Uley Wanilla

4.3.2 Coastal boundary

The coastal boundary is simulated using the Seawater Intrusion 2 (SWI2) package in MODFLOW2005. The SWI2 package allows for variable-density flow to be simulated with a 'sharp interface' between freshwater and seawater, rather than a dispersed mixing zone (Bakker et al., 2013). Diffusion and dispersion are not simulated with SWI2, and aquifers can be simulated with one layer, which makes SWI2 computationally more efficient than other density-dependent codes such as SEAWAT and SUTRA, while yielding results which are comparable to SEAWAT (Dausman et al., 2010). The SWI2 package has been used in regional groundwater modelling studies to investigate a diverse range of processes such as risks to coastal groundwater lenses in sand dunes (Kok et al., 2010); upconing of high salinity groundwater in inland supply fields (Luedeling et al., 2015); optimisation of well location for desalination (Baalousha, 2016); the impact of groundwater development on freshwater lenses under islands (Rotzoll et al., 2016); and the impact of sea level rise on seawater intrusion in coastal aquifers (Walter et al., 2016; Hughes & White, 2016; Fiore et al., 2018).

The SWI2 package was implemented following recommendations in Bakker et al. (2013). The domain is extended offshore by 2 km, so that the 'tip' cell of the seawater interface is not at the edge of the model domain. Model cells located offshore were set as head-dependent flux boundaries using the MODLFOW GHB package. The head values in these cells represent offshore equivalent freshwater heads at the ocean bottom (Bakker et al., 2013; Figure 4.4). The heads are constant in time, without tidal and seasonal variations in sea level. Dimensionless densities for freshwater and seawater are set at 0 and 0.025 respectively. The simulated interface approximates the 50% freshwater-seawater contour.

The slope for cells at the tip and toe of the interface (where the interface intersects the top and bottom of a model layer respectively) are based on recommendations in Bakker et al. (2013), who suggests assigning a value based on the coastal hydraulic gradient divided by the dimensionless density difference. Here we use a gradient of 0.0001 (1 m head change per 1000 m) to derive a slope of 0.04. However, the gradient close to the coast may vary across the Uley South Basin; hence the sensitivity of simulated interface to tip/toe slope parameters was tested using values of 0.03 (gradient of 1/1300) and 0.05 (gradient of 1/800), with results presented in Appendix B.

Conductance is set at 200 m^2/d across the coastal boundary. While a higher conductance may be anticipated for the QL aquifer due to high hydraulic conductivity, Bakker et al. (2013) note that instabilities with SWI2 may occur with large boundary conductance values. Furthermore, previous examples of the use of SWI2 have assigned

coastal boundary conductance using a trial and error approach to achieve a good match to expected interface elevation (Walter et al., 2016). Early calibration work on the model suggested coastal aquifer conductivities were generally lower than inland areas, and coastal boundary conductance values ranging from 50 to 200 m^2/d were tested, with no noticeable impact on SWI2 results. Hence conductance of 200 m^2/d is used, while acknowledging that coastal QL conductivity is an area of uncertainty that may require further investigation in the future. Other parameters are set at the defaults suggested by Bakker et al. (2013) (Table 4.1).

Table 4.1. Parameters used in the SWI2 package

Parameter	Value	Units
Maximum slope of toe cells (TOESLOPE)	0.04	(m/m)
Maximum slope of tip cells (TIPSLOPE)	0.04	(m/m)
Dimensionless density of freshwater	0	-
Dimensionless density of seawater	0.025	-
Density distribution options (ISTRAT)	1	
Number of surfaces (NPLN)	1	-
Fraction to move to an empty cell (ALPHA)	0.1	-
Fraction to move to non-empty cell (BETA)	0.1	-
Conductance of coastal GHB cells	200	m^2/d

4.3.3 Inactive cells

Inactive cells were added to areas where basement outcrops at the coast, and where the central part of the QL is dry (see Figure 4.4, Knowling et al., 2015 also simulated this area as dry). Inactive cells were further added in some of the locations where the TS aquifer is mapped as absent. However, there is an absence of lithology information in some areas (Figure 4.4), for example through the central part of the basin, and in the north in between the inflow boundaries from Uley East and Uley Wanilla. Initial simulations showed the TC layer was likely to be dry in areas where the TS has been mapped as absent outside of the QL saturated area, hence these areas were also assigned as inactive in layer 2 (see Figure 4.9 showing TC property distribution). In the central-eastern part of the domain, where the TS aquifer has been mapped as absent, inactive cells were not assigned, as layer elevation in this area is constrained by more drillhole information. In this area, part of the TS aquifer pinches out to become insignificantly thick, and has not been assigned as inactive (Figure 4.3, Figure 4.4).

4.4 Groundwater recharge and evapotranspiration

As discussed in section 2.5.5, numerous studies have investigated recharge to the QL aquifer in the Uley South Basin, and estimated rates range from less than 25 to more than 240 mm/y (Table 2.2). The methods used to estimate recharge include those based on sampling at points in time (e.g. chloride mass balance or CFCs) and those that provide transient/yearly estimates of recharge (e.g. the water table fluctuation method and unsaturated zone modelling). Given that groundwater levels are responsive to annual rainfall and recharge, transient estimates of recharge are used in the model, based on the water table fluctuation method.

Groundwater level observations from eight wells (Figure 4.6) have been used to estimate annual recharge from 1961–2017. At each well, the annual recharge is calculated via Equation 1, where Δh is the difference between annual maximum and minimum groundwater levels (Crosbie et al., 2015), Δt is 1 year, and S_y is 0.25 (based on the

modelled S_y typically ranging from 0.15 to 0.4, Table 3.1). This approach yielded recharge rates ranging from 3 to 323 mm/y; however, the maximum recharge rates only occur in 1968, when the highest rainfall for the Eyre Peninsula was recorded (Figure 2.2). High recharge is also estimated in ULE102 in 1964; however, in other years recharge rarely exceeds 240 mm/y, consistent with the range reported by previous studies (Table 2.2). The long term (1961–2017) average recharge estimate using this approach is 61 mm/y. However, after recharge was zoned according to vegetation type, preliminary transient model runs showed recharge was likely to be higher; hence the maximum recharge rate from all eight wells was used each year, giving a long-term average recharge estimate of 102 mm/y.

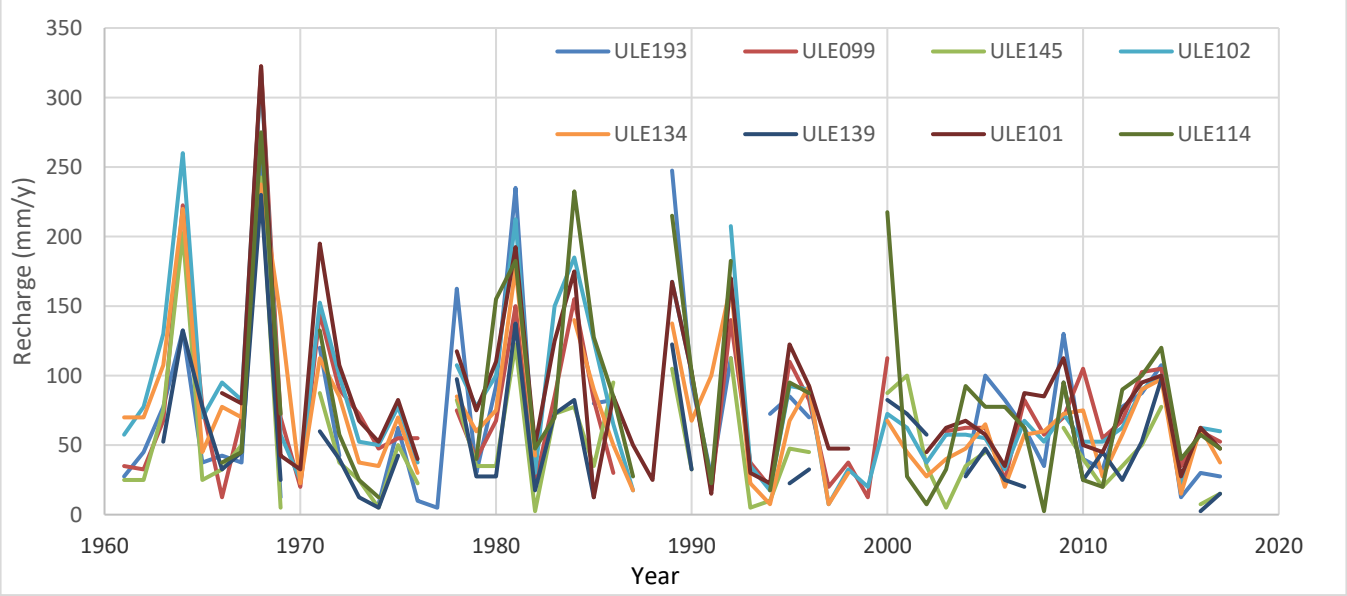
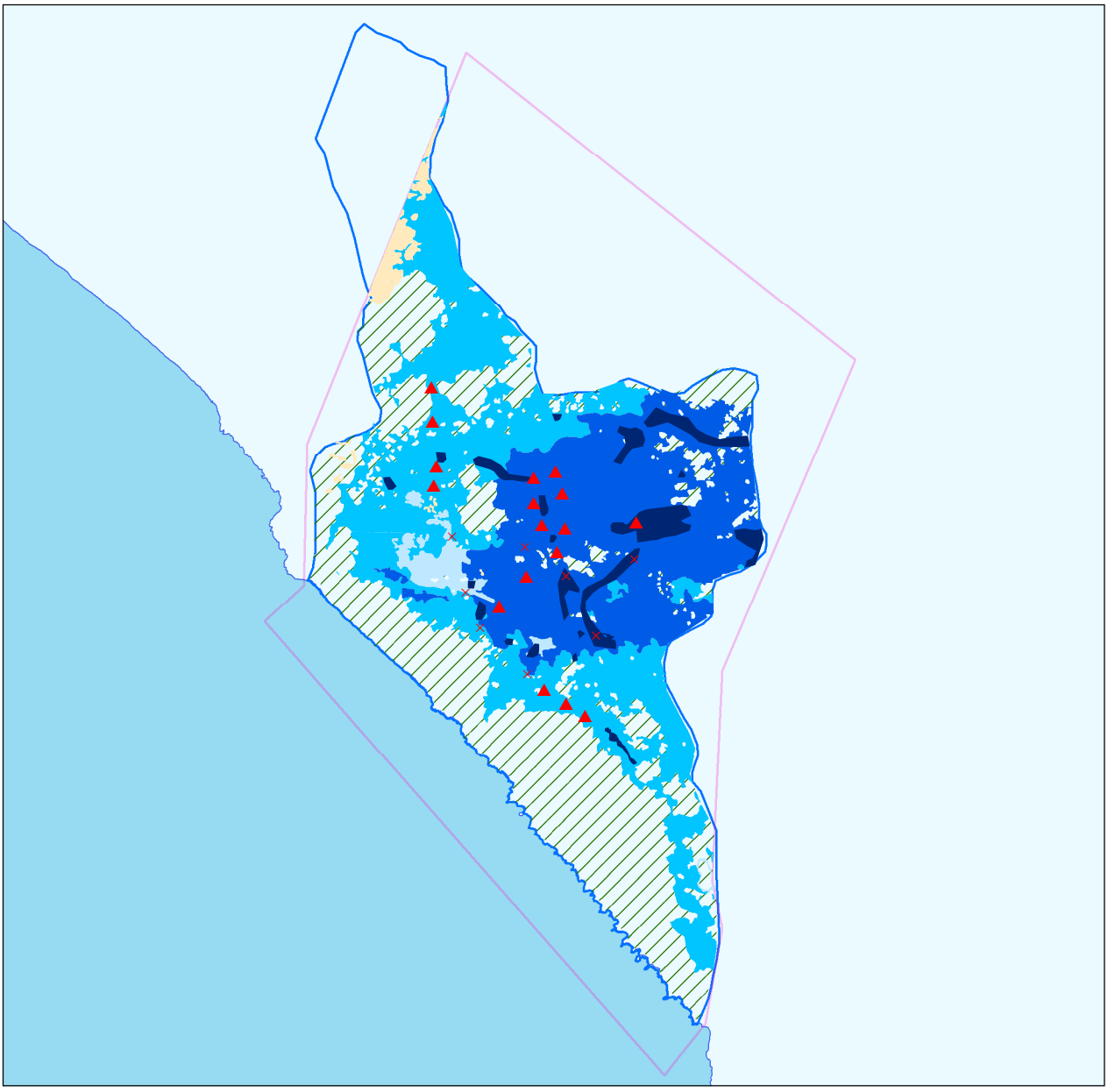


Figure 4.6. Transient recharge estimates from eight wells using the water table fluctuation method (gaps in the time series reflect gaps in observation records)

Recharge was applied in the model using a zoned approach, where zones were delineated based on vegetation mapping and recharge was adjusted through initial manual calibration (Figure 4.7). Areas of open grassland were assigned the full estimated recharge rates (long term average = 102 mm/y), while areas of coastal shrubs were assigned 95% of the full recharge (long term average = 97 mm/y). Areas where sinkholes have been mapped were assigned double the estimated recharge (long term average = 204 mm/y). Areas of remnant wetlands were assigned high recharge for the pre-development period (1961–1976) based on nearby observation wells showing large rises during this period when water tables were closer to the surface and the wetlands were likely to be seasonal recharge/discharge features (Morton and Steel, 1970). Following development and declines in water levels, the wetland areas are assigned the same recharge rate as grasslands, such that the long-term average is 136 mm/y.

Areas of mallee vegetation were assigned no recharge, based on studies of recharge under mallee in similar calcrete environments (Allison et al., 1985) as well as more recent water balance studies using satellite-based data sets, which indicate that evapotranspiration exceeds rainfall in mallee zones (Swaffer, 2017). The area of no recharge was also expanded to cover the coastal cliff areas, where the water table depth is up to 130 m below ground (Figure 4.7). A small area of sand dunes is present in the north-west edge of the model domain, and these were assigned a long-term average recharge rate of 20 mm/y, based on values in Allison et al. (1985) for similar sand dune environments. After zoning recharge, the long-term spatial and temporal average recharge rate for the transient model was 90 mm/y, in good agreement with that average of 84 mm/y used by Knowling et al., (2015).



Recharge zones

- Open grassland, 102 mm/y
- Coastal shrubland, 97 mm/y
- Remnant swamps, 136 mm/y
- Sand dunes, 20 mm/y
- Sinkhole area, 204 mm/y
- Coastal mallee and deep water table, 0 mm/y
- Recharge wells
- Town water supply wells



Figure 4.7 Recharge zones and average recharge rates

The recharge estimates derived from this method are typically half of those estimated in Somaratne (2019). Another recharge data set based on an alternative conceptualisation was also derived in consultation with SA Water. This involved calculating Δh using the antecedent recession curve to derive a minimum water level as described in Healy and Cook (2002), rather than maximum and minimum annual measured values. This approach yielded recharge values that were on average 1.4 times larger than initial values given in Figures 4.6 and 4.7. To accommodate this uncertainty in recharge, as well as stakeholder advocacy in model development, both recharge data sets were used to calibrate the two model versions. A further two models were calibrated by allowing recharge values to vary using recharge multipliers applied to each stress period in parameter estimation with PEST (Doherty, 2010). Recharge multipliers applied uniformly to all recharge zones. Thus, six versions of the model were constructed, as summarised in Table 4.2.

Table 4.2. Summary of model versions calibrated

Model version	TS to QL flow	Recharge
V1a	Vertical in areas where TC is absent	Water table fluctuation using antecedent recession min, long term average = 90 mm/y
V1b	Vertical in areas where TC is absent	Water table fluctuation using max/min annual values (Figure 4.6 and 4.7), long term average = 64 mm/y
V1c	Vertical in areas where TC is absent	V1a recharge allowed to vary in parameter estimation with recharge multiplier, long term average = 92 mm/y
V2a	Horizontal through Layer 1	Water table fluctuation using antecedent recession min, long term average = 90 mm/y
V2b	Horizontal through Layer 1	Water table fluctuation using max/min annual values (Figure 4.6 and 4.7), long term average = 64 mm/y
V2c	Horizontal through Layer 1	V2a recharge allowed to vary in parameter estimation with recharge multiplier, long term average = 78 mm/y

Evapotranspiration (ET) is considered to be a relatively small component of the water balance in Uley South. Evapotranspiration was applied using the ET package, with a rate of 1547 mm/y based on average annual pan evaporation data for the region, as described in Knowling et al., (2015). An extinction depth of 2 m was set, that is evapotranspiration only occurs when and where the water table is within 2 m of the land surface. The ET rate decreases linearly with depth from the surface to 2 m.

4.5 Groundwater extraction

The steady state model represents pre-development conditions and hence does not contain any groundwater extraction. The transient model simulates extraction from the TWS wells from 1976 to 2017. While there is a small amount of metered extraction data from these wells from 2013 to 2017, it is not sufficient to construct an entire extraction data set. Hence monthly groundwater extraction rates for individual bores were based on master meter extraction rates, as described in Section 2.5.8. These synthetic extraction rates show a reasonable correlation with metered extraction rates where data is available (Figure 2.19).

4.6 Aquifer parameters

Aquifer parameters were based on measured and previously modelled values and refined during calibration using the pilot point approach in PEST (see Appendix C for pilot point locations and ranges). Initial parameter values and bounds were based on ranges reported from aquifer test data (Appendix A), as well as values in other modelling studies (Table 4.3). The final aquifer parameter values used in each model are shown in Figures 4.8 to 4.13. Chapter 5 provides further information on the calibration approach with PEST.

Despite high specific yield values up to 0.7 being reported for the QL aquifer (Sibenaler, 1976), an upper limit of 0.4 was used in the final models, consistent with previous modelling (Knowling et al., 2015). For the models with higher recharge and horizontal flow from the TS aquifer (e.g. model versions 2a and 2c), this upper bound is reached extensively across the QL aquifer (Figure 4.11). Such consistently high parameter values may be a result of calibration, in terms of the model responding to higher simulated recharge rates and inflow volumes from the TS aquifer. However, previous models of the Uley South Basin have yielded very high parameter values. For example, Knowling et al. (2015) derived areas where the hydraulic conductivity was 10,000 m/d for the QL aquifer. In this study, the maximum is 2000 m/d, with one pilot point at a pumping test location having an upper limit of 4800 m/d based on Watkins et al. (2015). Hence the constraints placed on hydraulic conductivity, and the approach to simulating TS inflow in some model versions in this study may be influencing the calibration derived specific yield values. It should be noted though that such high specific yield values have been reported for Uley South (see Section 2.5.4).

Specific storage (S_s) for the TS aquifer was based on the storage value reported by Morton and Steel (1968) of 0.007, which gives an S_s value of ~4 x 10^{-4} m^{-1} when divided by aquifer thickness of 10 to 40 m, as well as values used in previous models (Table 3.1) and in the literature (De Marsily, 1986). However, more recent work by Rau et al. (2018) has shown that 1.3 x 10^{-5} m^{-1} is likely to be a physically plausible upper bound for S_s values. Hence the S_s parameters used in this model may be too high. However, this information was not available during the model calibration phase, hence re-calibrating using this information is considered beyond the scope of this project. Future work could be done to test the sensitivity of model results to TS parameters and refine the model further.

Layer 2 in the model represents the TC formation, however this formation is absent in some areas (Figure 2.5). Hence the majority of pilot points in Layer 2 use ranges for the TC formation as given in Table 4.3, and pilot points in areas where the TC is absent were assigned ranges based on the TS formation. Kriging was used to interpolate between pilot point values in the final model, hence a clear boundary between areas where the TC is present and absent is not marked. Nevertheless, zones of higher conductivity are apparent in Figure 4.9 along the northern boundary and the south-eastern edge of the basin. Consequently Table 4.4 gives the parameter ranges as applied to each layer in the model, rather than each formation.

Table 4.3. Aquifer parameter ranges used in model calibration

Aquifer parameter at pilot points	Range for pilot points (initial preferred value)	Units
QL horizontal conductivity (non-pump test pilot points) QL horizontal conductivity* (pump test pilot points)	5–2000 (200) 30–4800	m/d
QL specific yield (non-pump test pilot points) QL specific yield (pump test pilot points)	0.01–0.4 (0.2) 0.002–0.4	-
TC horizontal conductivity	$1x10^{-3}$–1 (0.1)	m/d
TC vertical conductivity	$1x10^{-5}$–$1x10^{-3}$ ($6.8x10^{-4}$)	m/d
TS horizontal conductivity	0.1–200 (20)	m/d
TS storage	$5x10^{-4}$–$1x10^{-1}$ ($1x10^{-4}$)	m^{-1}

(*see Appendix A for pump test values)

Table 4.4. Aquifer parameter ranges in calibrated models (see Figures 4.8 to 4.13 for spatial distributions)

Aquifer parameter at pilot points	Range in calibrated models (Figure 4.8 to 4.13)	Units
Layer 1 horizontal conductivity (QL)	7–4470	m/d
Layer 1 specific yield (QL)	0.008–0.4	-
Layer 2 horizontal conductivity (TC + TS)	$1x10^{-4}$ –37*	m/d
Layer 2 vertical conductivity (TC + TS)	$1x10^{-5}$–10*	m/d
Layer 3 horizontal conductivity (TS)	0.7–177	m/d
Layer 3 storage (TS)	$5x10^{-4}$–0.1	m^{-1}

(*higher conductivity values represent areas in Layer 2 where the TC formation is absent, see Figure 4.9)

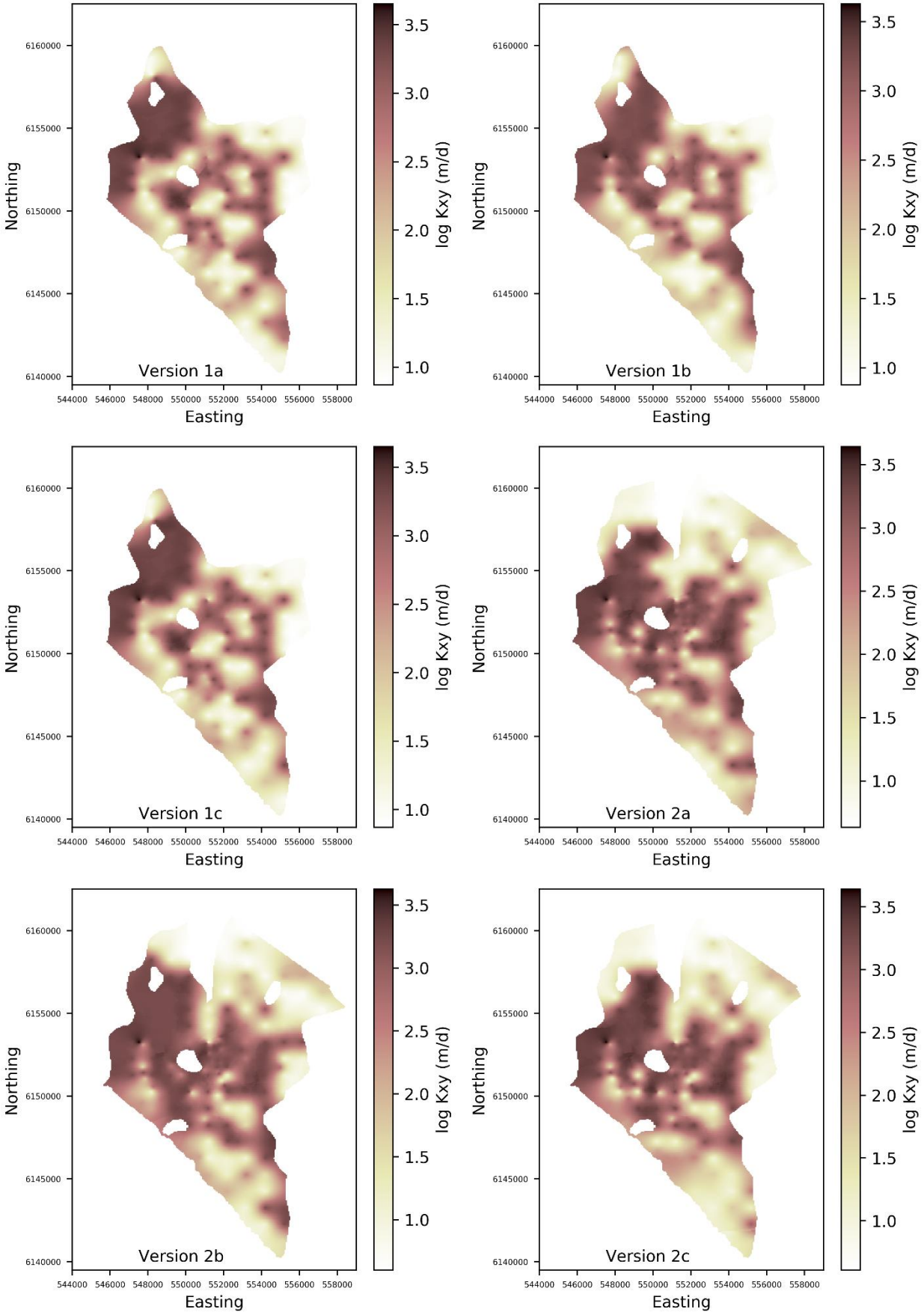


Figure 4.8. Layer 1 horizontal hydraulic conductivity values for the six models

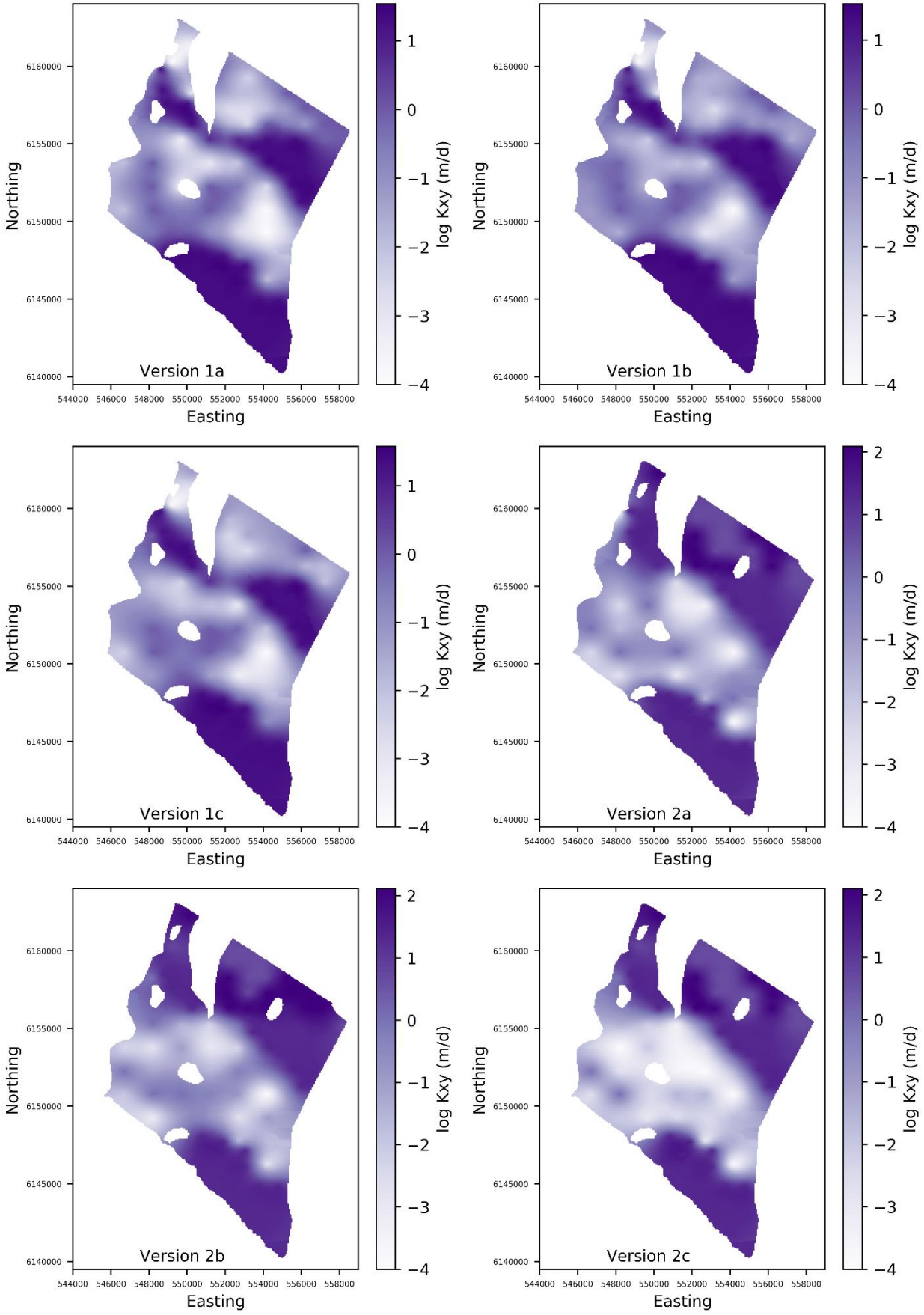


Figure 4.9. Layer 2 horizontal hydraulic conductivity values for the six models

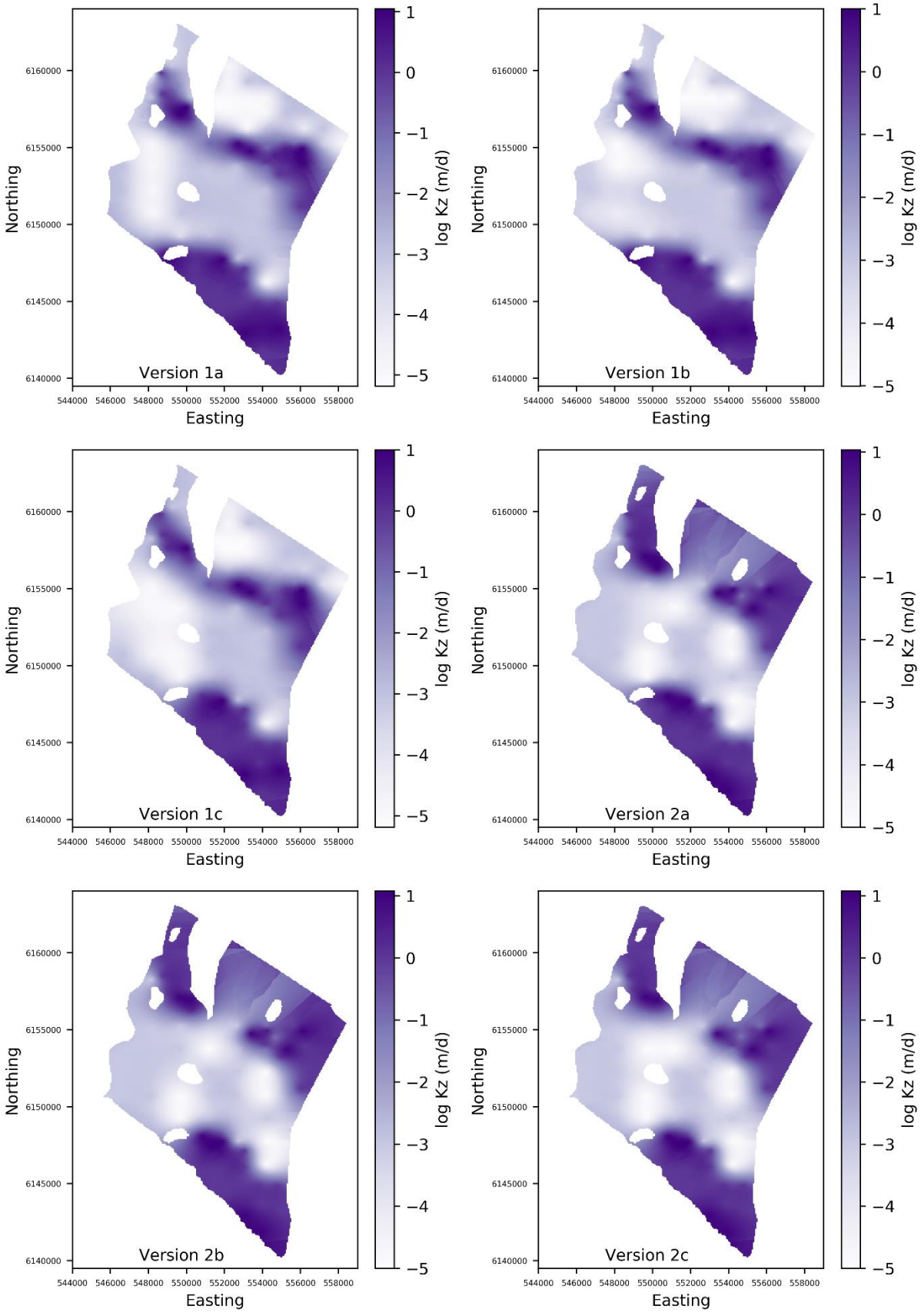


Figure 4.10. Layer 2 vertical hydraulic conductivity for the six models

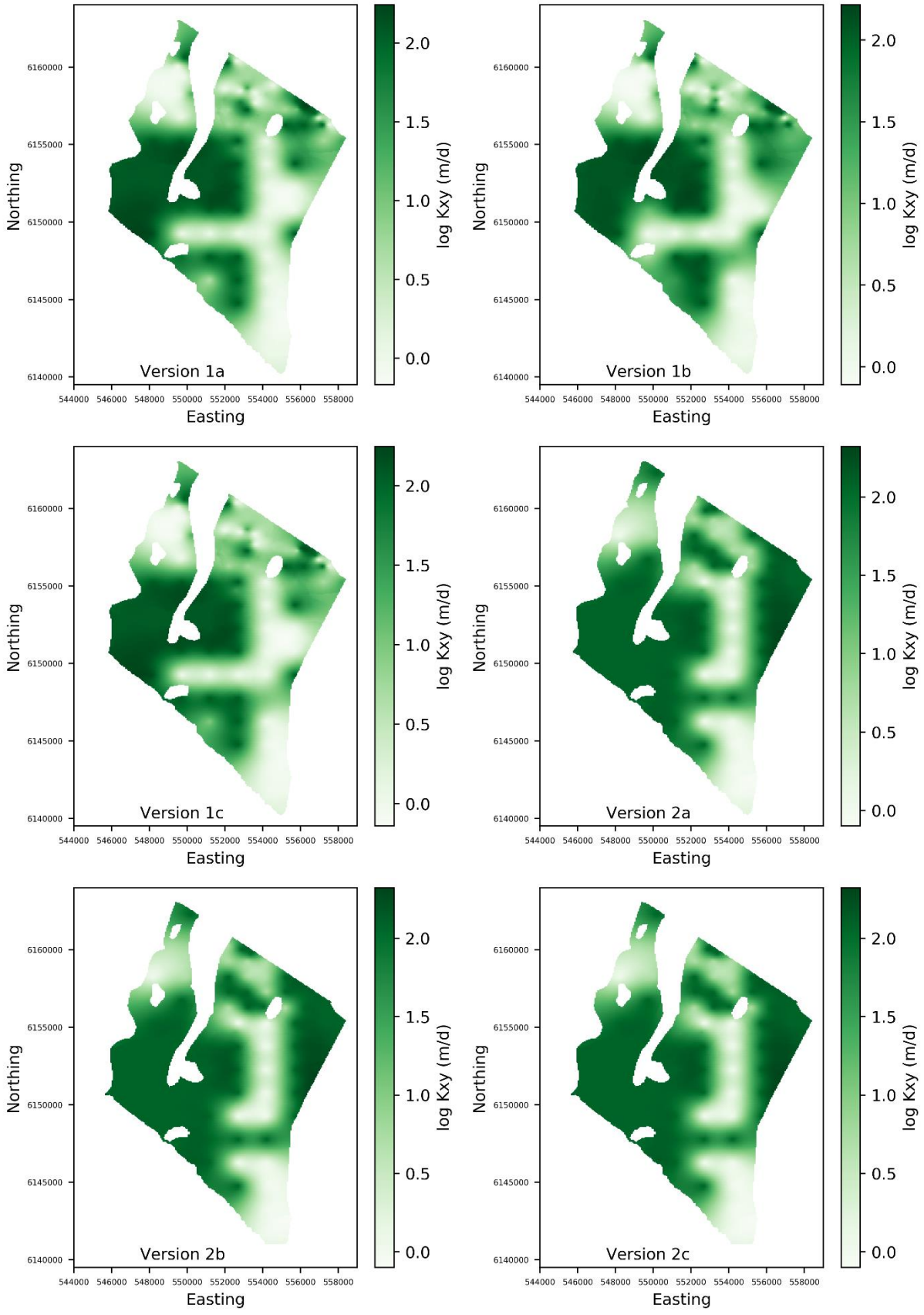


Figure 4.11. Layer 3 horizontal hydraulic conductivity for all six models

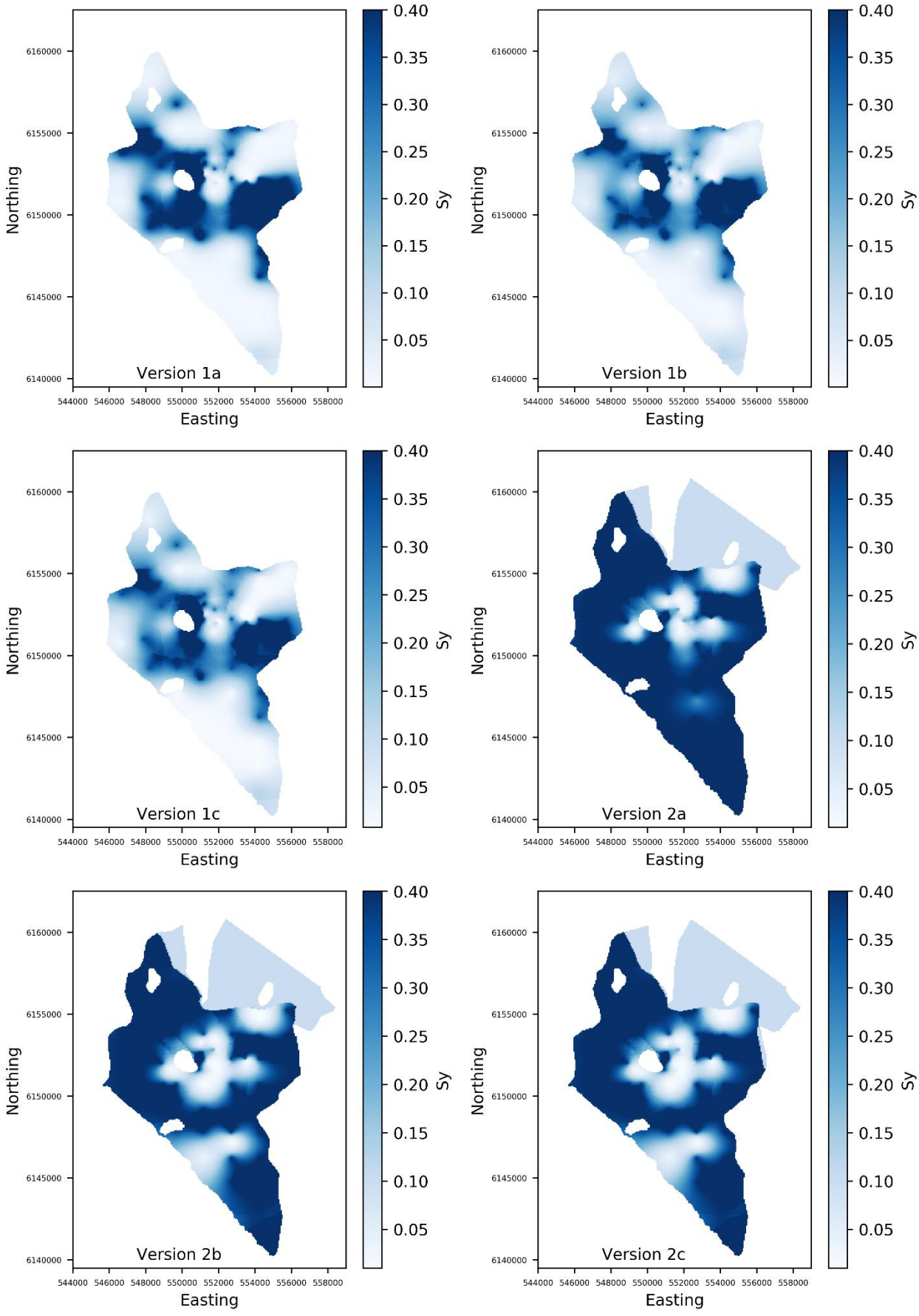


Figure 4.12. Layer 1 specific yield for the six models

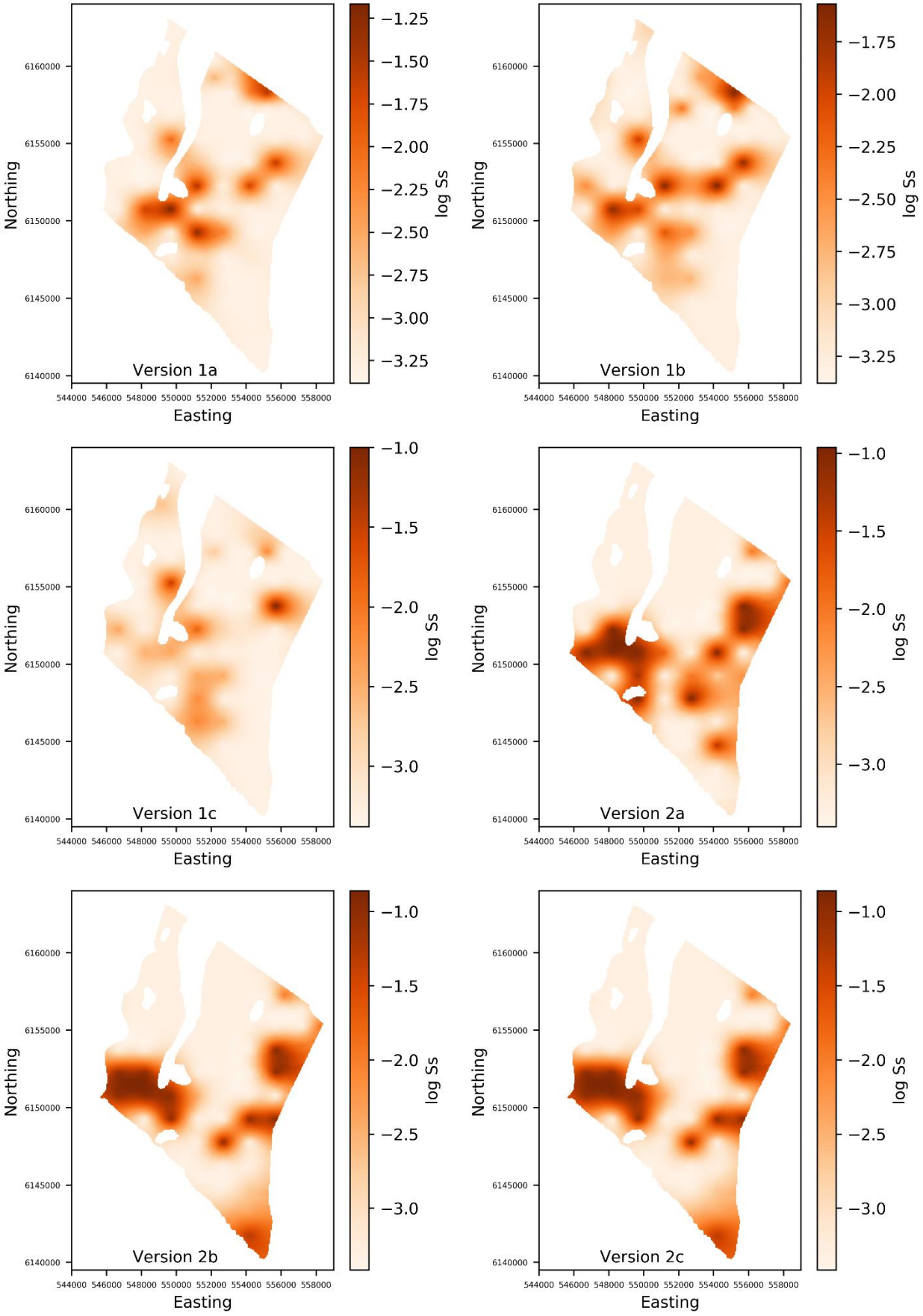


Figure 4.13. Layer 3 specific storage for the six models

4.7 Observation data and time discretisation

4.7.1 Steady state model

For the steady state model, average groundwater levels from 1960–63 were used for calibration, as this is the earliest time period for which a reasonable amount of data is available (45 QL wells and 8 TS wells). Groundwater levels were also relatively stable from 1960 to 1963 (Figure 2.8 to 2.12), when there was no groundwater extraction from the basin.

A pseudo-steady state model was then run for 10 years, with water balance fluxes held constant, to simulate long term average pre-development conditions. This was run in transient mode, with monthly stress periods and 100 time steps per stress period, so that the simulated seawater interface with SWI2 had sufficient time to reach steady state. As a check, the simulated interface from one run of the steady state model was imported as an initial condition in a second run, and checked to ensure the interface position was constant with time. The volumetric SWI2 budget saved in the MODFLOW list (.lst) file was also checked to ensure freshwater and seawater zones had reached steady state.

4.7.2 Transient model

The transient model was calibrated to 24,773 groundwater level measurements in the study area covering the 57-year period 1961 to 2017 (Figure 4.14). All groundwater level data in the study area was initially assessed for inclusion; however, some observation wells showed spurious or anomalous results, and so were removed from the calibration data set. Furthermore, some wells with good long-term records contained occasional anomalous readings, and these anomalous values were assigned low weights (0.2) in the PEST calibration. These include wells SLE005, ULE089, ULE105 and ULE130 (see Appendix D for individual hydrograph plots). The transient model has monthly stress periods with 10 time steps per stress period. As with the steady state model, 100 time steps per stress period were used for the SWI2 simulations.

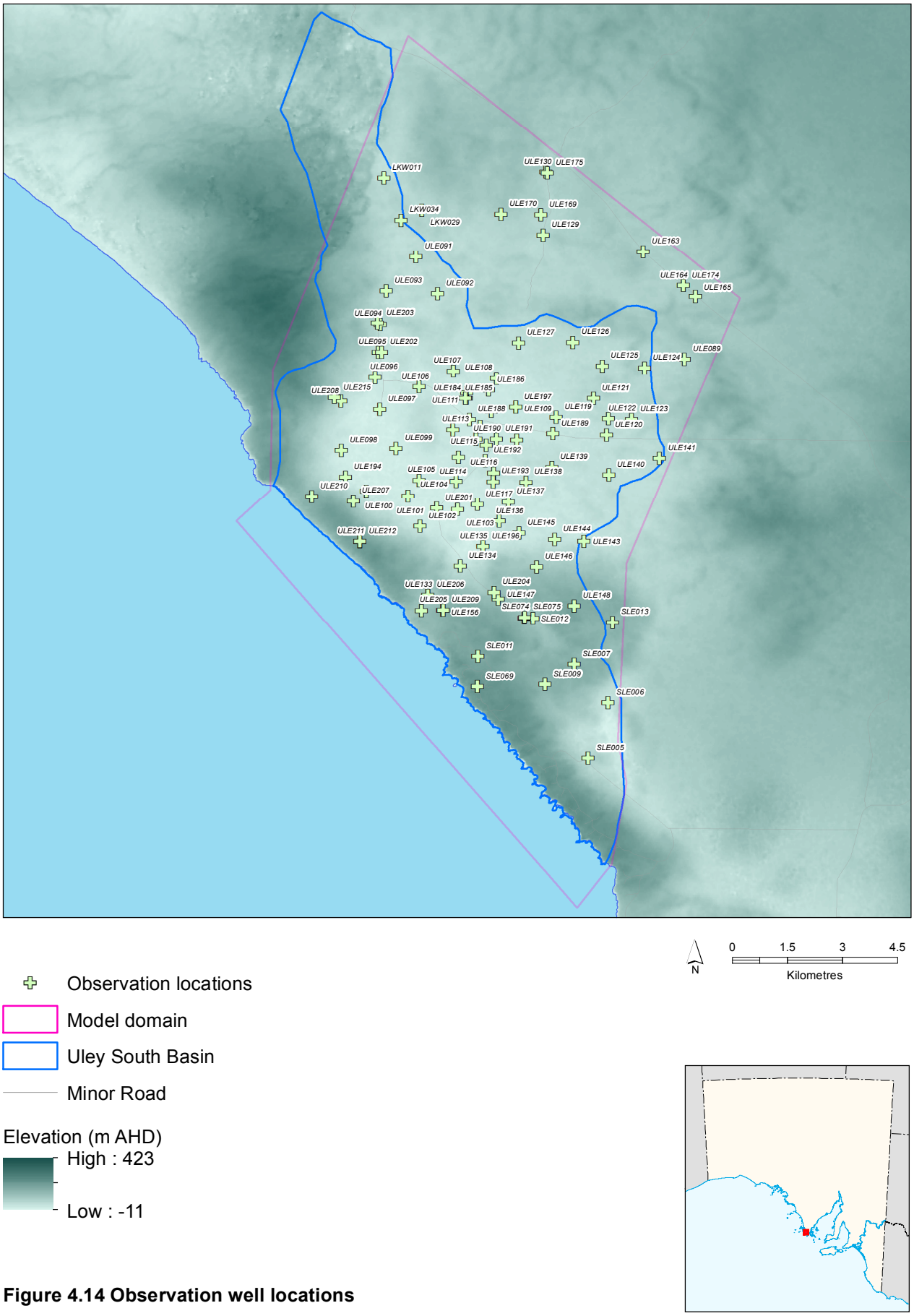


Figure 4.14 Observation well locations

4.7.3 Initial conditions

Initial conditions for groundwater levels in the steady state model are based on a potentiometric surface derived from average groundwater levels for the period 1960–63. Following approaches used in other studies (Hughes and White, 2016), the initial position of the seawater interface for the steady state model was based on the initial model heads for each layer and the Ghijben-Herzberg relation:

$$z = \frac{\rho_f}{\rho_s - \rho_f} h = \alpha h \qquad (5)$$

where z is the elevation of the interface below sea level (m), ρ_f and ρ_s are the densities of freshwater and seawater respectively, and h is the water table elevation. Here we assume density values of 1000 kg/m^3 for ρ_f and 1025 kg/m^3 for ρ_s, such that α is equal to 40 (Post et al., 2018).

Initial conditions for both groundwater level and the position of the seawater interface for the transient model are based on results from the steady state model.

5 Model calibration

5.1 Calibration approach

Six versions of the model (Table 4.2) were each calibrated separately. Calibration was achieved by altering hydraulic parameters (K_h, K_v, S_y and S, as in Table 4.3) in order to provide a good fit between measured and modelled potentiometric head in the QL, TC and TS formations. Parameter estimation software PEST (Doherty, 2010) was used with hydraulic parameters assigned at 560 pilot points. At locations where aquifer test data was available, pilot points were assigned preferred values based on pumping test results, with bounds of $\pm$ 10% (see Appendix A for aquifer test data). Vertical hydraulic conductivities (K_v) of the QL and TS aquifers were tied to horizontal conductivity (K_h) using a K_h:K_v ratio of 10, following previous examples (Werner, 2010). During calibration of model versions 2a, 2b and 2c, the northern part of Layer 1 is treated as part of the TS: the area was assigned hydraulic conductivity closer to expected TS values, assigned a uniform Sy value of 0.1 (Figure 4.12), and no recharge was simulated.

Given the large number of pilot point values used in calibration, super parameters were implemented with the SVD-Assist tools in PEST. Initial calibration was performed on steady state models; however, most of the calibration effort was spent on transient models. Parameters derived from calibrated transient models were re-run through steady state models to derive appropriate initial conditions for the final transient models.

No metrics were set to determine whether or not a model calibration was satisfactory; rather, overall model fits to absolute water levels and trends in key wells was judged qualitatively. Quantitative model error values are reported as root mean squared error (RMS) and scaled root mean squared error (SRMS), consistent with statistics often used in groundwater model studies (Barnett et al., 2012).

Given the long run-time (~5 hours) and large file sizes for transient SWI2 models, calibration was performed on flow models only. Furthermore, there is insufficient data on the position of the seawater interface over time with which to calibrate the SWI2 models, hence SWI2 simulations were run after final parameters had been assigned.

5.2 Steady state calibration

The purpose of the steady state models is to provide a broad match to 'average' pre-development groundwater levels. It should be noted that large groundwater fluctuations were observed prior to development, in response to high rainfall/recharge in years such as 1964 and 1968. Hence the steady state models are calibrated to average 1960–63 groundwater levels, as this was the earliest period during which there was no extraction, there is sufficient water level data, and groundwater levels were relatively stable (Figure 2.8–2.13). Modelled groundwater levels generally match measurements for the steady state models, with RMS error (RMSE) < 1 m and SRMS error typically < 5% (Figure 5.1).

5.3 Transient calibration

The transient models were run from January 1961 to December 2017 and calibrated to groundwater level measurements at 103 observation wells. All six models generally fit the measured data well, with RMSE ranging from 0.66–0.91 m, and SRMSE of 1.8–2.5% (Figure 5.2). Modelled water levels also generally replicate the potentiometric surface well, noting that the measured surface is based on point observations (Figure 5.3). Some of the misfit is related to model calibration and uncertainty in processes; however, some model misfit can likely be attributed to measurement issues such as surveyed well elevations. For example, all models simulate groundwater levels that are higher than measurements at well ULE130 in the northern part of the domain, where measured levels are ~30 m AHD and modelled levels are ~ 35 m AHD (see consistent outliers in Figure 5.2). Well ULE130 is in close proximity to ULE175, which shows higher water levels by about 6 m where measurements coincide at points

in time. Thus, there is likely an error in surveyed elevation for one of these wells. As ULE175 has a longer observation record, and is used to assist in assigning boundary conditions for the TS aquifer (see section 4.3.1), the poor calibration at ULE130 was considered of low importance by assigning a low weight (0.2) to observations during calibration.

Transient matches to water level trends are generally good for all models. For example, Figure 5.4 shows measured and modelled groundwater levels at ULE114 for all six models. For brevity, distributions of modelled groundwater level for all six models are shown for 17 wells with long term data records (Figures 5.5 to 5.21). The locations of these observation wells are shown in Figure 5.22. Complete calibration plots for model versions 1c and 2b (discussed further in section 5.5) can be found in Appendix D.

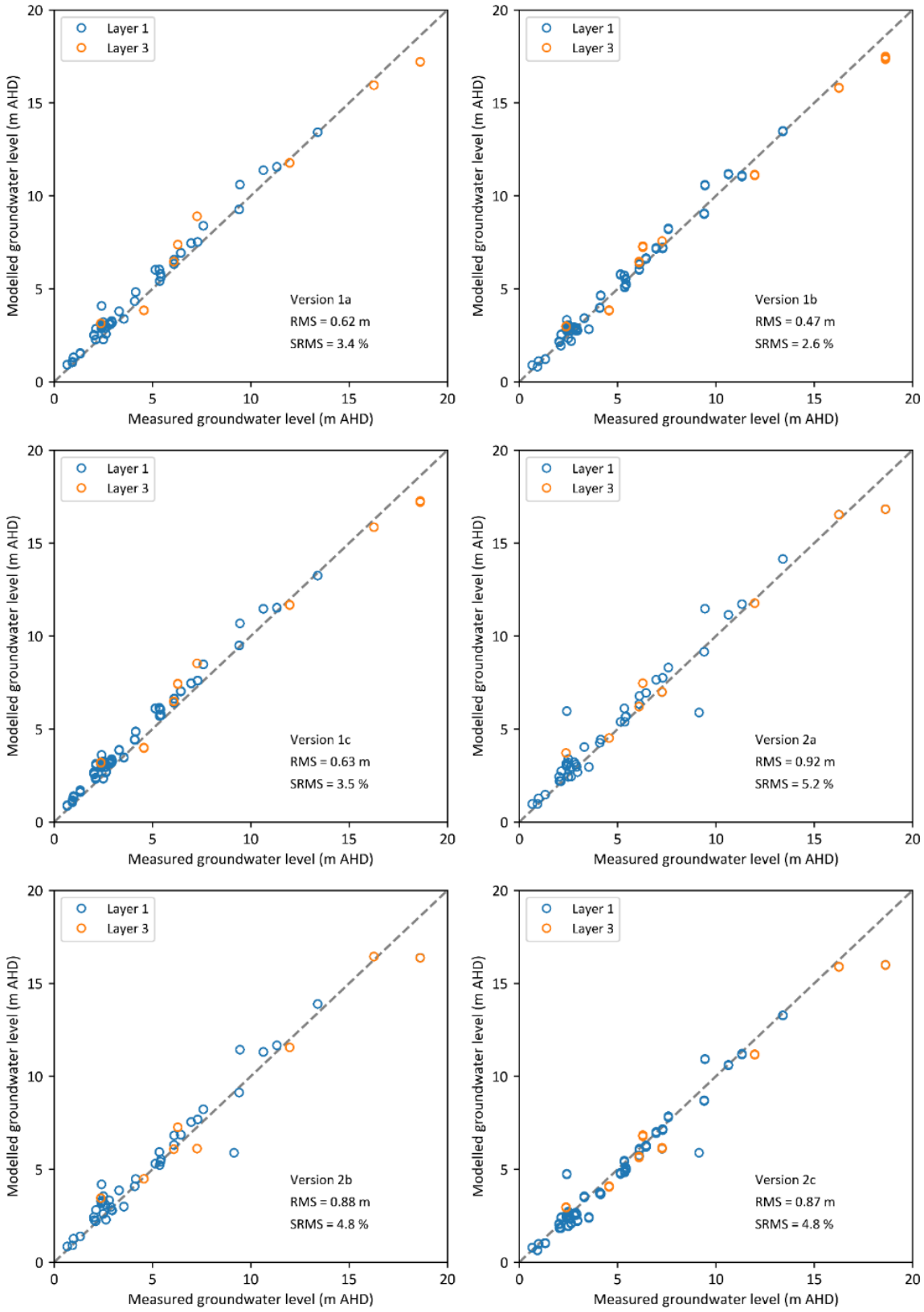


Figure 5.1. Steady state modelled vs measured groundwater levels

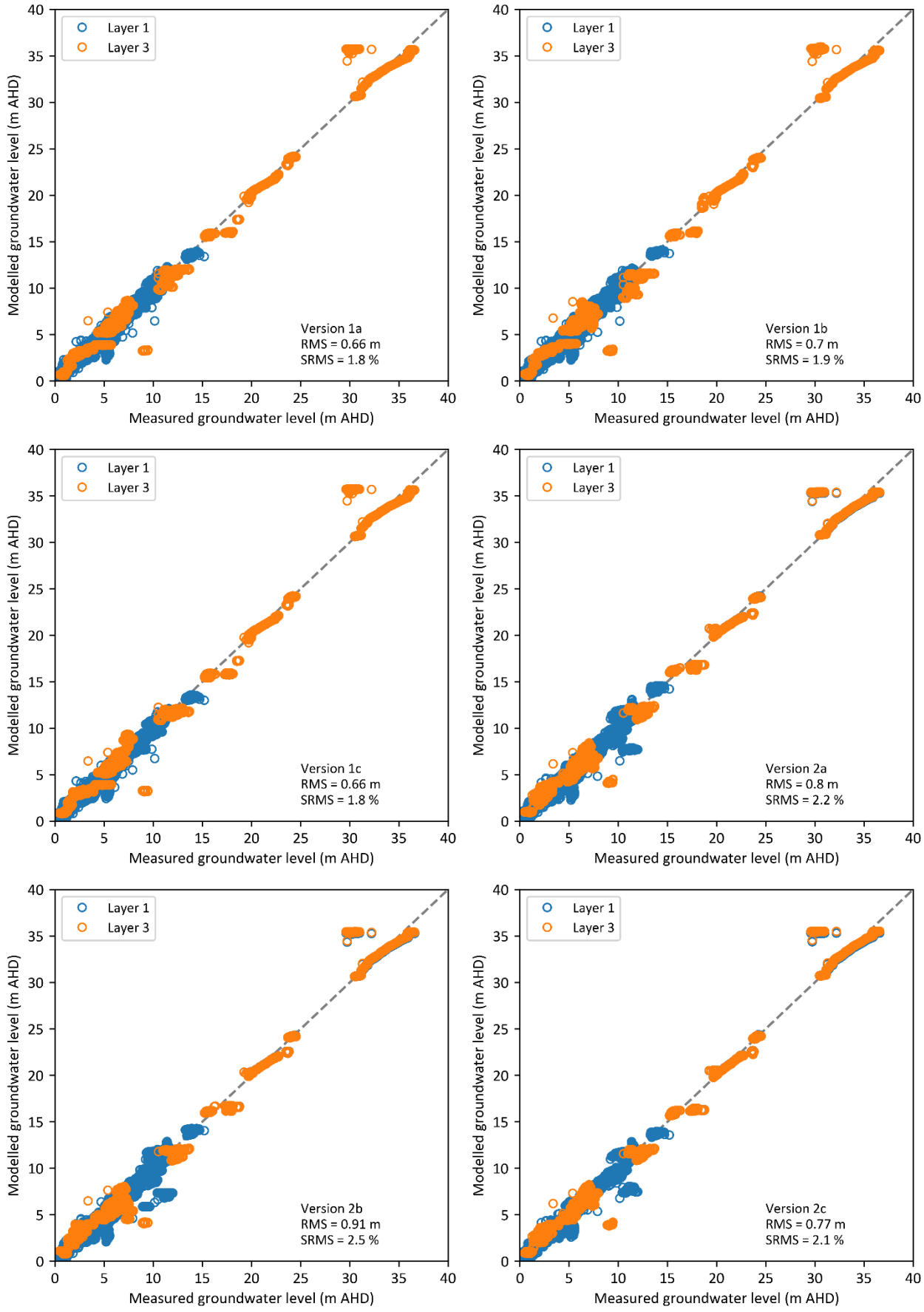


Figure 5.2. Transient modelled vs measured groundwater levels

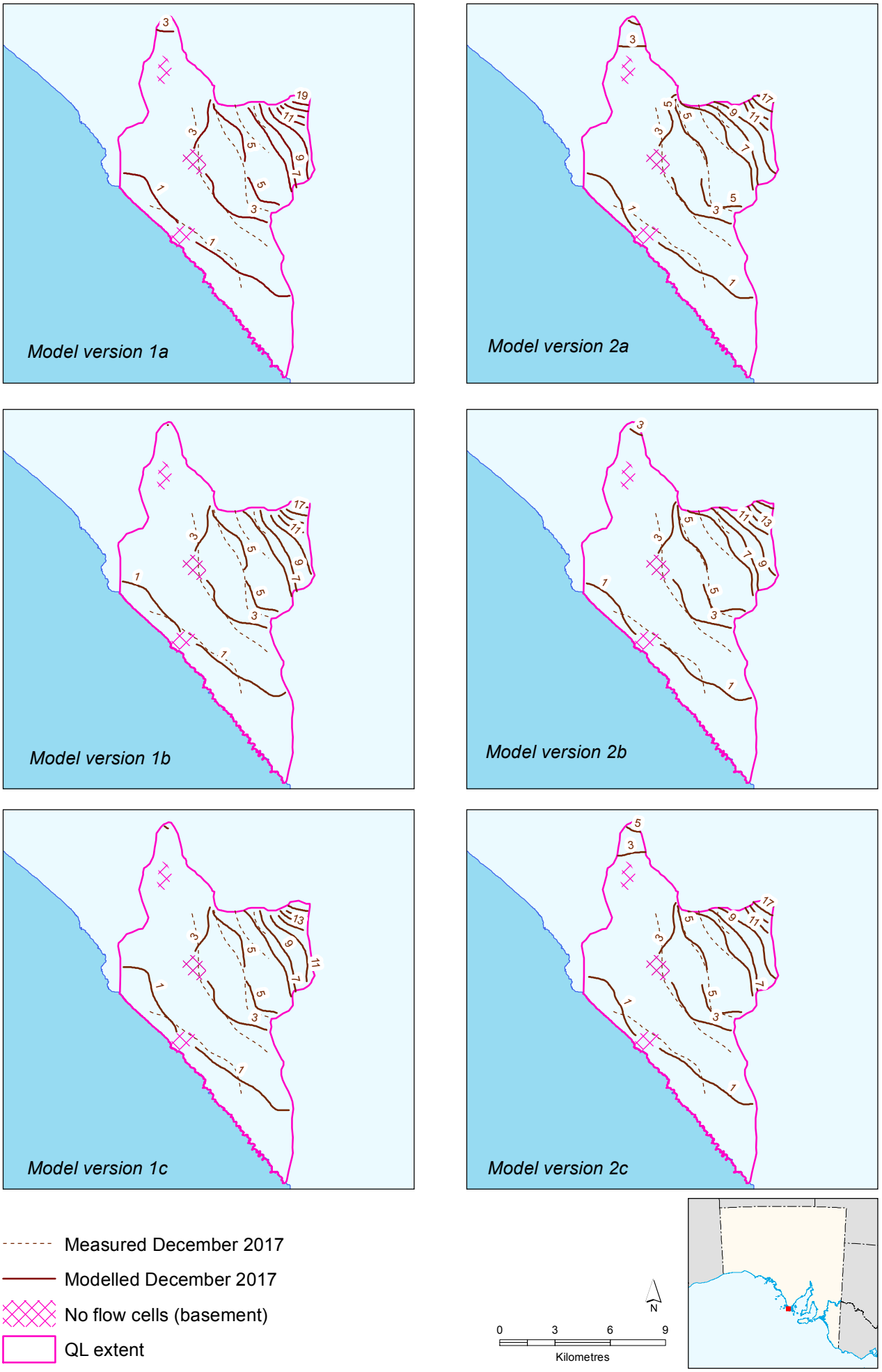


Figure 5.3 Measured and modelled potentiometric surfaces at December 2017

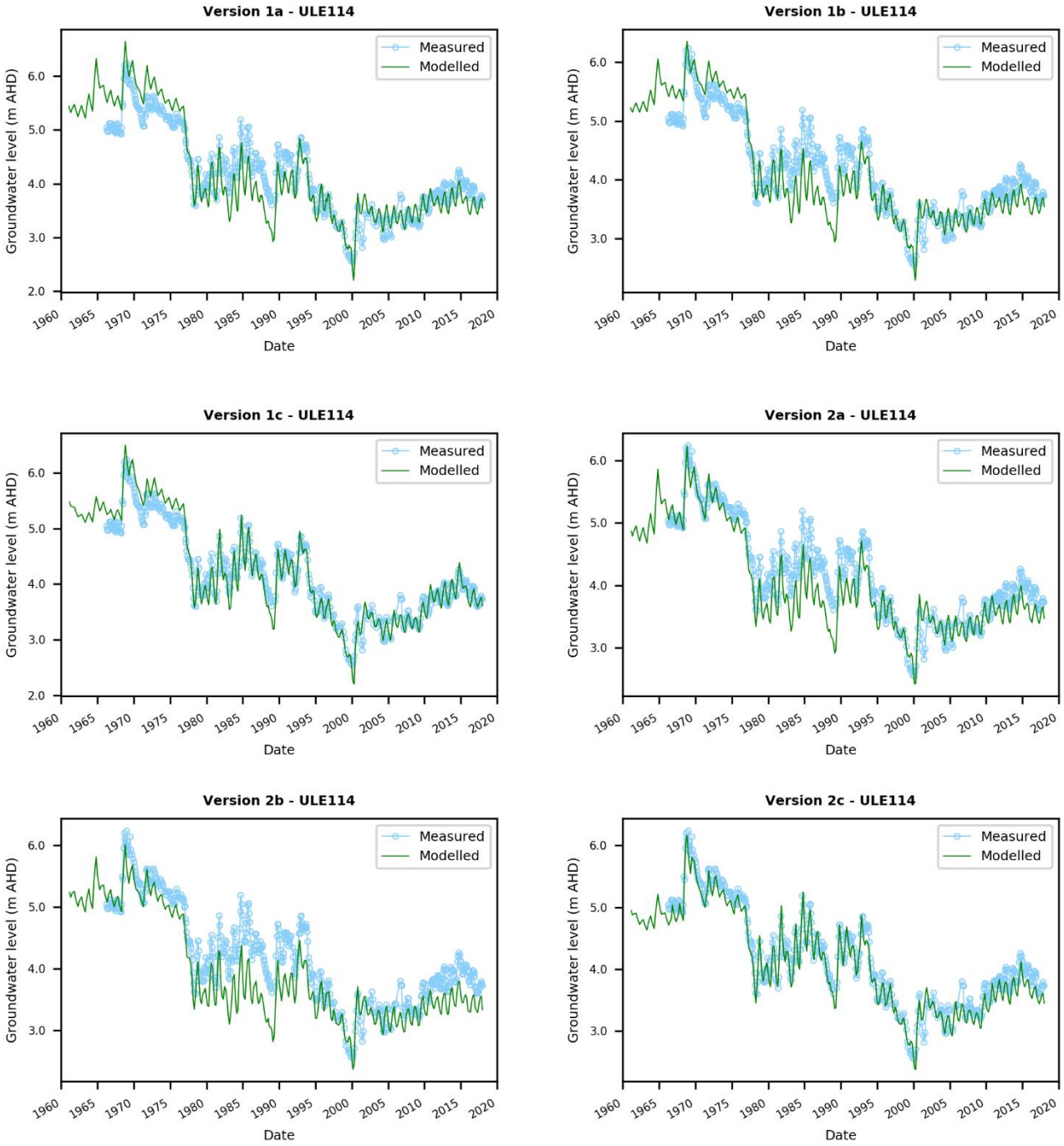


Figure 5.4. Transient modelled and measured groundwater levels at well ULE114 (QL) for all six models

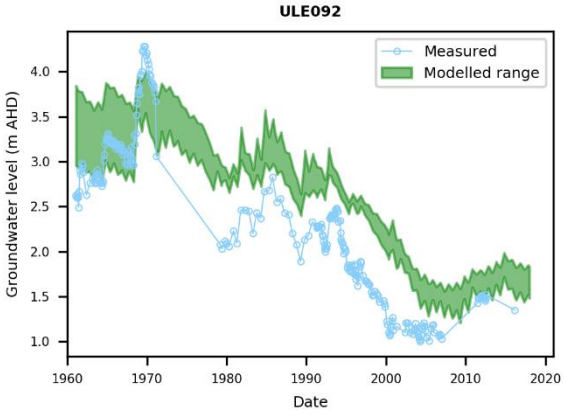


Figure 5.5. Transient modelled and measured groundwater levels at well ULE092 (QL) for all six models

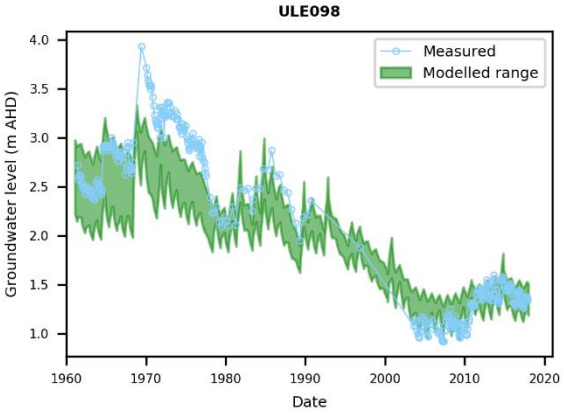


Figure 5.8. Transient modelled and measured groundwater levels at well ULE098 (QL) for all six models

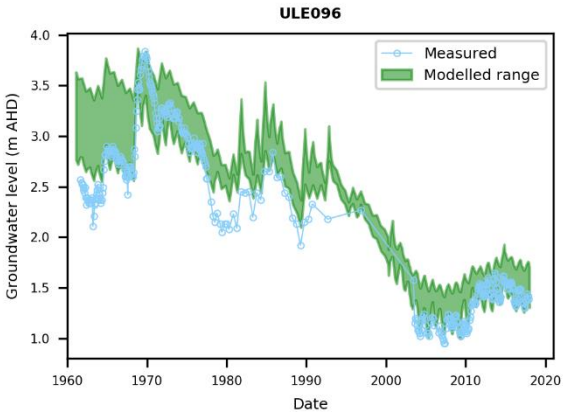


Figure 5.6. Transient modelled and measured groundwater levels at well ULE096 (QL) for all six models

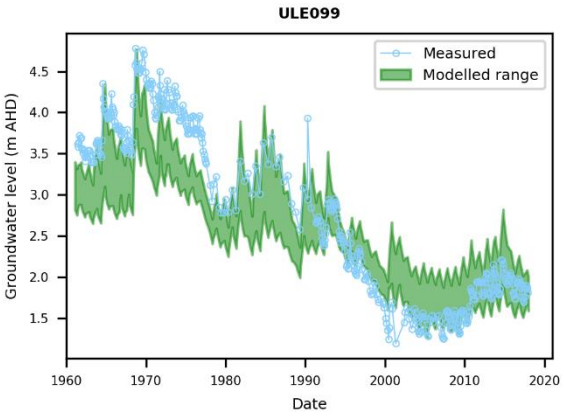


Figure 5.9. Transient modelled and measured groundwater levels at well ULE099 (QL) for all six models

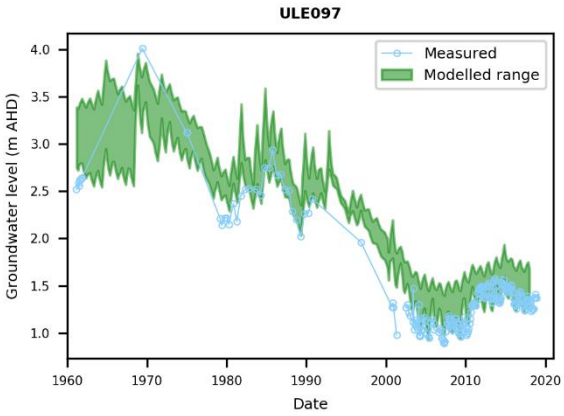


Figure 5.7. Transient modelled and measured groundwater levels at well ULE097 (QL) for all six models

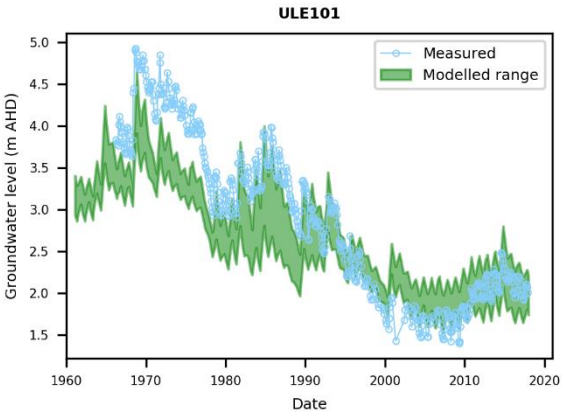


Figure 5.10. Transient modelled and measured groundwater levels at well ULE101 (QL) for all six models

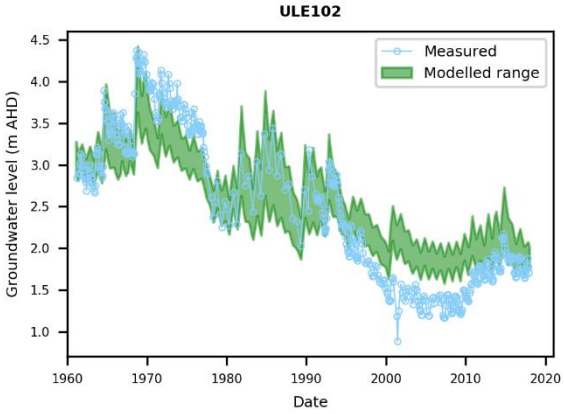


Figure 5.11. Transient modelled and measured groundwater levels at well ULE102 (QL) for all six models

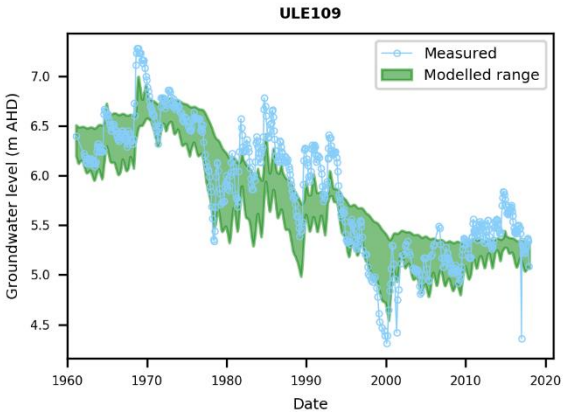


Figure 5.12. Transient modelled and measured groundwater levels at well ULE109 (TS) for all six models

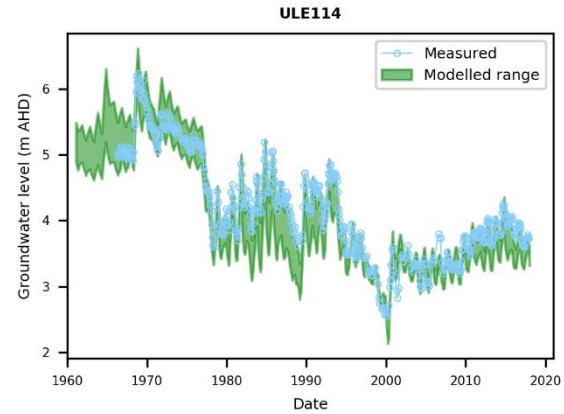


Figure 5.13. Transient modelled and measured groundwater levels at well ULE114 (QL) for all six models

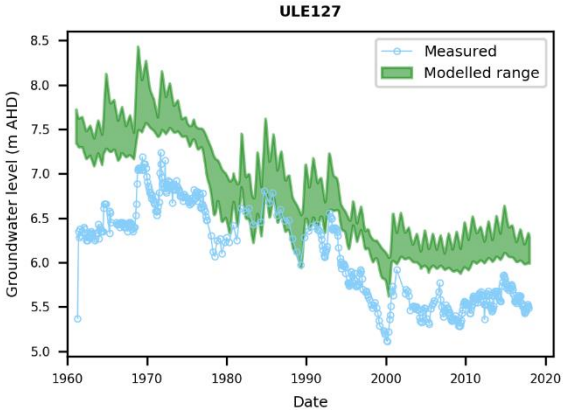


Figure 5.14. Transient modelled and measured groundwater levels at well ULE127 (TS) for all six models

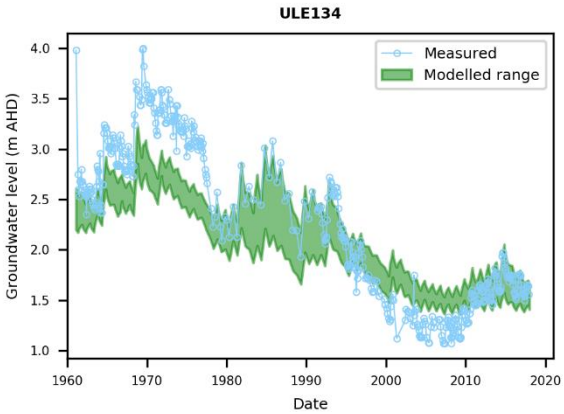


Figure 5.15. Transient modelled and measured groundwater levels at well ULE134 (QL) for all six models

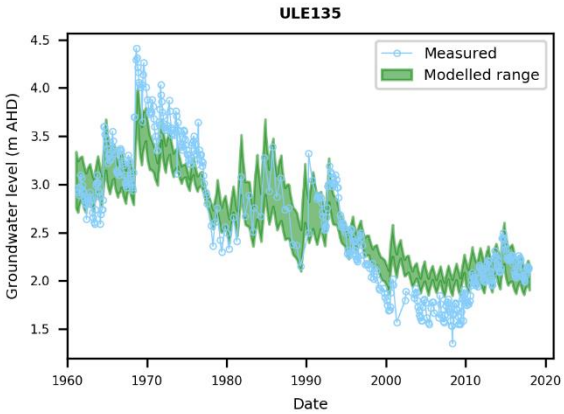


Figure 5.16. Transient modelled and measured groundwater levels at well ULE135 (QL) for all six models

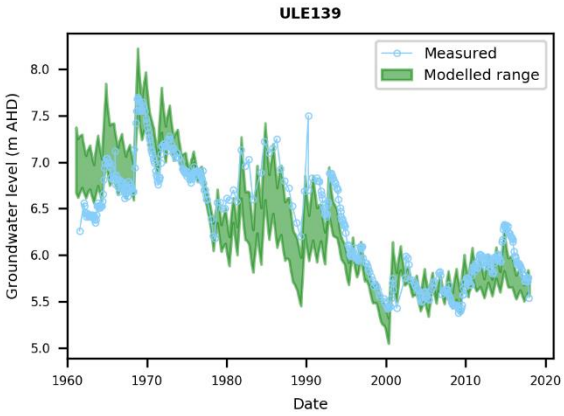


Figure 5.17. Transient modelled and measured groundwater levels at well ULE139 (QL) for all six models

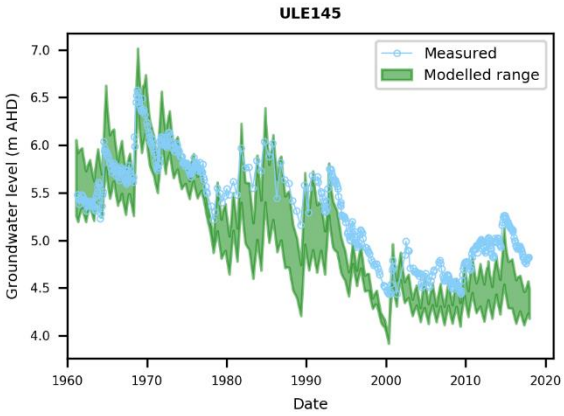


Figure 5.18. Transient modelled and measured groundwater levels at well ULE145 (QL) for all six models

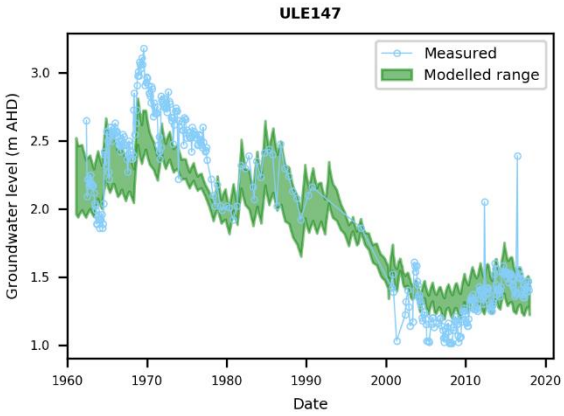


Figure 5.19. Transient modelled and measured groundwater levels at well ULE147 (QL) for all six models

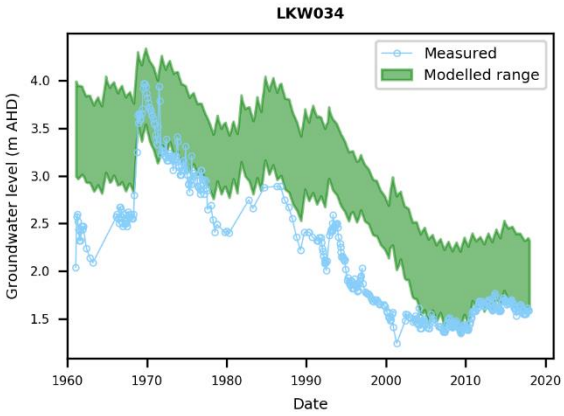


Figure 5.20. Transient modelled and measured groundwater levels at well LKW034 (TS) for all six models

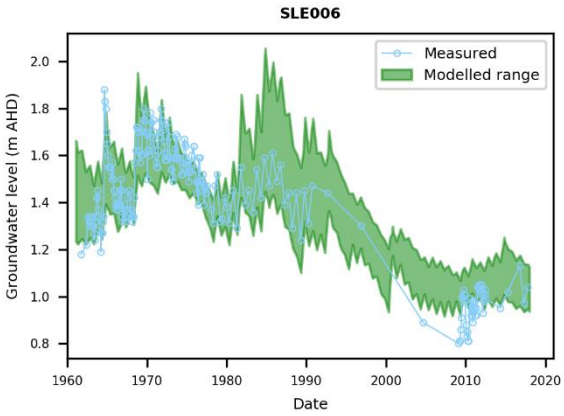


Figure 5.21. Transient modelled and measured groundwater levels at well SLE006 (QL) for all six models

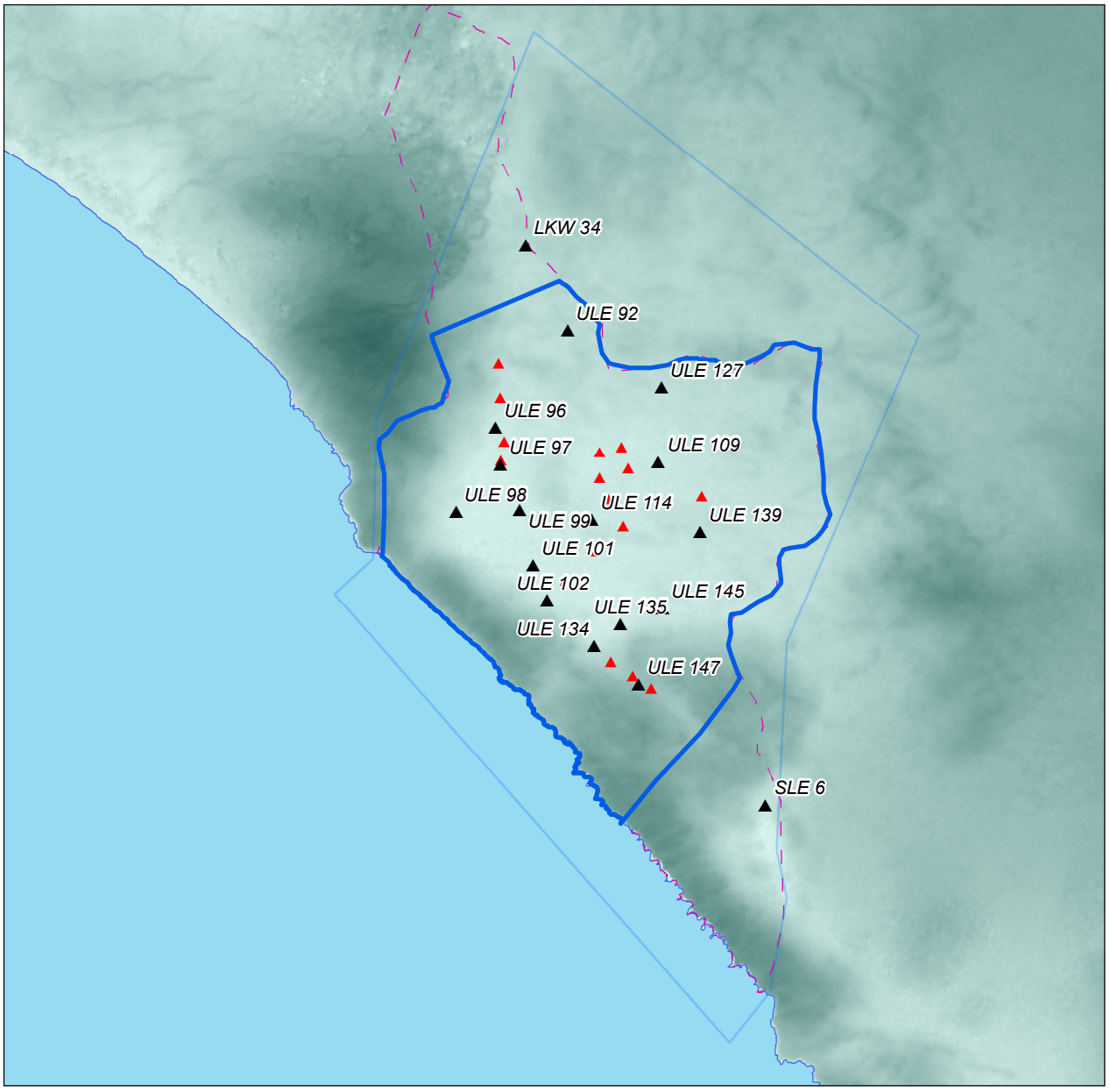


Figure 5.22 Mass balance area and long term observation wells for the QL aquifer

5.4 Mass balances

Average mass balances are given for the QL aquifer in the main recharge areas around the town water supply wells (Figure 5.22). The mass balances reported here are for a sub-section of the entire basin, hence not directly comparable with previously reported fluxes.

The mass balances vary for different time periods and different models, given the different way that processes are represented. Model versions 2a, 2b and 2c generally show larger inflow and outflow volumes, given the way that the QL aquifer is explicitly connected to the TS aquifer in the north of the domain through Layer 1. Fluxes are generally higher for pre-development periods (Table 5.1) compared to long-term averages (Table 5.2) and the last ten years (Table 5.3).

Mass balances for the pre-development period (1961–75) show the largest recharge and coastal groundwater discharge fluxes, given the high rainfall observed in the mid to late 1960s, and the absence of groundwater extraction (Table 5.1). Coastal discharge fluxes are within the ranges estimated by Evans (1997), however, lower than some other pre-development estimates (Table 2.3). These lower simulated fluxes can be attributed to the recharge used in this model, as well as the extent and architecture of the model domain (Figure 4.3), both of which are different to that used in previous models. Evapotranspiration also represents a small but noticeable part of the water balance during this period, as groundwater levels were higher than they currently are and discharge was likely to occur intermittently through swamps (Morton and Steel, 1970).

Table 5.1. Average pre-development (1961–75) mass balance for all six versions of the model

Pre-development (1961–75)	**Model version**					
Inflow (ML/y)	**v1a**	**v1b**	**v1c**	**v2a**	**v2b**	**v2c**
Recharge	9,847	7,059	8,095	9,778	7,035	7,300
Layer 2 inflow	4,595	4,961	4,429	7,554	7,613	7,818
Tertiary Sand inflow				2,640	3,733	2,448
Boundary inflow	2	2	2	1	1	2
Storage inflow	3,429	2,441	2,887	4,175	3,440	3,078
Surrounding QL inflow	900	505	946	1,959	1,367	1,534
Outflow (ML/y)						
Coastal discharge	6,631	5,783	6,567	9,169	9,315	8,721
Evapotranspiration	27	23	23	40	45	35
Layer 2 outflow	6,435	5,013	5,205	8,196	7,341	7,067
Tertiary sand outflow				401	461	232
Storage outflow	3,674	2,675	2,998	5,684	3,984	4,405
Surrounding QL outflow	2,009	1,475	1,565	2,620	2,052	1,725
Total inflow (ML/y)	18,774	14,968	16,359	26,108	23,188	22,180
Total outflow (ML/y)	18,775	14,969	16,358	26,110	23,198	22,184
Percent error (%)	-2.6E-03	-3.7E-03	1.2E-03	-7.5E-03	-4.1E-02	-1.8E-02

Post development (Table 5.2) and contemporary (2008–2017, Table 5.3) mass balances show declining recharge and coastal discharge fluxes compared to the pre-development period. This reflects declines in rainfall since the early 1990s, as well as the impact of pumping. The relative impacts of climate and pumping on groundwater levels have not been quantified in this study; however, pumping is likely to have contributed to aquifer decline more than climate, as was previously determined by Knowling et al. (2015). This is evident by running the model over the history matching period (1961–2017) with and without pumping (Figure 5.23).

Table 5.2. Average long-term post development (1976–2017) mass balance for all six versions of the model

Post-development (1976–2017)	Model version					
Inflow (ML/y)	**v1a**	**v1b**	**v1c**	**v2a**	**v2b**	**v2c**
Recharge	7,274	5,315	8,325	7,395	5,277	7,921
Layer 2 inflow	4,285	6,567	5,714	7,512	7,483	7,308
Tertiary Sand inflow				3,047	3,029	2,602
Boundary inflow	3	3	2	1	1	2
Storage inflow	3,627	2,696	3,732	4,737	3,689	5,060
Surrounding QL inflow	927	786	1,200	1,680	1,869	1,513
Outflow (ML/y)						
Coastal discharge	3,706	3,972	5,042	6,263	5,172	7,206
Pumping	5,436	5,436	5,436	5,436	5,436	5,436
Evapotranspiration	4	7	10	14	8	18
Layer 2 outflow	3,103	2,797	3,985	6,429	5,312	5,393
Tertiary sand outflow				414	429	355
Storage outflow	2,802	2,161	3,274	3,864	2,846	4,259
Surrounding QL outflow	1,066	995	1,228	1,951	2,147	1,740
Total inflow (ML/y)	16,116	15,367	18,973	24,372	21,348	24,406
Total outflow (ML/y)	16,117	15,368	18,975	24,371	21,350	24,407
Percent error (%)	-6.2E-03	-6.5E-03	-1.1E-02	4.1E-03	-9.4E-03	-4.1E-03

Table 5.3. Average contemporary (2008–2017) mass balance for all six versions of the model

Contemporary (2008–17)	Model version					
Inflow (ML/y)	**v1a**	**v1b**	**v1c**	**v2a**	**v2b**	**v2c**
Recharge	6267	4665	7720	6497	4620	6455
Layer 2 inflow	3093	5697	4746	7366	7344	7164
Tertiary Sand inflow				2827	2813	2426
Boundary inflow	4	3	3	1	1	2
Storage inflow	2763	2010	3021	3434	2511	3392
Surrounding QL inflow	701	657	972	1425	1631	1270
Outflow (ML/y)						
Coastal discharge	2098	2747	3601	5013	4013	5459
Pumping	5328	5328	5328	5328	5328	5328
Evapotranspiration	0	1	3	6	3	6
Layer 2 outflow	2160	2182	3393	5423	4407	4289
Tertiary sand outflow				406	424	351
Storage outflow	2542	2007	3155	3644	2806	3806
Surrounding QL outflow	699	768	982	1730	1939	1470
Total inflow (ML/y)	12828	13032	16462	21550	18920	20709
Total outflow (ML/y)	12827	13033	16462	21550	18920	20709
Percent error (%)	7.80E-03	-7.67E-03	0.00E+00	0.00E+00	0.00E+00	0.00E+00

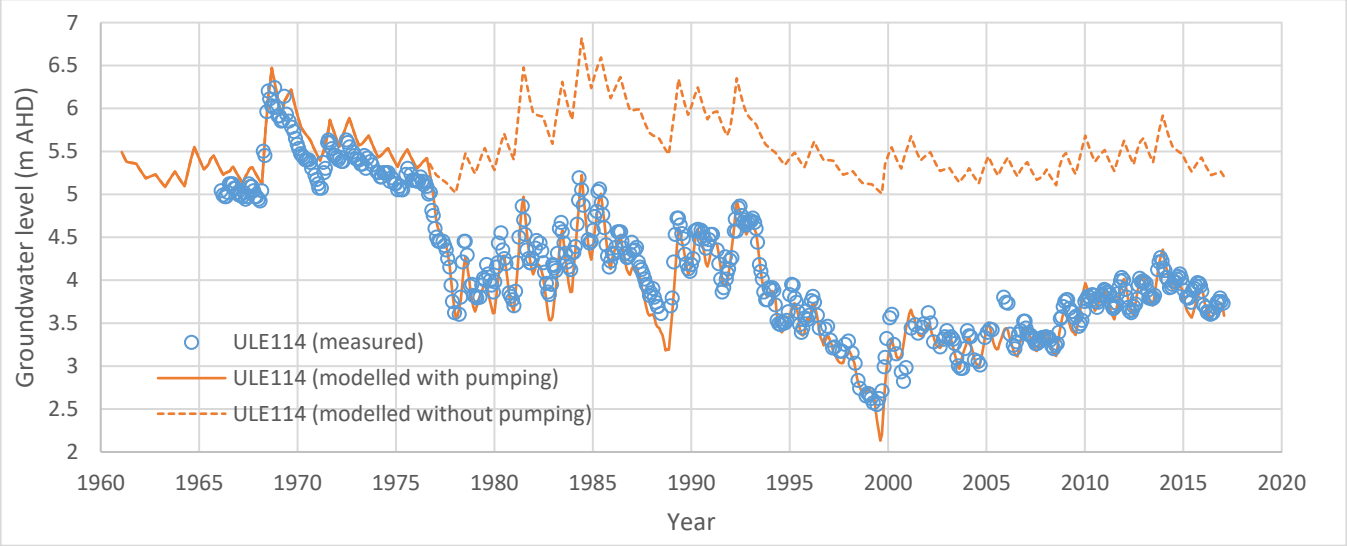


Figure 5.23. Simulated groundwater levels at ULE190 for the calibrated model (solid orange line) and with no pumping (dashed orange line)

The models do not simulate solute transport, which limits their application in determining risks to salinity in town water supply wells from increased inflow from the TS aquifer (see Section 2.5.9). However, some of the models do show temporal trends in inflow from Layer 2 (TS) to Layer 1 (QL) in the town water supply area that show similar trends to salinity in TWS 3/20 (Figure 5.24). Model version 1c in particular shows periods of sustained net inflow from TS to QL (total inflow from L2 to L1 minus total outflow from L1 to L2) corresponding with the period of higher salinity in TWS 3. This is distinct from the other models, which show sustained net inflow from TS to QL, as salinity in TWS3 was decreasing. Thus, model version 1c broadly matches the conceptual model of increased inflow from the underlying TS, resulting in increased salinity in the TWS well field. It should be noted that the salinity trend in TWS 3 is not observed in other town water supply wells; hence, while the overall flux from TS to QL in model version 1c 'fits the data', there may be spatial variability in fluxes between layers not captured by the models. Improving this would require an upgrade to a solute transport model to simulate salinity trends in the town water supply wells.

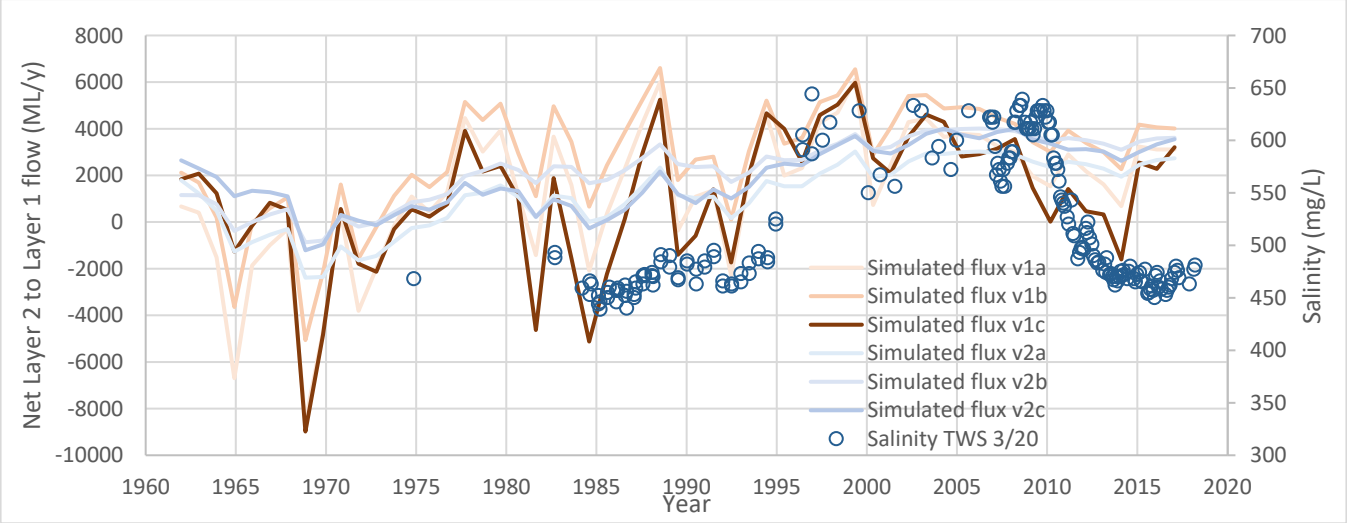


Figure 5.24. Modelled net inflow from Layer 2 (TS) to Layer 1 (QL) (positive values are net inflow, negative values are net outflow) in the TWS area in all six models, with measured salinity in TWS 3 and TWS 20

5.5 Seawater interface simulations

The SWI2 package (Bakker et al., 2013) was used to simulate the position and movement of the saltwater-freshwater interface in the Uley South Basin. Model results show the impact of basement outcrops and model layering on the position of the interface (Figure 5.25), with the coastal zone essentially being divided in two by basement outcrops in the area referred to as Shoal Point East by Bestland (2010). The different models simulate different toe locations for the seawater wedge in the QL aquifer, owing to different fluxes and aquifer parameters in the different models (Table 5.4). It should be noted that implementation of the SWI2 package in this project means the toe represents the 50% seawater-freshwater interface. The results are within the ranges reported by previous studies for post-development conditions. Werner and Dang (2013) and Badaruddin (2017) show the toe migrating further inland under post-development conditions. However, these models simulate seawater intrusion using MODHMS and SEAWAT (respectively) which consider full dispersive mixing. Thus, simulating the 50% seawater-freshwater interface using SWI2 may underestimate the full extent of seawater intrusion into the aquifer.

Table 5.4. Simulated maximum inland extent of the 50% seawater-freshwater interface toe in the QL aquifer in December 2017

Model version	Maximum inland extent of toe in QL aquifer, western half of basin (m)	Maximum inland extent of toe in QL aquifer, eastern half of basin (m)
1a	740	770
1b	785	568
1c	720	836
2a	561	648
2b	450	794
2c	508	988

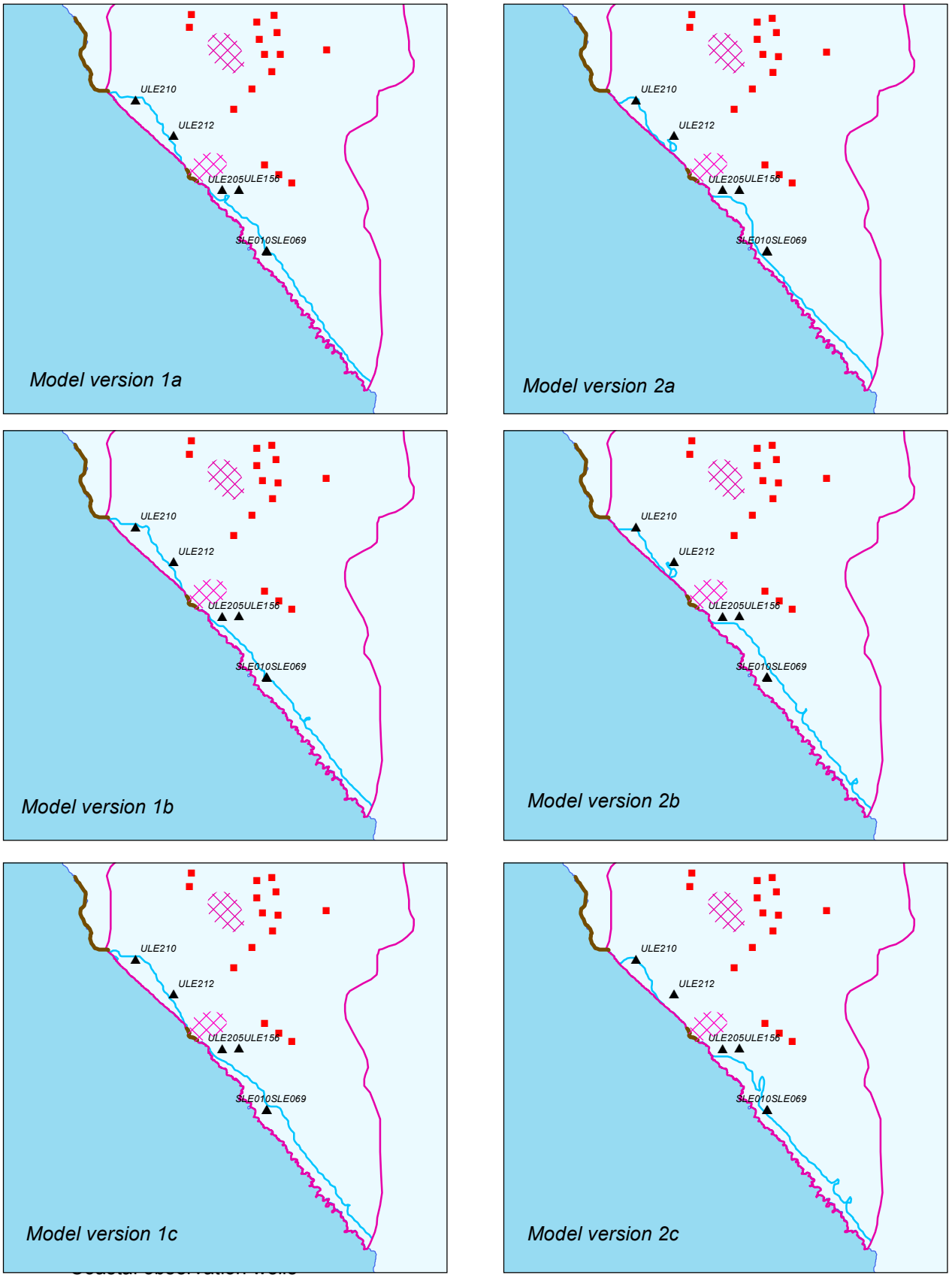


Figure 5.25 Simulated seawater interface toe locations in the QL aquifer, December 2017

As discussed in Section 2.5.10, measurements of the position of the seawater-freshwater interface over time in Uley South are limited to vertical profiles in wells SLE010, SLE069 and ULE205. SLE069 is of particular interest, as it shows the seawater-freshwater interface being present in the QL aquifer. These measurements have been made in long-screened wells which straddle both the QL and TS aquifers, and thus may give an inaccurately high measurement of the interface elevation, due to hydraulic 'short-circuiting' in the well (Shalev et al., 2009). Nevertheless, they provide the only available information on the relative position of the interface over time. Thus two metrics regarding the position of the interface over time are plotted in Figure 5.26: (1) the depth over which there is a transition between freshwater and seawater from measurements in SLE069 (and SLE010 in 1962) and (2) the depth at which the 50% seawater-freshwater salinity is observed in salinity profiles. The 50% salinity here is 30,535 µS/cm, which is the mid-point between freshwater and seawater, based on minimum and maximum salinities measured in the sonde profiles of 1350 µs/cm (fresh) and 59,720 µS/cm (saline) in the salinity profiles.

The simulated elevation of the interface at location SLE069 over time varies for each of the models. Model versions 1c and 2b appear to give the most accurate position of the interface over time (Figure 5.26). These models still generally plot the 50% interface lower than that observed in the sonde profiles; however, as discussed earlier, the long screen in well SLE069 may be raising the interface position (Shalev et al., 2009). Some of the models, such as versions 2a and 2c, show the interface elevation 10–12 m lower than these models. Again, observations of the interface elevation are limited and hence the reliability of these results is difficult to constrain. But based on observations in SLE010 and SLE069, it would appear these models significantly underestimate the position of the seawater interface.

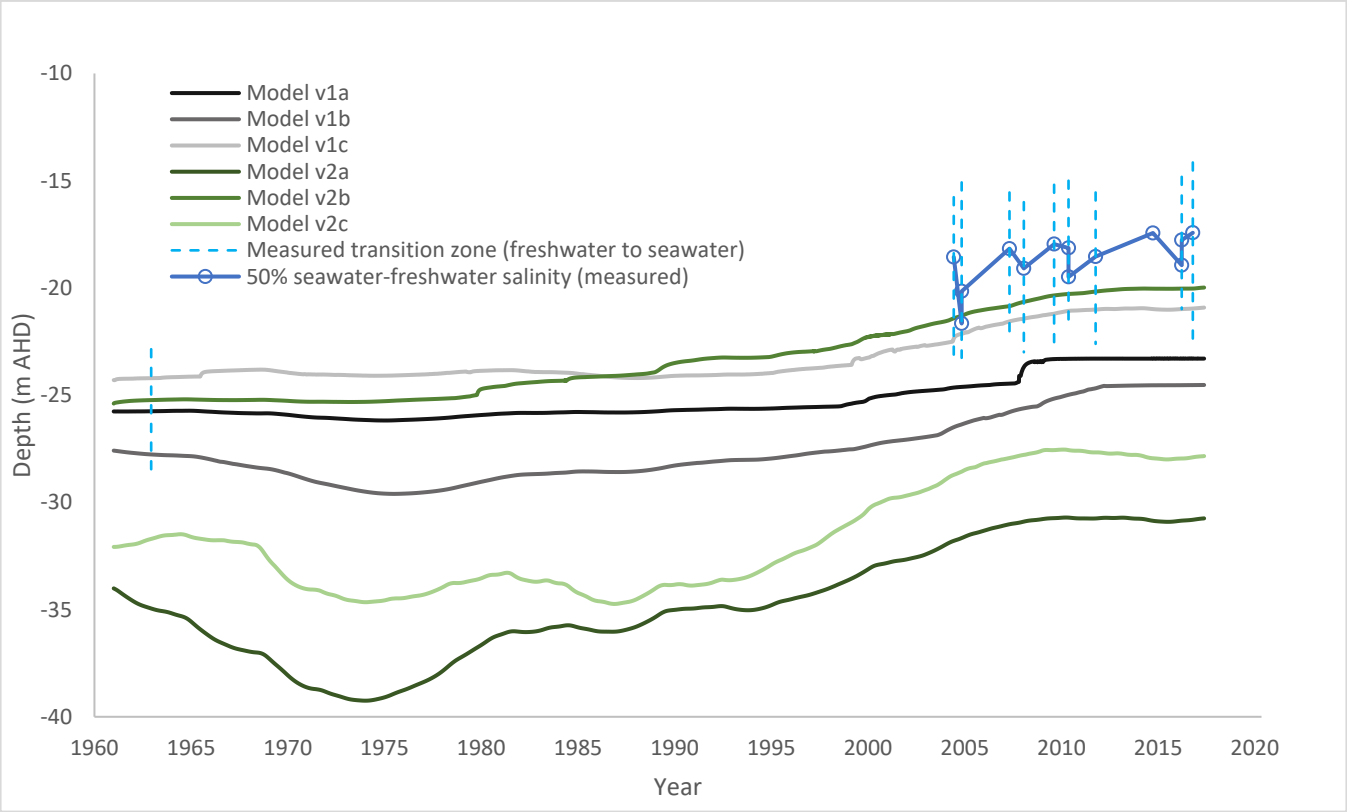


Figure 5.26. Simulated and measured elevation of the seawater interface in SLE010 (1962) and SLE069 for all six models

In the vicinity of SLE069, the TC is generally absent (Figure 2.5), hence the model simulates Layer 2 as higher hydraulic conductivity than the surrounding TC formation in this area (Figure 4.9). Consequently, the interface intrudes further inland in the underlying TS aquifer (Figure 5.27). It should be noted here that model basement elevations (Layer 3 bottom in Figure 5.27) are based primarily on basement elevations from drillhole data.

Interpreted basement elevations from AEM data (Fitzpatrick et al., 2009) have not been used to assign basement elevations in the model at this location due to difficulties correlating AEM-derived aquifer elevations with observed data from drillholes (Somaratne et al., 2018). Hence the full TS thickness may be underestimated in some parts of the model domain, and the modelled inland extent of the interface in the TS formation (Figure 5.27) can only be considered indicative. Furthermore, the AEM data described in Fitzpatrick et al. (2009) does not cover the coastal zone where SLE069 is located, possibly due to the presence of the Cathedral Rocks Wind Farm. Hence it is difficult to correlate modelled seawater interface with AEM interpreted conductivity with depth. Further work could be done in future to re-interpret the AEM data to better constrain basement elevation and to fill in gaps in the AEM data near SLE069, possibly with ground-based geophysics.

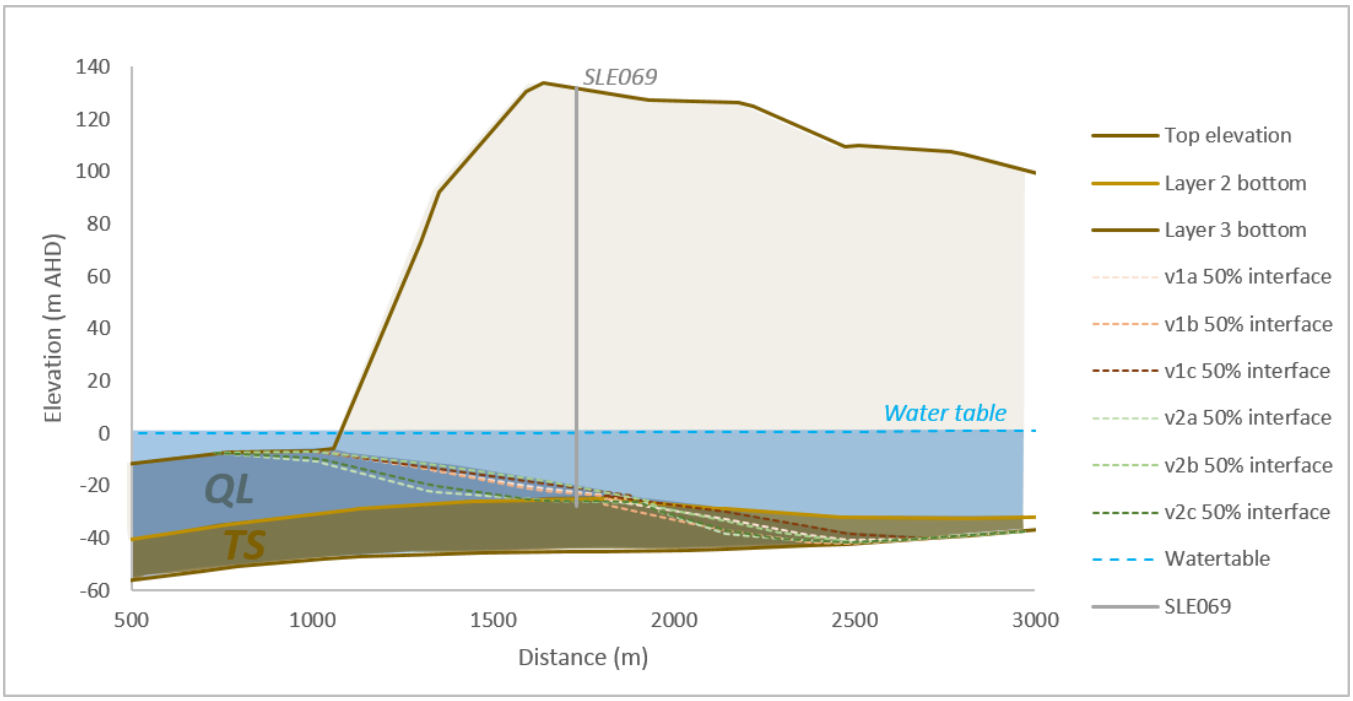


Figure 5.27. Simulated inland extent of the seawater interface parallel to coast (transect running through SLE069)

5.6 Summary of transient models

The modelling approach considers conceptual uncertainty and stakeholder concerns regarding aquifer connection (TS flow into QL) and recharge. The result is a suite of six transient groundwater flow models, calibrated to groundwater level. All models reproduce groundwater levels reasonably well. However, not all models give accurate representations of the position of the freshwater-seawater interface over time, noting that measurements of the interface are limited.

One of the key purposes of the modelling is to simulate the potential future impact of different climate and recharge scenarios on groundwater resources in the Uley South Basin. The key risks to groundwater resources in Uley South include depletion of groundwater levels, increased salinity from TS inflow, and seawater intrusion. Thus, for the purposes of running scenarios, only the models which give the most accurate simulation of the seawater interface (version 1c and 2b) will be considered further. Model version 1c also gives the soundest representation of Layer 2 inflow to Layer 1 in terms of matching salinity trends in the QL aquifer (Figure 5.24).

6 Model uncertainty and limitations

6.1 Uncertainty analysis

Uncertainty in groundwater model results arise from multiple sources. Middlemis et al. (2019) discuss four primary sources of uncertainty:

- structural/conceptual uncertainty – hydrogeological conceptualisation assumptions applied to the model, which cannot be varied in an automated way to assess uncertainty;
- parameter uncertainty – hydrogeological property assumptions applied to the model, which can be varied in an automated way;
- measurement error – uncertainty associated with measured values used in the model (e.g. groundwater level) or upscaling/downscaling issues (e.g. climate data);
- scenario uncertainty – assumptions applied to future scenarios (e.g. future climate, future groundwater extraction. time-varying boundary conditions and land use change).

The development of six models in this study goes some way to address conceptual uncertainty in TS flow into the QL aquifer and uncertainty in recharge. Further areas of conceptual uncertainty can be identified such as thickness of the TS aquifer, location and movement of the seawater interface, and vertical connection between the TS and QL aquifers in the TWS well field as it relates to salinity variations in the QL aquifer (section 2.5.9). However, further studies may be required before considering multiple models to address conceptual uncertainty in these processes (see Recommendations in Section 8.2).

As discussed in section 5.5, model versions 1c and 2b give the most accurate representation of the seawater interface (based on limited data), hence for the purpose of running scenarios these two models are used to capture some of the conceptual uncertainty in predictions. To address the impact of parameter uncertainty on model results, a null space Monte Carlo uncertainty analysis was run on model version 1c using PEST (Doherty 2010). PEST utilities were run through the Groundwater Vistas GUI to generate 1000 parameter sets. This was done with the utility FIELDGEN, which creates 'noisy' parameter fields based on the variogram (structure) used in kriging pilot point values in the original model calibration (where kriging options were based on the recommendations in Rumbaugh and Rumbaugh (2017)). The utility PPSAMP then takes pilot point values from these fields, before the PNULPAR utility assembles parameter value files that PEST uses as starting point in each parameter set (Doherty, 2007). The parameters varied were hydraulic conductivity, specific yield, storage and recharge multipliers. The degree to which the calibration performance of the 1000 models was affected was determined by assessing their objective function:

$$\emptyset = \sum(w_i r_i)^2 \qquad (6)$$

Where ϕ is the objective function for i measurements, r is the residual (difference between modelled and measured groundwater level) and w is the weight assigned to observations. Of the 1000 random parameter sets, 355 had objective functions within 20% of that of the calibrated model (where the original ϕ was 23,899, Figure 4.1).

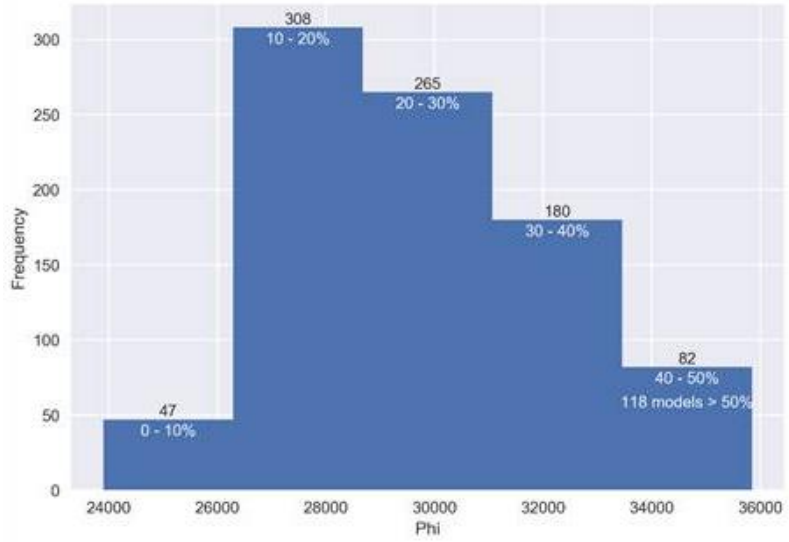


Figure 6.1. Range of objective function values for models generated for the null space Monte Carlo simulations

The mean modelled groundwater level, plus the distribution of results from all 1000 models for well ULE114 shows that all models generally fit the trend in groundwater levels quite well (Figure 6.2). ULE114 is used for illustrative purposes, as it is located close to the central TWS well field and models generally reproduce trends here well. However, despite the generally good fit, some models show overall misfit of >1 m. The weighted mean and 95% confidence intervals for the subset of 355 models with ϕ within 20% of the original calibrated model show a narrower distribution (Figure 6.3). Here the mean is weighted based on the objective function (weight = 1/objective function) to give greater weighting to models with lower objective functions. Figures 6.4–6.7 show the weighted mean and 95% confidence intervals for all wells with long term observation records and wells located close to town water supply pumping wells.

As described by Tonkin and Doherty (2009), these new parameter fields can be recalibrated with a small number of model runs. However, early attempts to recalibrate all models proved too time consuming, as the calibration performance of some models was significantly affected due to model non-linearity. Hence for using the models in scenarios, the 47 models with an objective function (measurement of model error) within 10% of the calibrated model were selected, similar to the study described by Hayes and Nicol (2017).

The results of the parameter uncertainty on one model (version 1c), in terms of the distribution of modelled groundwater levels at ULE114, is similar to that given by considering all six conceptual models (Figure 6.3). However, a quantitative comparison between conceptual and parameter uncertainty would require further work including re-calibrating alternative parameter sets, and investigating conceptual model differences, possibly with model averaging techniques (Ye et al. 2010). Nevertheless, both parameter and a degree of conceptual model uncertainty have been considered, and results generally show a good match between measured and modelled groundwater levels and trends. Consequently, the impact of uncertainty on model predictions will be demonstrated by displaying distributions of predicted groundwater levels.

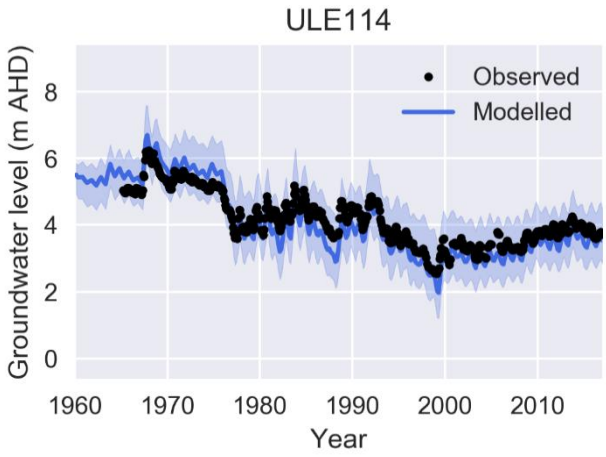


Figure 6.2. Mean (solid blue line) and range (blue cloud) of modelled groundwater levels at ULE114, based on 1000 model runs with different parameter sets

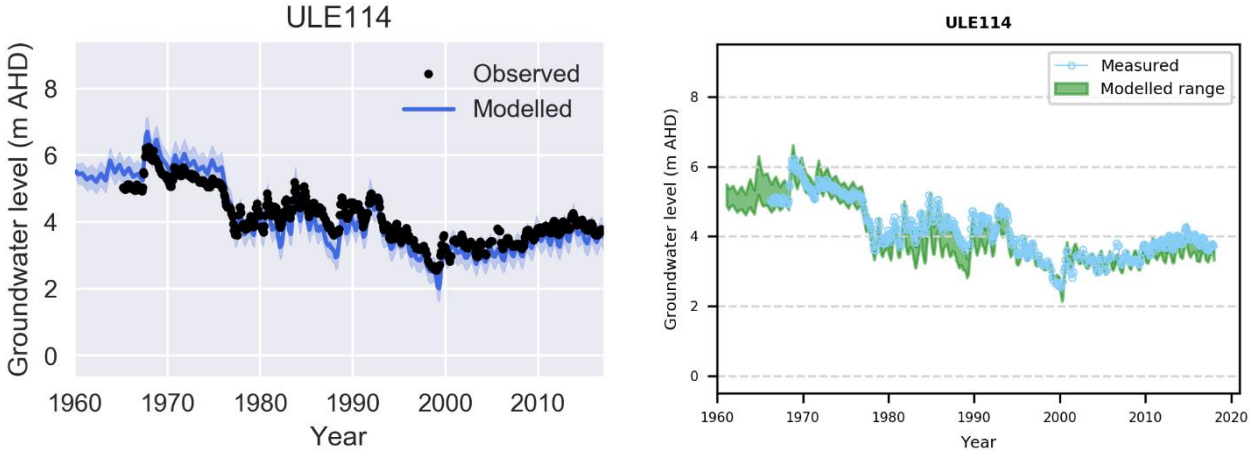


Figure 6.3. Weighted mean (solid blue line) and 95% confidence interval (blue cloud) of modelled groundwater levels at ULE114, based on 355 models with phi <20% of original model (left figure) and modelled range of groundwater levels from all six calibrated conceptual models (right figure)

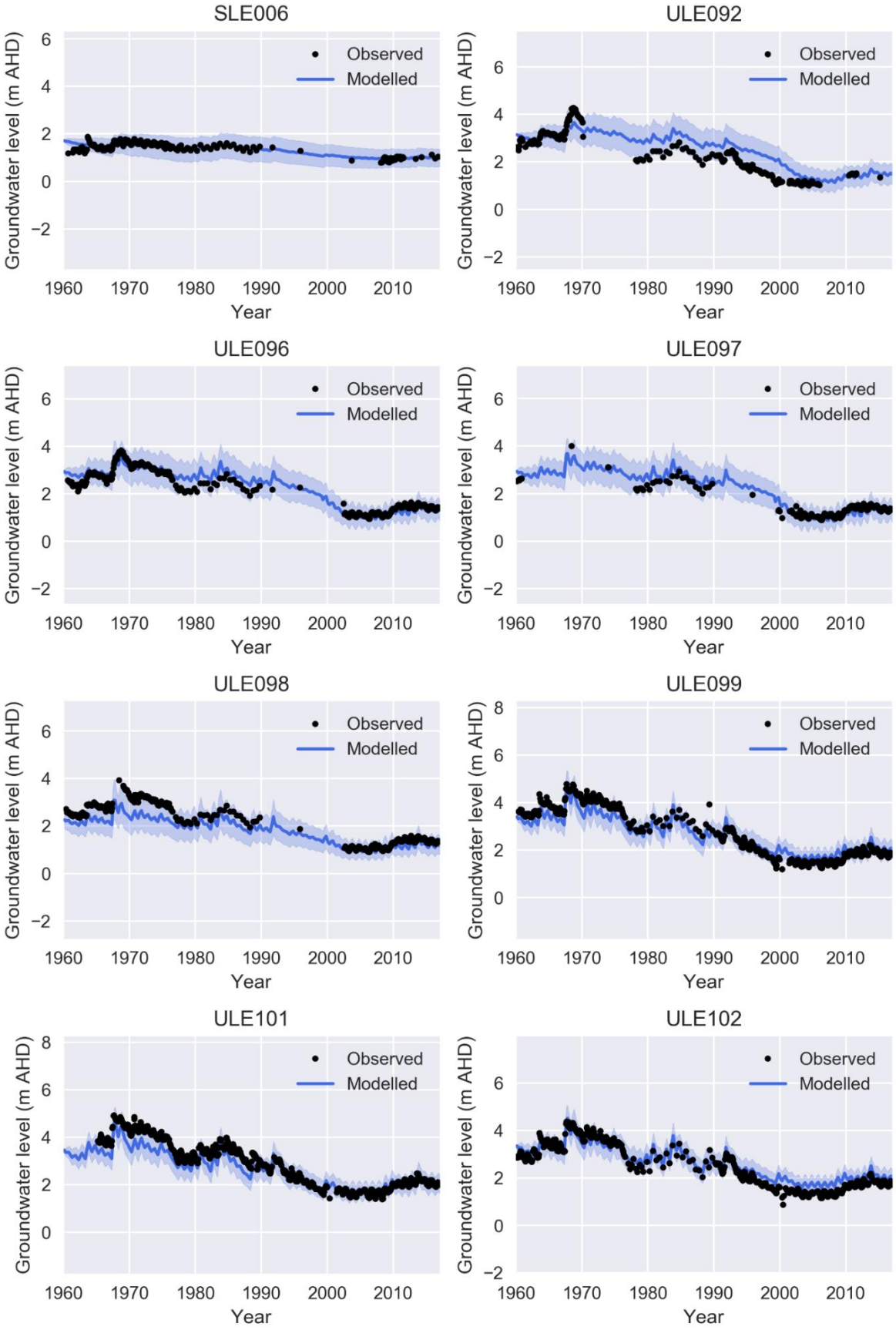


Figure 6.4. Weighted mean (solid blue line) and 95% confidence interval (blue cloud) of modelled groundwater levels (SLE006–ULE102), based on 355 models with phi <20% of original model

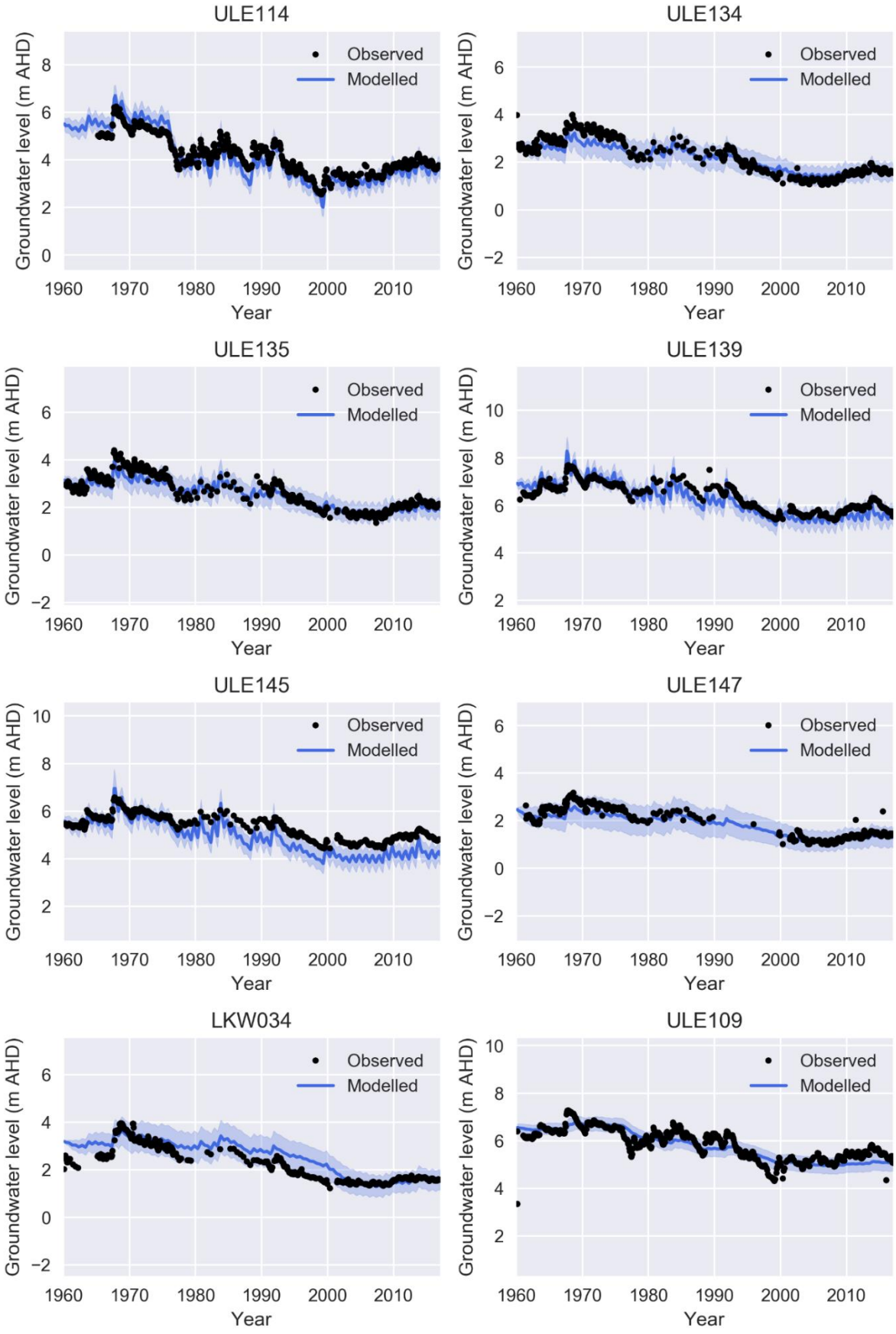


Figure 6.5. Weighted mean (solid blue line) and 95% confidence interval (blue cloud) of modelled groundwater levels (ULE114–ULE109), based on 355 models with phi <20% of original model

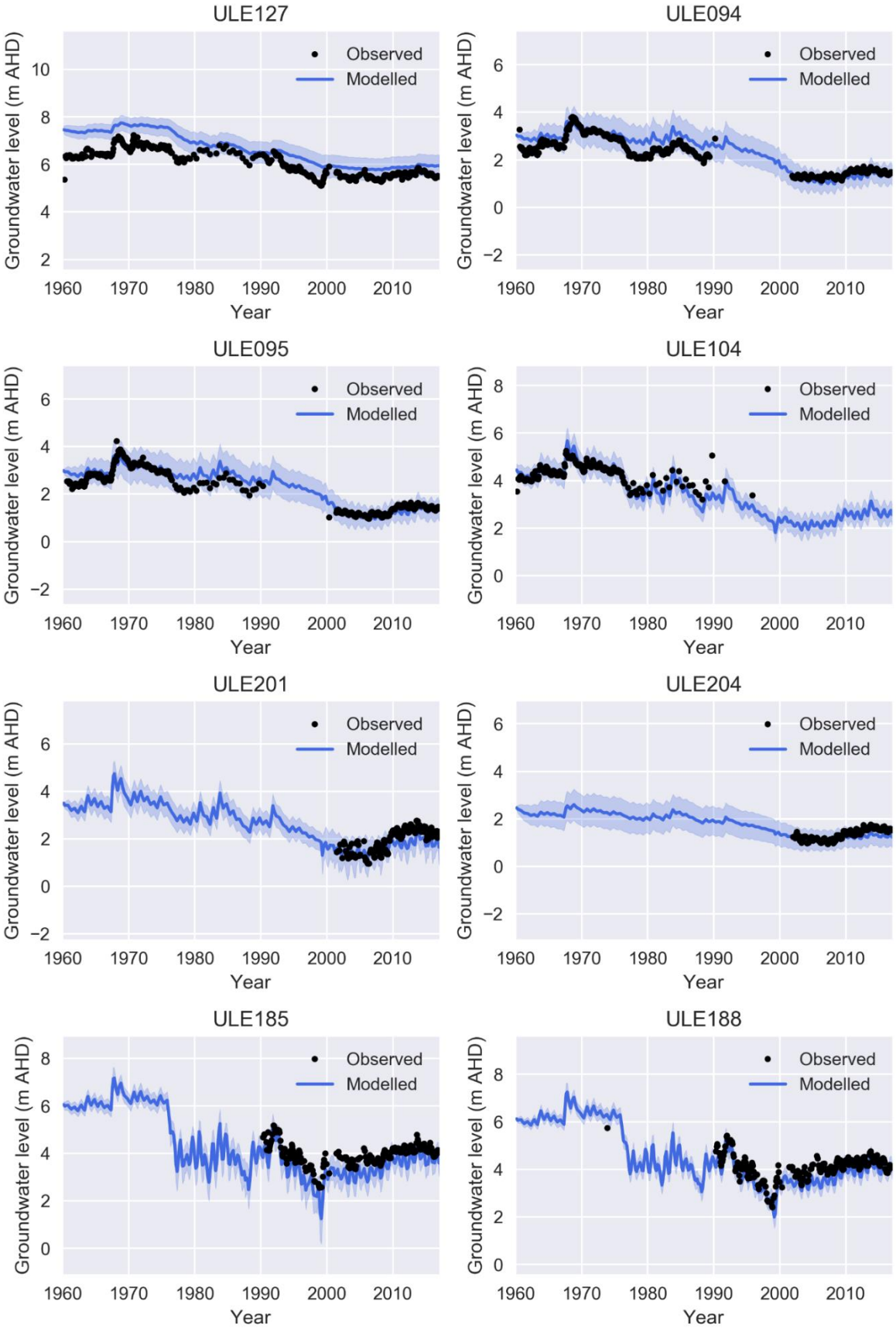


Figure 6.6. Weighted mean (solid blue line) and 95% confidence interval (blue cloud) of modelled groundwater levels (ULE127–ULE188), based on 355 models with phi <20% of original model

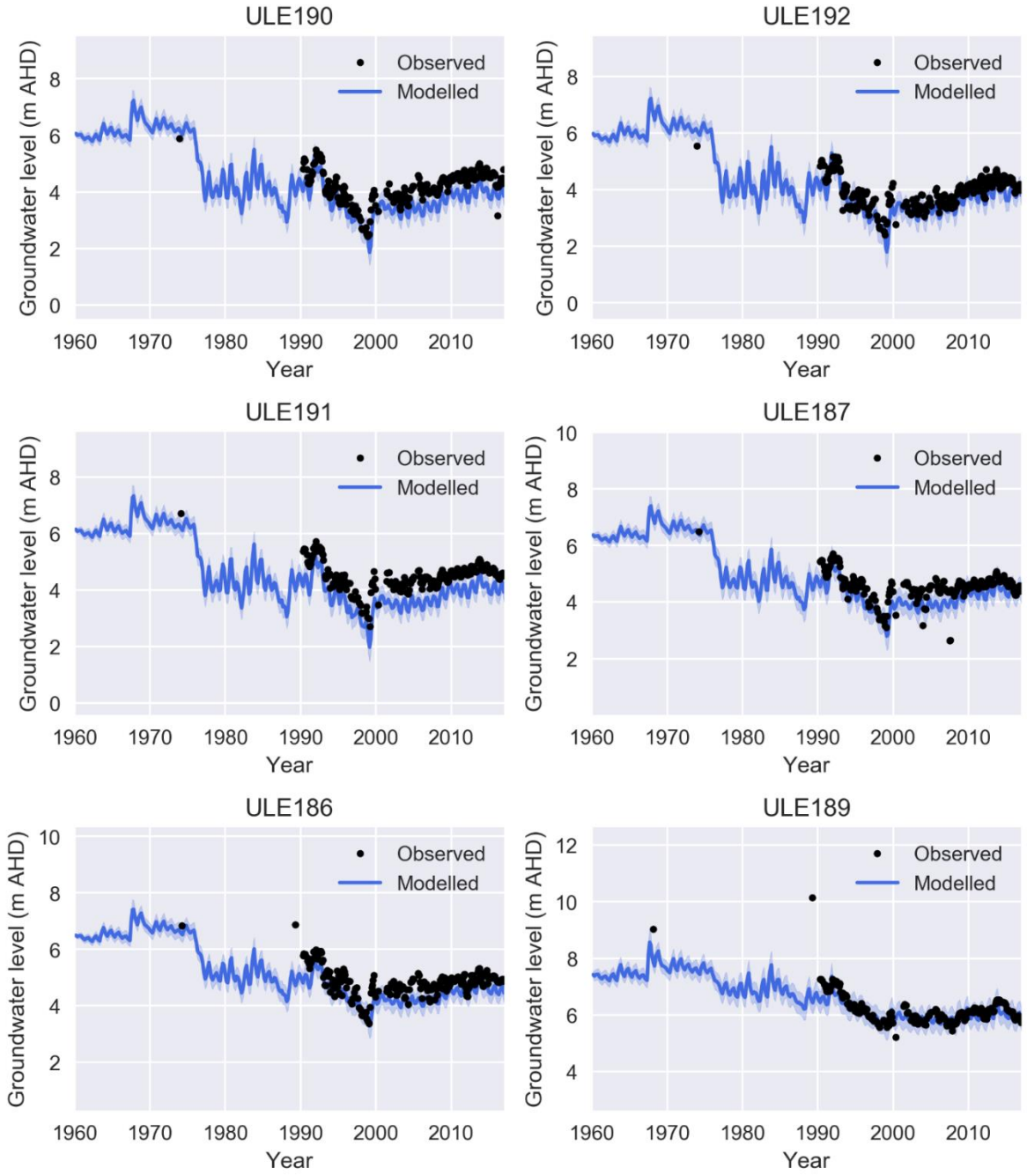


Figure 6.7. Weighted mean (solid blue line) and 95% confidence interval (blue cloud) of modelled groundwater levels (ULE190–ULE189), based on 355 models with phi <20% of original model

6.2 Model capability, limitations and uncertainty

It is important to define the model capabilities and limitations, in order to manage expectations on the model results.

The capability of the model reflects its intended purpose to simulate the potential impact of different pumping and climate change scenarios on groundwater levels and position of the seawater interface in the QL aquifer, and can be summarized as follows:

- The model is capable of simulating historical groundwater levels in the QL aquifer in the Uley South Basin. The inclusion of multiple models with different recharge and TS inflow setups helps address combined conceptual and parameter uncertainty. The modelled groundwater level fluctuations from the 6 model versions match observed levels, and declines are shown to be driven mainly by changes in pumping over time (Figure 5.23) as well as changes in recharge, consistent with findings from previous studies.
- Two versions (v1c and v2b) of the model are capable of simulating the position and movement of the seawater interface in the QL aquifer in a way that is consistent with the limited data available (Figure 5.26).
- One model version (1c) has also been subject to parameter uncertainty analysis (K_h, S_y, S and recharge), as it gives the best simulation of the seawater interface as well as the net inflow from the TS to QL aquifers (layer 2 to layer 1) consistent with QL salinity trends.

Two versions of the model (v1c and v2b) may be used to simulate the potential impact of future groundwater extraction and recharge scenarios on groundwater levels and position of the seawater interface in the QL aquifer in the Uley South Basin. The model limitations also stem from its intended purpose, and can be summarized as follows:

- The model simulates groundwater flow and movement of the seawater interface, not solute transport. While changes in flow between layers appear to match changes in salinity in the TWS well field for some versions of the model (Figure 5.24), the model cannot be used to simulate or predict changes in salinity over time (although the model forms a suitable basis to develop a solute transport model in the future).
- The model simulates seawater interface movement with the SWI2 package (Bakker et al., 2013). Hence only the 50% seawater-freshwater interface is simulated as a 'sharp interface'. The full extent of seawater intrusion and dispersive mixing at the interface may therefore be underestimated.
- While the model simulates flow in the QL and TS aquifers, observation data and knowledge of the full TS thickness is limited compared to the QL aquifer. Further data such as TS thickness, possibly derived through re-interpretation of the AEM data (Fitzpatrick et al., 2009) would be required before the model can be used to predict changes in seawater intrusion in the TS aquifer over time.

Some of the model limitations arise from knowledge gaps and areas of conceptual and parameter uncertainty. While uncertainty analyses can constrain the impact on model predictions, in some cases additional studies and data may be required. Key areas that would benefit from additional studies and data are also discussed further in recommendations (Chapter 8) and include:

- Position and movement of the seawater interface in the QL and TS aquifers – regardless of the ability to simulate these processes, improved understanding and monitoring of the position of the seawater interface in Uley South is needed. This is unlikely to be achieved through monitoring salinity profiles in observation wells with long screens (see discussion in section 5.5).
- Hydraulic parameters in the coastal zone – the majority of aquifer test parameters that are available in Uley South are for the TWS area in the centre of the basin. However, the simulation of seawater interface at the coast may be sensitive to variations in aquifer parameters in near-coastal areas. This sensitivity has not been fully explored in this study, and such a sensitivity analysis would benefit from more information on hydraulic parameters of the QL aquifer close to the coast.
- Thickness and extent of the TS aquifer – as discussed in limitations, the model may not be suitable for predicting the full extent of seawater intrusion in the TS aquifer, due to limited knowledge of the full TS thickness and extent in the coastal area.
- TS flow into QL at the basin boundary – this process is conceptualised to occur, and has been simulated in two different ways in this study. However, modelled fluxes are not currently constrained by estimates, which would require further studies.

- Inter-aquifer mixing within the basin and its impact on TWS salinity – the models do not simulate solute transport, and further information on the spatial variability of salinity in the TS aquifer would be required to accurately simulate inter-aquifer mixing in the model.
- Time series pumping data from extraction wells – despite the advent of metering of individual extraction wells, accurate pumping data is still lacking in Uley South (Figure 2.19), and there is still uncertainty in monthly pumping rates at individual wells in the model.

7 Model scenarios

7.1 Overview

As discussed in the previous chapter, the best-performing model versions 1c and 2b are used for running predictive scenarios. Model scenarios were developed in consultation with SA Water and focus on three groundwater extraction regimes, from 2018 to 2040:

- Extraction 1: Extraction reduces to 3.8 GL/y, assuming water supply to Eyre Peninsula is augmented.
- Extraction 2: Extraction continues at the current rate of 5 GL/y.
- Extraction 3: Extraction increases with time to 6.8 GL/y by 2040, consistent with 50th percentile projections of water demand for Eyre Peninsula excluding supply from the Iron Knob-Kimba pipeline (Department for Environment and Water, 2018b).

In all three regimes, pumping volumes are scaled proportionally from those used during the calibration period. It is worth noting that in extraction scenario 3, extraction rates are increased year by year from 2018 to 2040, to reach a maximum rate of 6.8 GL/y. Thus, the potential impact of a sudden increase in extraction has not been simulated. Each extraction scenario was simulated with two recharge projections from 2018 to 2040, again developed in consultation with SA Water:

- Recharge A: Recharge is based on the previous 10 years recharge (2008–2017) repeated on a cycle.
- Recharge B: Recharge is based on the previous 10 years recharge (2008–2017) repeated on a cycle, with recharge decreasing over time based on climate change projections taken from Charles and Fu (2015a) assuming a high emissions scenario.

Assumptions related to the implementation of climate change scenarios and pumping are discussed further below. Table 7.1 summarises the model scenarios.

Table 7.1. Summary of model scenarios

Scenario	Pumping	Recharge
1A	3.8 GL/y	Recharge based on 2008–17
1B	3.8 GL/y	Recharge based on project climate change (RCP 8.5)
2A	5 GL/y	Recharge based on 2008–17
2B	5 GL/y	Recharge based on project climate change (RCP 8.5)
3A	Up to 6.8 GL/y by 2040	Recharge based on 2008–17
3B	Up to 6.8 GL/y by 2040	Recharge based on project climate change (RCP 8.5)

7.2 Climate change impacts on rainfall and recharge

Climate change impacts on recharge are based on rainfall projections provided by Charles and Fu (2015a), and a relationship between rainfall and recharge provided by Green et al. (2012). Charles and Fu produced climate projections based on downscaled climate simulations from 15 Global Climate Models (GCMs), which were calibrated to observed rainfall at a number of rainfall stations across South Australia, including 28 in the Eyre Peninsula. The calibrated models were used to simulate climate projections based on two Representative Concentration Pathways (RCP) for future greenhouse gas and aerosol concentrations. The RCPs represent an intermediate emission scenario (RCP 4.5) and a high emission scenario (RCP 8.5). Projections are given relative to the 20 year 'baseline' period from 1986 to 2005. For the Eyre Peninsula, Charles and Fu reported median changes

of -7% and -7.5% in annual rainfall by 2030 for RCP 4.5 and 8.5 respectively (the full range is shown in Figure 7.1). The authors made further projections for 2050, 2070 and 2090. However, for groundwater model scenarios run to 2040 in this study, the 2030 climate projections are used.

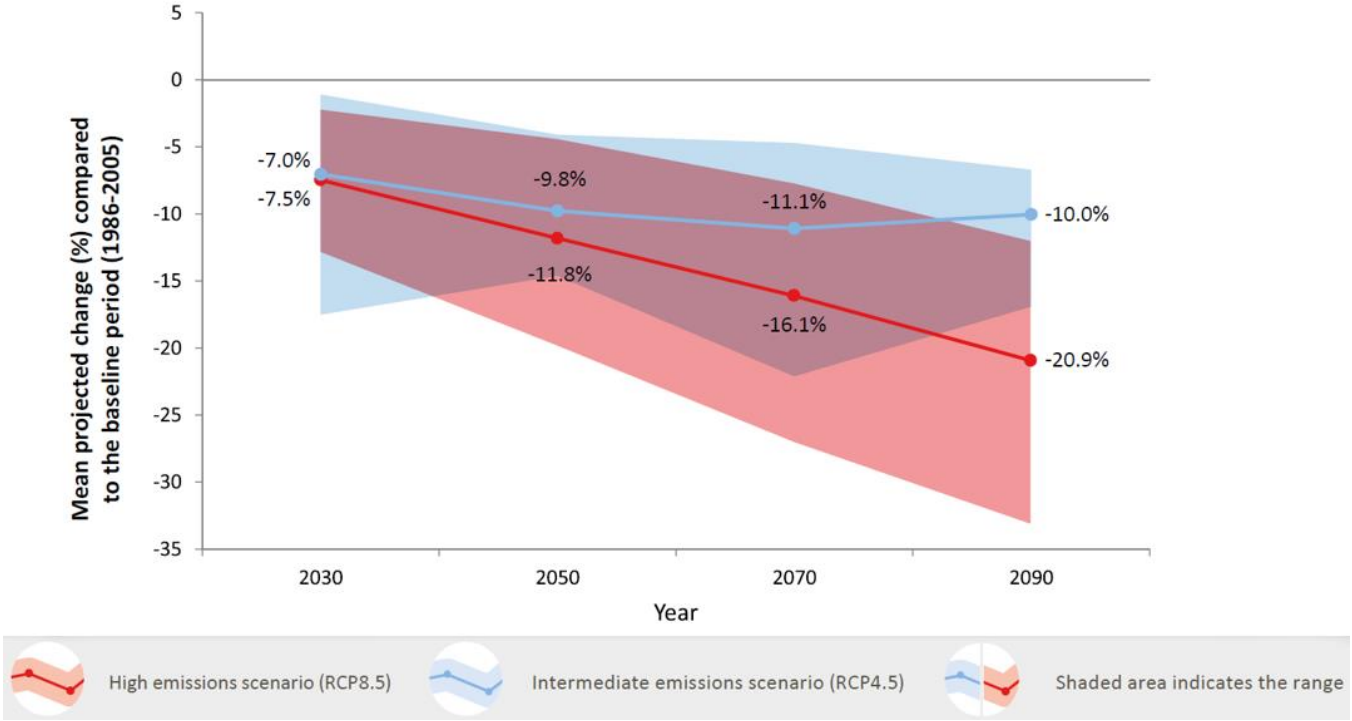


Figure 7.1. Projected changes in mean annual rainfall for the Eyre Peninsula, based on RCP 4.5 (blue) and RCP 8.5 (red), taken from Charles and Fu (2015b).

The changes in rainfall from Charles and Fu (2015a) were scaled to changes in recharge using the relationship between annual rainfall and recharge developed by Green et al. (2012). Green et al. (2012) used unsaturated zone models to simulate rainfall infiltration and drainage past the root zone, which was equated to recharge. Models were developed with parameters based on representative soil and lithology types on the Eyre Peninsula and calibrated to past conditions by comparing drainage fluxes with recharge estimated from the water table fluctuation method. These models were then used to simulate changes in recharge based on future climate data generated by four GCMs and two emissions scenarios (low and high). The results from all models are summarized in Figure 7.2. Relevant to the Charles and Fu annual rainfall projections, the modelling of Green et al. (2012) suggests that -7% and -7.5% changes in annual rainfall will lead to -22% and -24% changes in recharge by 2030.

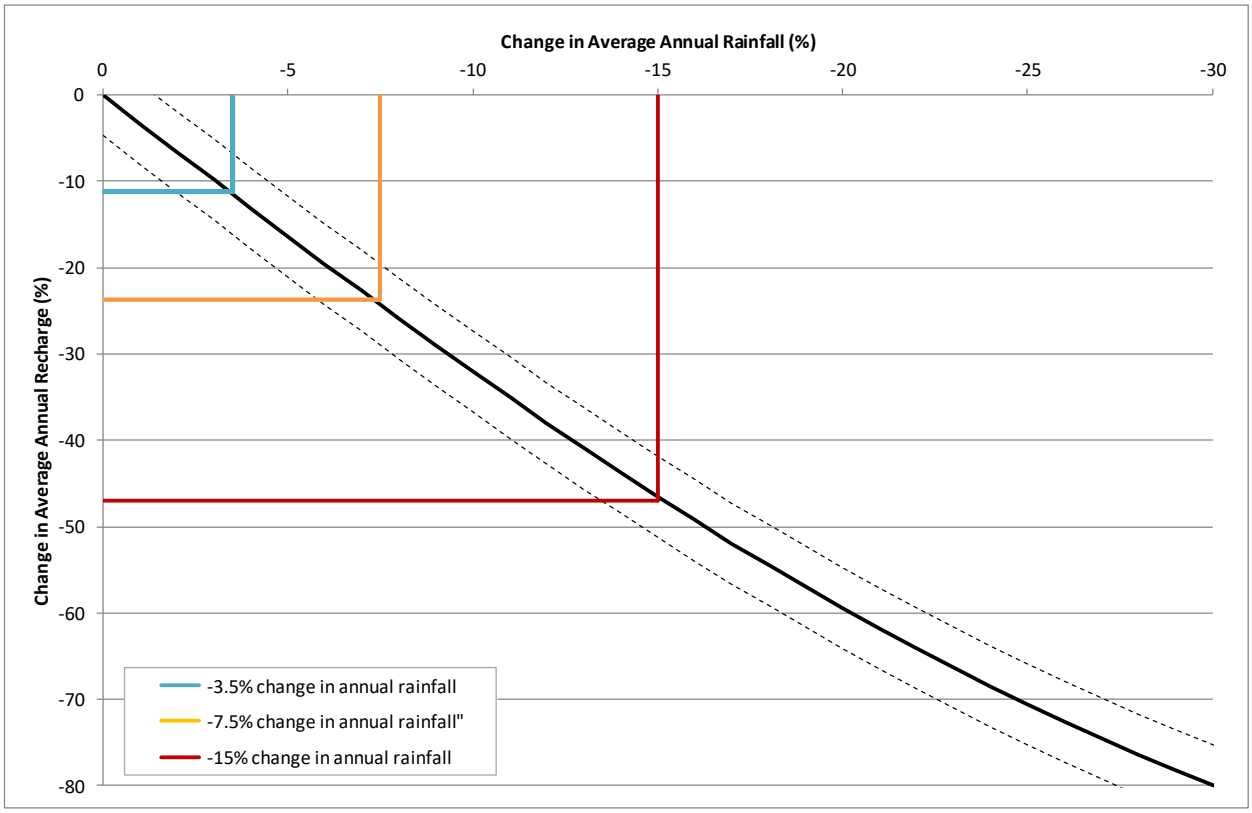


Figure 7.2. Simulated change in average annual recharge for given changes in average annual rainfall based on unsaturated zone modelling, dashed lines represent 95% confidence intervals (figure taken from Green et al., 2012)

The changes projected by Charles and Fu (2015a) are relative to averages for the period from 1986 to 2005. Assuming a constant rate of rainfall decline over 25 years (2006 to 2030), a -22% to -24% change in recharge means a -0.88 % to -0.96% change in recharge per year. These rates compare well with observations of recharge since 2005. For example, recharge calculated using the water table fluctuation method in this study gives an average recharge rate (applied to grassland areas in the model, Figure 4.7) of 95 mm/y for the 1986 to 2005 period. For the period 2006 to 2017, the average is 85 mm/y, which equates to a -0.88% per year change. Although the approach to estimating climate change impacts on recharge is simple and ignores the potential influence of changes in rainfall seasonality, it is considered adequate for the purposes of this study, and consistent with observations over the past 12 years.

In applying these projected changes in recharge to the model, recharge estimates from the last 10 years are used, acknowledging observations of year to year rainfall variability. Recharge is then reduced at a constant rate each year, such that by 2030, the average recharge rate (based on a 10-year moving average) is 22% to 24% less than the 1986 to 2005 average. Thus, for an average recharge rate of 95 mm/y (1986 to 2005 average), the average recharge rate by 2030 is 72 and 74 mm/y for RCP 4.5 and RCP 8.5 respectively (Figure 7.3). Scenarios are further projected to 2040 using the same rate of recharge decline. Given the similarity in projections for RCP 4.5 and 8.5 (Figure 7.3), it was decided to run more conservative simulations using RCP 8.5 only.

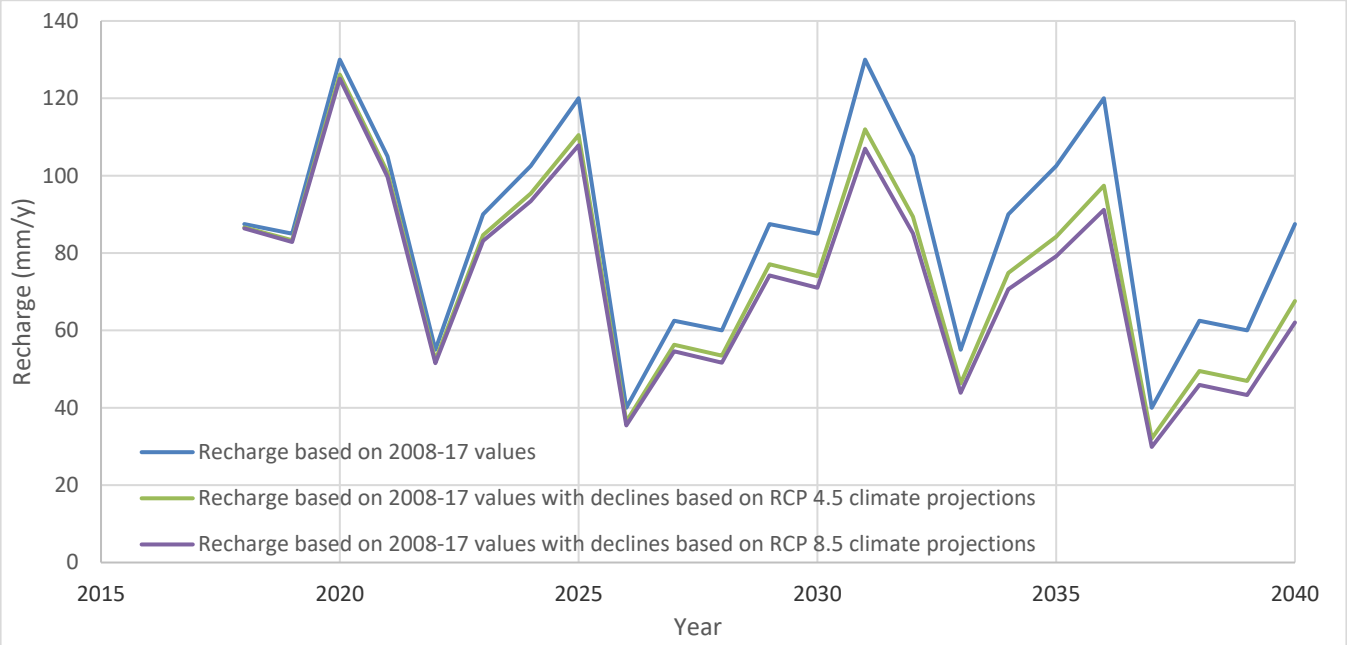


Figure 7.3. Example of scenario recharge time series for model areas where the average recharge from 1986 to 2005 was 95 mm/y

The calibrated models simulate inflow from the TS aquifer in the vicinity of Uley Wanilla with a time-varying general head boundary, where the water level declines from the 1990s onwards based on measured trends in ULE175 and ULE169 (see Section 4.3.1). For scenarios, this declining trend is continued forward to 2040 (Figure 7.4). The assumption here is that declining water levels in Uley Wanilla, thought to be driven by declines in recharge, continue into the future at the same rate. Given that the scenarios assume recharge is projected to decline at a similar rate to that observed in Uley South since 2005, this assumption is considered appropriate.

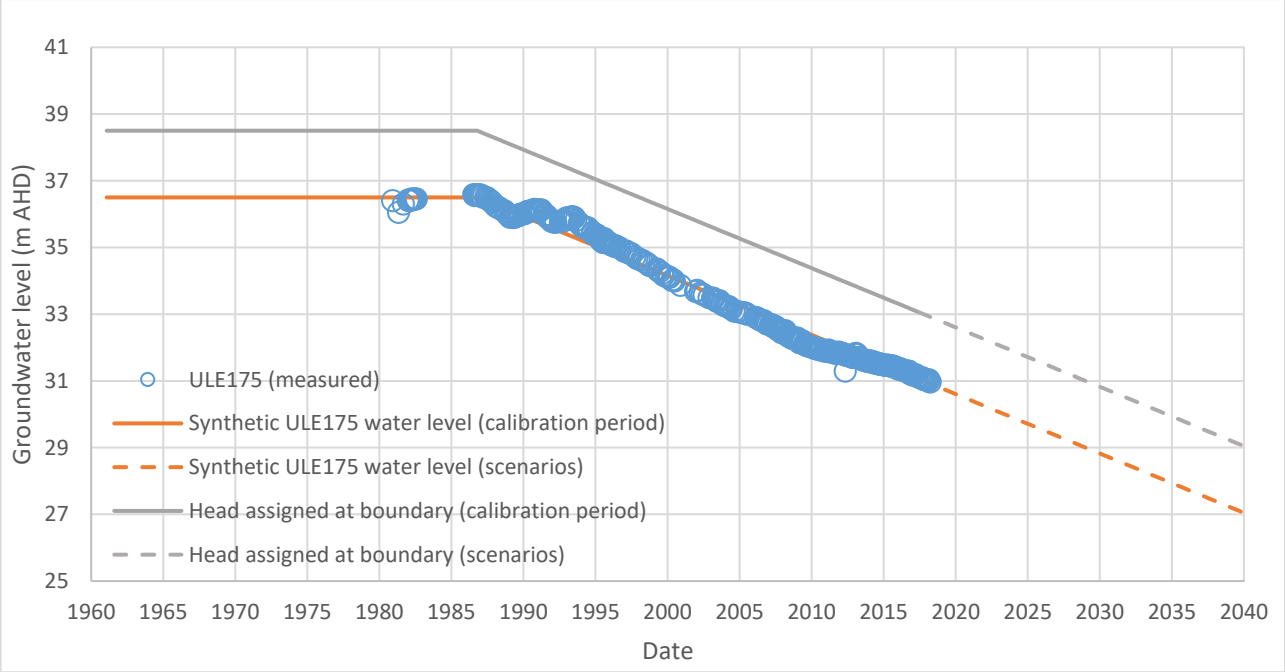


Figure 7.4. Measured and synthetic water levels used as TS boundary inflow from Uley Wanilla

7.3 Scenario results

Scenario results are presented in terms of hydrographs at ULE190 and projected seawater interface movement at SLE069. ULE190 is located closest to TWS 3 and 20, which showed increased salinity in the late 1990s as groundwater extraction increased and groundwater levels declined (Figure 2.22). SLE069 is the one observation well with measurements of the seawater interface in the QL aquifer (problematic as those measurements may be – see discussion in section 2.5.10), against which the performance of SWI2 models has been judged (Figure 5.26).

7.3.1 Scenarios 1A and 1B – pumping 3.8 GL/y

Scenarios 1A and 1B simulate a reduction in pumping from the basin from the current rate of approximately 5 GL/y to 3.8 GL/y, and continued pumping at this rate from 2018 to 2040. A continuation of the last 10 years (2008–2017) rainfall recharge is simulated, as is reduced rainfall recharge from climate change, based on an RCP 8.5 emissions scenario (Section 7.2). With the reduction in groundwater extraction, groundwater levels generally show recovery in the town water supply well field (Figure 7.5). Longer-term declines are observed under the reduced rainfall scenarios; however, groundwater levels only reach a minimum of 3.89 to 4.09 m AHD (for model versions 1c and 2b respectively), which is similar to modelled groundwater levels in 2017. Groundwater levels do not decline to the historic low that was observed in the late 1990s, suggesting that groundwater salinity should not increase in relation to TS inflow (Figure 2.22). The longer-term declines in water level would nevertheless need to be monitored into the future, along with ongoing monitoring of groundwater salinity.

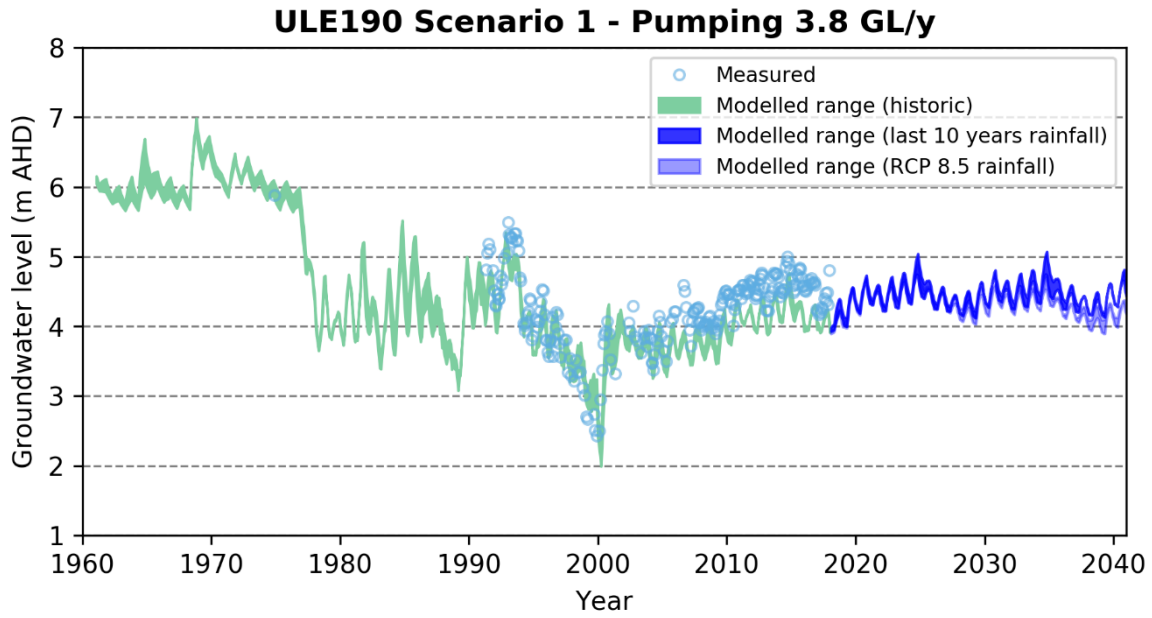


Figure 7.5. Scenarios 1A and 1B: Historic and projected modelled groundwater levels in ULE190 (adjacent to TWS 3/20) with pumping reduced to 3.8 GL/y from 2018 onwards

7.3.2 Scenarios 2A and 2B – pumping 5 GL/y

Since 2011, extraction from Uley South has varied from 4.7–5.4 GL/y (Figure 2.17), thus Scenario 2 continues pumping at a constant rate of 5 GL/y from 2018 to 2040. Both a continuation of the recharge from 2008–2017 and reduced recharge from climate change is simulated. Projected groundwater levels are generally stable to 2025, but show longer-term declines towards 2040 (Figure 7.6). It should be re-iterated here that recharge scenarios are based around the last 10 years rainfall recharge, as requested by SA Water. This data set includes five above and five below average rainfall years – hence the longer-term trends are based on the assumption that an equal proportion of above and below average rainfall continues in the future. This assumption may not be accurate. Predicted groundwater levels do not decline to the historic low recorded in the late 1990s. However, under

reduced rainfall recharge, levels do decline to a minimum of 3.5 m AHD, which is similar to levels recorded in the mid-2000s, when salinity in TWS 3 was higher (Figure 2.22), due to sustained extraction of 5–7 GL/y from the late 1990s to 2010 (Figure 2.17). Thus, under a scenario of continued pumping at 5 GL/y, groundwater level and salinity in the TWS well field would need to be carefully monitored to ensure no adverse trends occur.

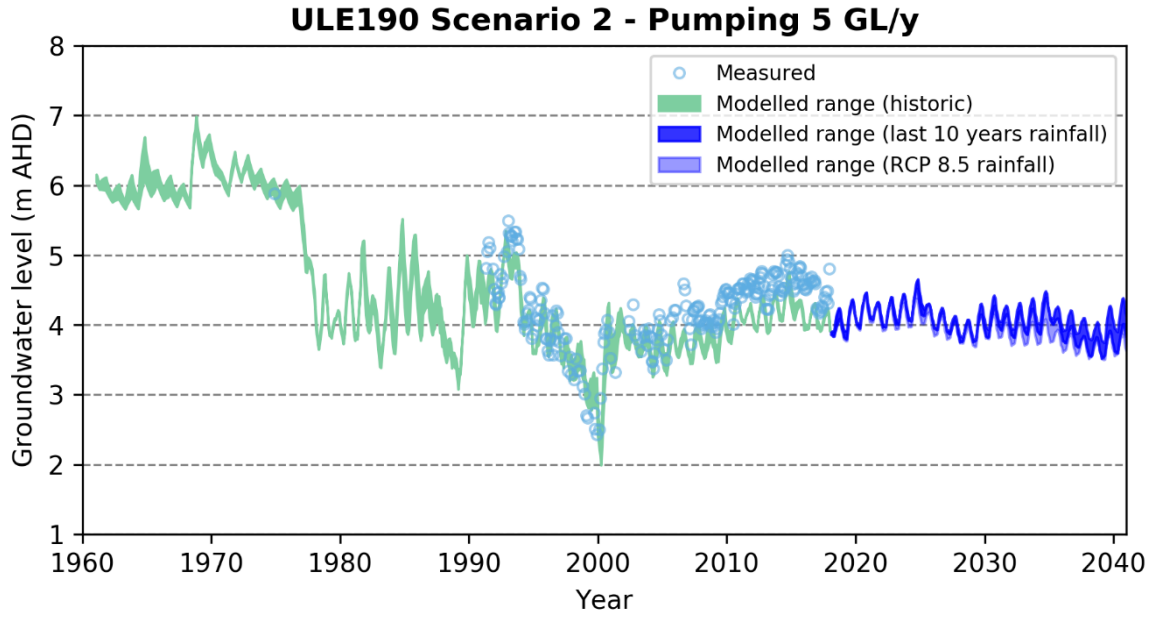


Figure 7.6. Historic and projected modelled groundwater levels in ULE190 (adjacent to TWS 3/20) with pumping continued at 5 GL/y from 2018 onwards

7.3.3 Scenario 3A and 3B – pumping up to 6.8 GL/y

Scenario 3 simulates the impact of an increase in extraction from 5 GL/y to 6.8 GL/y by 2040. The increase in extraction is based on 50th percentile projections of water demand from Uley South assuming supply is not augmented (Department for Environment and Water, 2018b). Groundwater levels are projected to decline under this scenario (Figure 7.7). Declines are greatest assuming reduced rainfall recharge from climate change, with levels reaching a minimum of ~3 m AHD. This level is approaching the same levels observed in the late 1990s when salinity in TWS 3 increased (Figure 2.22), due to sustained extraction of 5-7 GL/y from the late 1990s to 2010 (Figure 2.17). Thus, continued pumping from Uley South to meet projected demand is likely to cause groundwater level decline and a decadal downwards trend, which may in turn impact the salinity of water from production wells. Close monitoring of groundwater level and salinity will be needed if extraction is to increase, and negative impacts to the groundwater resource should be anticipated.

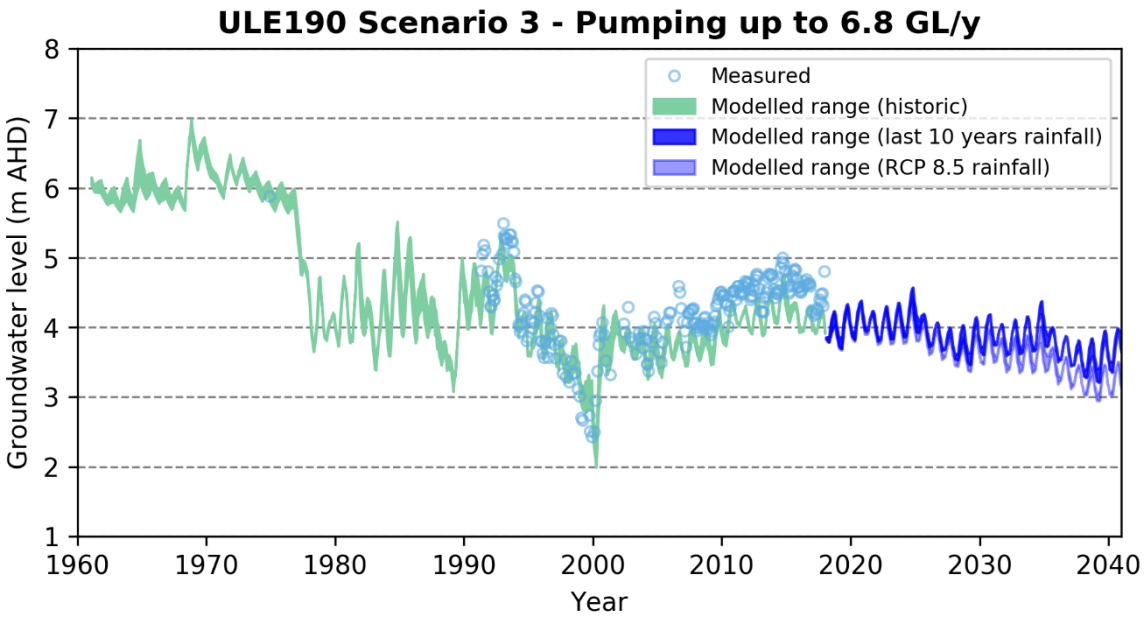


Figure 7.7. Historic and projected modelled groundwater levels in ULE190 (adjacent to TWS 3/20) with pumping increased up to 6.8 GL/y from 2018 onwards

7.3.4 Seawater intrusion

Model versions 1c and 2b were selected for scenario analysis as they both gave simulated seawater interface positions that seemed most consistent with the limited data available (Figure 5.26). Given the large file sizes and long run times for the SWI2 models, SWI2 scenario analysis was only conducted for the reduced rainfall recharge scenarios (scenarios 1B, 2B and 3B in Table 7.1). It should be noted that the potential impact of climate change on sea level rise is not simulated in these scenarios; hence the extent of seawater intrusion may be underestimated.

For model version 1c, the 3.8 GL/y extraction scenarios shows the interface position staying relatively stable to 2030, and increasing in elevation slightly towards 2040, consistent with longer-term groundwater level declines. Thus, reduced extraction to 3.8 GL/y is not likely to cause seawater intrusion in the short term; however, a small amount of seawater intrusion may continue in the future as rainfall recharge reduces. Continued extraction at the current rate of 5 GL/y with reduced recharge from climate change resulted in some enhanced seawater intrusion in the short term compared to the 3.8 GL/y scenario, while increased extraction to meet projected demand is likely to result in ongoing seawater intrusion, with the simulated interface elevation in SLE069 increasing over time (Figure 7.8).

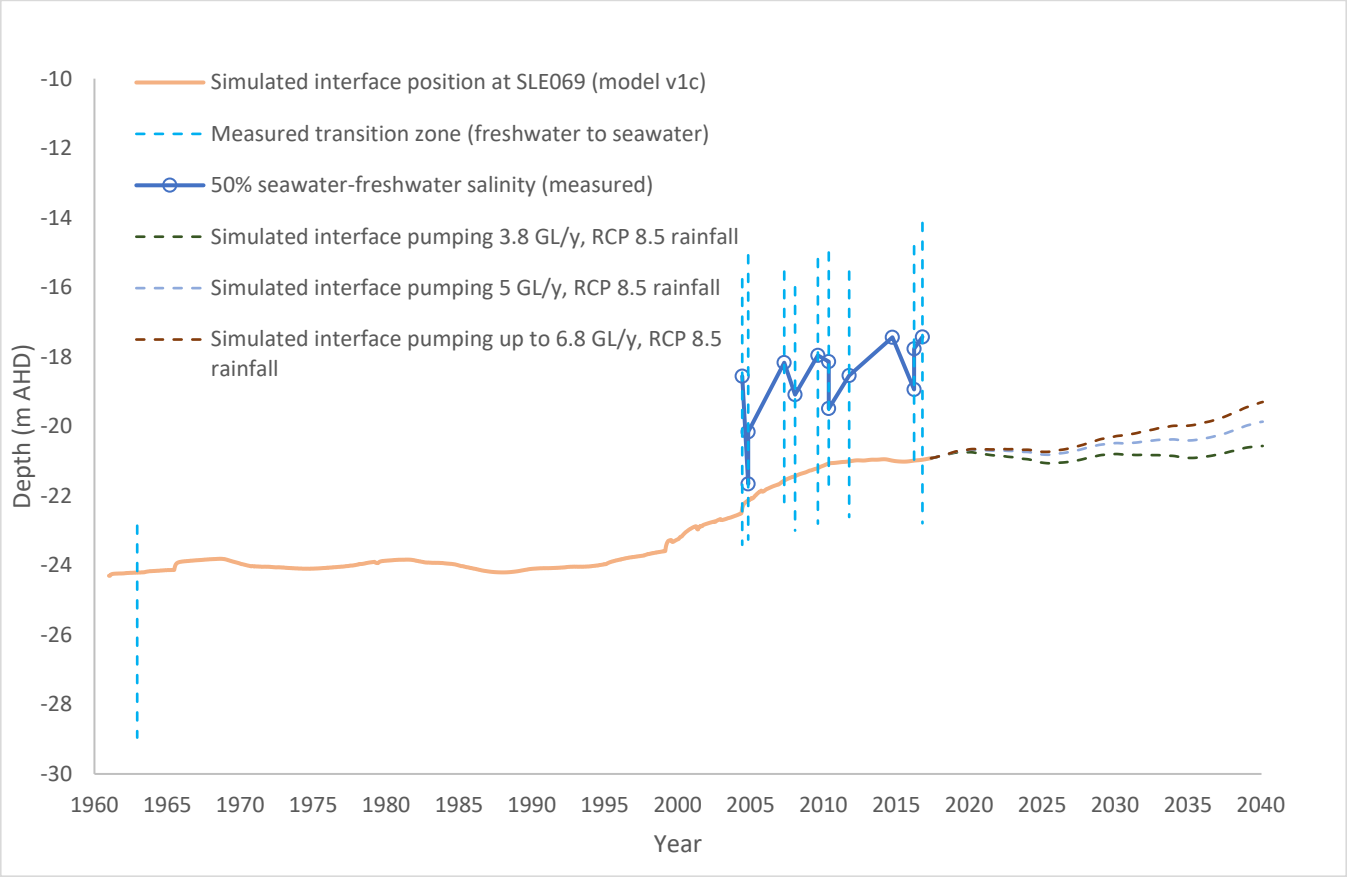


Figure 7.8. Historic and projected modelled seawater interface position at SLE069 for model version 1c

Model version 2b shows similar results to v1c, in that increased extraction to meet projected demand is likely to result in an increase in the elevation of the seawater interface at SLE069, as seawater intrusion occurs (Figure 7.9). Reduced extraction to 3.8 GL/y shows the interface remains relatively stable to 2025, with only relatively small increases to 2040 (as rainfall recharge reduces). Continued extraction at the current rate of 5 GL/y and increased extraction to 6.8 GL/y shows similar results to 2025, after which seawater intrusion is enhanced in both cases.

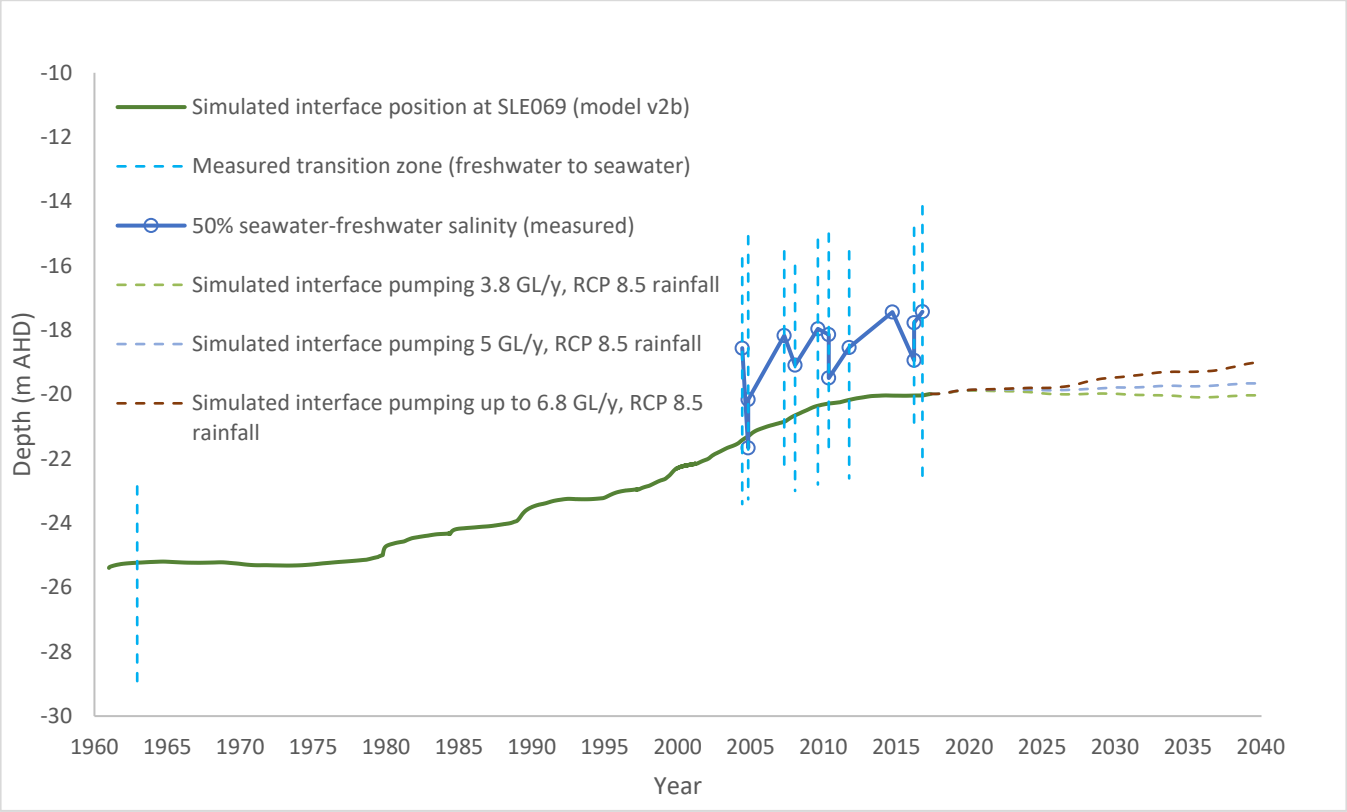


Figure 7.9. Historic and projected modelled seawater interface position at SLE069 for model version 2b

7.4 Predictive parameter uncertainty

To assess the impact of parameter uncertainty on predicted groundwater levels, uncertainty scenarios were run using the 47 realisations of model version 1c with different parameter distributions but acceptable calibration performance (Figure 6.1). Due to the large file sizes involved in running each scenario 47 times, SWI2 simulations were not run and only scenarios simulating reduced rainfall recharge based on RCP 8.5 projections were run (scenarios 1B, 2B and 3B in Table 7.1).

The projected groundwater levels at ULE190 for scenario 1B, 2B and 3B are given in Figures 7.10–7.12. The results are similar to those given in Figures 7.5–7.7 for the two different conceptual models (v1c and v2b); however, the modelled distributions are wider due to the use of the 47 different parameter sets on model version 1c. Nevertheless, all model results generally show the same trends:

- Reduced extraction to 3.8 GL/y is likely to result in some groundwater level recovery, but a subtle trend downwards in levels is predicted due to reduced rainfall projections. Groundwater levels are likely to remain above the historic minimum over the next 20 years, but reduced rainfall is likely to promote conditions for seawater intrusion.
- Continued extraction of 5 GL/y will be accompanied by long-term groundwater level decline; however, groundwater levels are likely to remain above the historic minimum. These declines are likely to result in longer-term seawater intrusion as rainfall recharge reduces.
- Increased extraction to meet projected demand (up to 6.8 GL/y by 2040) will result in continued groundwater level decline. Groundwater levels may get close to historic minimums, and seawater intrusion is likely to increase.

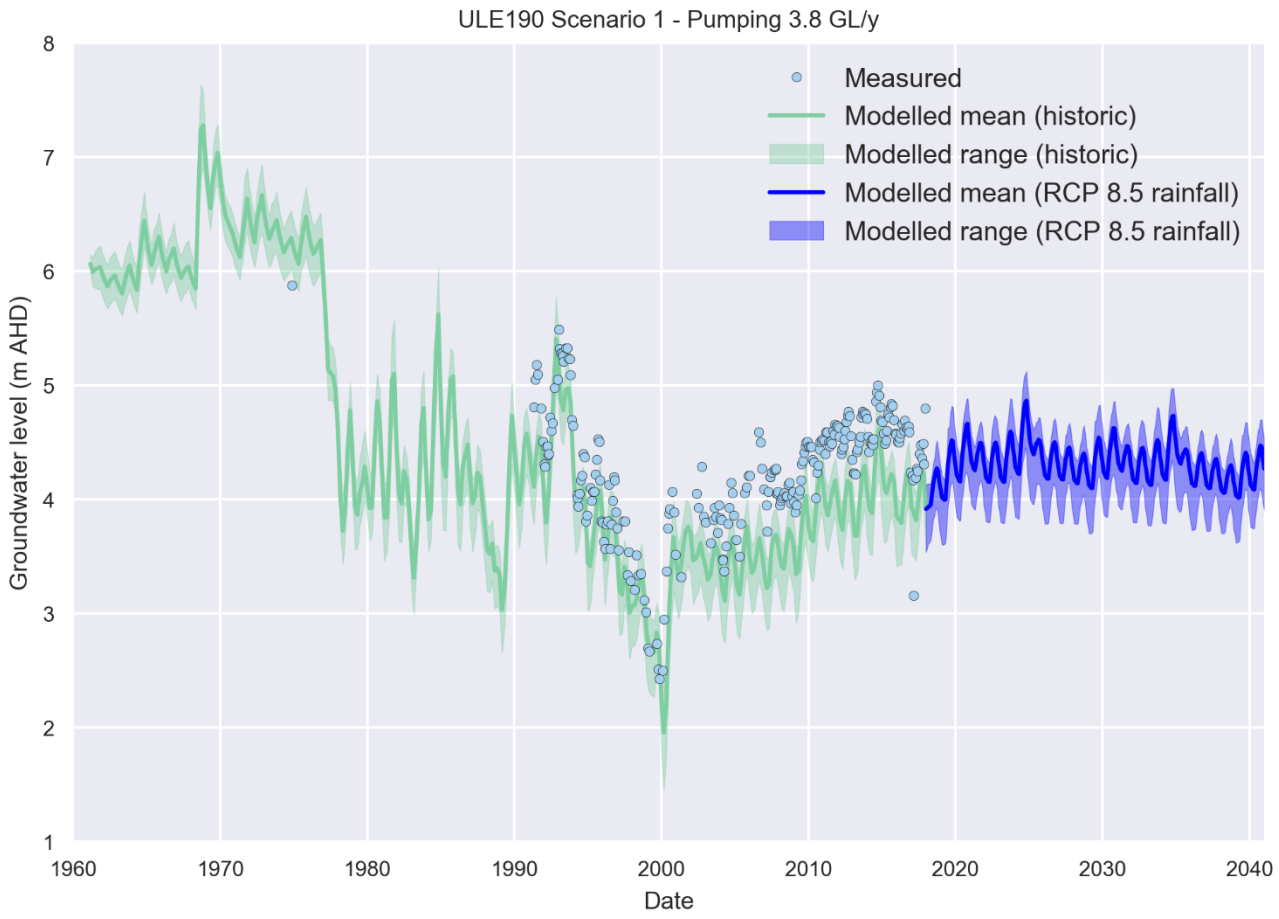


Figure 7.10. Historic and projected groundwater levels for predictive uncertainty model scenario 1b (3.8 GL/y)

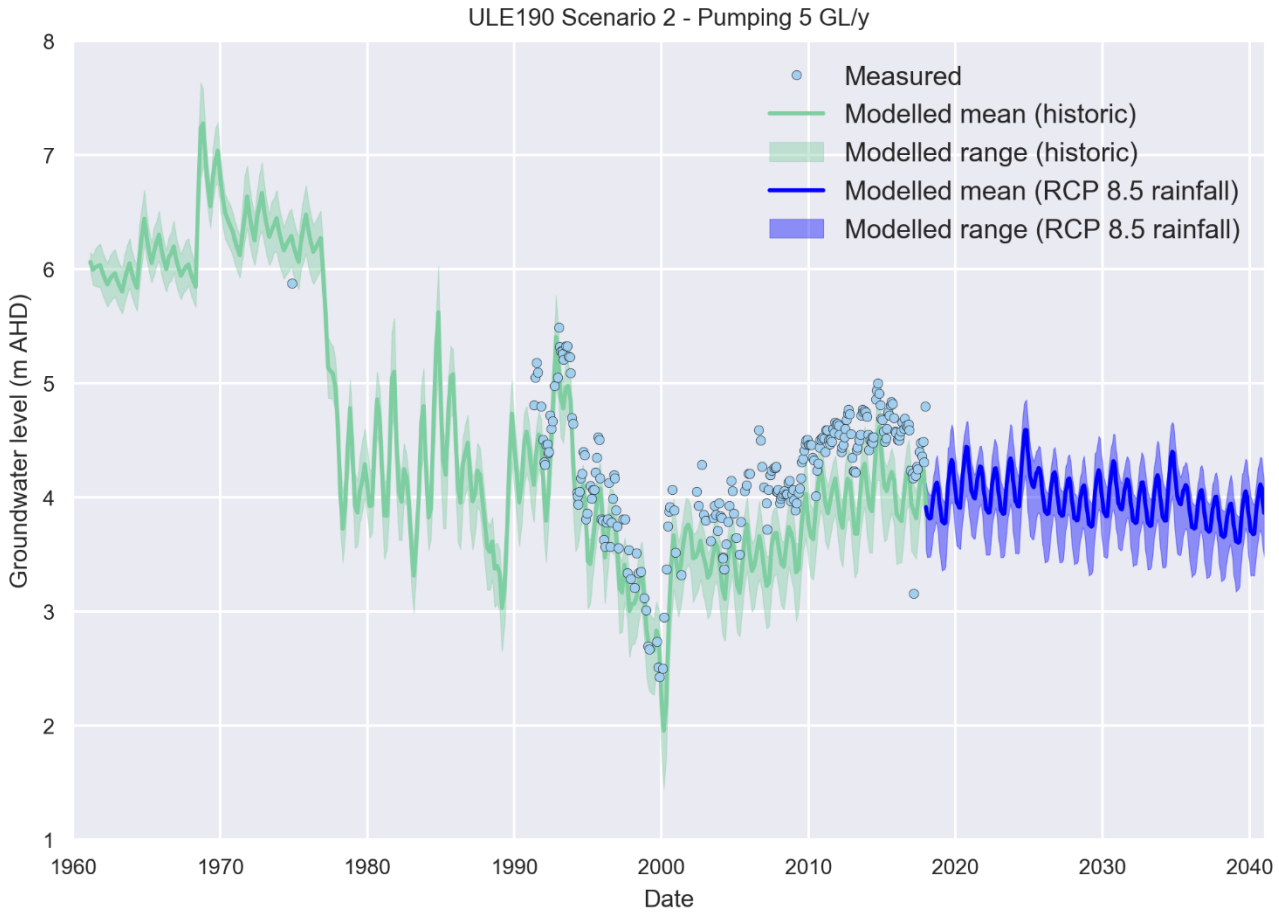


Figure 7.11. Historic and projected groundwater levels for predictive uncertainty scenario 2b (5 GL/y)

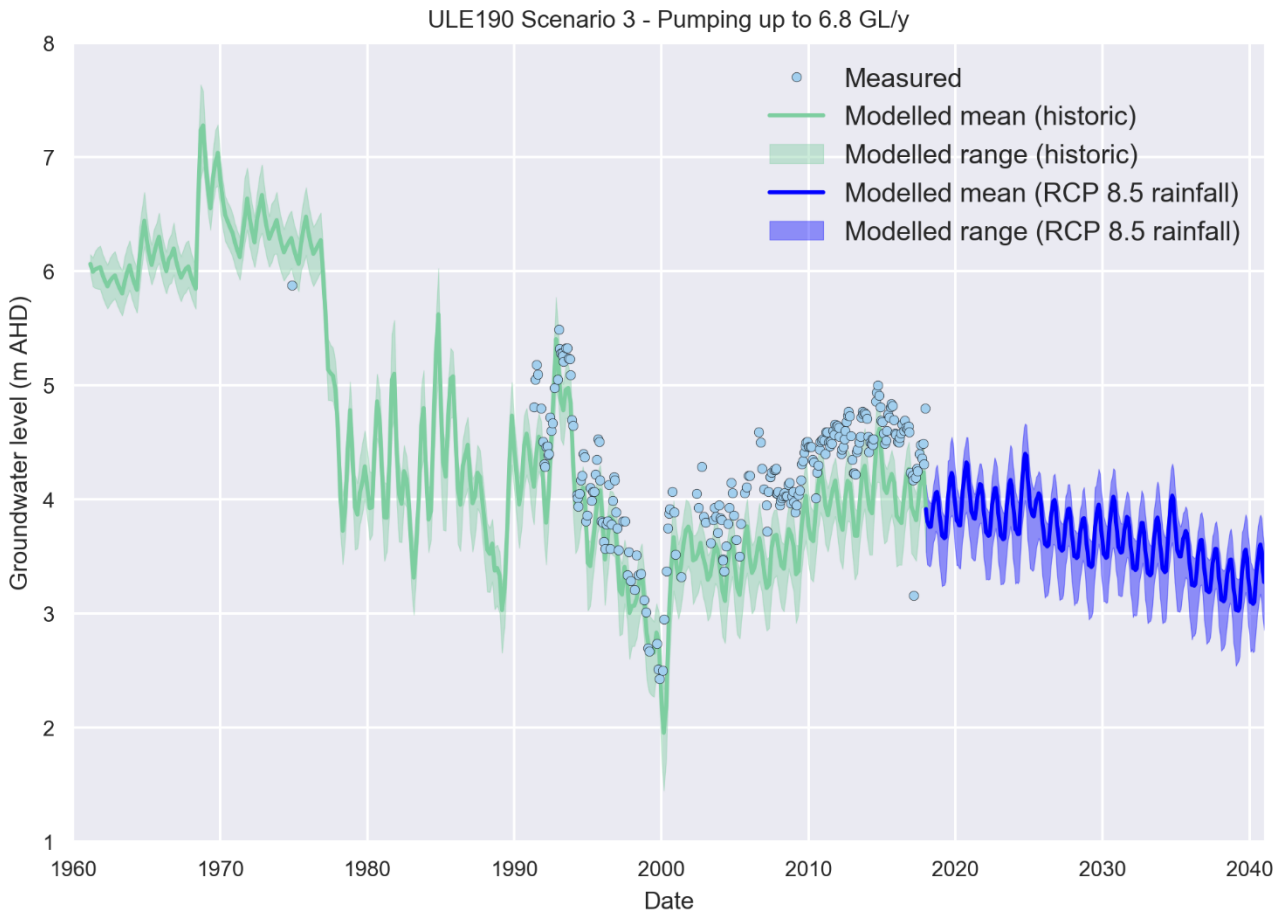


Figure 7.12. Historic and projected groundwater levels for predictive uncertainty scenario 3b (6.8 GL/y)

8 Conclusions and recommendations

8.1 Conclusions

A multi-model approach has been taken to simulating groundwater flow in the QL aquifer in the Uley South Basin. The multi-model approach addressed a range of conceptual and parameter uncertainties. However, further areas of uncertainty and limitations of the model have been identified. The SWI2 package has been used to simulate the position and movement of the seawater-freshwater interface in the aquifer over time. While all the multi-models reproduced groundwater levels well, only two models (1c and 2b) showed seawater intrusion results that are consistent with observations, although observations of the position and movement of the seawater interface in Uley South are limited.

Based on the results of the SWI2 simulations, two versions of the model were used for seawater intrusion scenario analysis. Scenarios assessed the potential impact of reduced pumping (3.8 GL/y), continued pumping (5 GL/y) and increased pumping (up to 6.8 GL/y) on groundwater levels in the TWS well field, and position of the seawater interface at the coast. The scenarios included continued recharge based on the last 10 years recharge, and reduced rainfall recharge based on climate change impacts. Scenario results show that:

- Reduced groundwater extraction (3.8 GL/y) leads to some recovery in groundwater levels. Longer-term declines are predicted to occur as a result of reduced rainfall recharge, and ongoing monitoring of groundwater level and salinity will be needed. The seawater interface is likely to be relatively stable in the short-term; however, seawater intrusion may continue in future as recharge reduces.
- Continued pumping at current rates (5 GL/y) leads to relatively stable groundwater levels to 2025; but with a longer-term declining trend. Groundwater levels do not reach the minimum level recorded in the late-1990s; however, they may reach the same level as recorded in the mid-2000s, when groundwater salinity in TWS 3 was higher due to sustained extraction at 5-7 GL/y. Thus, careful monitoring of groundwater level and salinity will be required for continued pumping at current rates. The seawater interface is likely to be relatively stable in the short-term; however, seawater intrusion is likely to occur in future as recharge reduces.
- Increased extraction to meet projected demand (up to 6.8 GL/y by 2040) shows groundwater levels are likely to decline, potentially to the same level as the late 1990s, when salinity in TWS 3 increased. Adverse impacts such as increased salinity in the TWS wells would be anticipated, and close monitoring would be essential to detect adverse impacts of increased pumping. The increase in extraction with decreases in recharge is also likely to result in enhanced seawater intrusion which is undesirable.

Regardless of future groundwater pumping and recharge conditions in Uley South, close monitoring of groundwater level and salinity will be important. It is reiterated that the recharge scenarios are based on the last 10 years rainfall recharge, as requested by SA Water. This data set includes five above and five below average rainfall years – hence the longer-term trends are based on the assumption that an equal proportion of above and below average rainfall continues in the future. This assumption may not be accurate, and further work would be required to address this as an area of scenario uncertainty (see section 6.1).

8.2 Recommendations

The model results can be considered suitable for assessing potential impacts of different pumping and recharge scenarios on groundwater levels and the position of the seawater interface in the QL aquifer in the Uley South Basin. However, given the sensitivity of groundwater levels in Uley South to changes in pumping and recharge, monitoring of groundwater level and salinity will need to continue into the future.

Several improvements could be made to the modelling of groundwater flow and seawater intrusion described in this study. However, additional data may be required to further constrain modelled processes. Hence further recommendations for future work in relation to groundwater in the Uley South Basin are presented below.

Recommendations for data collection and conceptualisation:

1. Replacement of long-screened coastal wells (e.g. SLE069 and ULE205) with short-screened wells constructed with PVC: Salinity profiles with depth in long-screened wells may give an inaccurate measure of the seawater interface elevation (Shalev et al., 2009), and another method such as geophysical logging on PVC wells with short screens (Kamps et al., 2016), or installation and sampling of nested wells with short screens may be more appropriate.

2. Re-interpretation of AEM data (Fitzpatrick et al., 2009): This may offer more insight into the position of the freshwater-seawater interface, which could be used to better constrain the SWI2 simulations. Supplementary data collection may be required close to the coast, where AEM data is missing. This could also improve constraints on basement elevation, to give a better understanding of the TS thickness across the basin (particularly in coastal areas).

3. Elevation surveys where required: Accurate elevation surveys on all wells should be carried out, as discrepancies in water table elevation like those at sites ULE130 andULE175 (see Section 5.3) may be due to inaccurate survey elevation data.

Recommendations for modelling:

1. Assessing the impact of scenario uncertainty on model predictions: The scenarios here consider future rainfall trends based on 2008-2017 rainfall, which includes an equal proportion of above and below average rainfall. Further work is recommended to consider the impact of other rainfall scenarios on groundwater resources e.g. successive years of below average rainfall.

2. Improved understanding of the connection between the TS and QL aquifer: Current understanding and assumptions regarding TS flow into QL are conceptual, based on comparisons in ion chemistry in both aquifers, and changes in salinity that have been observed in the TWS wells over time. A better understanding of the connection between the two formations is needed. The development of a solute transport model (e.g. based on this flow model) may be one such way to test the conceptual model for interaction between the TS and QL aquifers.

3. Assessing the potential impact of rapid changes in pumping: Scenarios have only considered constant (3.8 and 5 GL/y) and gradual increases in extraction, not the potential impact of a sudden increase in groundwater extraction, for example the increase that was observed between 1999 (5.89 GL/y) and 2000 (7.2 GL/y, Figure 2.17). Should a sudden increase in groundwater extraction be anticipated, the potential impact should be simulated.

4. Further work on climate change scenarios: Climate change scenarios modelled here only consider changes in mean annual rainfall. However, Charles and Fu (2015a) show the seasonality of rainfall is likely to change in the Eyre Peninsula, with larger declines in spring rainfall compared with other seasons. Further work will be required to determine the impact of changing seasonal rainfall on recharge and groundwater processes in the Uley South Basin.

5. Incorporation of metered pumping data: Monthly pumping data from each SA Water town water supply well should be included in the model as it becomes available, and the model re-run with updated data to test model performance.

6. Assessing the impact of parameter uncertainty on SWI2 simulations: This has not been assessed, due to large file sizes and processing time required for SWI2 simulations. However, further work could be done with preferred model version 1c to derive parameter sets which represent the 5th, 50th and 95th percentiles

of the modelled distributions (e.g. modelled distributions in Figure 7.10) and run SWI2 simulations on this subset of models.

7. Further work on parameter uncertainty: The approach taken to assessing parameter uncertainty in this study was limited in scope compared with a full null space Monte Carlo analysis, in that models were not recalibrated due to time constraints (model non-linearity resulted in a large number of models with an objective function (phi) significantly higher than the calibrated model). Further work could be done to recalibrate all realisations, and possibly use a technique such as polynomial chaos expansion (which provides progressive estimates of the reduction in confidence limits) to assess the number of realisations that should be used for scenario analysis (Miller et al., 2018).

8. Further work on modelling TS to QL interlayer flow in the northern part of the basin: Conversion to MODFLOW-USG would help appropriately handle flow between layers, as MODFLOW-USG allows layers to 'pinch-out' and horizontal flow to occur between layers.

9. Further work on seawater intrusion modelling: Conversion of the MODFLOW/SWI2 model to a SEAWAT model or MODFLOW-USG, to better understand impact of dispersive mixing on coastal groundwater salinity. However, improved measurement and monitoring of the seawater interface may be required before modelling seawater-freshwater mixing in a more detailed way.

10. Assessing the potential impact of sea level rise on seawater intrusion: The scenarios do not include the potential impact of sea level rise, which should be assessed as it may impact the simulated extent of intrusion (i.e. current scenario results may underestimate seawater intrusion).

11. Sensitivity analysis of SWI2 results: Particular attention should be paid to the sensitivity of seawater intrusion scenarios to coastal hydraulic conductivity. Despite variation in recharge and pumping, the simulated position of the interface will also depend upon the hydraulic conductivity of cells close to the coast, for which there is limited data. Improved conceptualisation of hydraulic conductivity in the coastal region will improve confidence in simulations of the interface position. Geophysical techniques such as NMR may provide improved understanding of the spatial variability of aquifer properties in the coastal zone.

9 Appendices

A. Aquifer test data

The following table gives reported hydraulic conductivity values from the literature and analysis performed as part of this study. All values are for the QL aquifer except 6028-0895, the last entry in the table, which is the sole value for the TS aquifer. Figure 9.1 shows the average hydraulic conductivity and range reported for wells where multiple tests have been conducted.

Table 9.1. Aquifer test data for the Uley South Basin, all values are for the QL aquifer unless specified

Bore ID	Easting	Northing	T (m^2/d)	Aquifer thickness (m)	K (m/d)	Sy	S	Reference
6028-0699	553530	6152134	10420	8	1367	0.017		Painter (1968)
6028-0777	549815	6151425	11150	14	813	0.028		Painter (1968)
6028-0703	551132	6153175	3973	10	391	0.692		Morton & Steel (1970)
6028-0782	552177	6149818	1894	6	314	0.138		Morton & Steel (1970)
6028-0696	551642	6153301	3000	7	426			Sibenaler (1976)
6028-0697	551798	6152800	13000	10	1287			Sibenaler (1976)
6028-0697	551798	6152800	12000	10	1188	0.347		Sibenaler (1976)
6028-0698	551866	6151986	10000	10	1024	0.08		Sibenaler (1976)
6028-0698	551866	6151986	12000	10	1228	0.079		Sibenaler (1976)
6028-0699	553530	6152134	10000	8	1312	0.0172		Sibenaler (1976)
6028-0700	551681	6151436	5000	11	468	0.03		Sibenaler (1976)
6028-0700	551681	6151436	4000	11	375	0.026		Sibenaler (1976)
6028-0701	551336	6152061	12000	11	1071	0.08 to 0.12		Sibenaler (1976)
6028-0701	551336	6152061	10000	11	893	0.124 to 0.079		Sibenaler (1976)
6028-0702	551134	6152575	22000	10	2259	0.15 to 0.72		Sibenaler (1976)
6028-0702	551134	6152575	10000	10	1027	0.722 to 0.146		Sibenaler (1976)
6028-0703	551132	6153175	6500	10	666	0.05 to 0.178		Sibenaler (1976)
6028-0777	549815	6151425	11000	14	803	0.288		Sibenaler (1976)
6028-0782	552177	6149818	1000	7	148	0.102		Sibenaler (1976)
6028-0905	554252	6154743	2000	12	171	0.007		Barnett (1978)
6028-2795	551735	6153390	2043	8	253			Watkins et al. (2015)
6028-2795	551735	6153390	2935	8	364	0.02		Watkins et al. (2015)
6028-2797	547582	6153205	87854	18	4848			Watkins et al. (2015)
6028-2798	551641	6151458	2196	10	220			Watkins et al. (2015)
6028-2798	551641	6151458	4608	10	463	0.02		Watkins et al. (2015)
6028-2799	553546	6152209	8785	8	1164			Watkins et al. (2015)
6028-2799	553546	6152209	10163	8	1346	2.00E-04		Watkins et al. (2015)
6028-2800	551126	6153178	13178	10	1367			Watkins et al. (2015)
6028-2800	551126	6153178	10034	10	1041	0.04		Watkins et al. (2015)
6028-2801	551954	6152047	13178	10	1373			Watkins et al. (2015)
6028-2801	551954	6152047	11517	10	1200	0.01		Watkins et al. (2015)
6028-2802	552742	6147187	52712	37	1431			Watkins et al. (2015)
6028-2802	552742	6147187	59000	37	1602	0.002		Watkins et al. (2015)

6028-2803	551221	6152572	8785	12	707			Watkins et al. (2015)
6028-2803	551221	6152572	11880	12	957	0.07		Watkins et al. (2015)
6028-2804	551829	6152797	5549	9	623			Watkins et al. (2015)
6028-2804	551829	6152797	9832	9	1105	0.08		Watkins et al. (2015)
6028-2806	551395	6152041	4392	8	586			Watkins et al. (2015)
6028-2806	551395	6152041	6534	8	871	0.05		Watkins et al. (2015)
6028-2160	550340	6150175	484	16	30			SA Water, unpublished data
6028-2164	551900	6147910	13000	16	790			SA Water, unpublished data
6028-2798	551641	6151458	4162	10	418			DEW, unpublished
6028-2798	551641	6151458	3953	10	397			DEW, unpublished
6028-0754	547745	6151752			1			Davis (2012)
6028-0752	549245	6151804			>360			Davis (2012)
6028-0775	550945	6151573			>350			Davis (2012)
6028-0744	550992	6148604			0.2 to 50			Davis (2012)
6028-0795	551891	6150894			1 to 13			Davis (2012)
6028-1747	547857	6151029			10 to 300			Davis (2012)
6028-2317	547736	6153092			3 to 140			Davis (2012)
*6028-0895 (TS aquifer)	552582	6154685	682	32	22		0.007	Morton & Steel (1970)

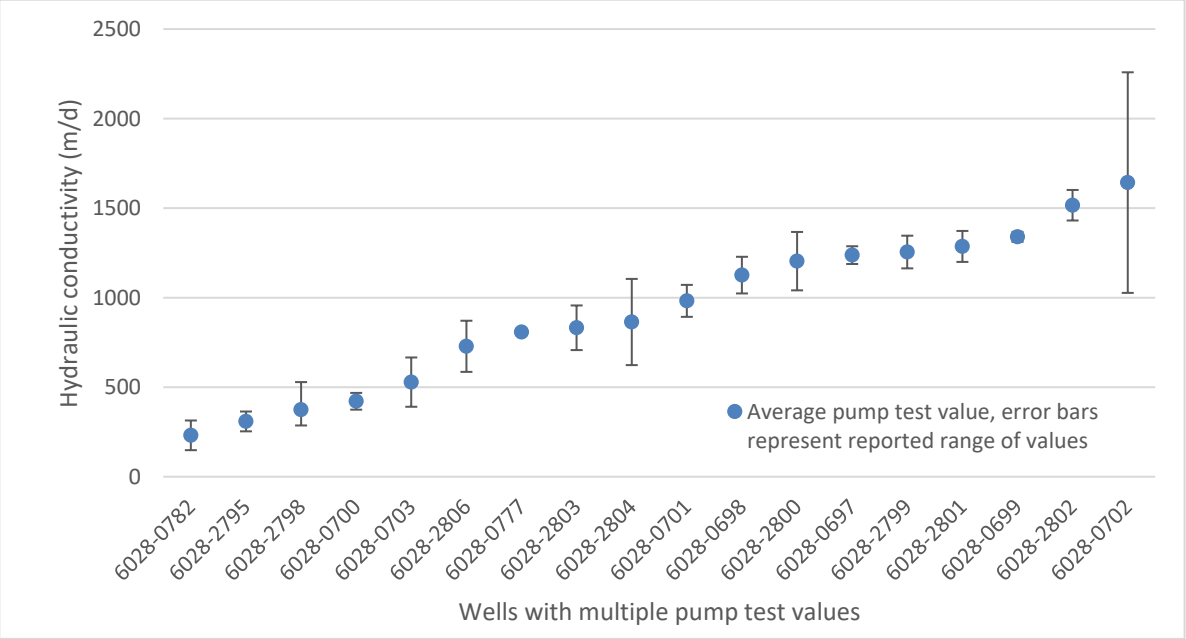


Figure 9.1. Average hydraulic conductivity values and their range, for wells with multiple pumping tests

As noted in Table 9.1, Results from 6028-2160 and 6028-2164 (town water supply wells 14 and 16) were unpublished, and the data had not previously been interpreted. Both wells are completed in the QL aquifer, and the tests were both step drawdown tests conducted between July and August 1999. Following previous interpretation methods for step tests in the Uley South Basin (Sibenaler, 1976; Watkins et al., 2015) and similar karst environments (Magarey and Slater, 2011), the data was analysed using the Eden-Hazel method as described in Kruseman and de Ridder (1990). The tests were only 150 minutes (6028-2160) and 1000 minutes (6028-2164) long and drawdown responses were not able to be perfectly fitted for all the data. Nevertheless, reasonable fits to the majority of data were obtained (Figures 9.2 and 9.3) to give transmissivities of 484 m^2/d (6028-2160) and 13,000 m^2/d (6028-2164). These values should not be considered the most reliable values for the aquifer at this

location, as the duration of the tests was relatively short. Nevertheless, they provide a useful guide to assist in model development and calibration.

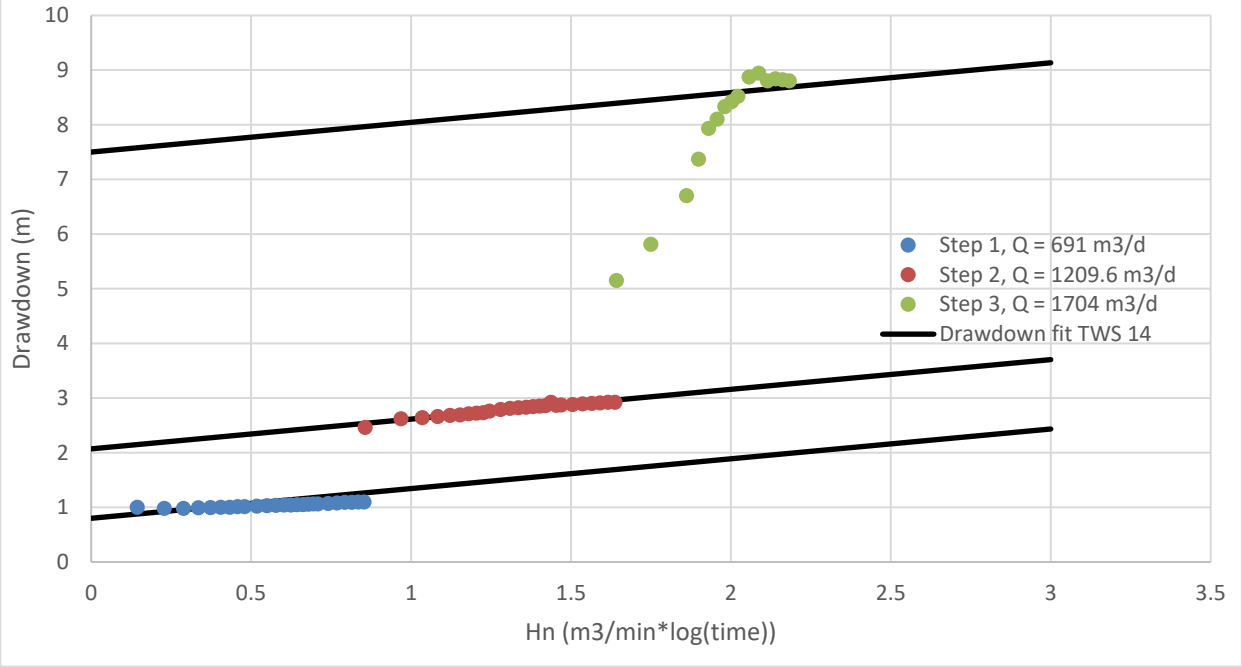


Figure 9.2. Drawdown curves for the step drawdown test in 6028-2160 (TWS 14), T = 484 m2/d (Q = flow rate)

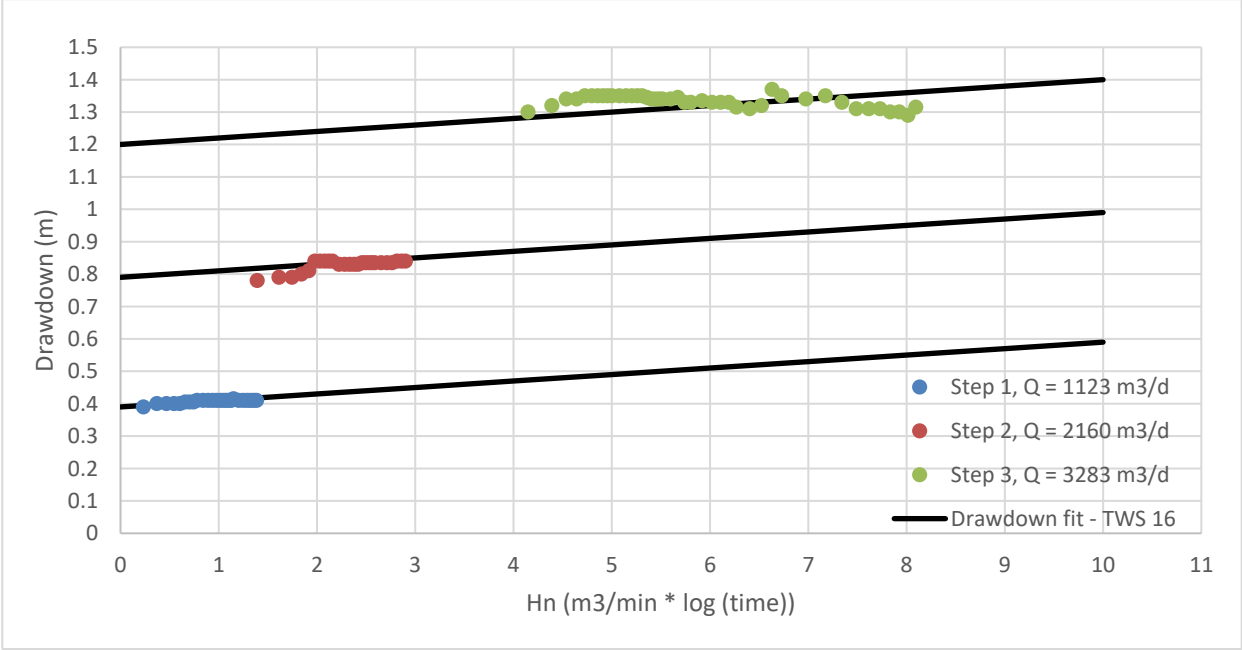


Figure 9.3. Drawdown curves for the step drawdown test in 6028-2164 (TWS 16), T = 13,000 m2/d (Q = flow rate)

B. Sensitivity of simulated interface to changes in TIPSLOPE and TOESLOPE

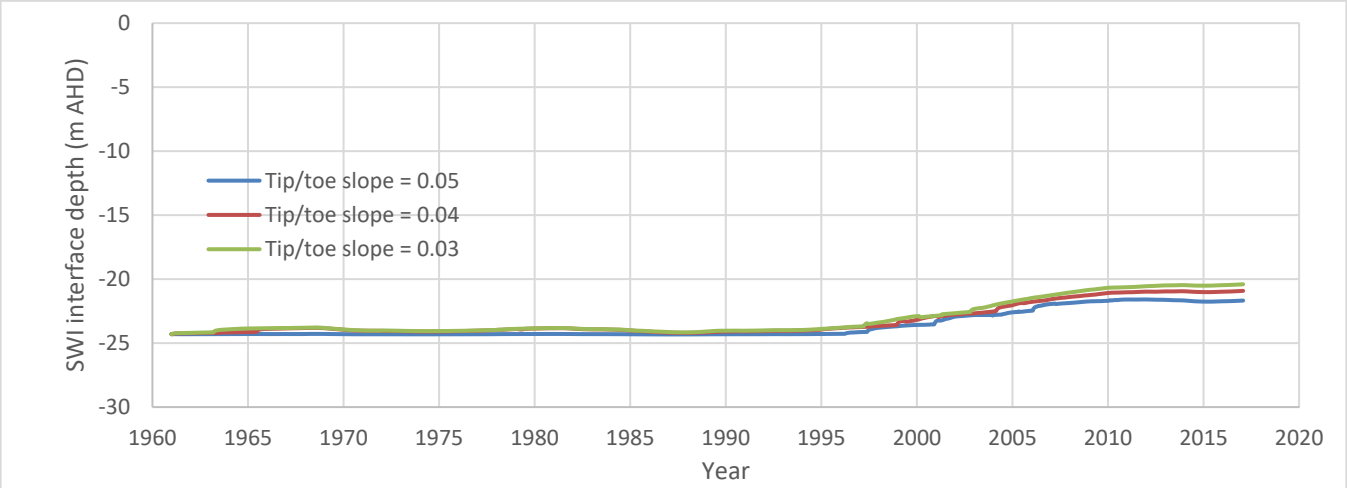
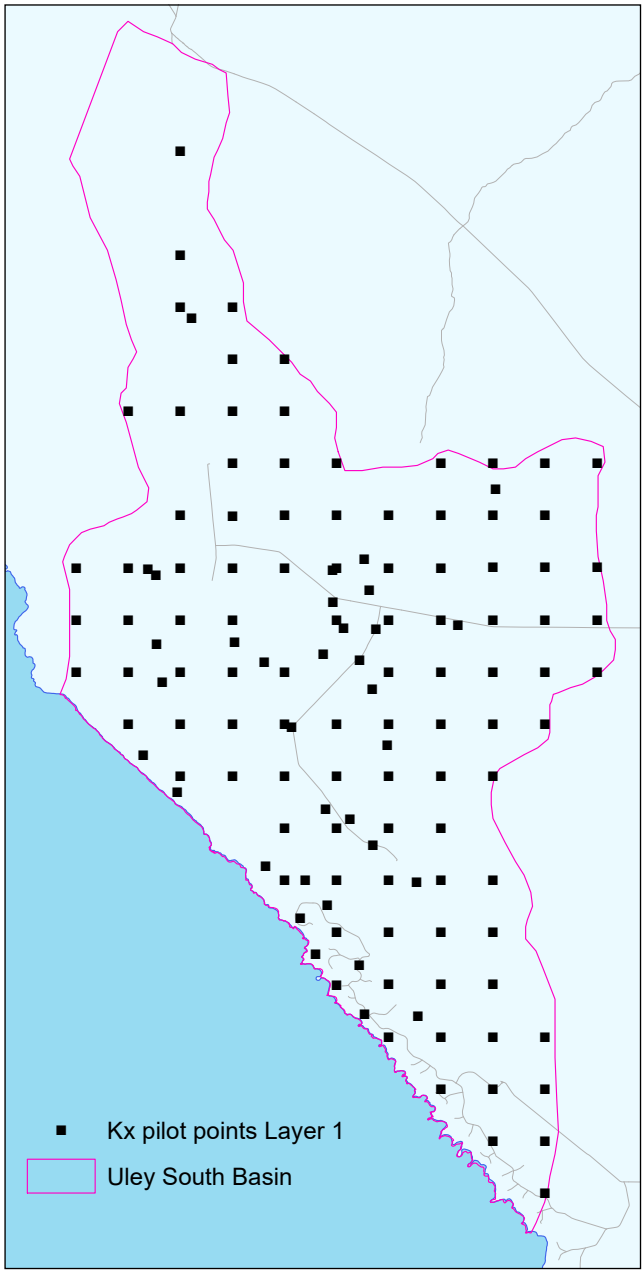


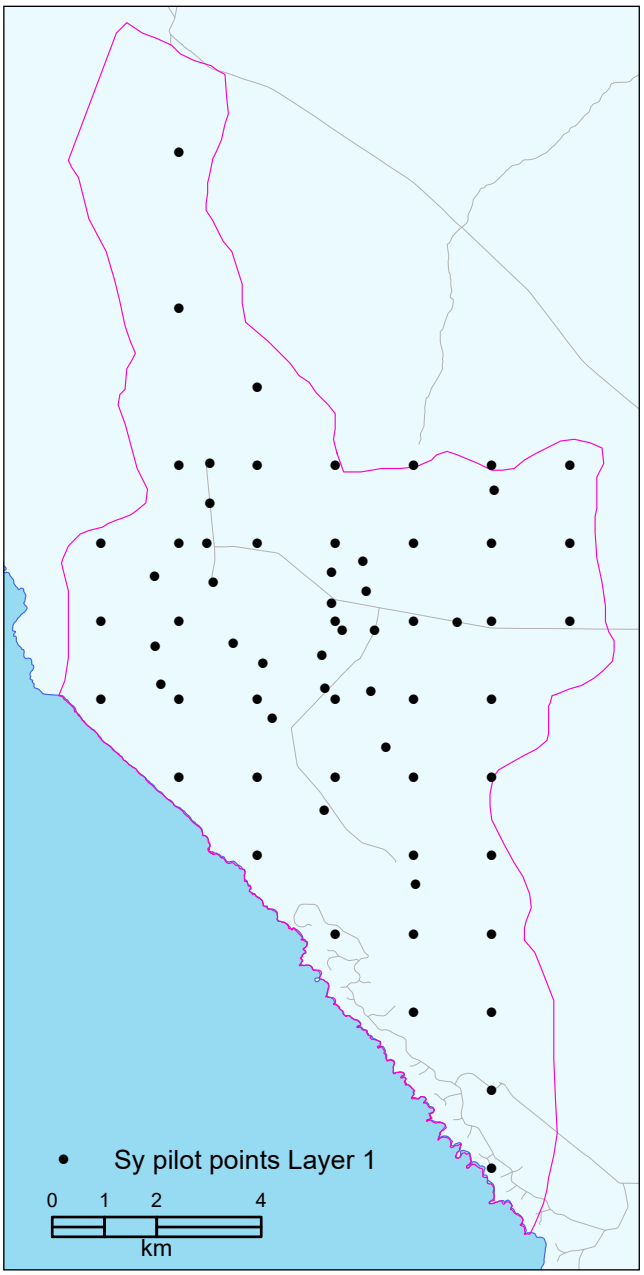
Figure 9.4. Simulated seawater interface depth at SLE069 for model version 1c with different tip/toe slope parameters

Different TIPSLOPE and TOESLOPE values ranging from 0.03 to 0.05 were tested on model version 1c. The results show that changes in this parameter will influence the overall position of the seawater interface at the end of a transient simulation (Figure 9.4). However, the difference in parameters does not influence the overall trend in interface movement. Furthermore, given the uncertainty in the position of the interface from lack of reliable measurements, this difference is not considered significant. Also, the SWI2 package simulates a sharp interface representing the 50% seawater-freshwater interface and so results are only approximate. Therefore, constant TIPSLOPE and TOESLOPE parameters of 0.04 are used in all models.

C. Pilot point locations

The following figures give the locations and ranges assigned to pilot point parameters in the model calibration.



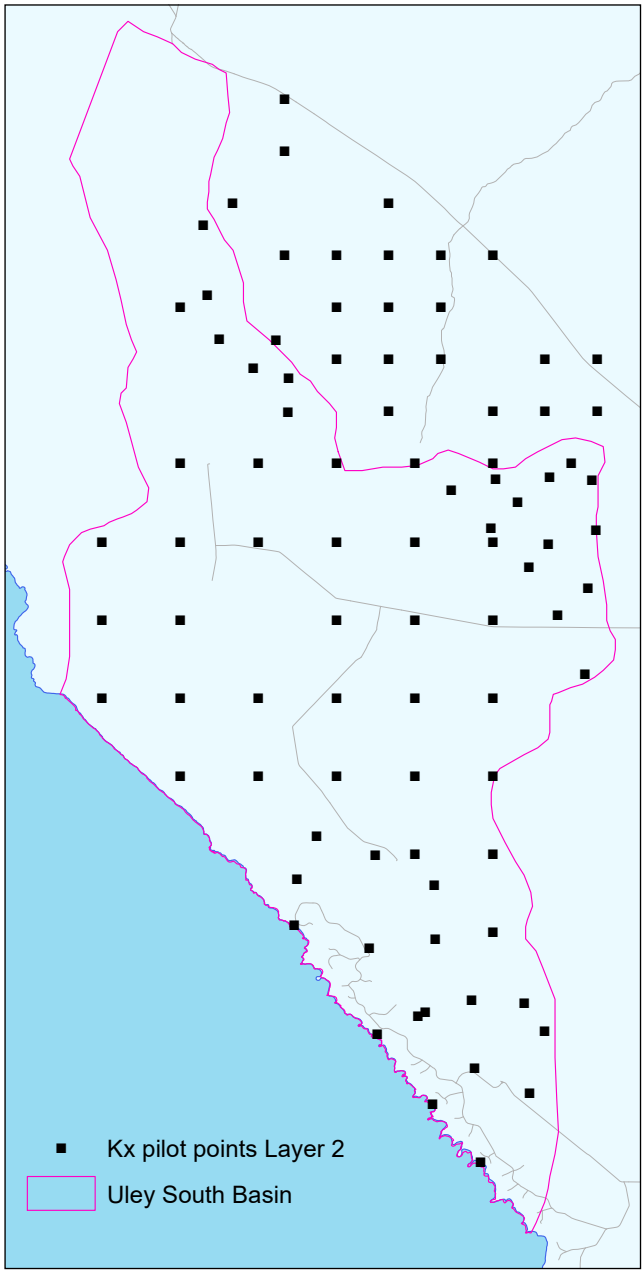


Kx pilot point range 5 - 2000 m/d, except where pump test data is available and ranges are based on esimtated value +/- 10% (see Figure 2.14 and Table 9.1)

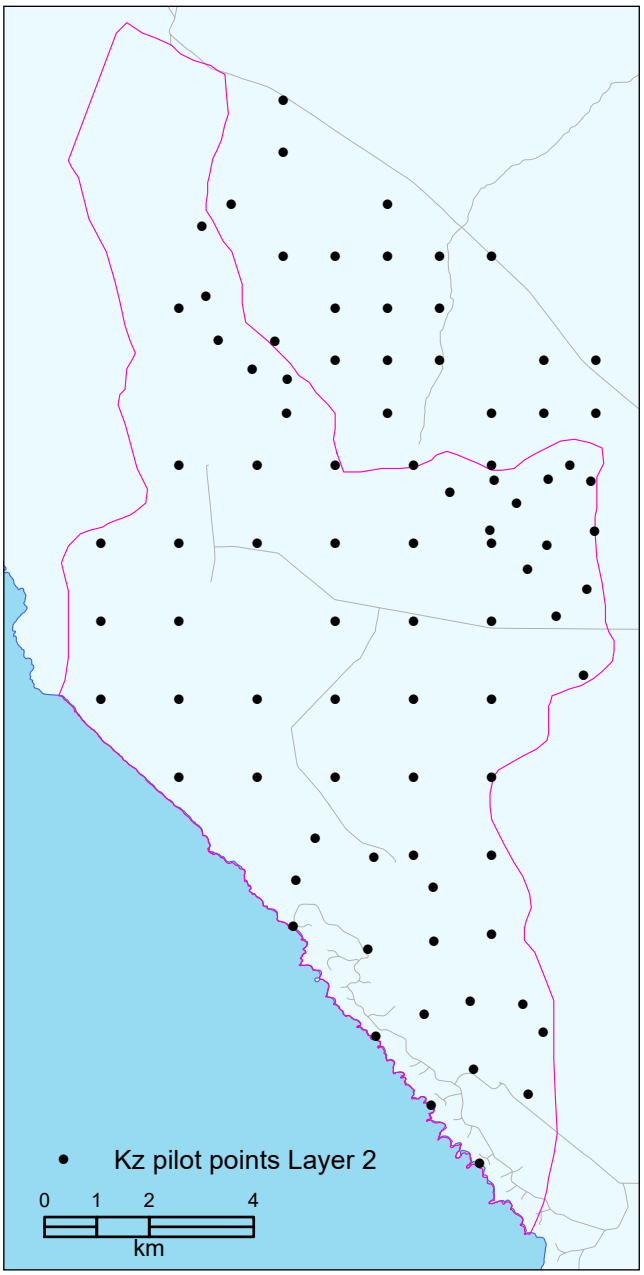
Sy pilot point range 0.01 - 0.4, except where pump test data is available and ranges are based on estimated values +/- 5% (see Figure 2.14 and Table 9.1)



Figure 9.5 Pilot point locations in Layer 1



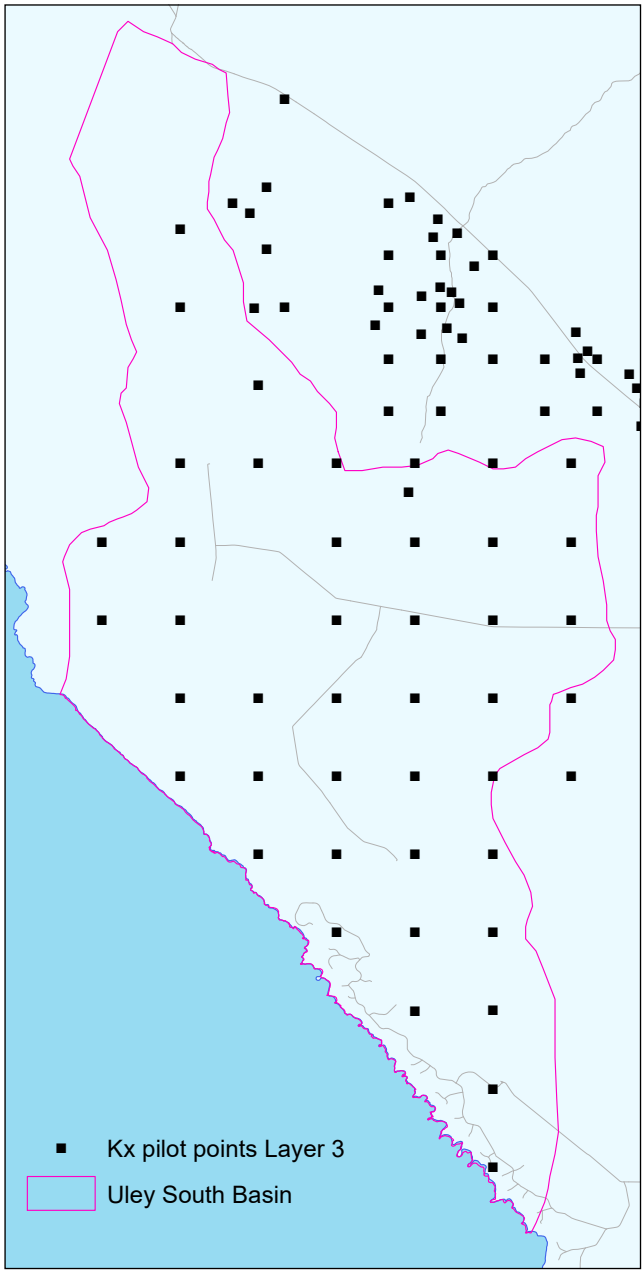
Kx pilot point range 1E-3 to 1 m/d.



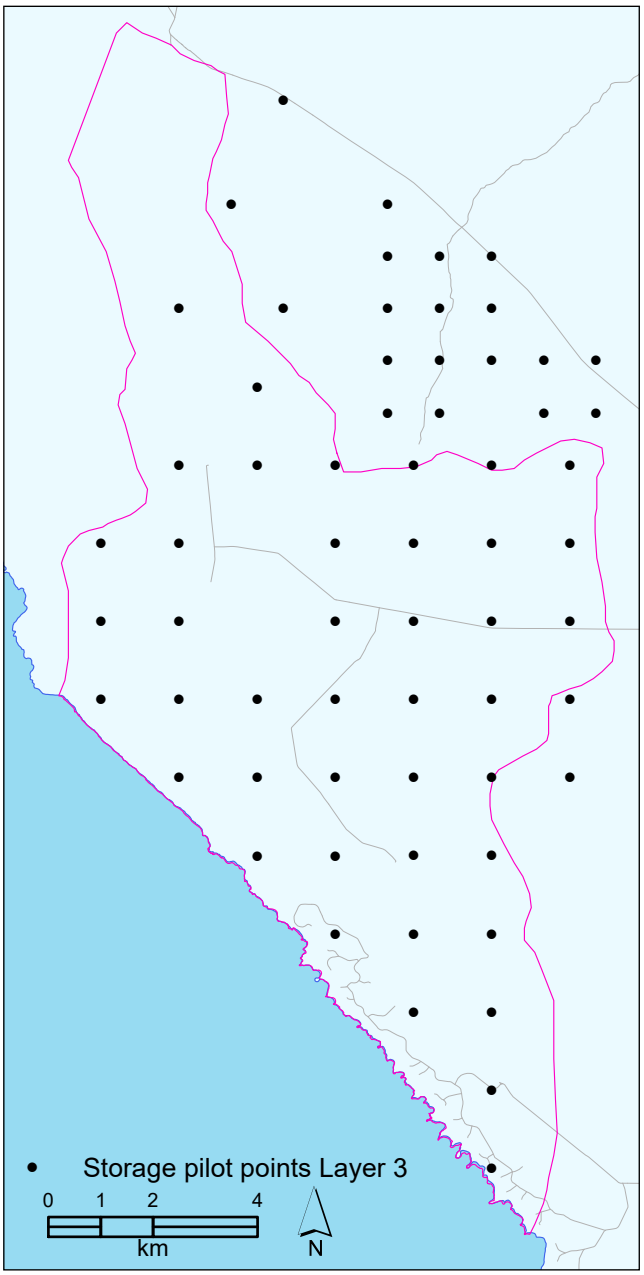
Kz pilot point range 1E-5 to 1E-3 m/d.



Figure 9.6 Pilot point locations in Layer 2



Kx pilot point range 1 to 200 m/d.



Storage pilot point range 5E-4 to 1E-1.

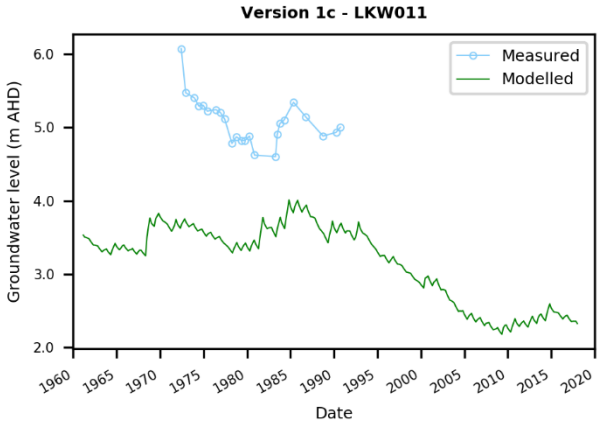


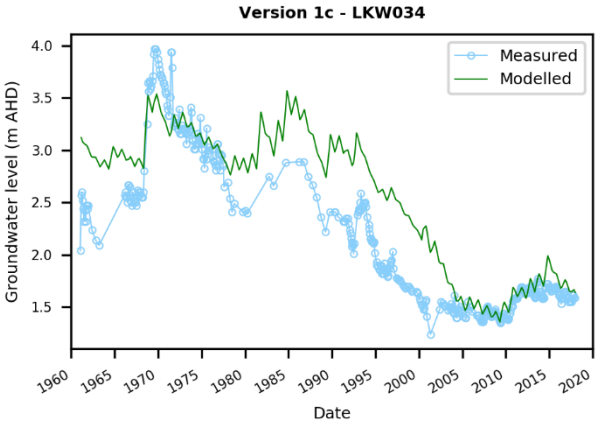
Figure 9.7 Pilot point locations in Layer 3

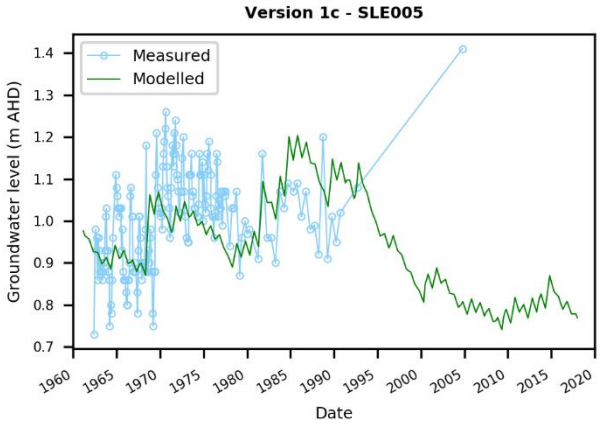
D. Calibration hydrographs

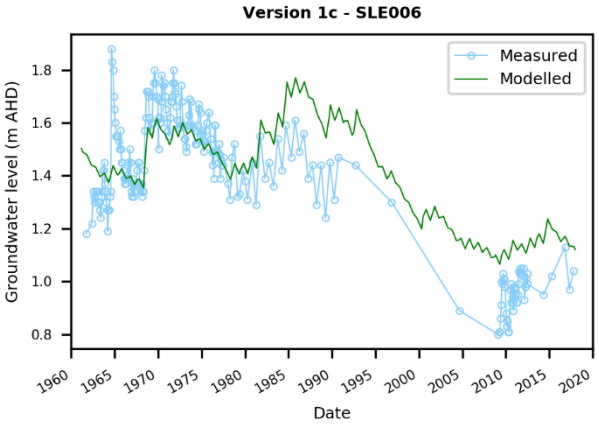
Given that model versions 1c and 2b only are used for scenario analysis, calibration hydrographs from these two models are presented here.

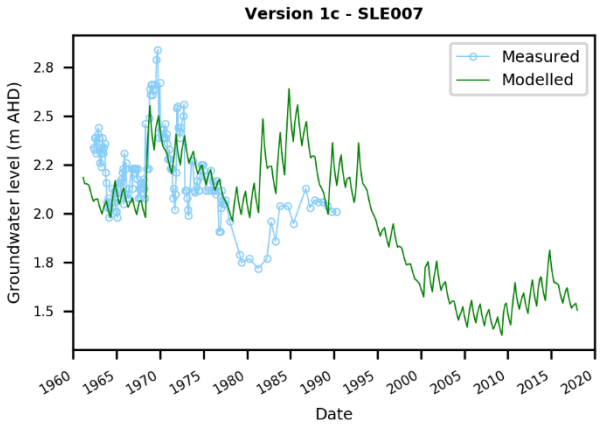
D.1 Calibration hydrographs from model version 1c

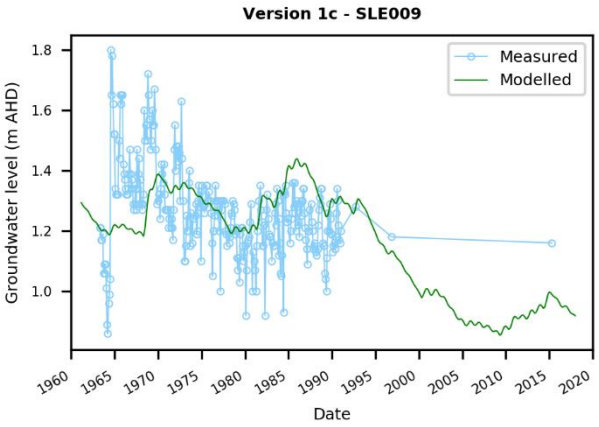


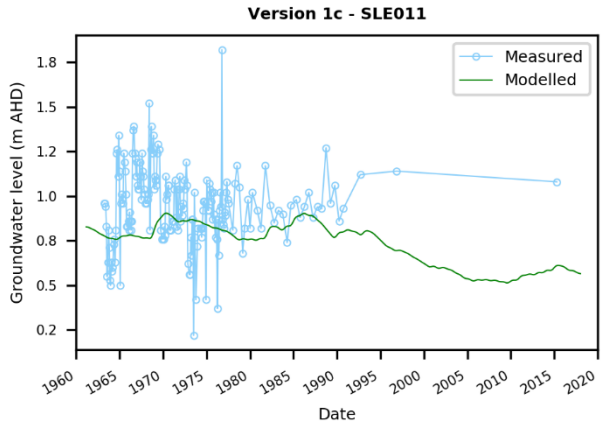


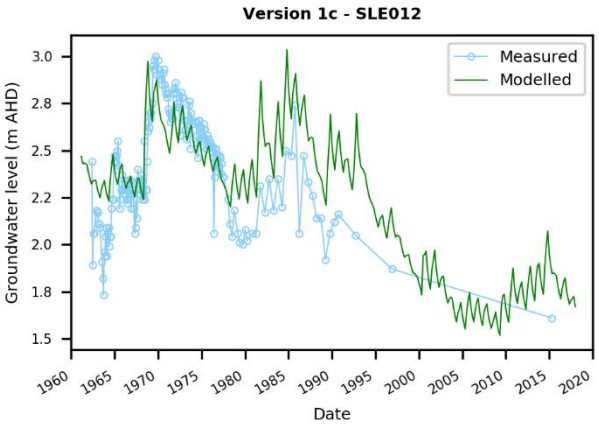


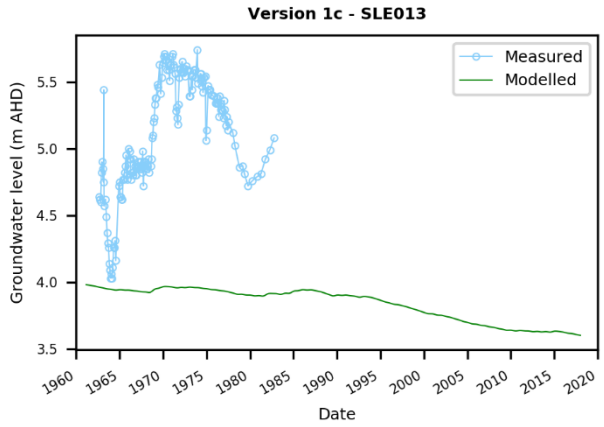


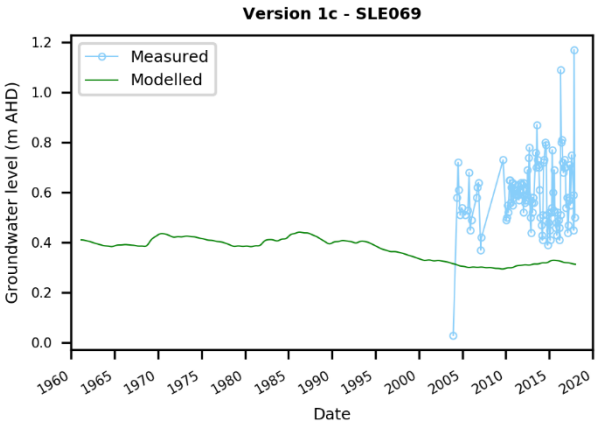


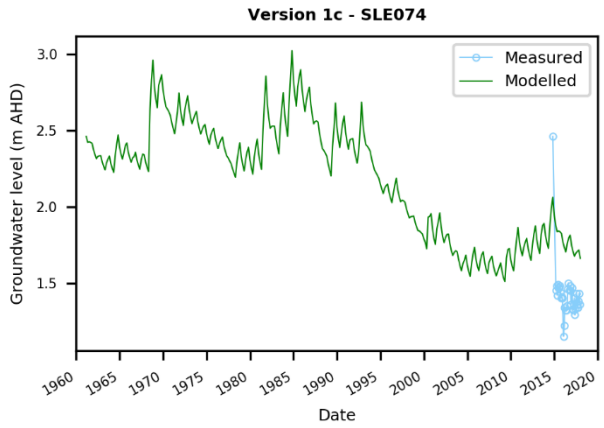


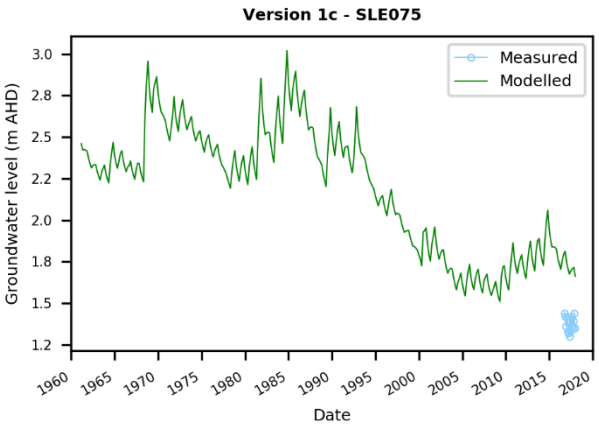

Version 1c - SLE011
Measured
Modelled
Groundwater level (m AHD)
Date

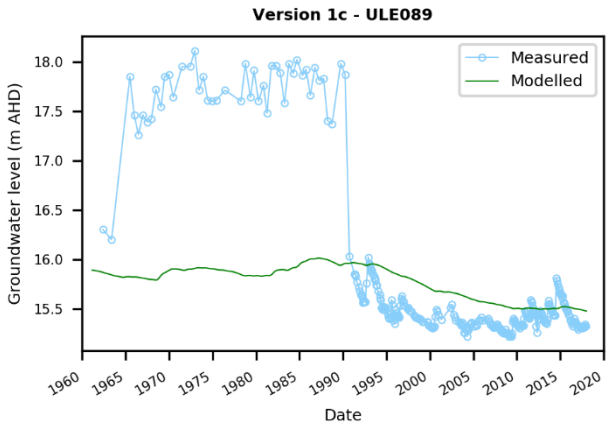

Version 1c - SLE012
Measured
Modelled
Groundwater level (m AHD)
Date

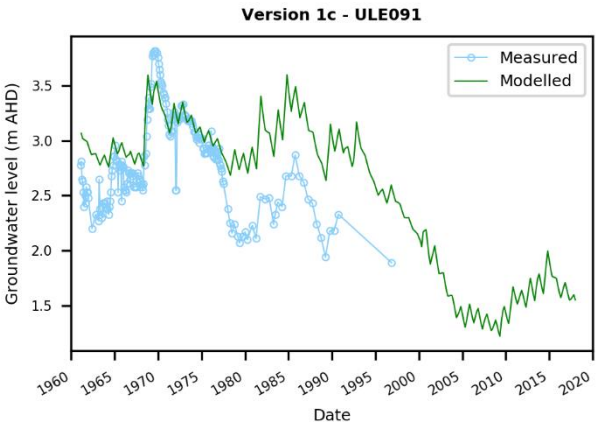

Version 1c - SLE013
Measured
Modelled
Groundwater level (m AHD)
Date

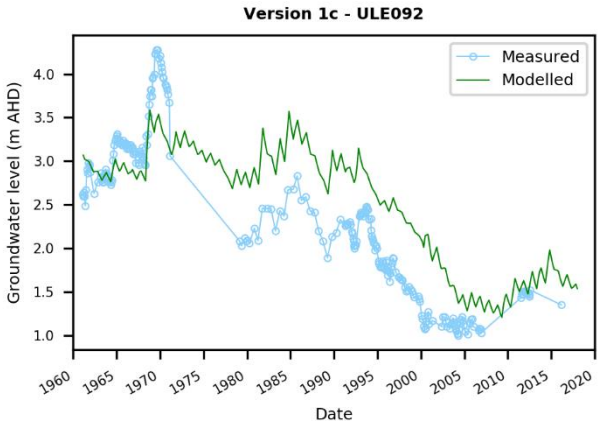

Version 1c - SLE069
Measured
Modelled
Groundwater level (m AHD)
Date

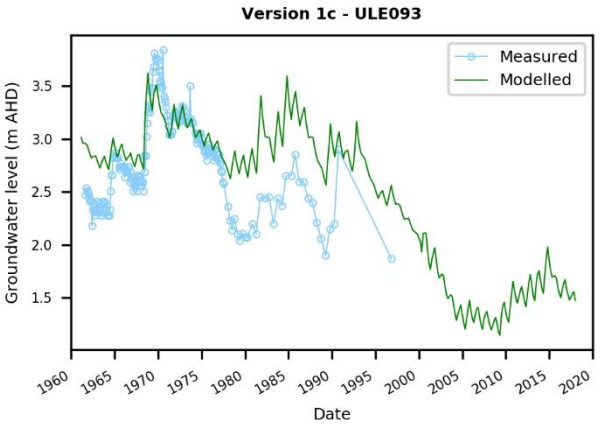

Version 1c - SLE074
Measured
Modelled
Groundwater level (m AHD)
Date

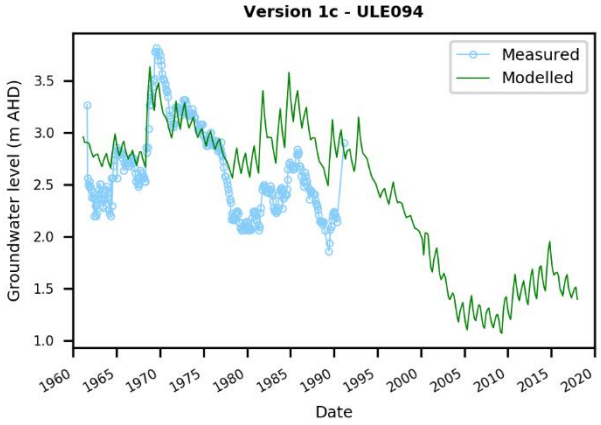

Version 1c - SLE075
Measured
Modelled
Groundwater level (m AHD)
Date

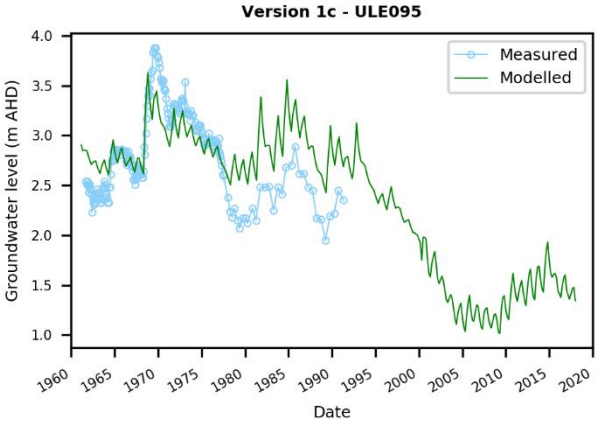

Version 1c - ULE089
Measured
Modelled
Groundwater level (m AHD)
Date

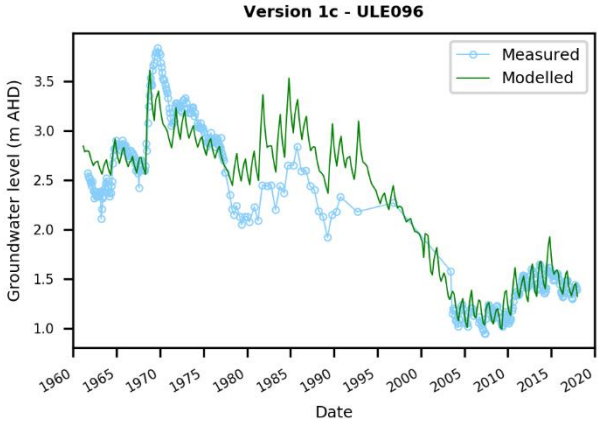

Version 1c - ULE091
Measured
Modelled
Groundwater level (m AHD)
Date

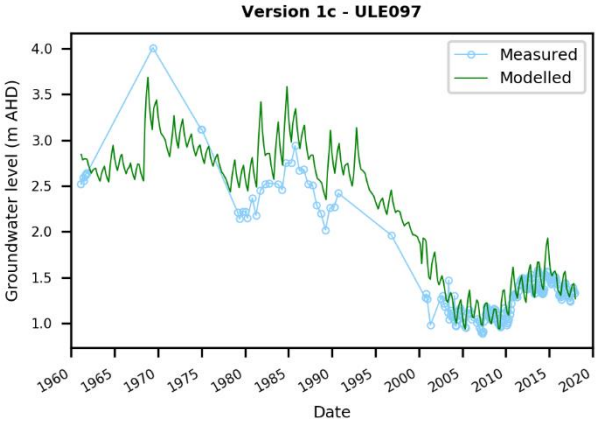

Version 1c - ULE092
Measured
Modelled
Groundwater level (m AHD)
Date

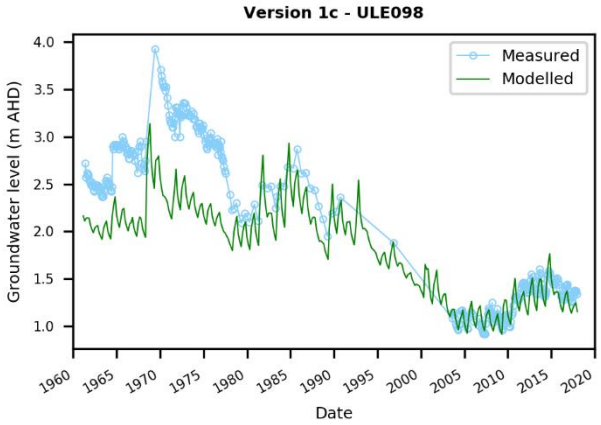

Version 1c - ULE093
Measured
Modelled
Groundwater level (m AHD)
Date

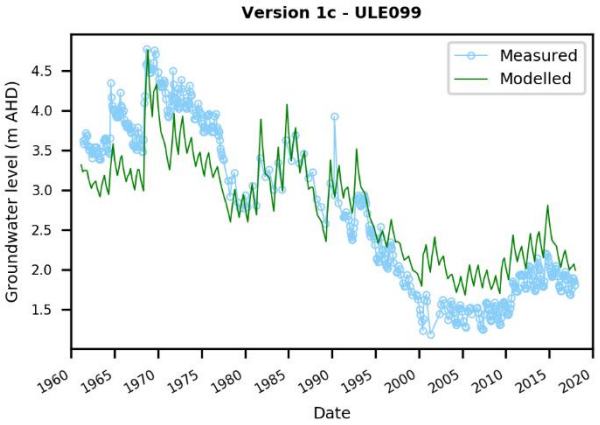

Version 1c - ULE094
Measured
Modelled
Groundwater level (m AHD)
Date

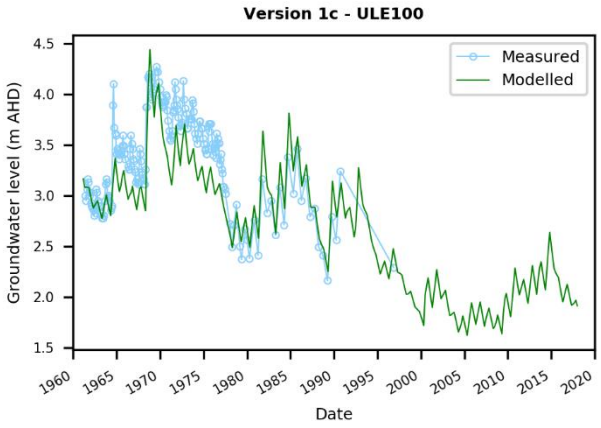

Version 1c - ULE095
Measured
Modelled
Groundwater level (m AHD)
Date

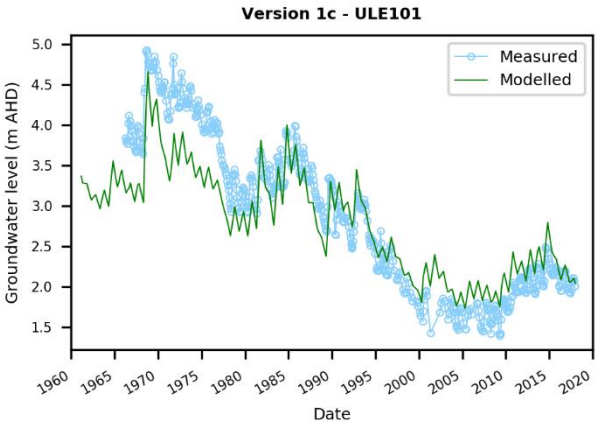

Version 1c - ULE096
Measured
Modelled
Groundwater level (m AHD)
Date

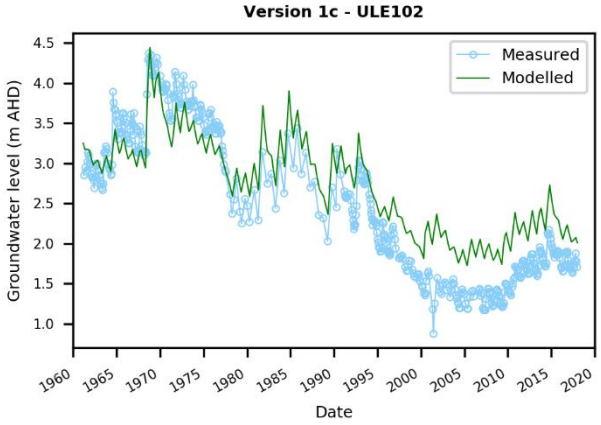

Version 1c - ULE097
Measured
Modelled
Groundwater level (m AHD)
Date

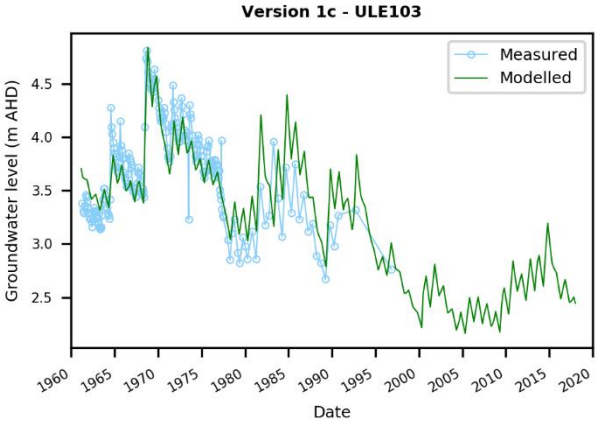

Version 1c - ULE098
Measured
Modelled
Groundwater level (m AHD)
Date

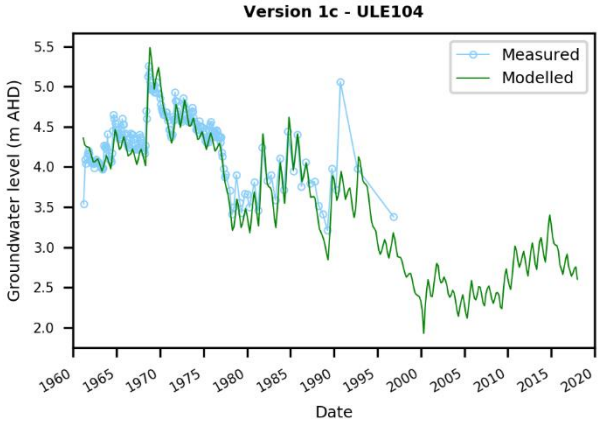

Version 1c - ULE099
Measured
Modelled
Groundwater level (m AHD)
Date

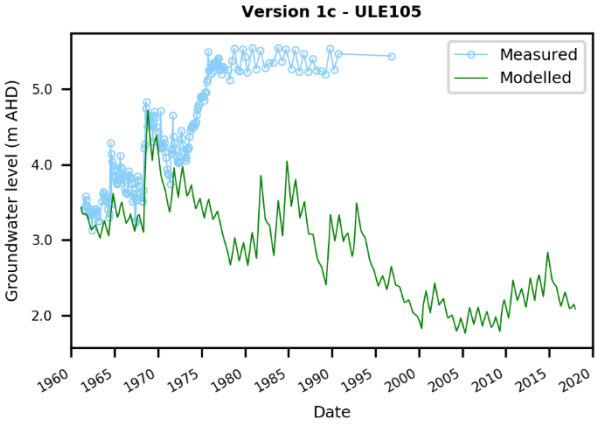

Version 1c - ULE100
Measured
Modelled
Groundwater level (m AHD)
Date

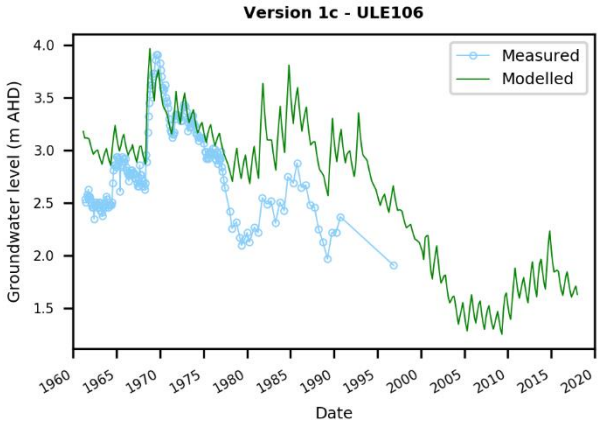

Version 1c - ULE101
Measured
Modelled
Groundwater level (m AHD)
Date

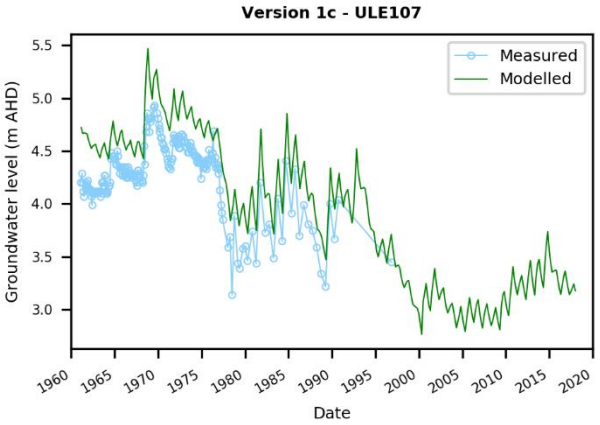

Version 1c - ULE102
Measured
Modelled
Groundwater level (m AHD)
Date

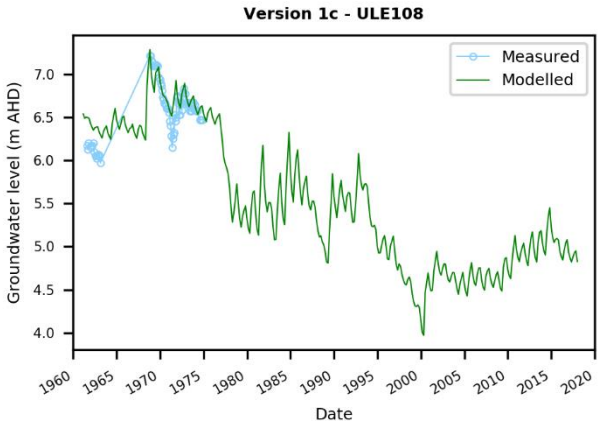

Version 1c - ULE103
Measured
Modelled
Groundwater level (m AHD)
Date

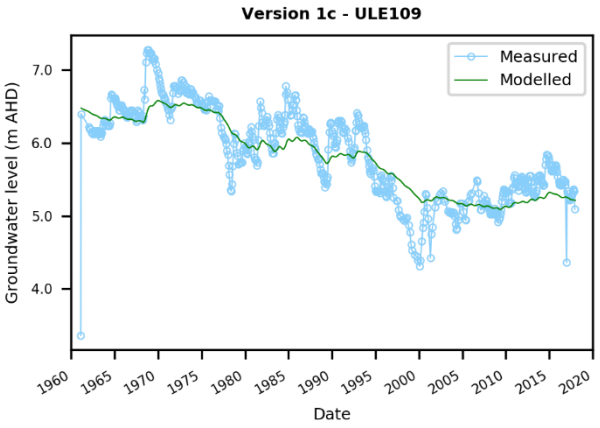

Version 1c - ULE104
Measured
Modelled
Groundwater level (m AHD)
Date

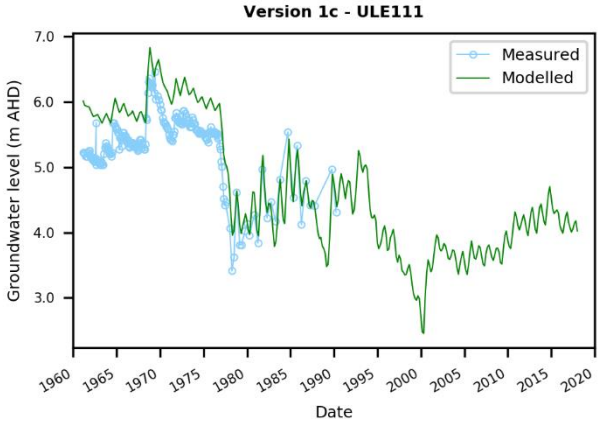

Version 1c - ULE105
Measured
Modelled
Groundwater level (m AHD)
Date

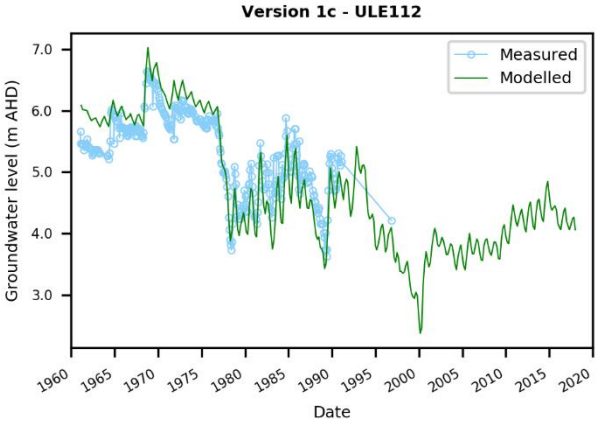

Version 1c - ULE106
Measured
Modelled
Groundwater level (m AHD)
Date

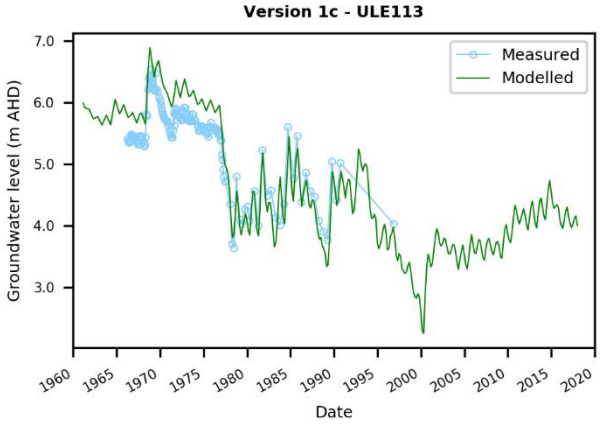

Version 1c - ULE107
Measured
Modelled
Groundwater level (m AHD)
Date

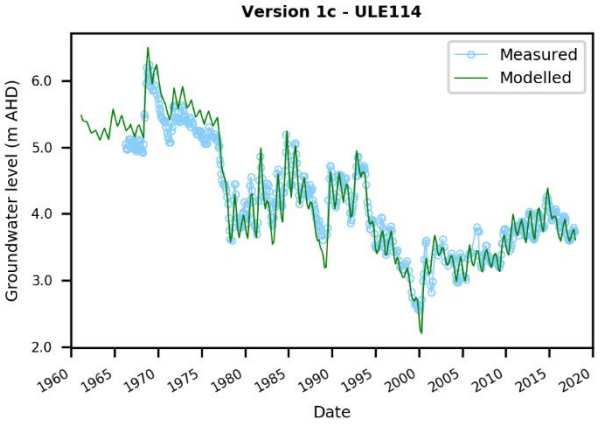

Version 1c - ULE108
Measured
Modelled
Groundwater level (m AHD)
Date

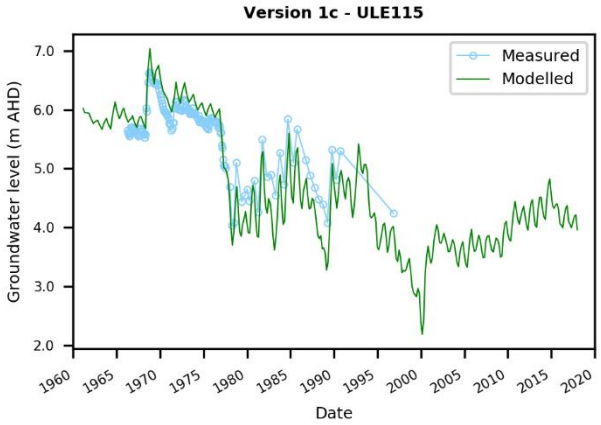

Version 1c - ULE109
Measured
Modelled
Groundwater level (m AHD)
Date

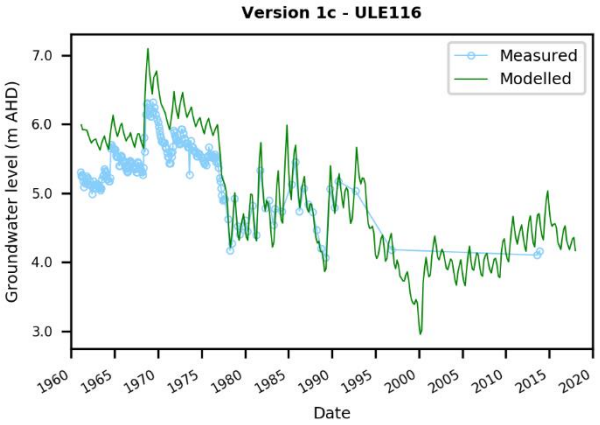

Version 1c - ULE111
Measured
Modelled
Groundwater level (m AHD)
Date

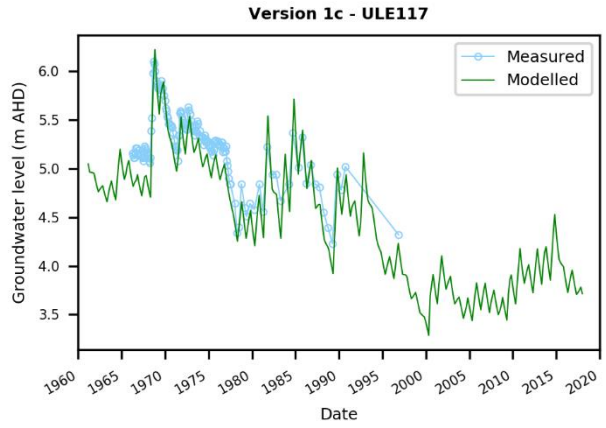

Version 1c - ULE112
Measured
Modelled
Groundwater level (m AHD)
Date

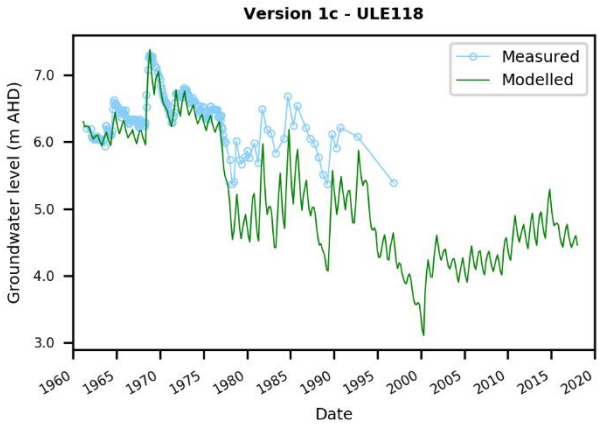

Version 1c - ULE113
Measured
Modelled
Groundwater level (m AHD)
Date

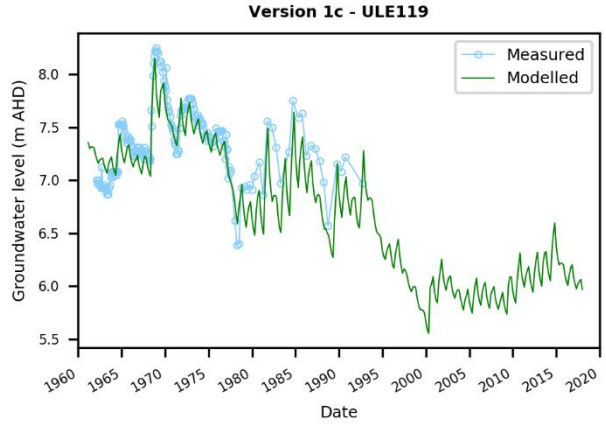

Version 1c - ULE114
Measured
Modelled
Groundwater level (m AHD)
Date

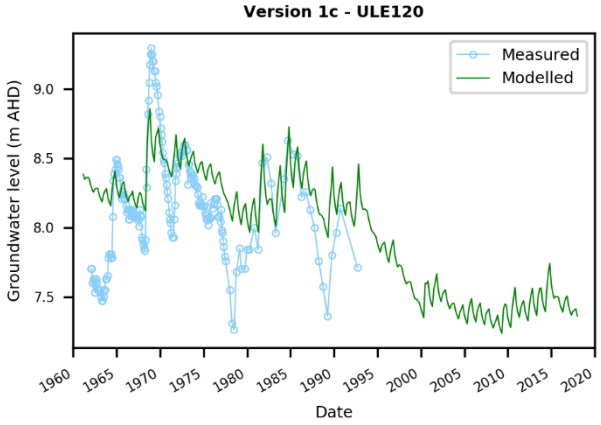

Version 1c - ULE115
Measured
Modelled
Groundwater level (m AHD)
Date

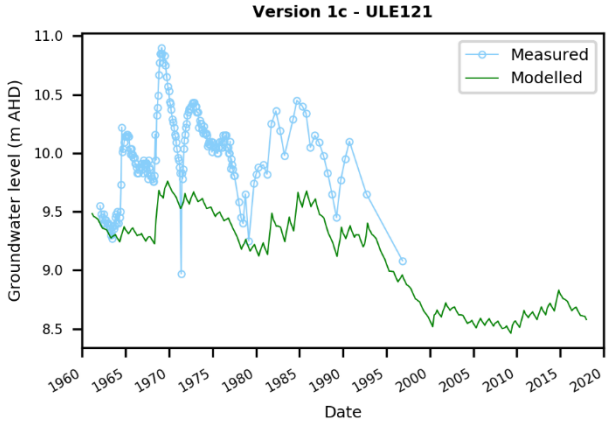

Version 1c - ULE116
Measured
Modelled
Groundwater level (m AHD)
Date

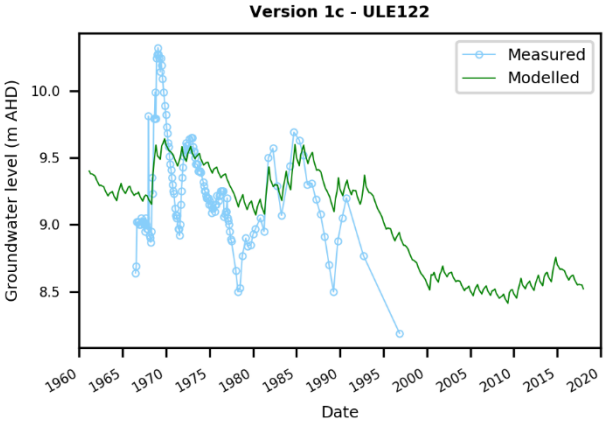

Version 1c - ULE117
Measured
Modelled
Groundwater level (m AHD)
Date

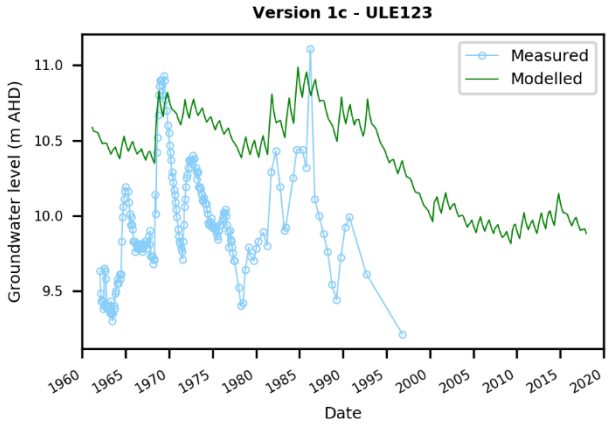

Version 1c - ULE118
Measured
Modelled
Groundwater level (m AHD)
Date

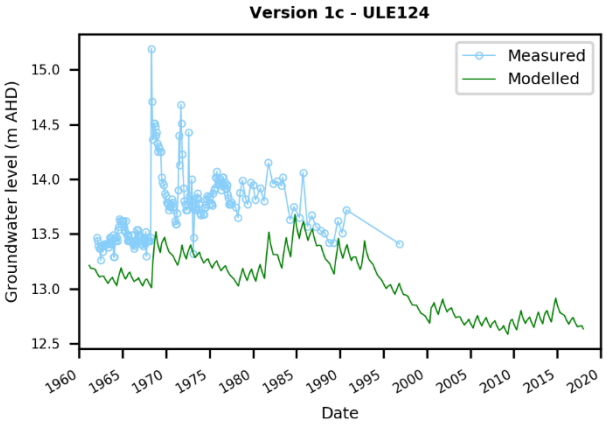

Version 1c - ULE119
Measured
Modelled
Groundwater level (m AHD)
Date

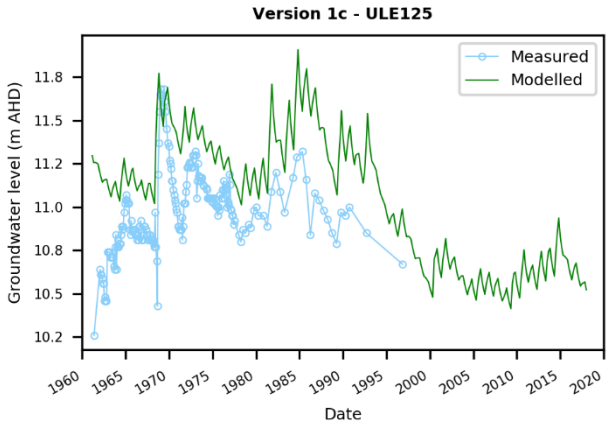

Version 1c - ULE120
Measured
Modelled
Groundwater level (m AHD)
Date

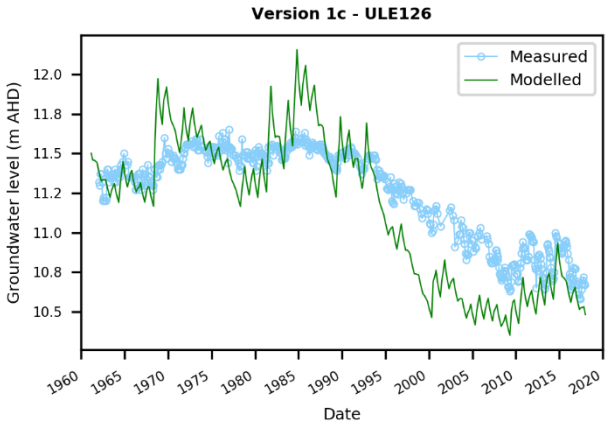

Version 1c - ULE121
Measured
Modelled
Groundwater level (m AHD)
Date

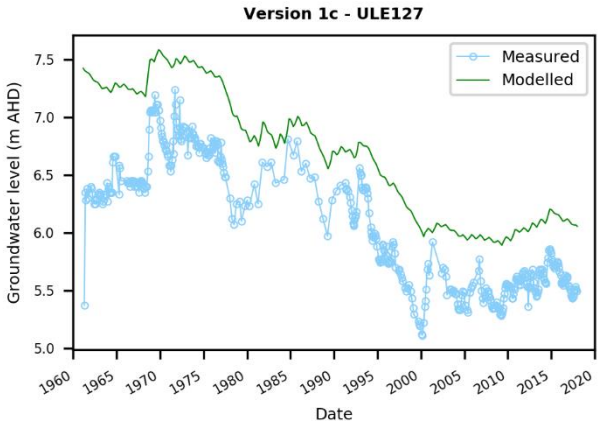

Version 1c - ULE122
Measured
Modelled
Groundwater level (m AHD)
Date

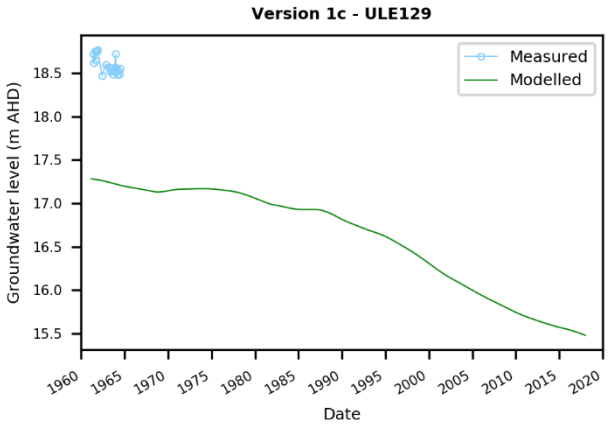

Version 1c - ULE123
Measured
Modelled
Groundwater level (m AHD)
Date

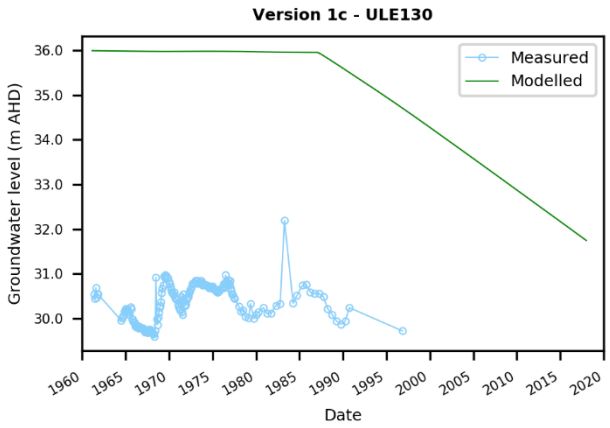

Version 1c - ULE124
Measured
Modelled
Groundwater level (m AHD)
Date

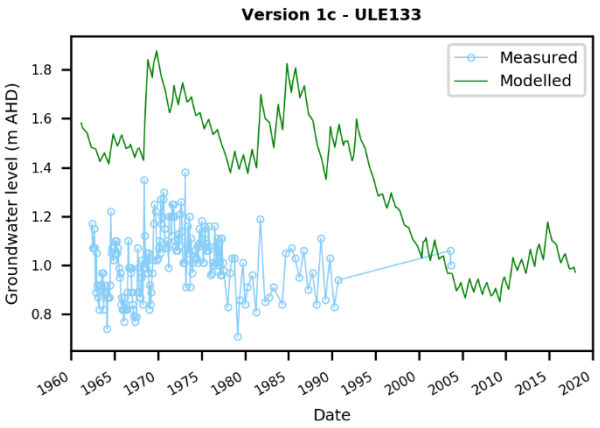

Version 1c - ULE125
Measured
Modelled
Groundwater level (m AHD)
Date

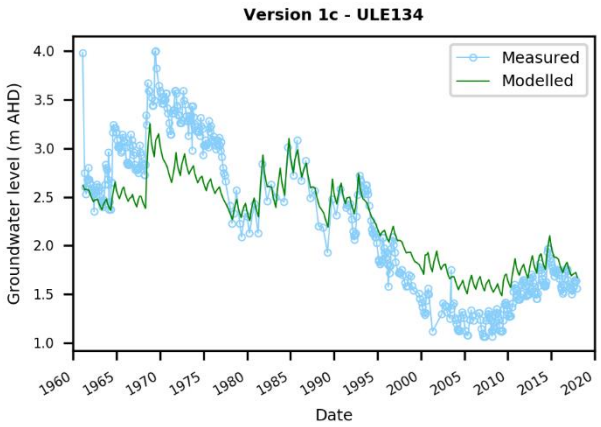

Version 1c - ULE126
Measured
Modelled
Groundwater level (m AHD)
Date

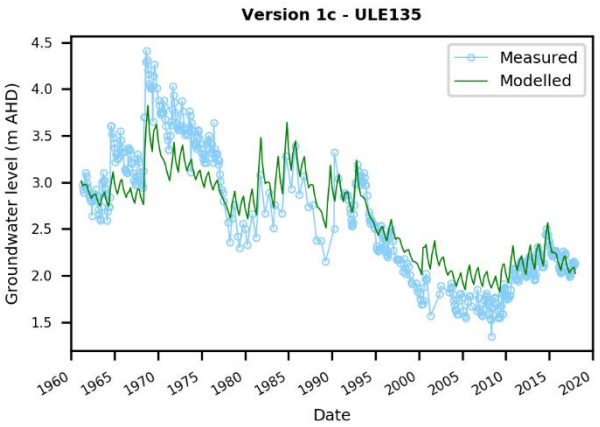

Version 1c - ULE127
Measured
Modelled
Groundwater level (m AHD)
Date

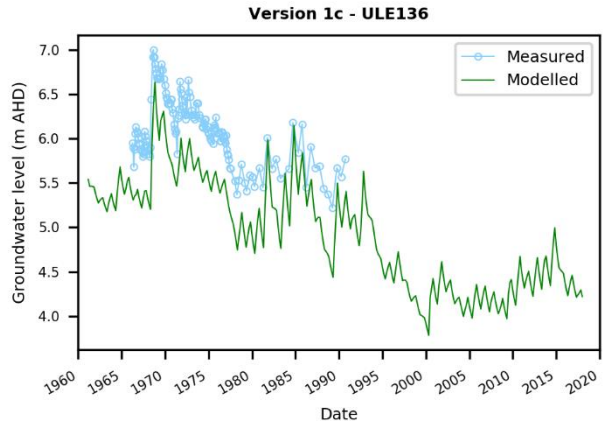

Version 1c - ULE129
Measured
Modelled
Groundwater level (m AHD)
Date

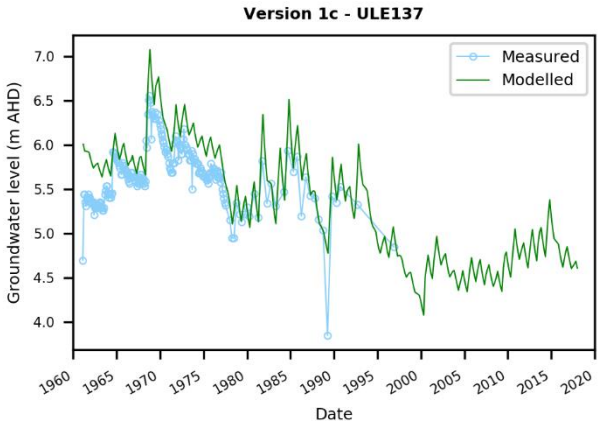

Version 1c - ULE130
Measured
Modelled
Groundwater level (m AHD)
Date

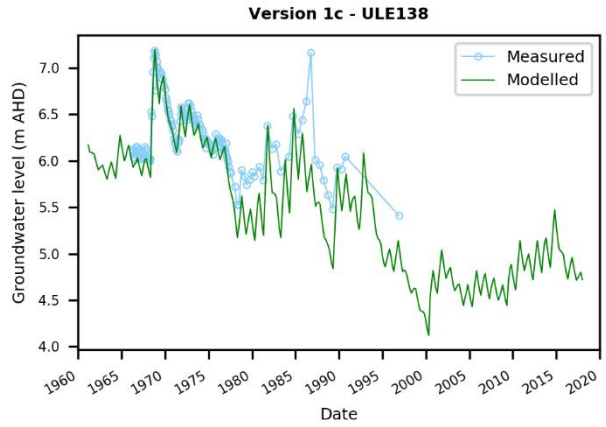

Version 1c - ULE133
Measured
Modelled
Groundwater level (m AHD)
Date

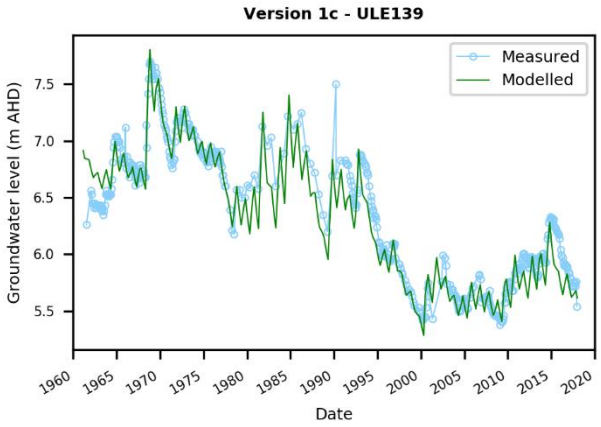

Version 1c - ULE134
Measured
Modelled
Groundwater level (m AHD)
Date

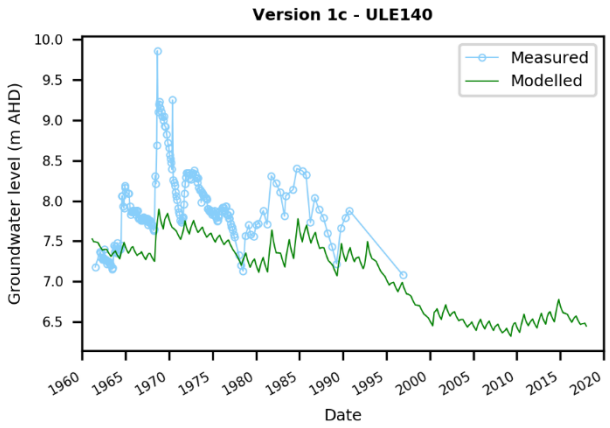

Version 1c - ULE135
Measured
Modelled
Groundwater level (m AHD)
Date

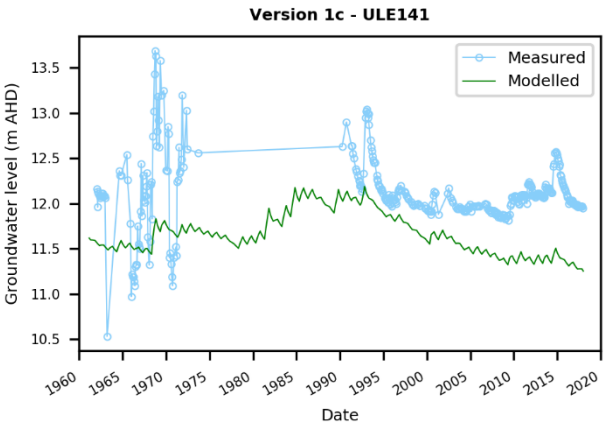

Version 1c - ULE136
Measured
Modelled
Groundwater level (m AHD)
Date

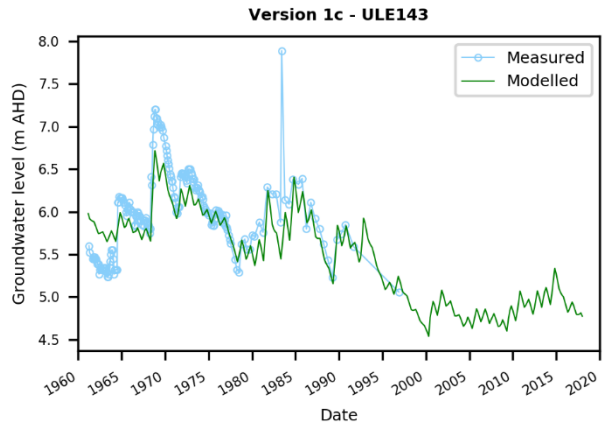

Version 1c - ULE137
Measured
Modelled
Groundwater level (m AHD)
Date

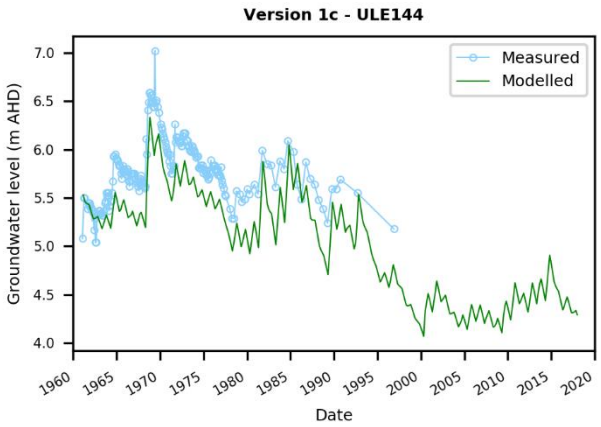

Version 1c - ULE138
Measured
Modelled
Groundwater level (m AHD)
Date

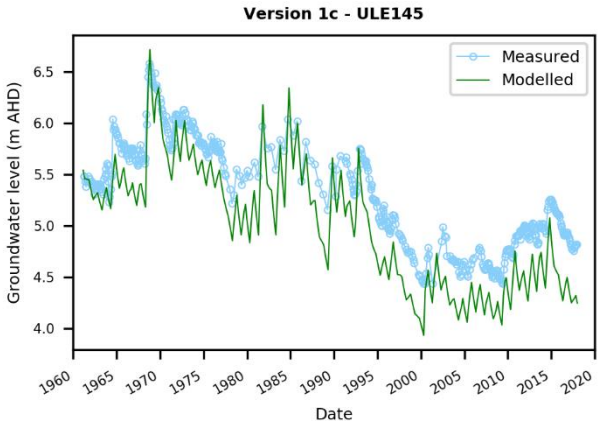

Version 1c - ULE139
Measured
Modelled
Groundwater level (m AHD)
Date

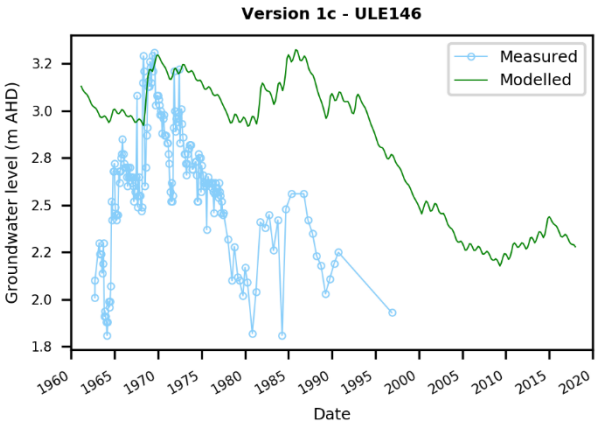

Version 1c - ULE140
Measured
Modelled
Groundwater level (m AHD)
Date

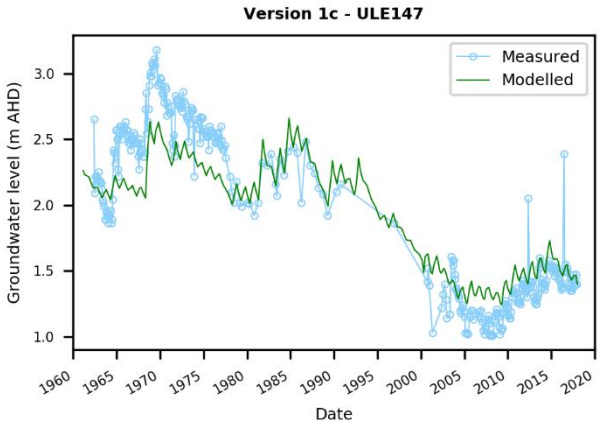

Version 1c - ULE141
Measured
Modelled
Groundwater level (m AHD)
Date

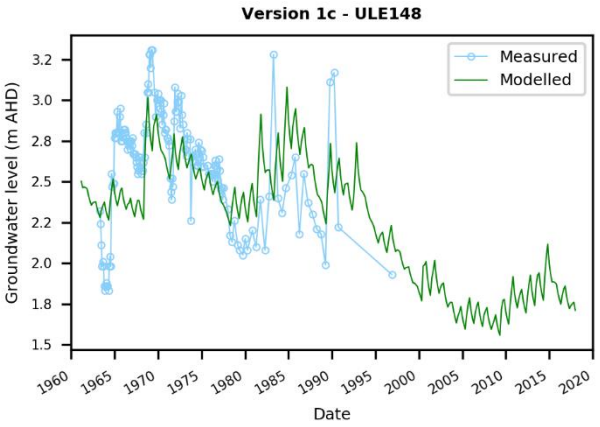

Version 1c - ULE143
Measured
Modelled
Groundwater level (m AHD)
Date

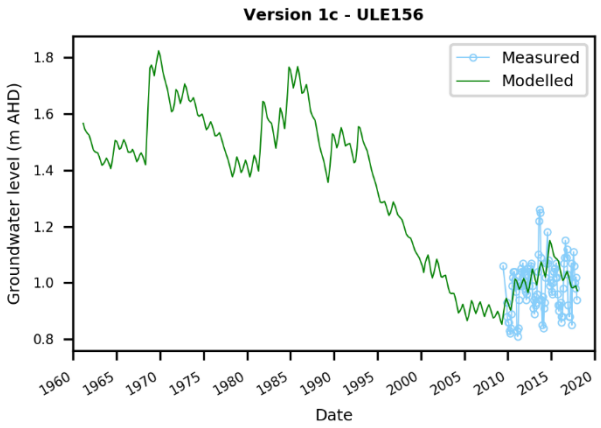

Version 1c - ULE144
Measured
Modelled
Groundwater level (m AHD)
Date

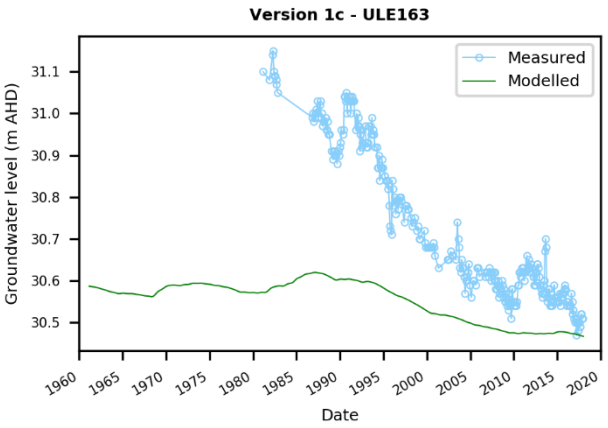

Version 1c - ULE145
Measured
Modelled
Groundwater level (m AHD)
Date

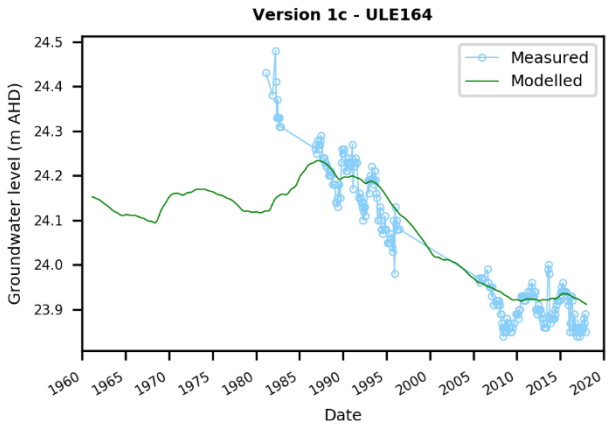

Version 1c - ULE146
Measured
Modelled
Groundwater level (m AHD)
Date

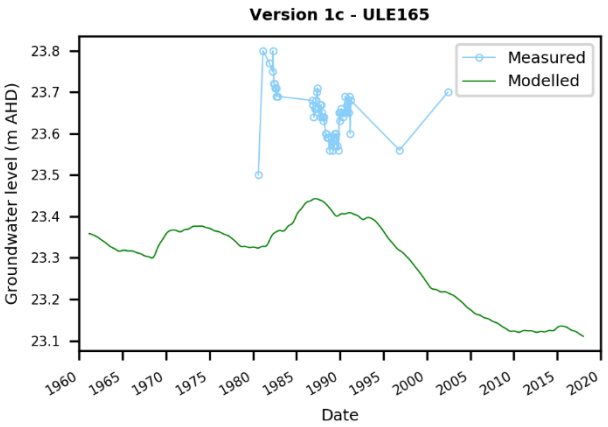

Version 1c - ULE147
Measured
Modelled
Groundwater level (m AHD)
Date

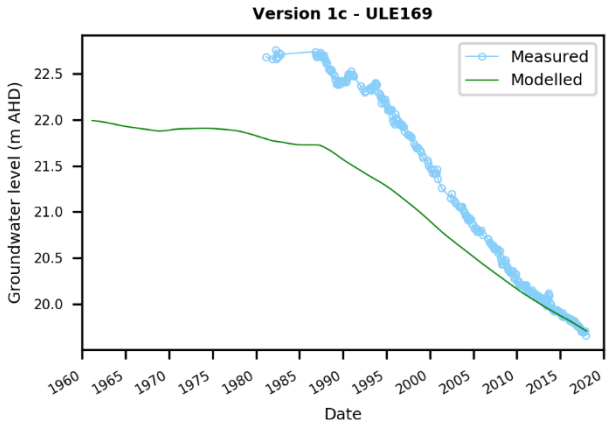

Version 1c - ULE148
Measured
Modelled
Groundwater level (m AHD)
Date

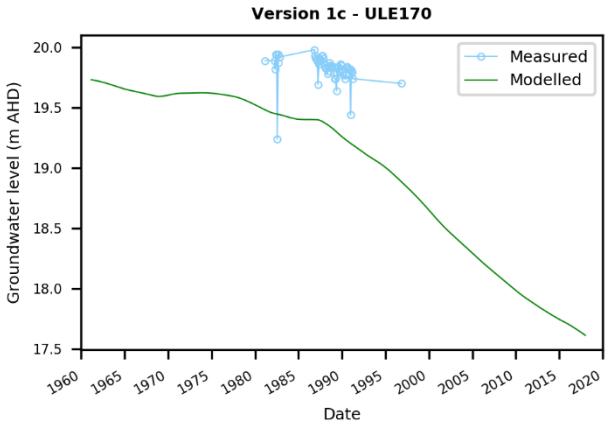

Version 1c - ULE156
Measured
Modelled
Groundwater level (m AHD)
Date

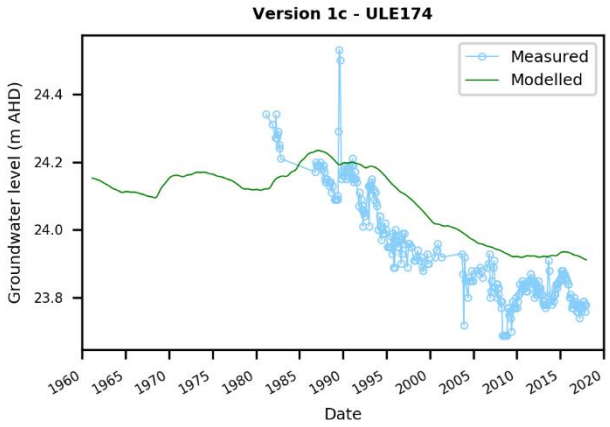

Version 1c - ULE163
Measured
Modelled
Groundwater level (m AHD)
Date

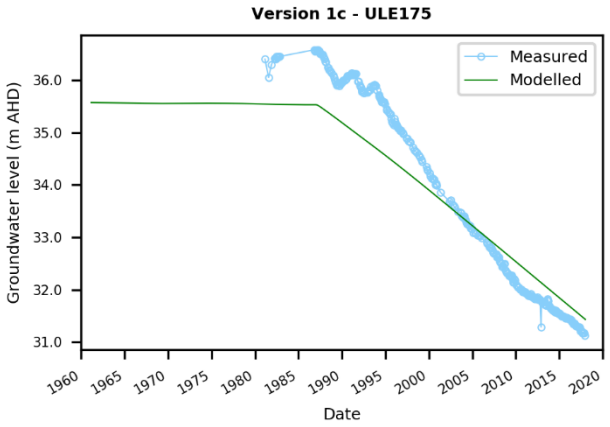

Version 1c - ULE164
Measured
Modelled
Groundwater level (m AHD)
Date

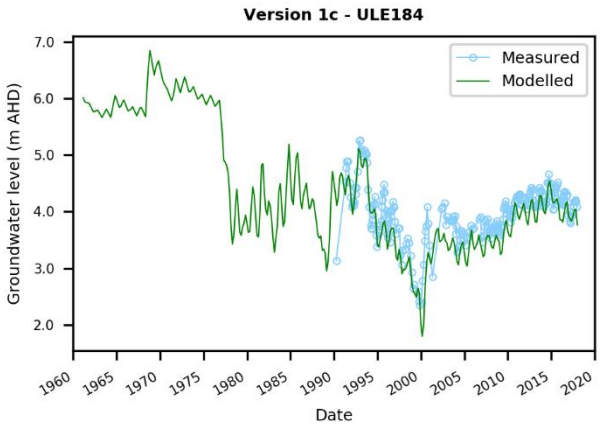

Version 1c - ULE165
Measured
Modelled
Groundwater level (m AHD)
Date

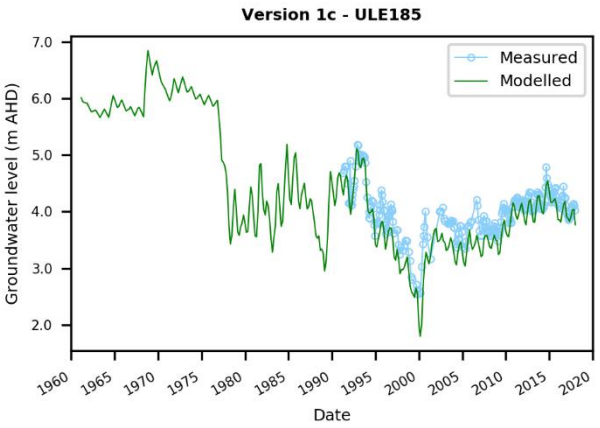

Version 1c - ULE169
Measured
Modelled
Groundwater level (m AHD)
Date

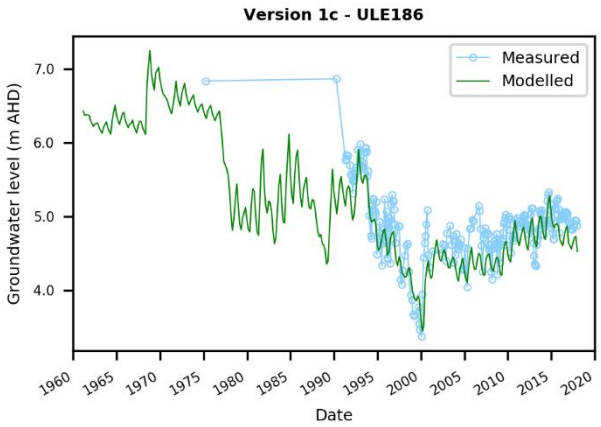

Version 1c - ULE170
Measured
Modelled
Groundwater level (m AHD)
Date

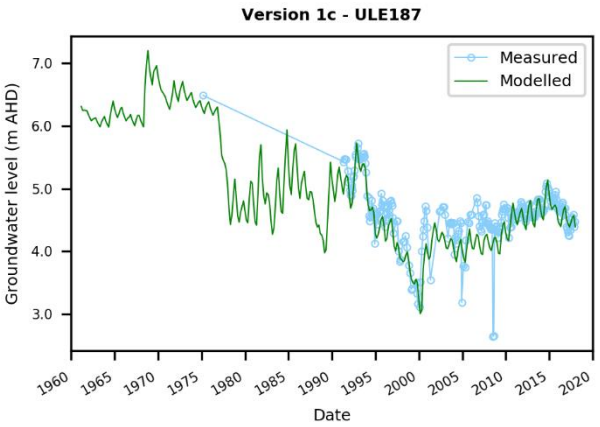

Version 1c - ULE174
Measured
Modelled
Groundwater level (m AHD)
Date

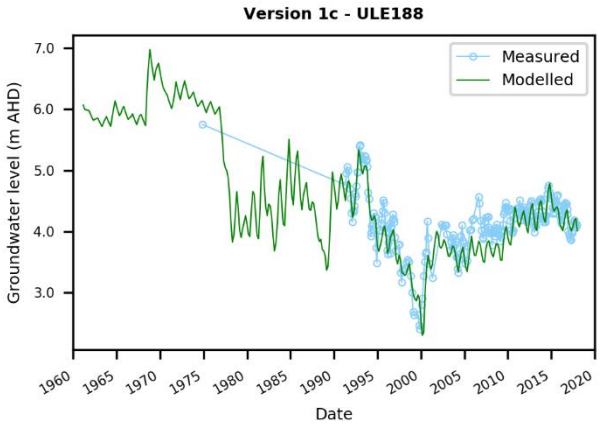

Version 1c - ULE175
Measured
Modelled
Groundwater level (m AHD)
Date

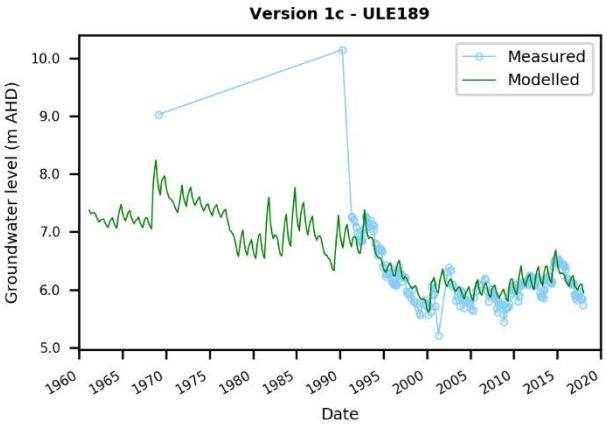

Version 1c - ULE184
Measured
Modelled
Groundwater level (m AHD)
Date

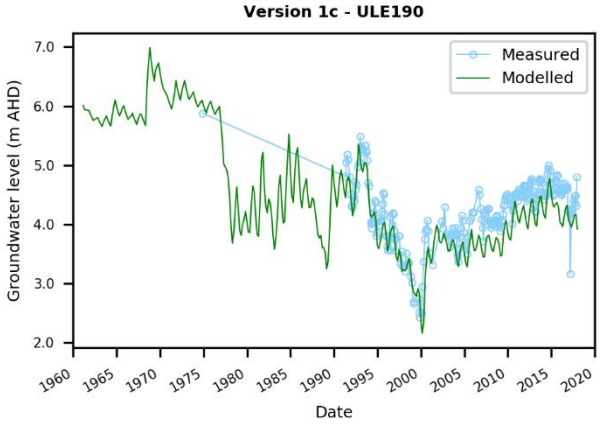

Version 1c - ULE185
Measured
Modelled
Groundwater level (m AHD)
Date

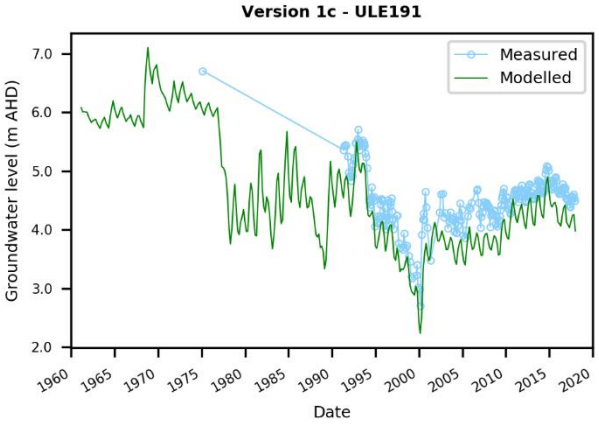

Version 1c - ULE186
Measured
Modelled
Groundwater level (m AHD)
Date

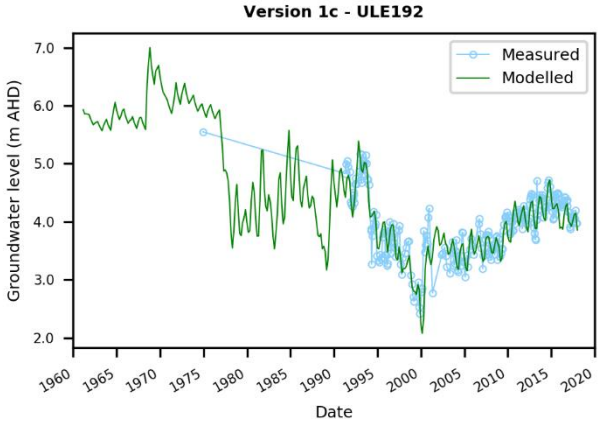

Version 1c - ULE187
Measured
Modelled
Groundwater level (m AHD)
Date

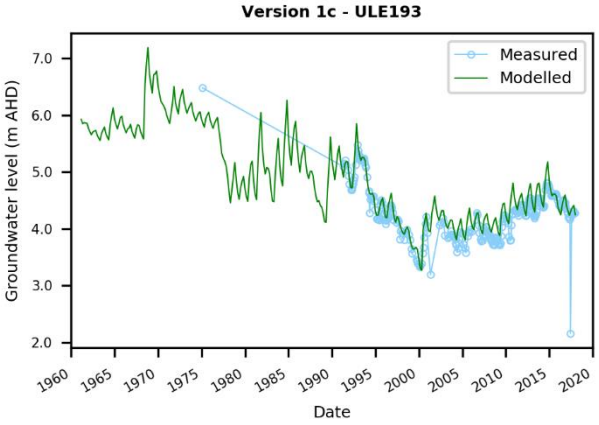

Version 1c - ULE188
Measured
Modelled
Groundwater level (m AHD)
Date

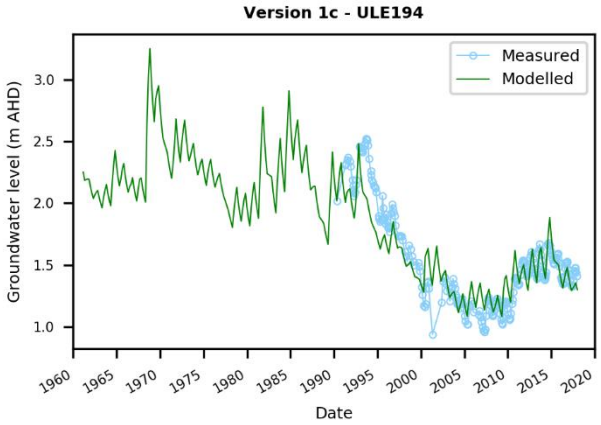

Version 1c - ULE189
Measured
Modelled
Groundwater level (m AHD)
Date

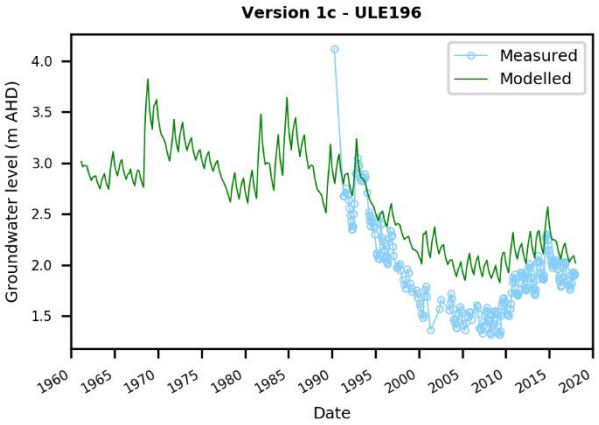

Version 1c - ULE190
Measured
Modelled
Groundwater level (m AHD)
Date

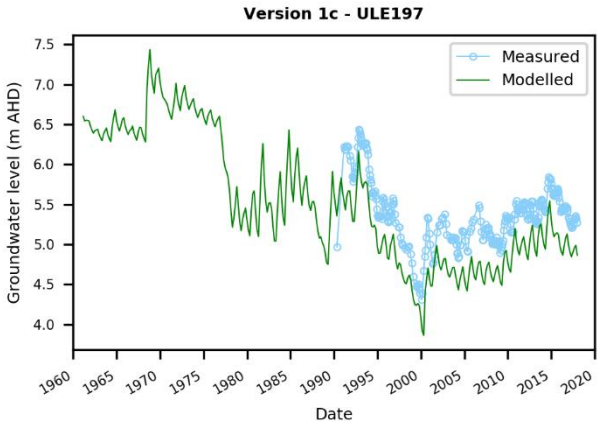

Version 1c - ULE191
Measured
Modelled
Groundwater level (m AHD)
Date

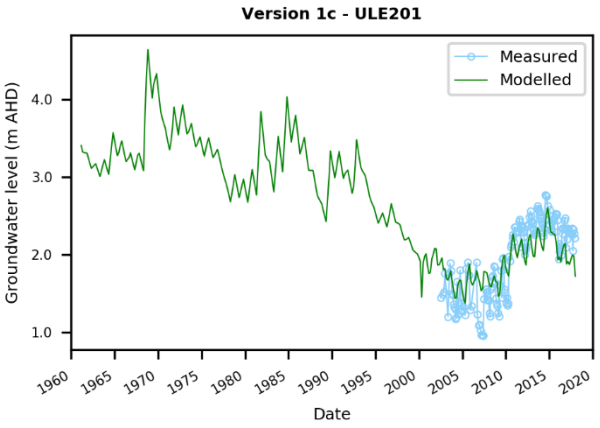

Version 1c - ULE192
Measured
Modelled
Groundwater level (m AHD)
Date

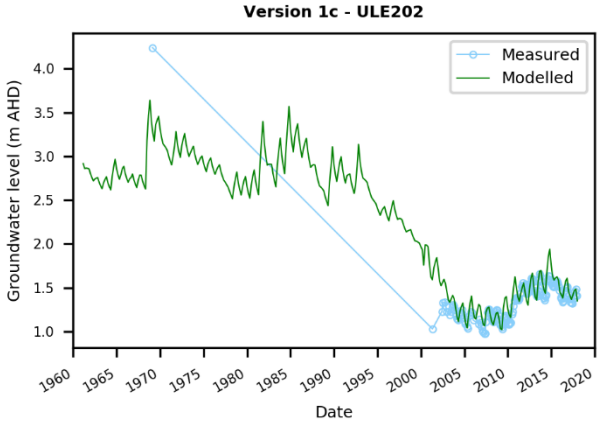

Version 1c - ULE193
Measured
Modelled
Groundwater level (m AHD)
Date

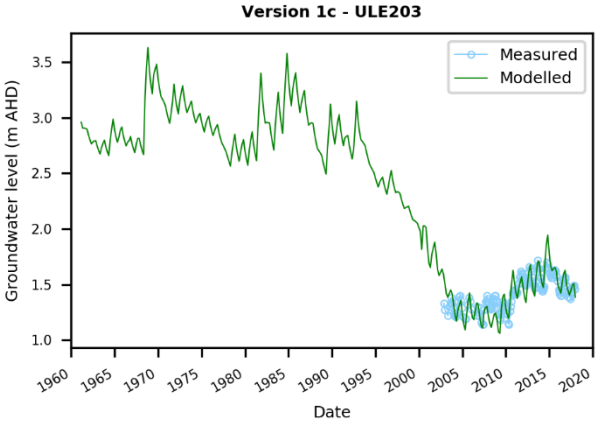

Version 1c - ULE194
Measured
Modelled
Groundwater level (m AHD)
Date

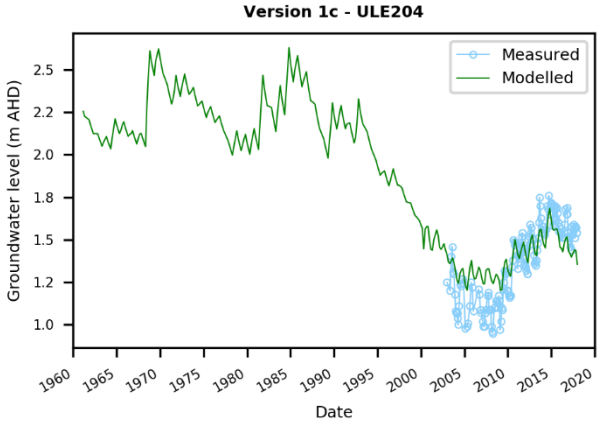

Version 1c - ULE196
Measured
Modelled
Groundwater level (m AHD)
Date

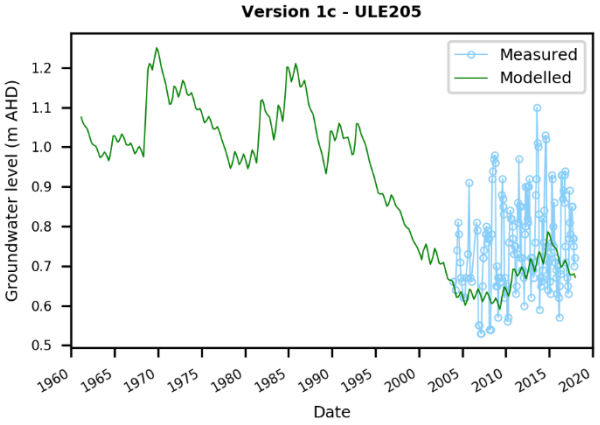

Version 1c - ULE197
Measured
Modelled
Groundwater level (m AHD)
Date

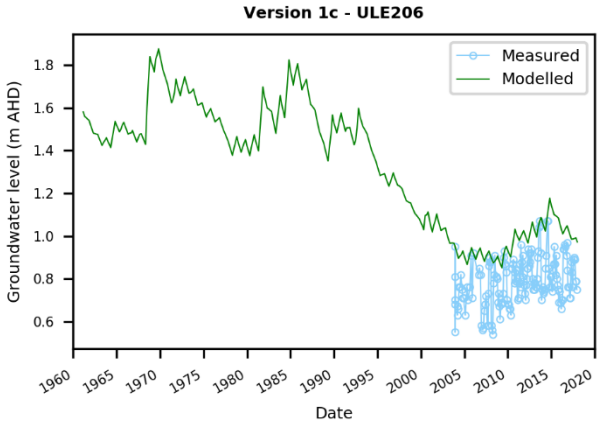

Version 1c - ULE201
Measured
Modelled
Groundwater level (m AHD)
Date

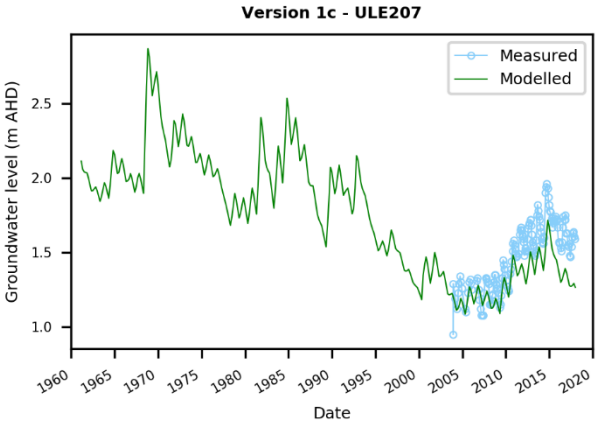

Version 1c - ULE202
Measured
Modelled
Groundwater level (m AHD)
Date

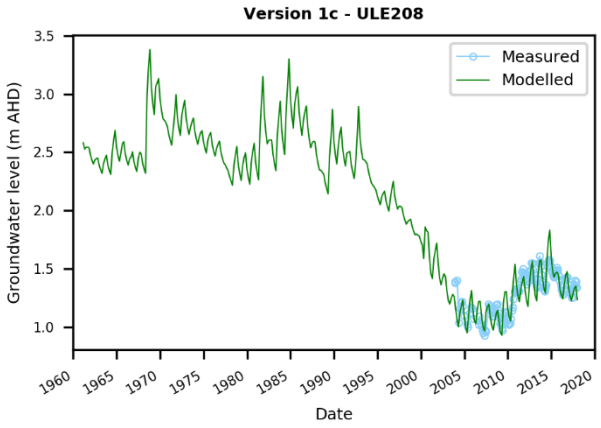

Version 1c - ULE203
Measured
Modelled
Groundwater level (m AHD)
Date

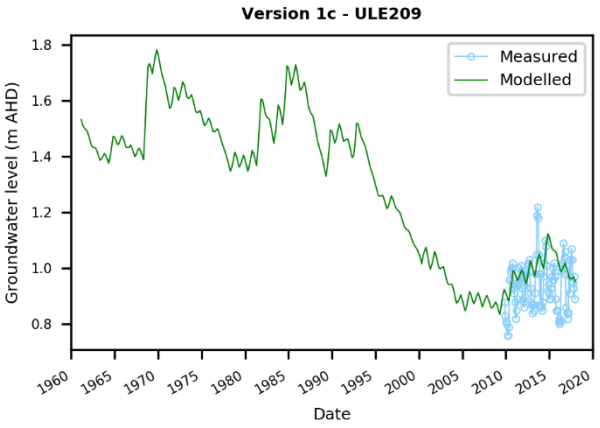

Version 1c - ULE204
Measured
Modelled
Groundwater level (m AHD)
Date

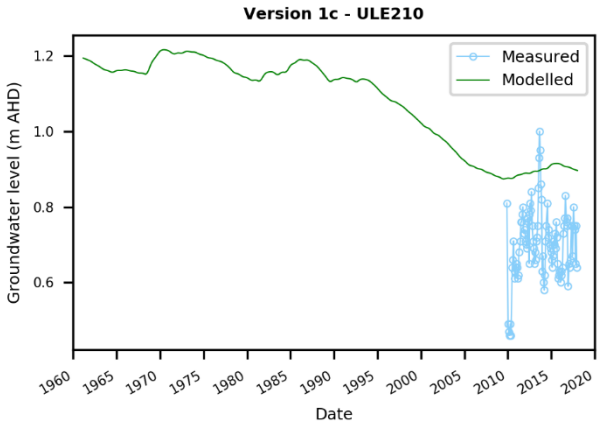

Version 1c - ULE205
Measured
Modelled
Groundwater level (m AHD)
Date

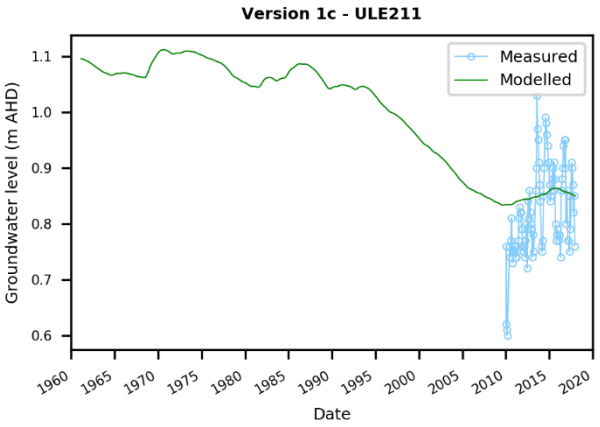

Version 1c - ULE206
Measured
Modelled
Groundwater level (m AHD)
Date

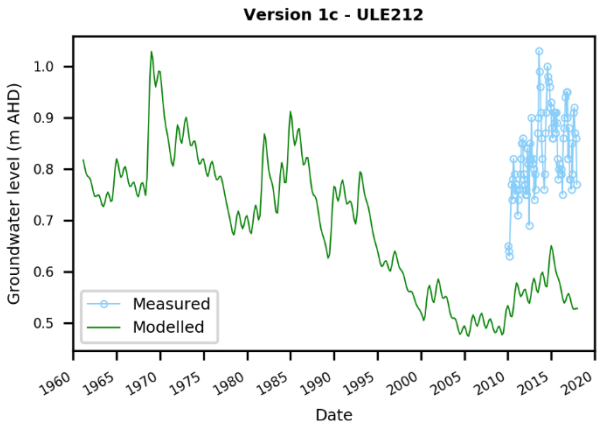

Version 1c - ULE207
Measured
Modelled
Groundwater level (m AHD)
Date

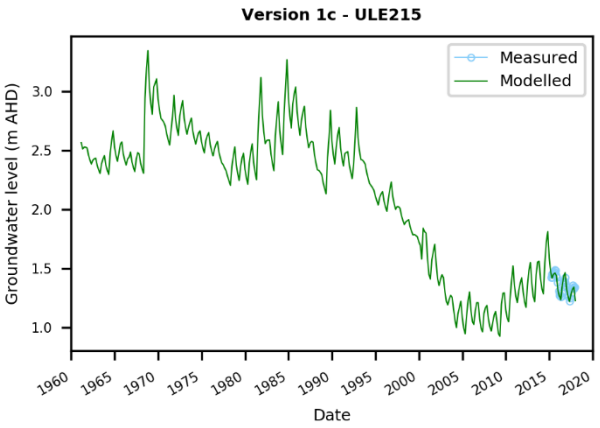

Version 1c - ULE208
Measured
Modelled
Groundwater level (m AHD)
Date


Version 1c - ULE209
Measured
Modelled
Groundwater level (m AHD)
Date

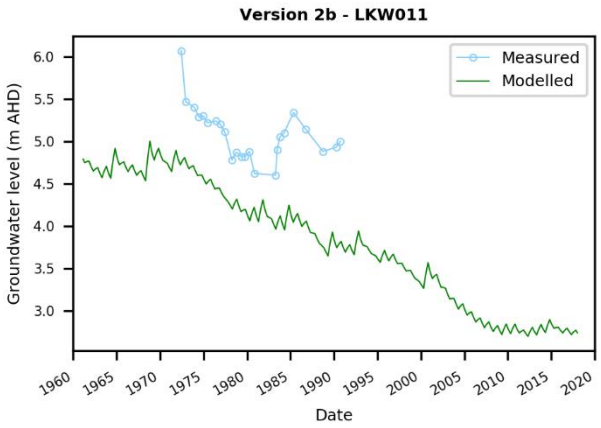

Version 1c - ULE210
Measured
Modelled
Groundwater level (m AHD)
Date

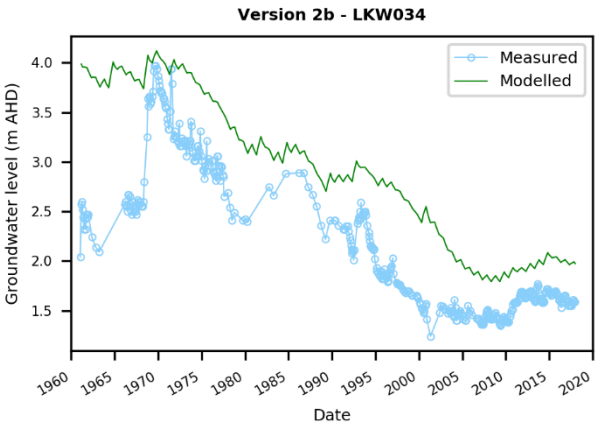

Version 1c - ULE211
Measured
Modelled
Groundwater level (m AHD)
Date

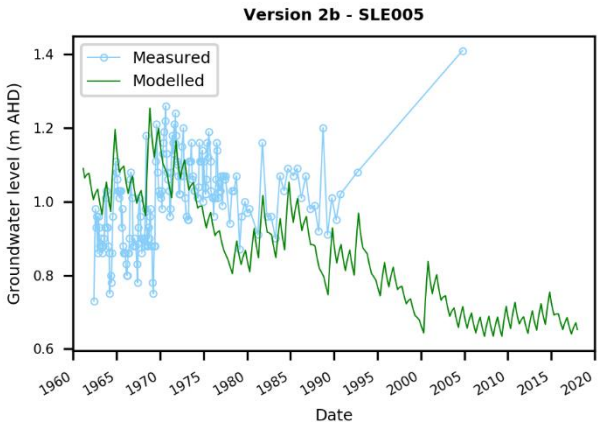

Version 1c - ULE212
Measured
Modelled
Groundwater level (m AHD)
Date

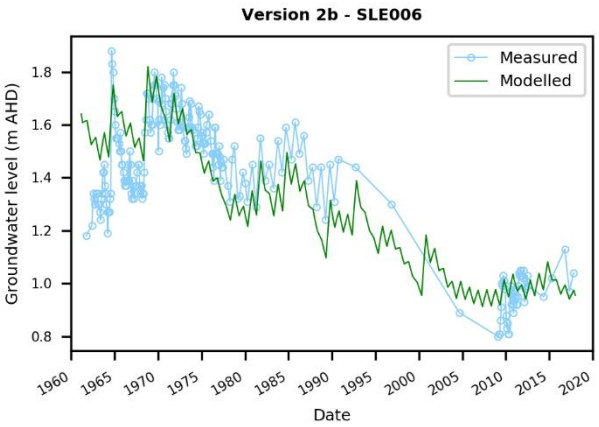

Version 1c - ULE215
Measured
Modelled
Groundwater level (m AHD)
Date

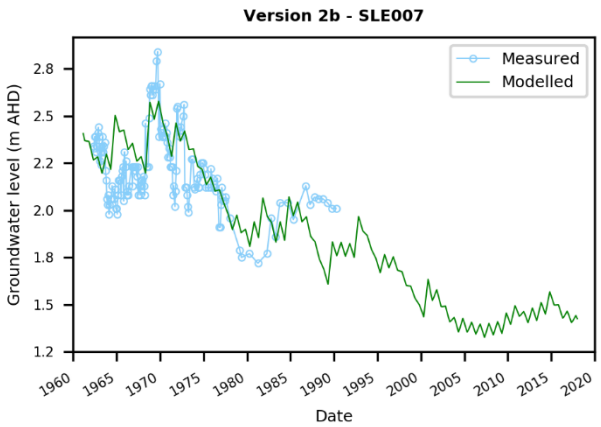
D.2 Calibration hydrographs from model version 2b

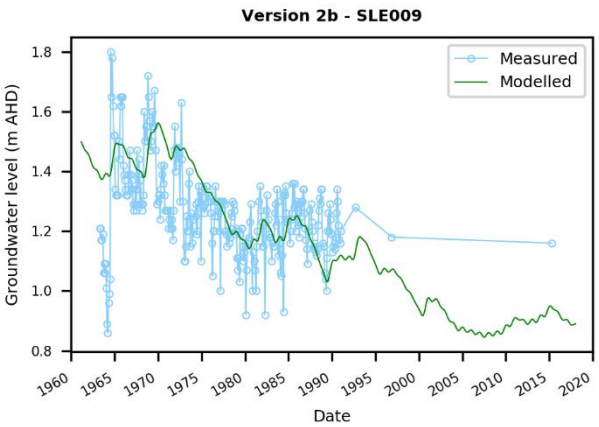


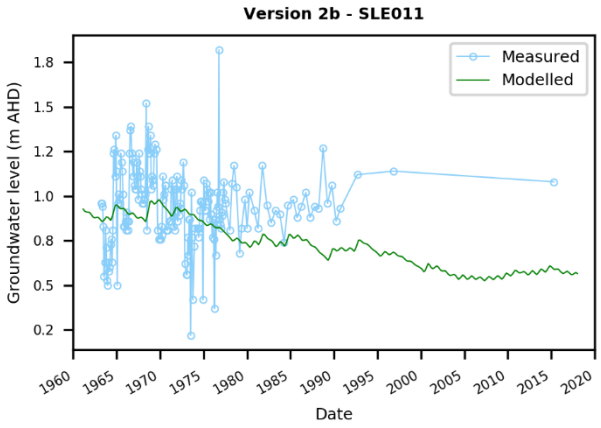


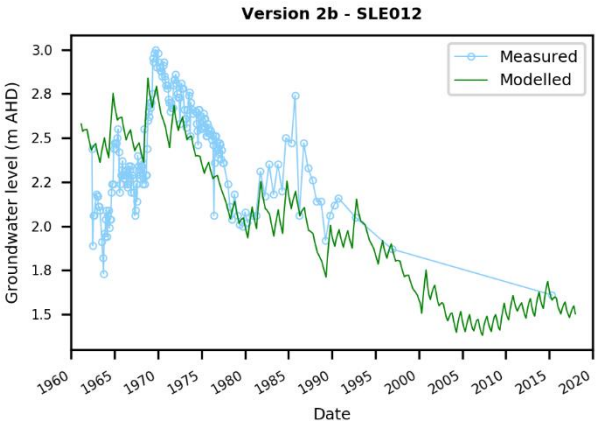


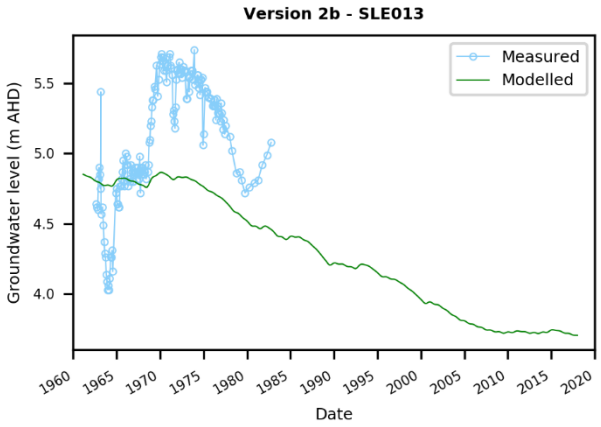


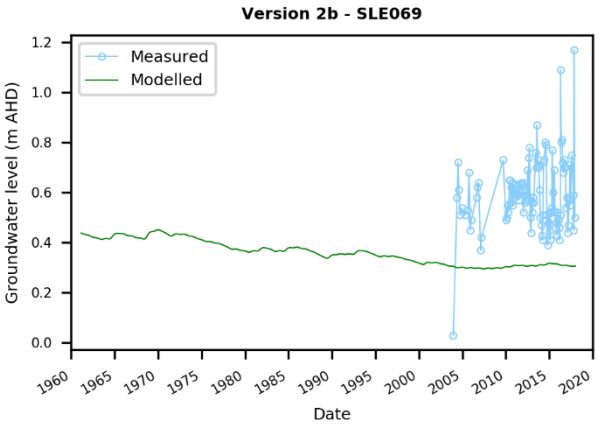


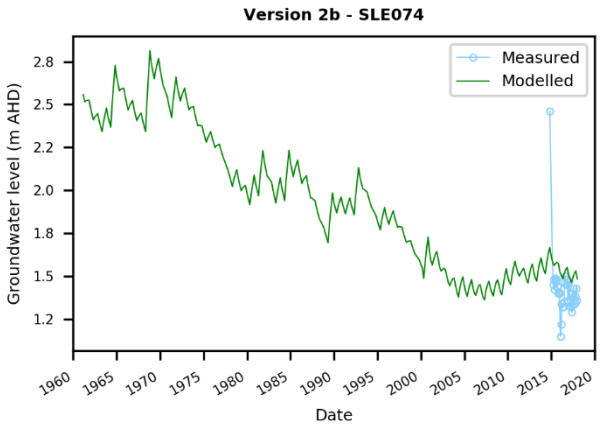


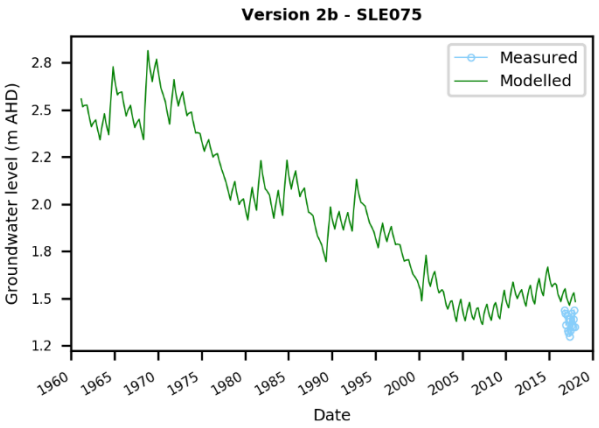

Version 2b - SLE011
Measured
Modelled
Groundwater level (m AHD)
Date

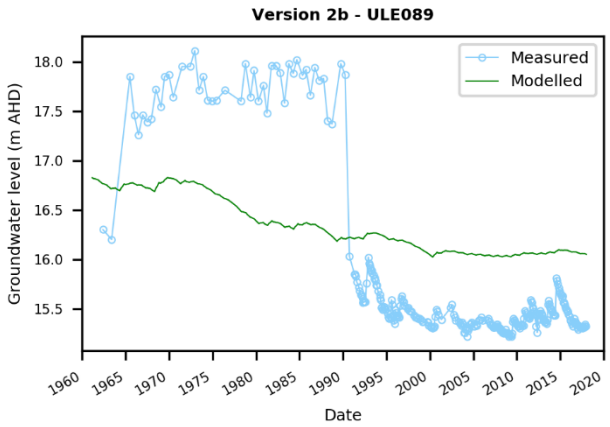

Version 2b - SLE012
Measured
Modelled
Groundwater level (m AHD)
Date

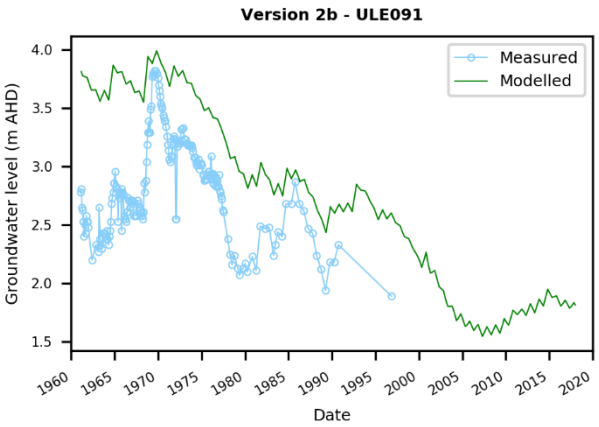

Version 2b - SLE013
Measured
Modelled
Groundwater level (m AHD)
Date

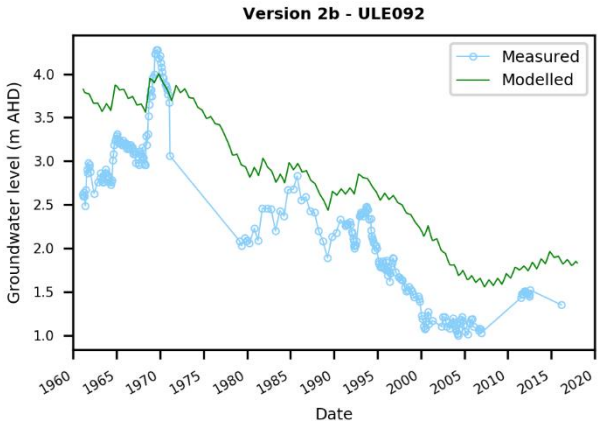

Version 2b - SLE069
Measured
Modelled
Groundwater level (m AHD)
Date

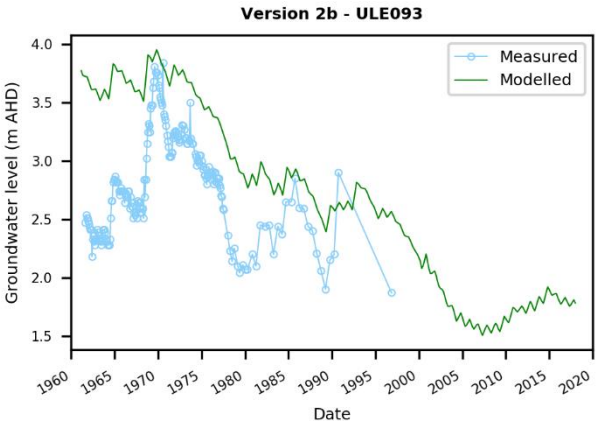

Version 2b - SLE074
Measured
Modelled
Groundwater level (m AHD)
Date

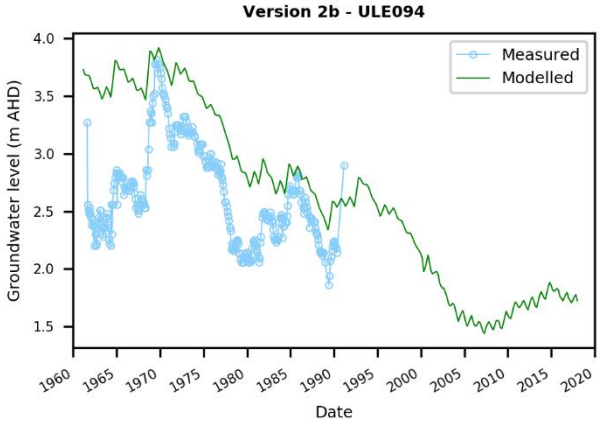

Version 2b - SLE075
Measured
Modelled
Groundwater level (m AHD)
Date

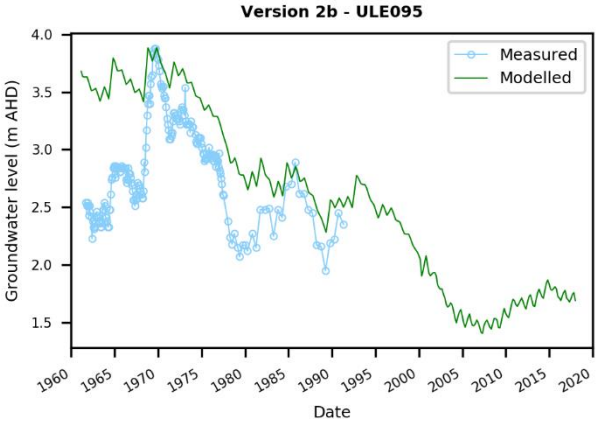

Version 2b - ULE089
Measured
Modelled
Groundwater level (m AHD)
Date

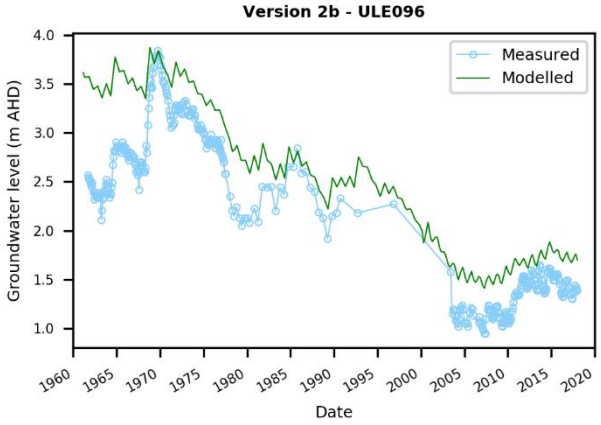

Version 2b - ULE091
Measured
Modelled
Groundwater level (m AHD)
Date

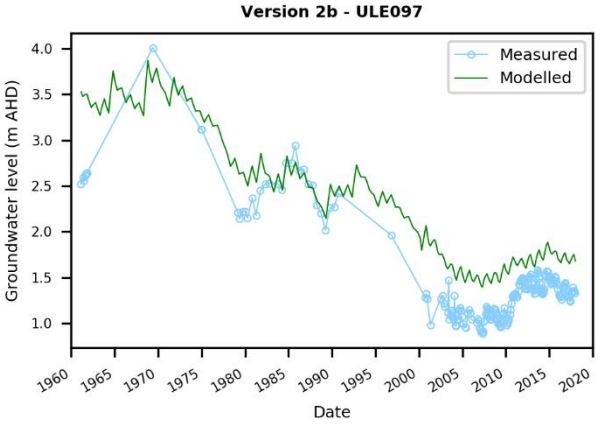

Version 2b - ULE092
Measured
Modelled
Groundwater level (m AHD)
Date

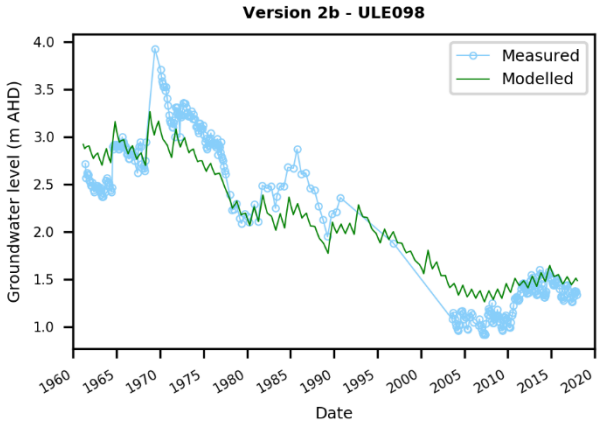

Version 2b - ULE093
Measured
Modelled
Groundwater level (m AHD)
Date

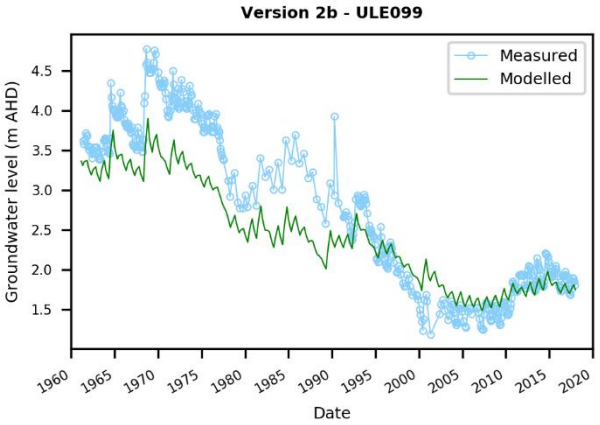

Version 2b - ULE094
Measured
Modelled
Groundwater level (m AHD)
Date

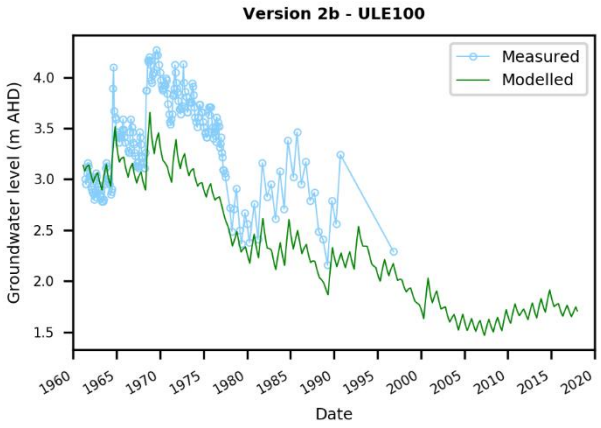

Version 2b - ULE095
Measured
Modelled
Groundwater level (m AHD)
Date

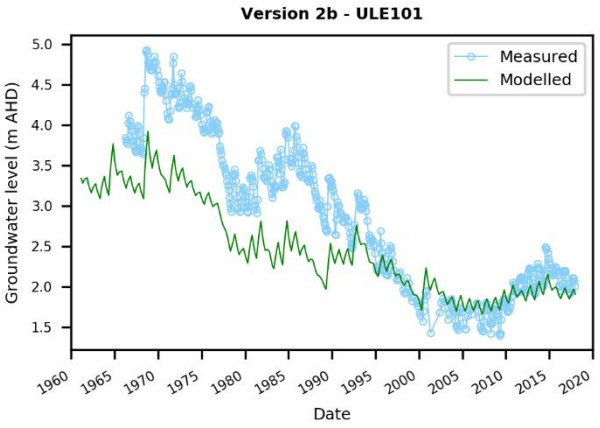

Version 2b - ULE096
Measured
Modelled
Groundwater level (m AHD)
Date

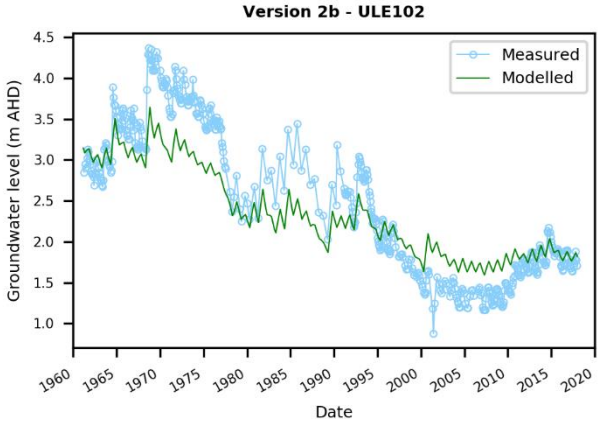

Version 2b - ULE097
Measured
Modelled
Groundwater level (m AHD)
Date

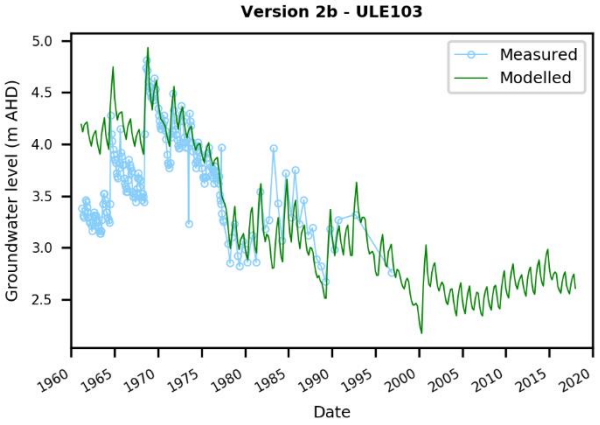

Version 2b - ULE098
Measured
Modelled
Groundwater level (m AHD)
Date

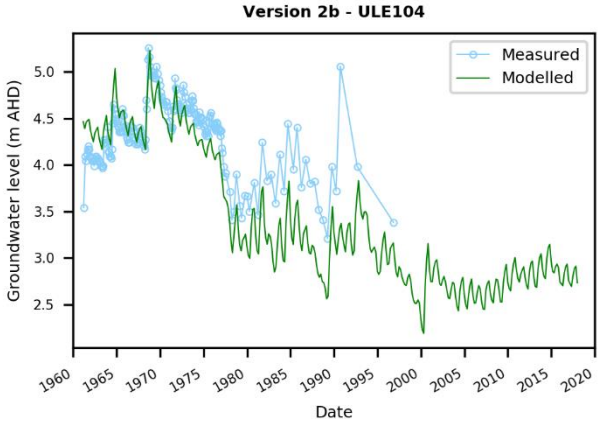

Version 2b - ULE099
Measured
Modelled
Groundwater level (m AHD)
Date

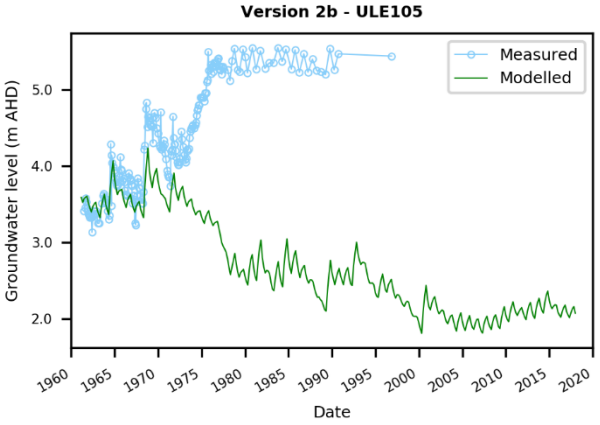

Version 2b - ULE100
Measured
Modelled
Groundwater level (m AHD)
Date

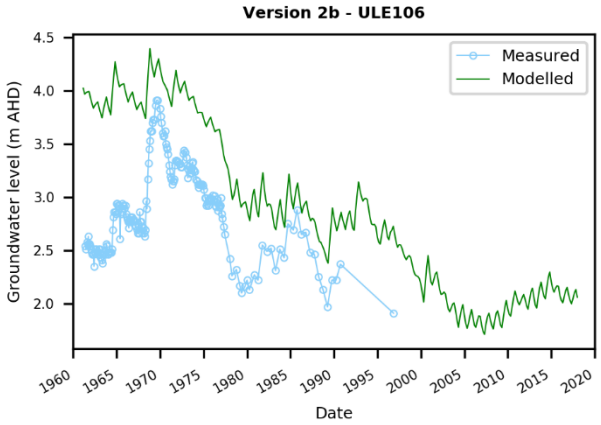

Version 2b - ULE101
Measured
Modelled
Groundwater level (m AHD)
Date

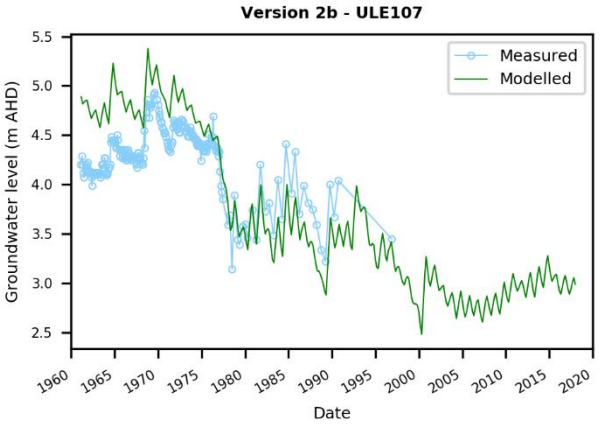

Version 2b - ULE102
Measured
Modelled
Groundwater level (m AHD)
Date

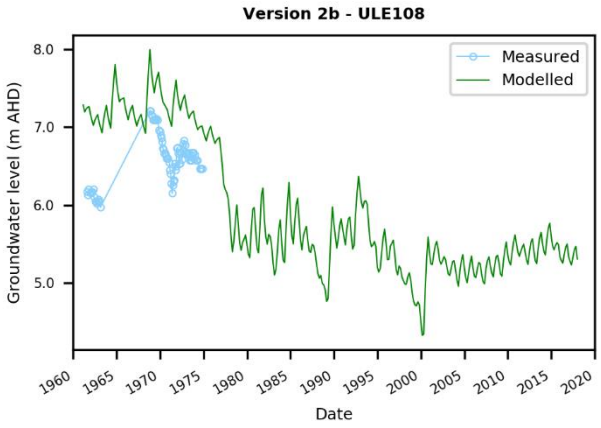

Version 2b - ULE103
Measured
Modelled
Groundwater level (m AHD)
Date

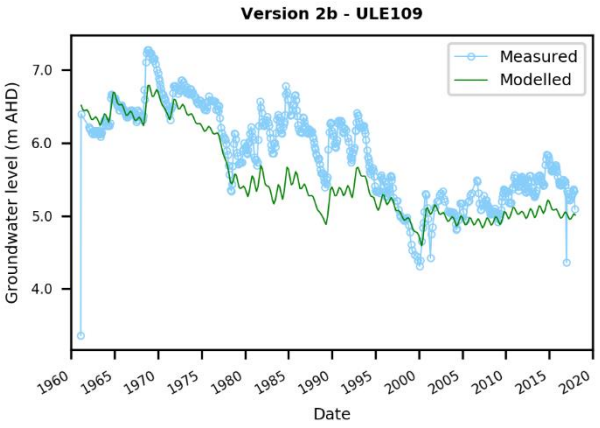

Version 2b - ULE104
Measured
Modelled
Groundwater level (m AHD)
Date

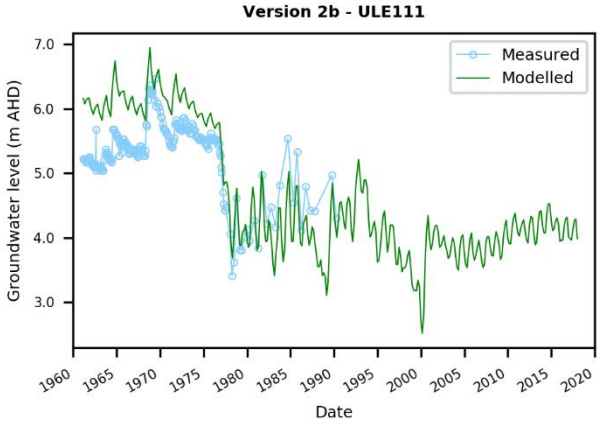

Version 2b - ULE105
Measured
Modelled
Groundwater level (m AHD)
Date

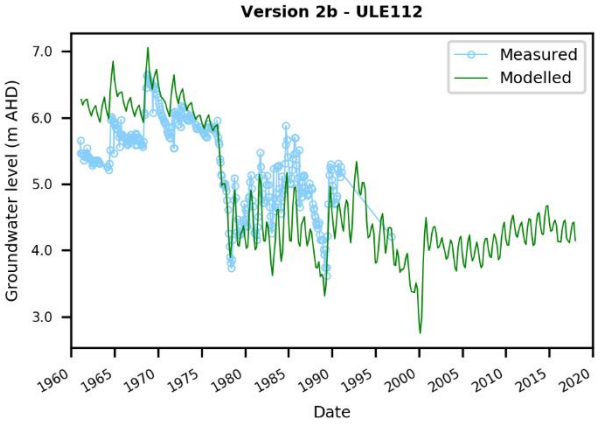

Version 2b - ULE106
Measured
Modelled
Groundwater level (m AHD)
Date

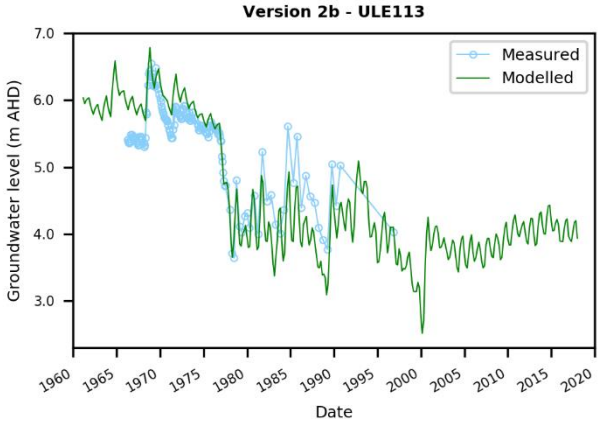

Version 2b - ULE107
Measured
Modelled
Groundwater level (m AHD)
Date

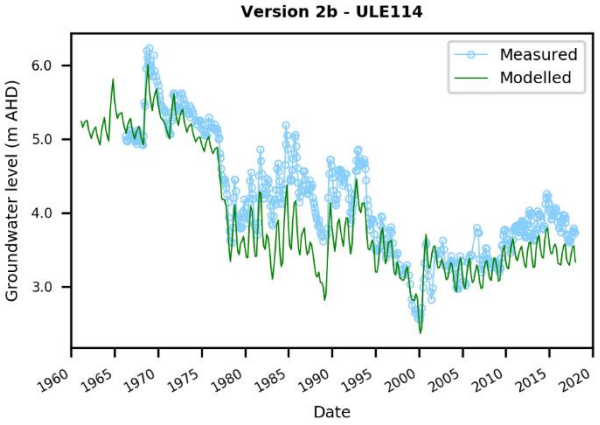

Version 2b - ULE108
Measured
Modelled
Groundwater level (m AHD)
Date

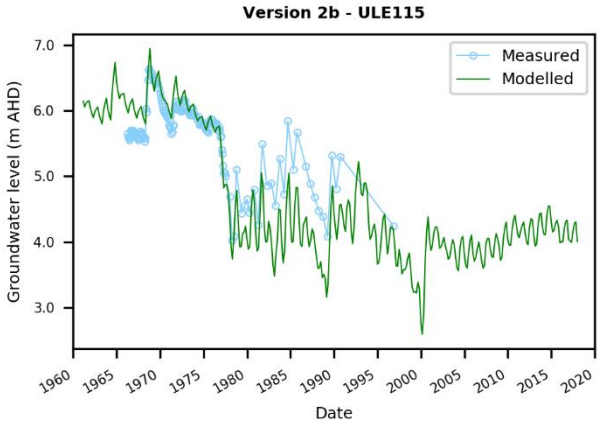

Version 2b - ULE109
Measured
Modelled
Groundwater level (m AHD)
Date

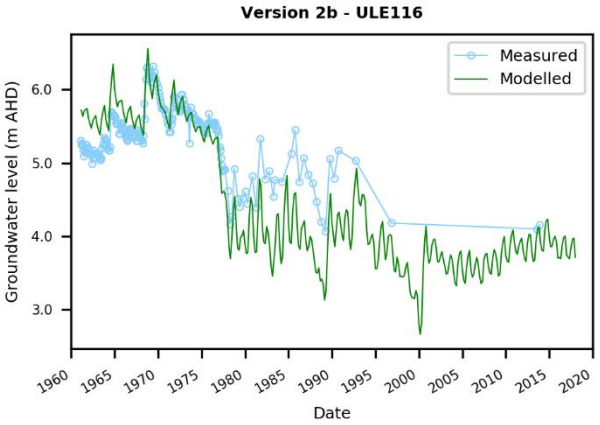

Version 2b - ULE111
Measured
Modelled
Groundwater level (m AHD)
Date

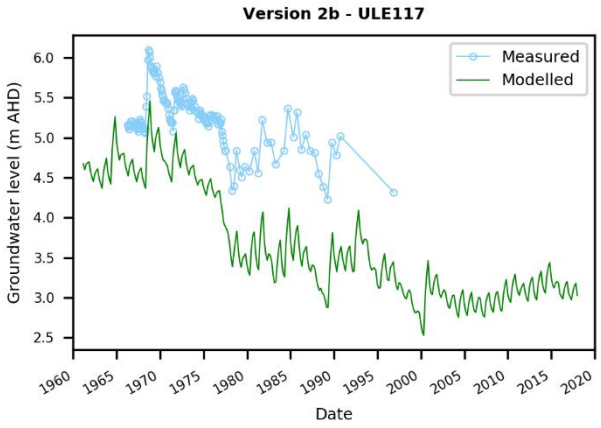

Version 2b - ULE112
Measured
Modelled
Groundwater level (m AHD)
Date

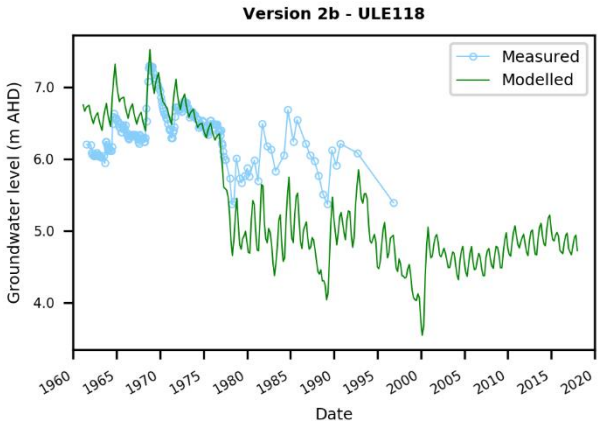

Version 2b - ULE113
Measured
Modelled
Groundwater level (m AHD)
Date

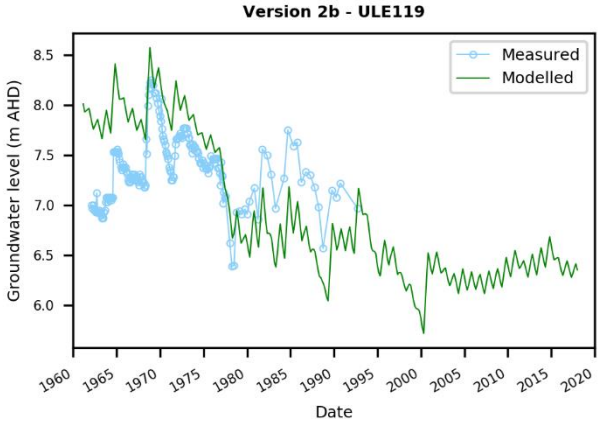

Version 2b - ULE114
Measured
Modelled
Groundwater level (m AHD)
Date

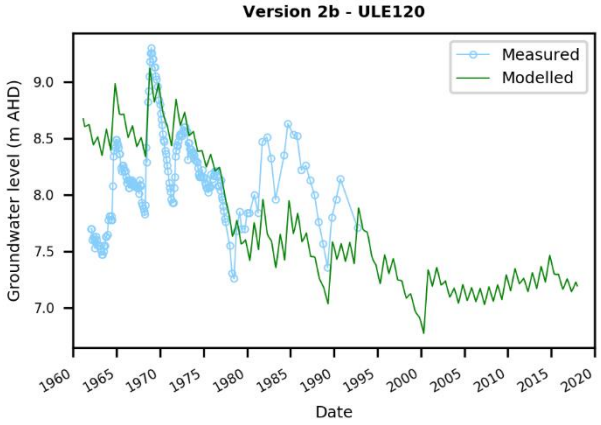

Version 2b - ULE115
Measured
Modelled
Groundwater level (m AHD)
Date

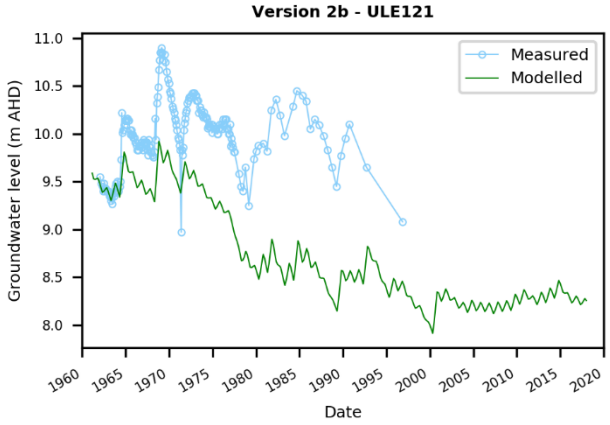

Version 2b - ULE116
Measured
Modelled
Groundwater level (m AHD)
Date

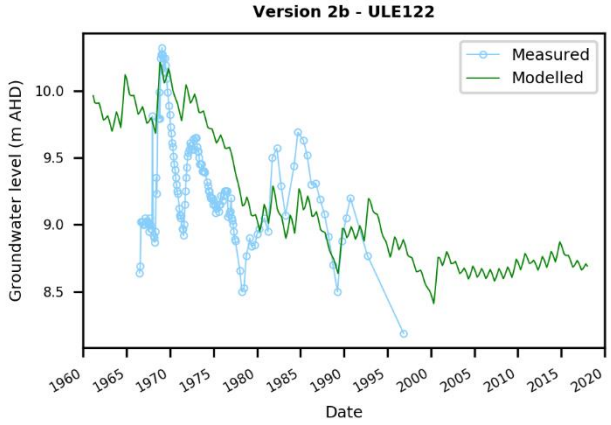

Version 2b - ULE117
Measured
Modelled
Groundwater level (m AHD)
Date

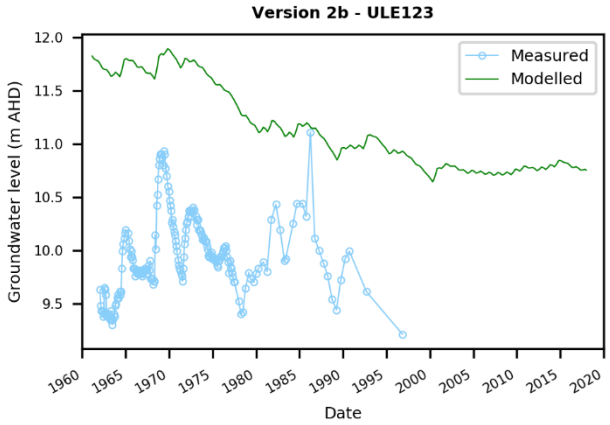

Version 2b - ULE118
Measured
Modelled
Groundwater level (m AHD)
Date

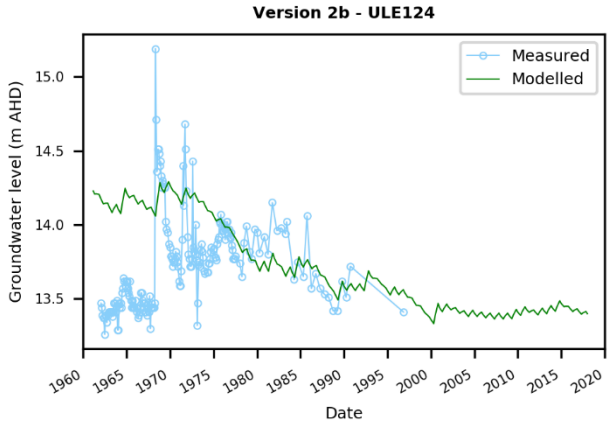

Version 2b - ULE119
Measured
Modelled
Groundwater level (m AHD)
Date

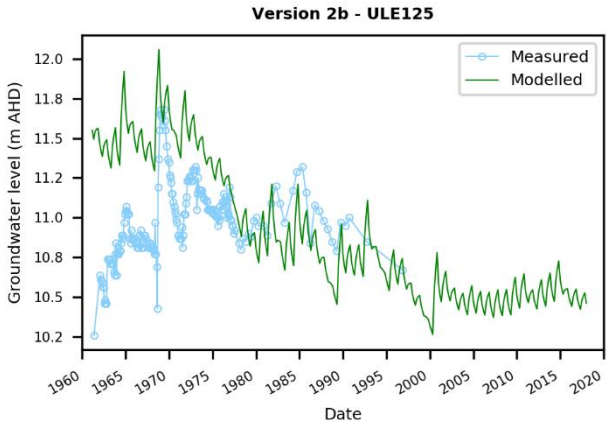

Version 2b - ULE120
Measured
Modelled
Groundwater level (m AHD)
Date

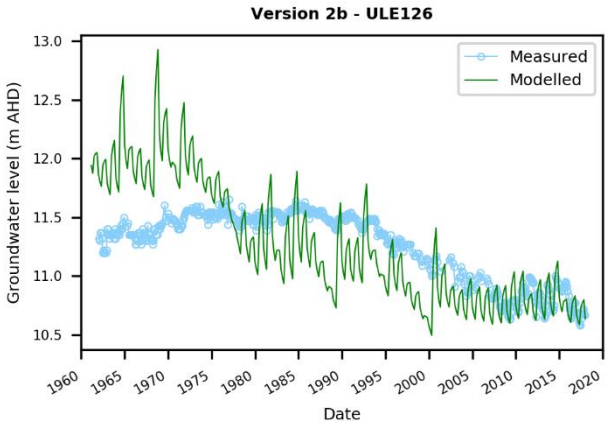

Version 2b - ULE121
Measured
Modelled
Groundwater level (m AHD)
Date

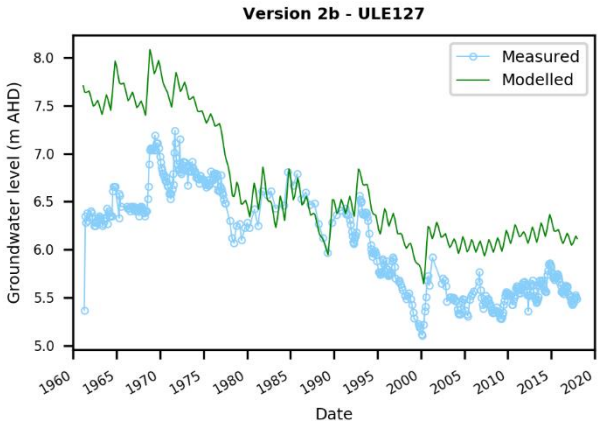

Version 2b - ULE122
Measured
Modelled
Groundwater level (m AHD)
Date

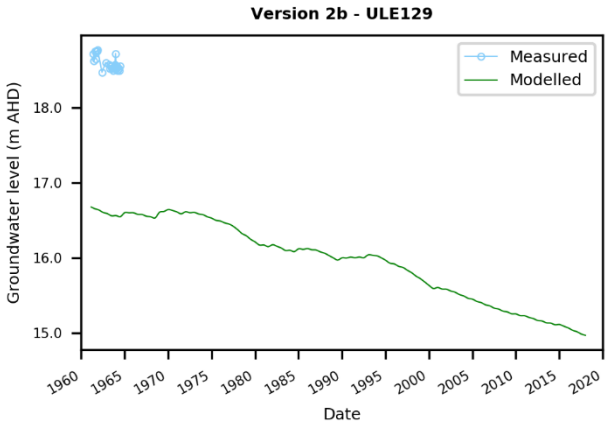

Version 2b - ULE123
Measured
Modelled
Groundwater level (m AHD)
Date

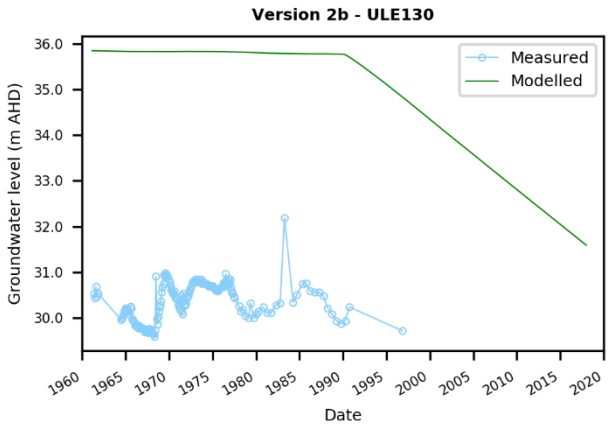

Version 2b - ULE124
Measured
Modelled
Groundwater level (m AHD)
Date

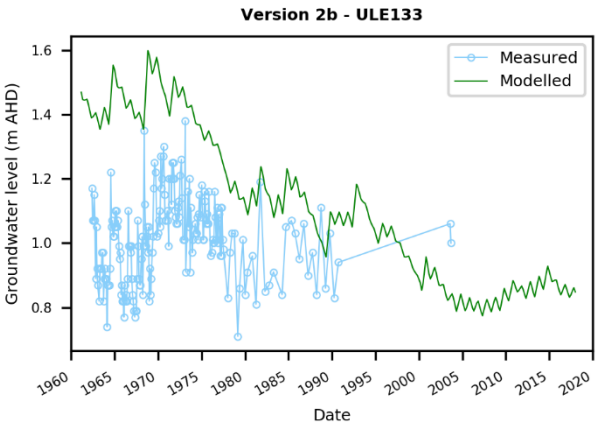

Version 2b - ULE125
Measured
Modelled
Groundwater level (m AHD)
Date

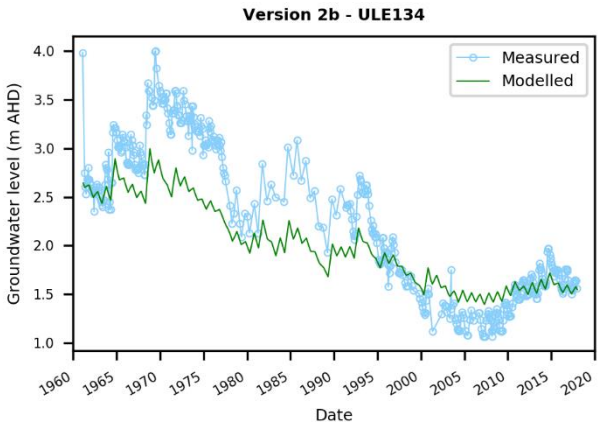

Version 2b - ULE126
Measured
Modelled
Groundwater level (m AHD)
Date

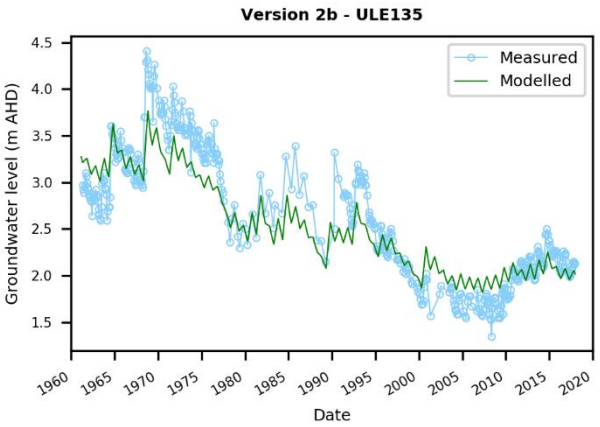

Version 2b - ULE127
Measured
Modelled
Groundwater level (m AHD)
Date

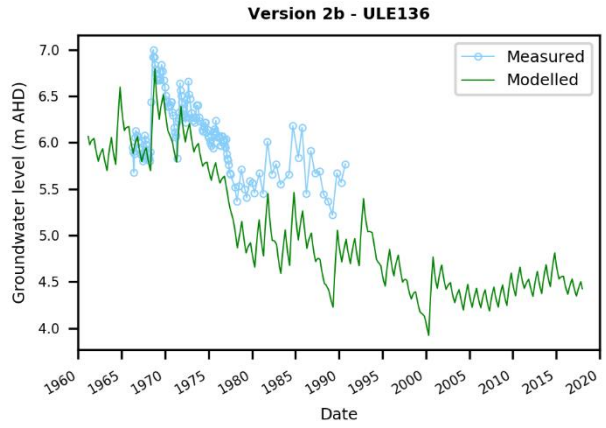

Version 2b - ULE129
Measured
Modelled
Groundwater level (m AHD)
Date

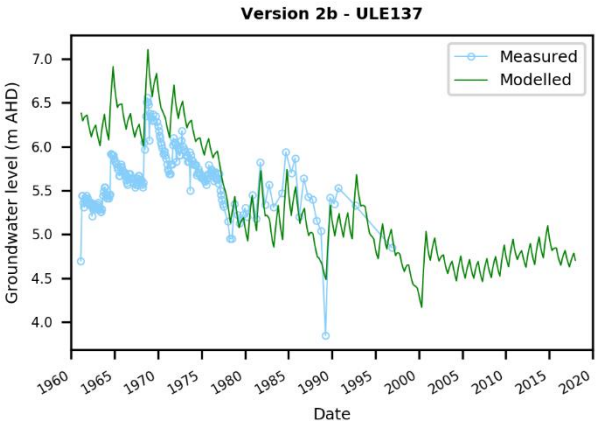

Version 2b - ULE130
Measured
Modelled
Groundwater level (m AHD)
Date

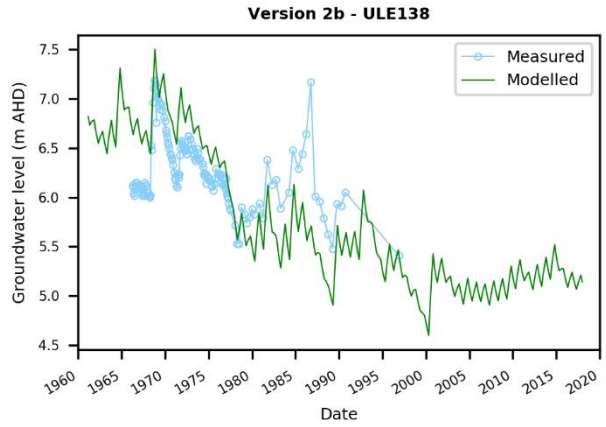

Version 2b - ULE133
Measured
Modelled
Groundwater level (m AHD)
Date

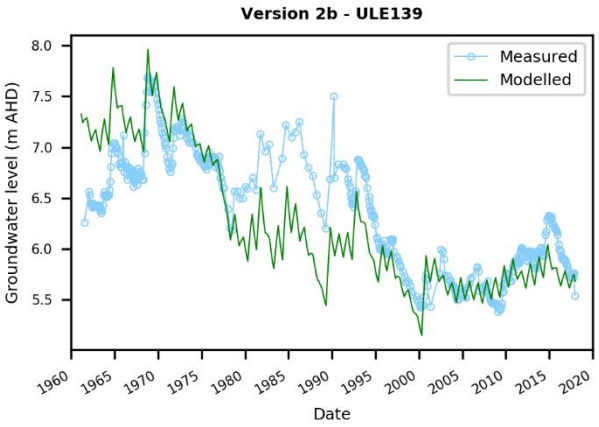

Version 2b - ULE134
Measured
Modelled
Groundwater level (m AHD)
Date

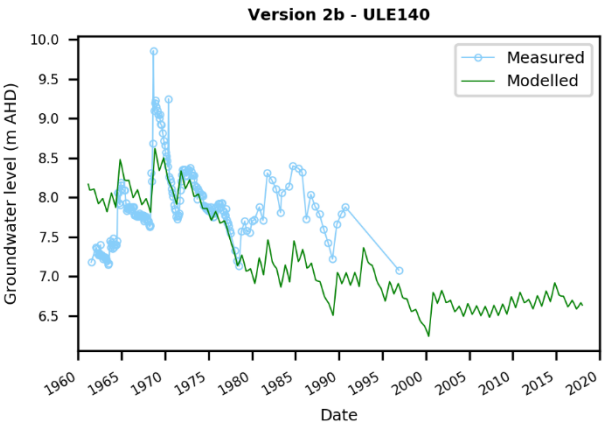

Version 2b - ULE135
Measured
Modelled
Groundwater level (m AHD)
Date

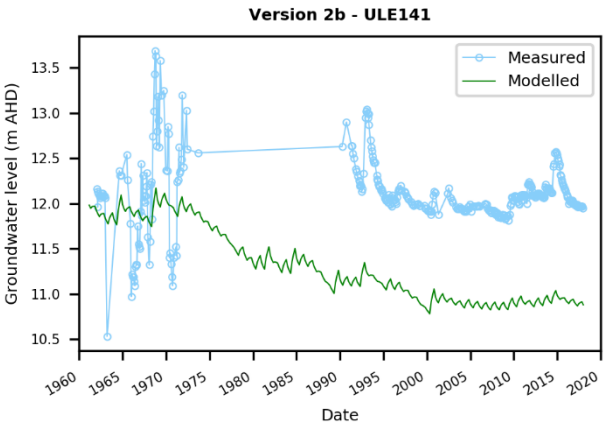

Version 2b - ULE136
Measured
Modelled
Groundwater level (m AHD)
Date

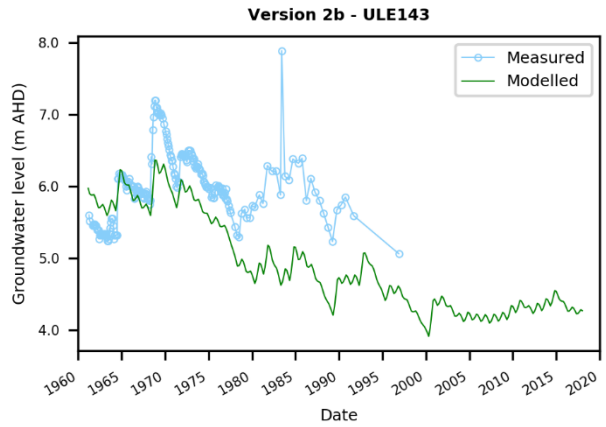

Version 2b - ULE137
Measured
Modelled
Groundwater level (m AHD)
Date

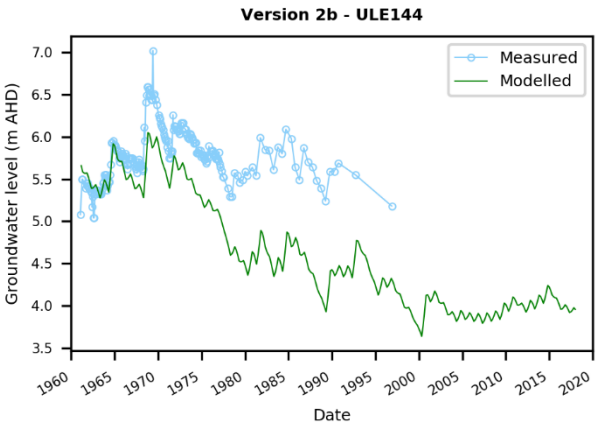

Version 2b - ULE138
Measured
Modelled
Groundwater level (m AHD)
Date

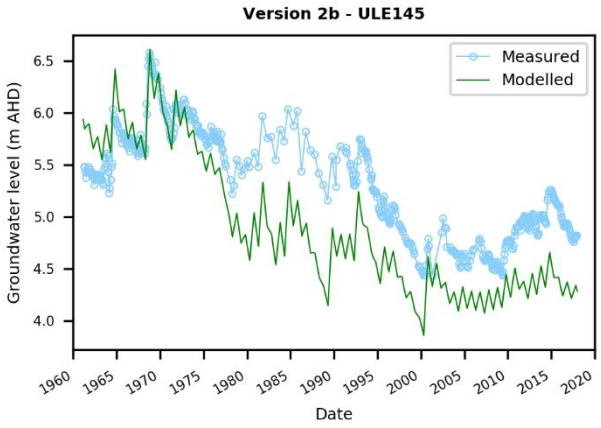

Version 2b - ULE139
Measured
Modelled
Groundwater level (m AHD)
Date

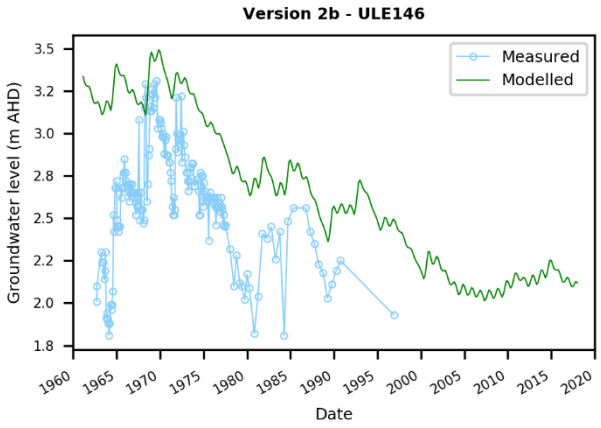

Version 2b - ULE140
Measured
Modelled
Groundwater level (m AHD)
Date

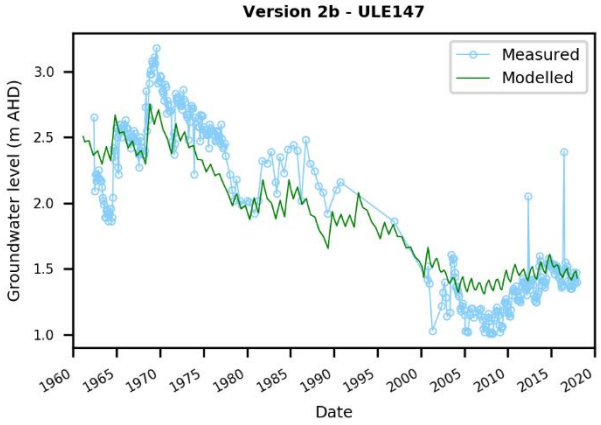

Version 2b - ULE141
Measured
Modelled
Groundwater level (m AHD)
Date

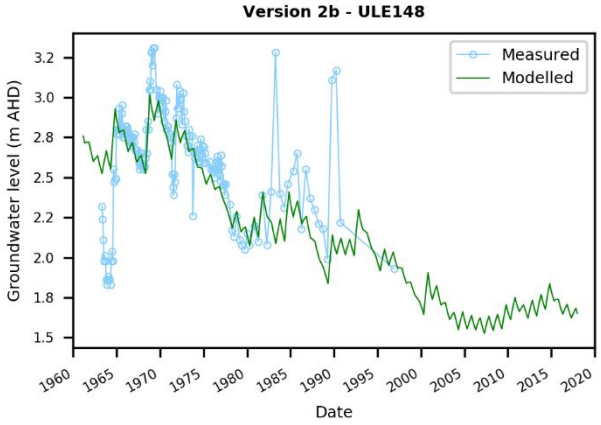

Version 2b - ULE143
Measured
Modelled
Groundwater level (m AHD)
Date

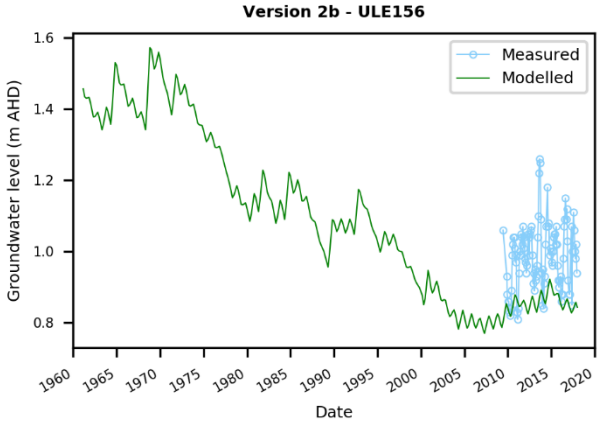

Version 2b - ULE144
Measured
Modelled
Groundwater level (m AHD)
Date

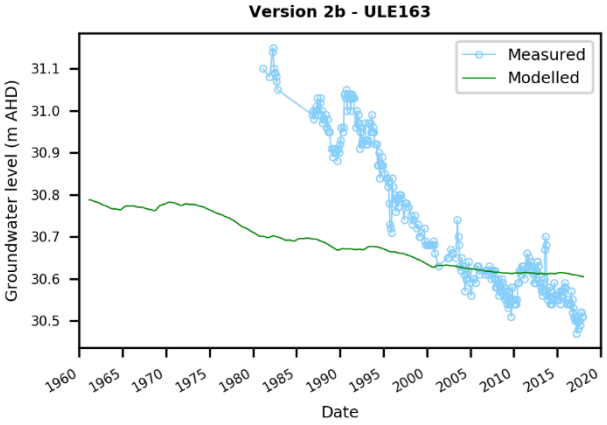

Version 2b - ULE145
Measured
Modelled
Groundwater level (m AHD)
Date

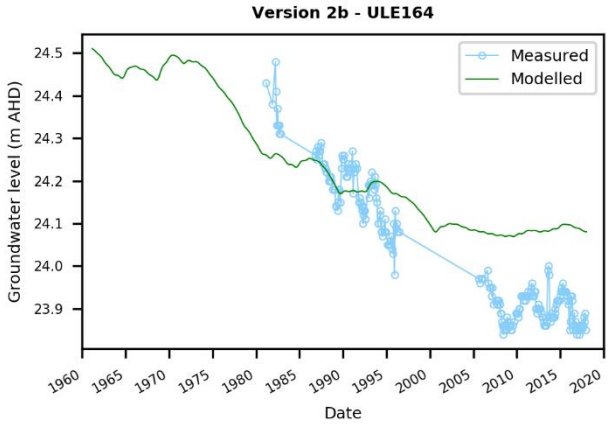

Version 2b - ULE146
Measured
Modelled
Groundwater level (m AHD)
Date

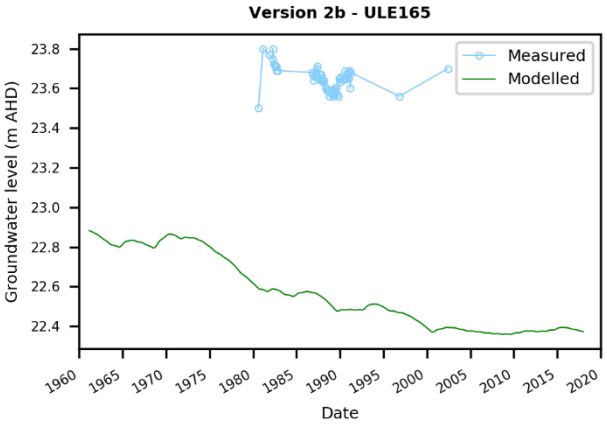

Version 2b - ULE147
Measured
Modelled
Groundwater level (m AHD)
Date

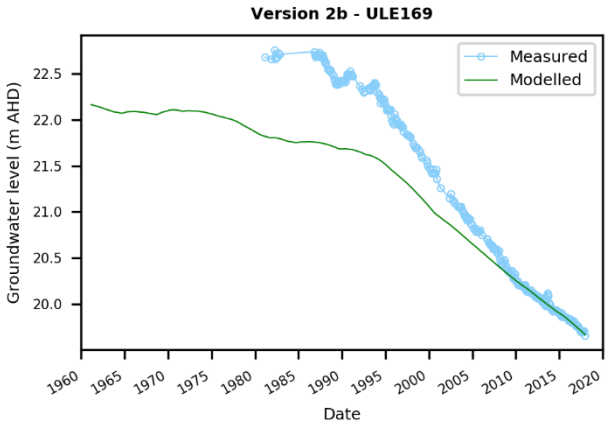

Version 2b - ULE148
Measured
Modelled
Groundwater level (m AHD)
Date

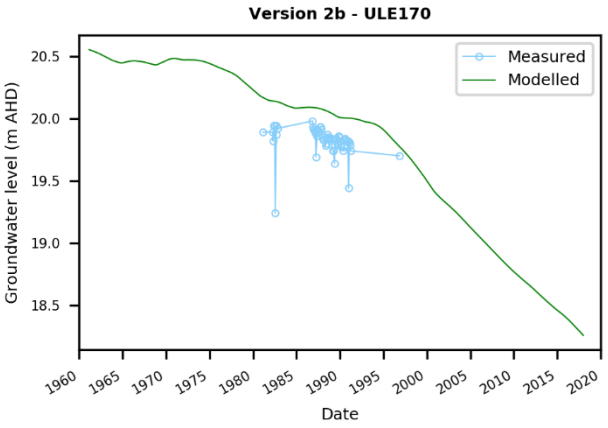

Version 2b - ULE156
Measured
Modelled
Groundwater level (m AHD)
Date

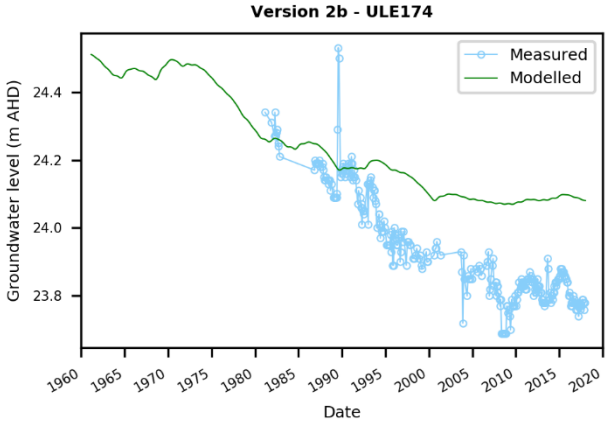

Version 2b - ULE163
Measured
Modelled
Groundwater level (m AHD)
Date

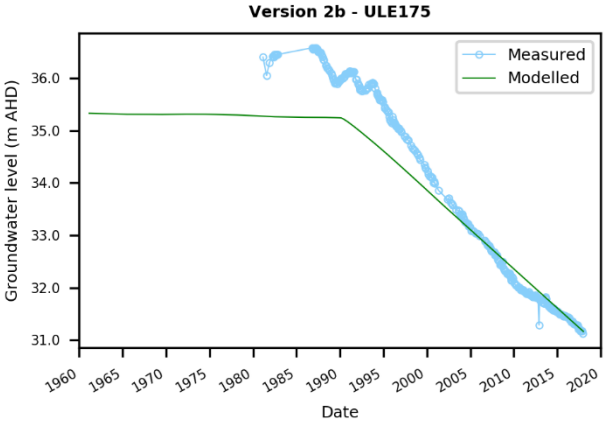

Version 2b - ULE164
Measured
Modelled
Groundwater level (m AHD)
Date

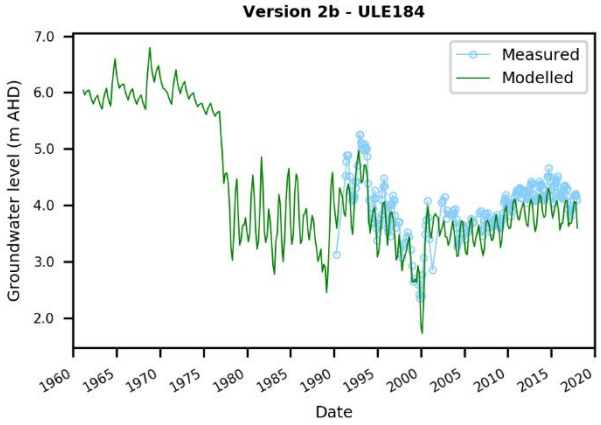

Version 2b - ULE165
Measured
Modelled
Groundwater level (m AHD)
Date

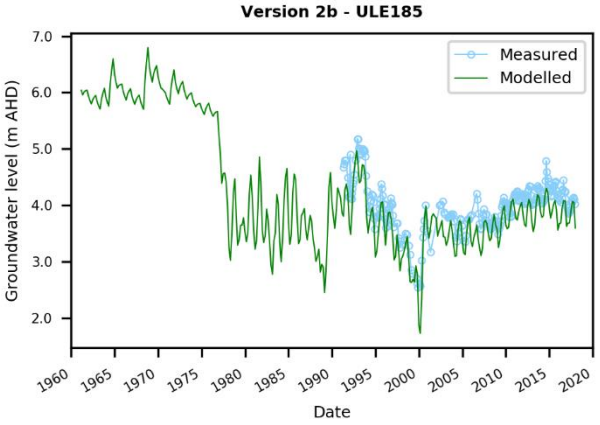

Version 2b - ULE169
Measured
Modelled
Groundwater level (m AHD)
Date

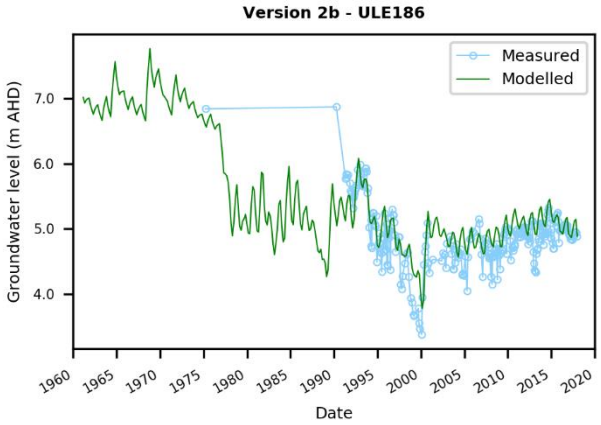

Version 2b - ULE170
Measured
Modelled
Groundwater level (m AHD)
Date

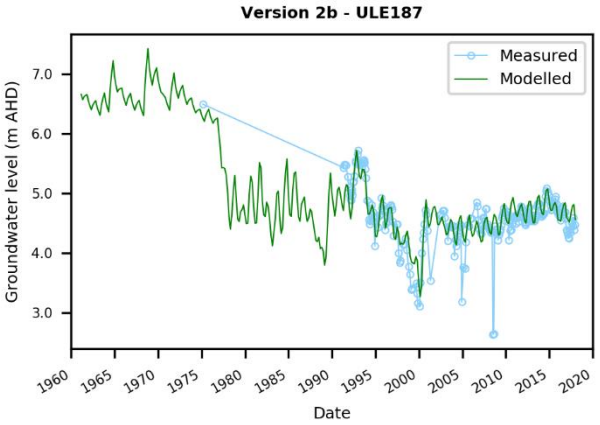

Version 2b - ULE174
Measured
Modelled
Groundwater level (m AHD)
Date

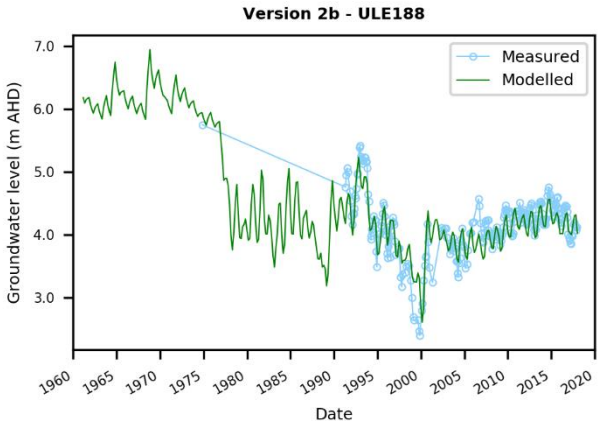

Version 2b - ULE175
Measured
Modelled
Groundwater level (m AHD)
Date

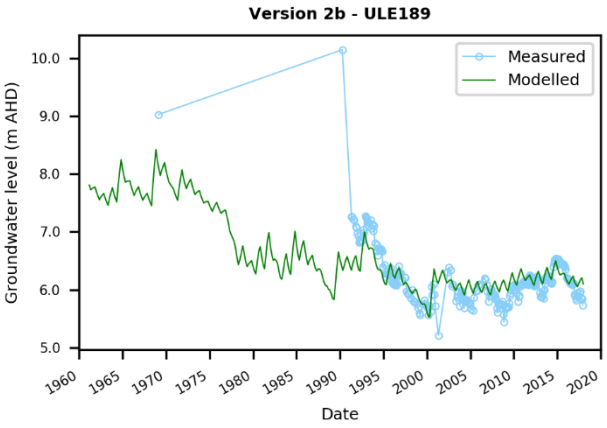

Version 2b - ULE184
Measured
Modelled
Groundwater level (m AHD)
Date

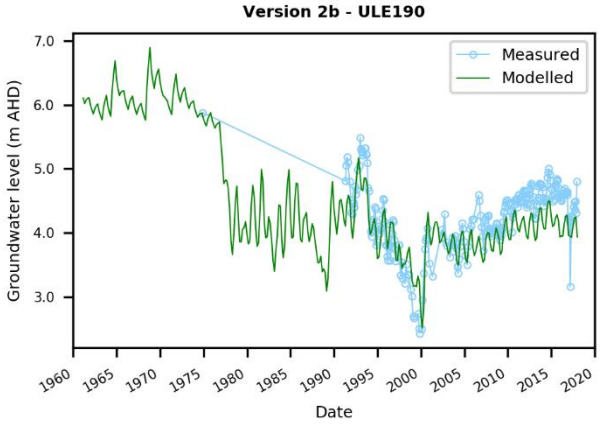

Version 2b - ULE185
Measured
Modelled
Groundwater level (m AHD)
Date

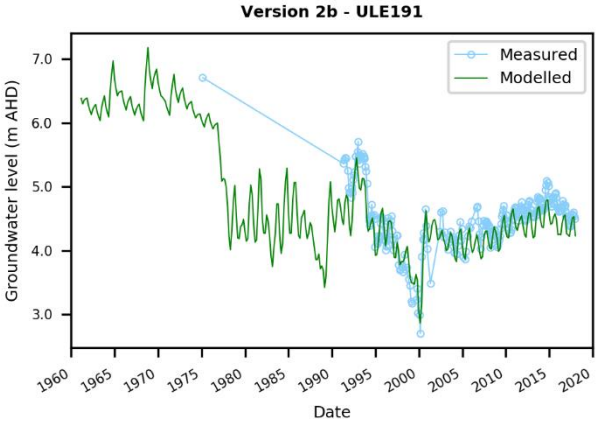

Version 2b - ULE186
Measured
Modelled
Groundwater level (m AHD)
Date

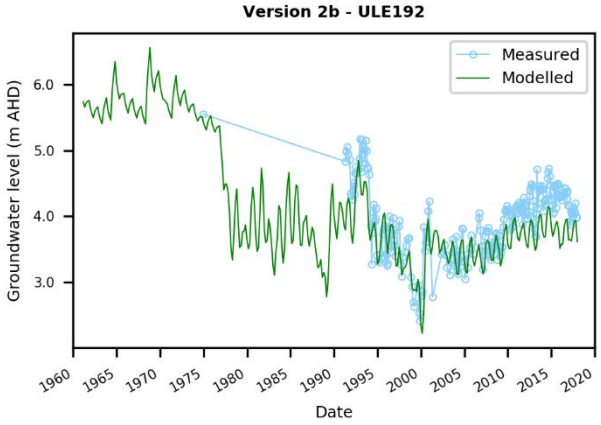

Version 2b - ULE187
Measured
Modelled
Groundwater level (m AHD)
Date

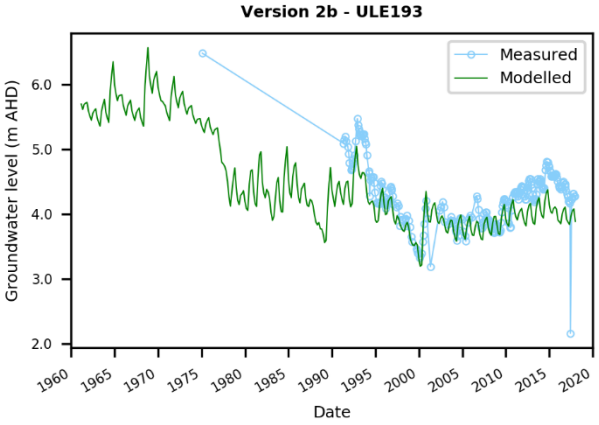

Version 2b - ULE188
Measured
Modelled
Groundwater level (m AHD)
Date

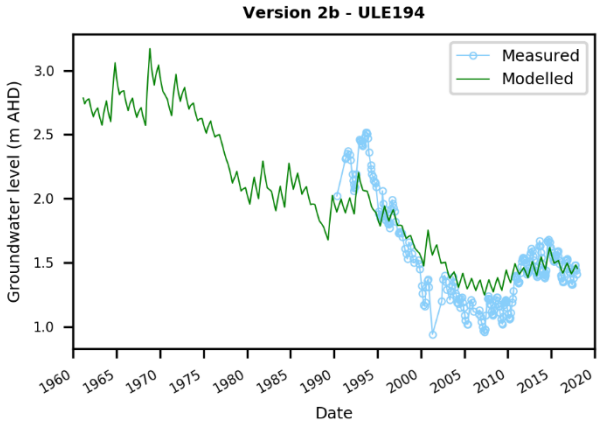

Version 2b - ULE189
Measured
Modelled
Groundwater level (m AHD)
Date

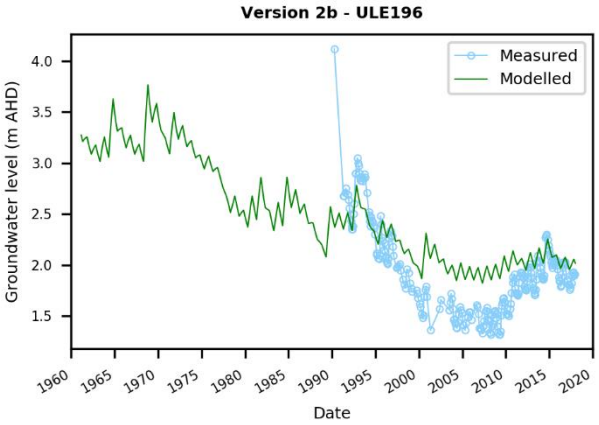

Version 2b - ULE190
Measured
Modelled
Groundwater level (m AHD)
Date

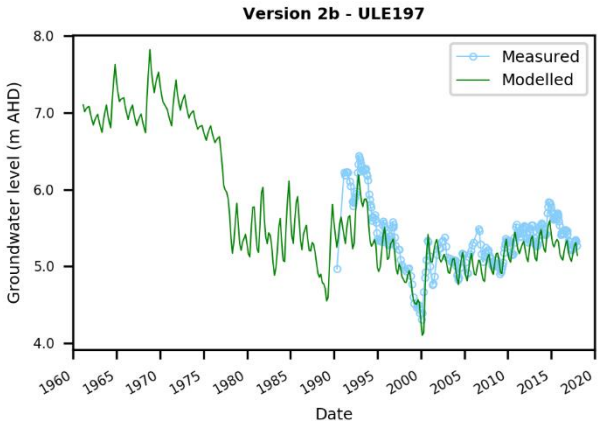

Version 2b - ULE191
Measured
Modelled
Groundwater level (m AHD)
Date

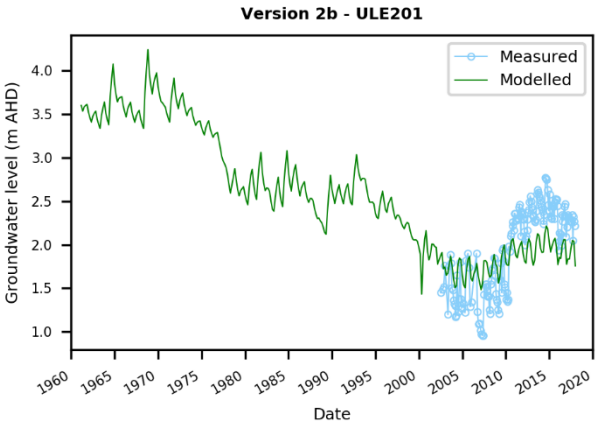

Version 2b - ULE192
Measured
Modelled
Groundwater level (m AHD)
Date

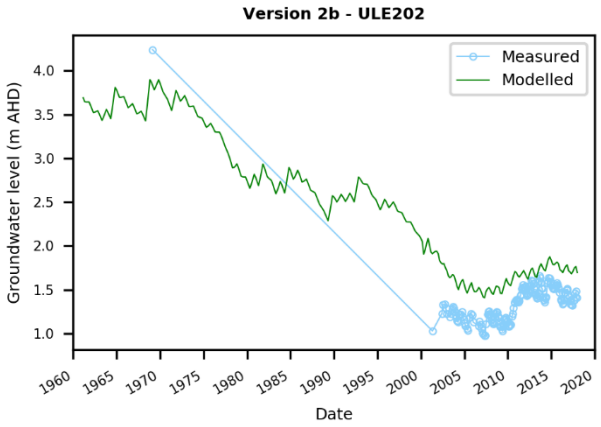

Version 2b - ULE193
Measured
Modelled
Groundwater level (m AHD)
Date

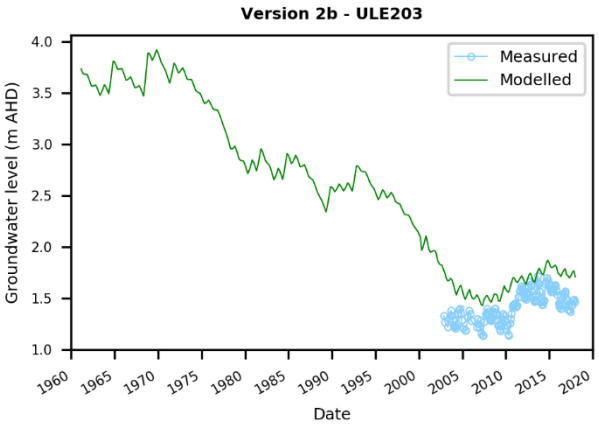

Version 2b - ULE194
Measured
Modelled
Groundwater level (m AHD)
Date

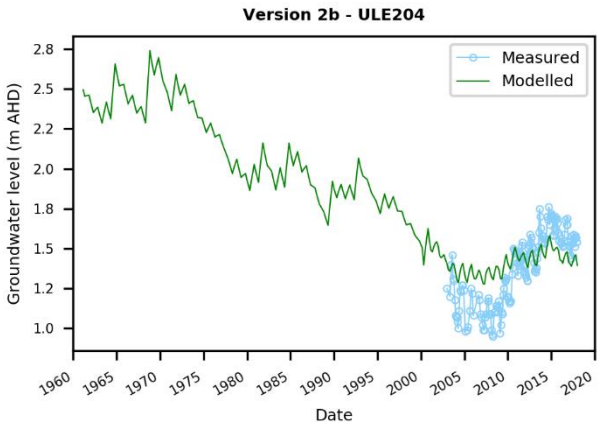

Version 2b - ULE196
Measured
Modelled
Groundwater level (m AHD)
Date

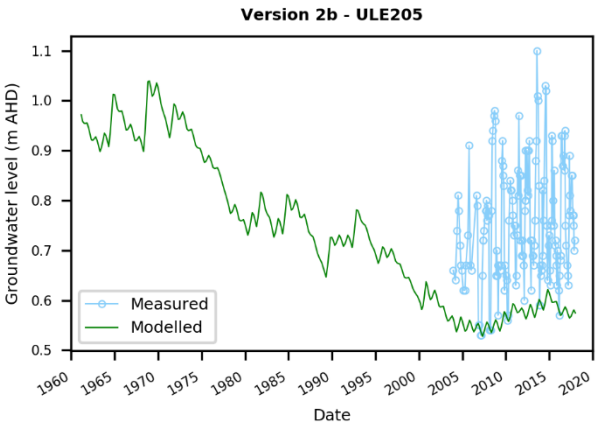

Version 2b - ULE197
Measured
Modelled
Groundwater level (m AHD)
Date

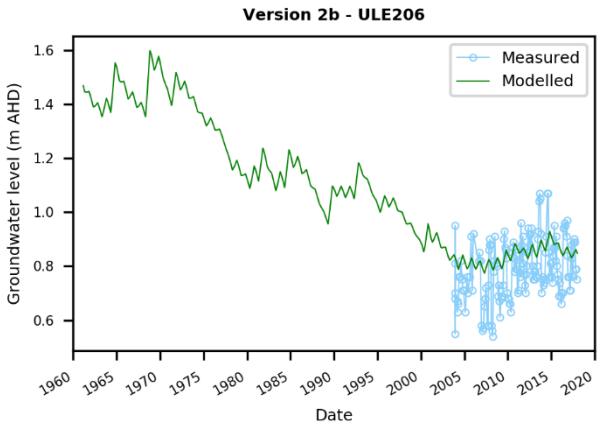

Version 2b - ULE201
Measured
Modelled
Groundwater level (m AHD)
Date

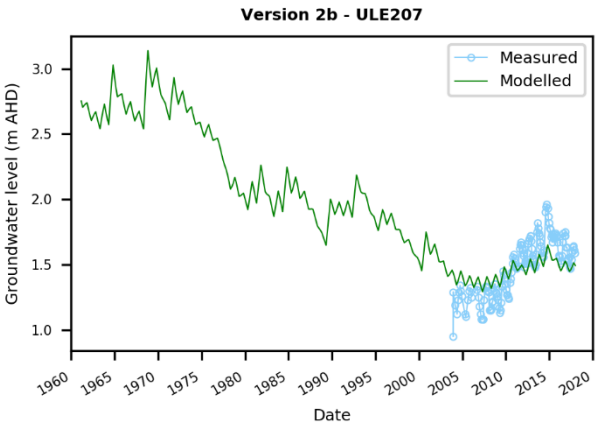

Version 2b - ULE202
Measured
Modelled
Groundwater level (m AHD)
Date

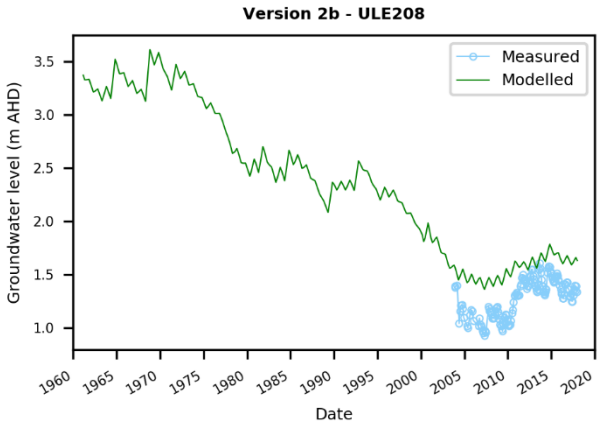

Version 2b - ULE203
Measured
Modelled
Groundwater level (m AHD)
Date

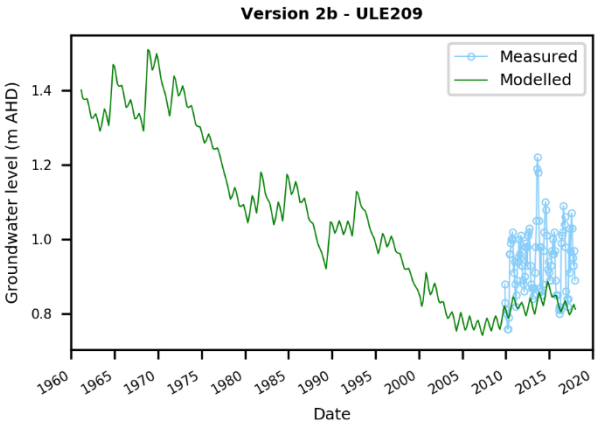

Version 2b - ULE204
Measured
Modelled
Groundwater level (m AHD)
Date

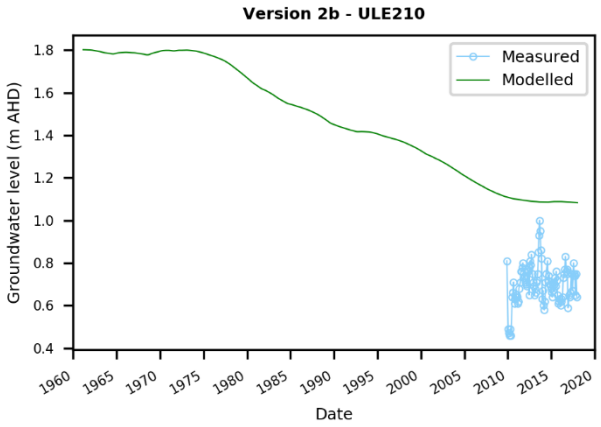

Version 2b - ULE205
Measured
Modelled
Groundwater level (m AHD)
Date

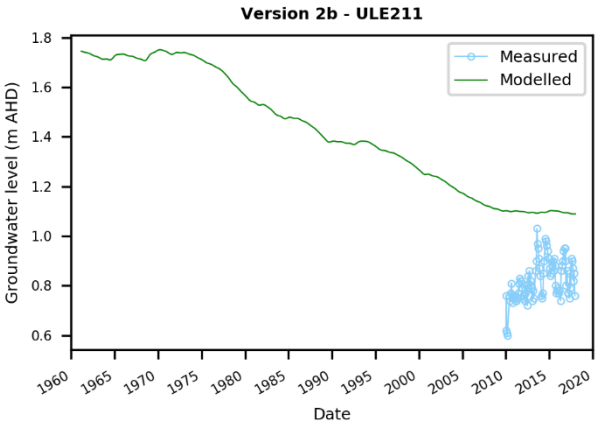

Version 2b - ULE206
Measured
Modelled
Groundwater level (m AHD)
Date

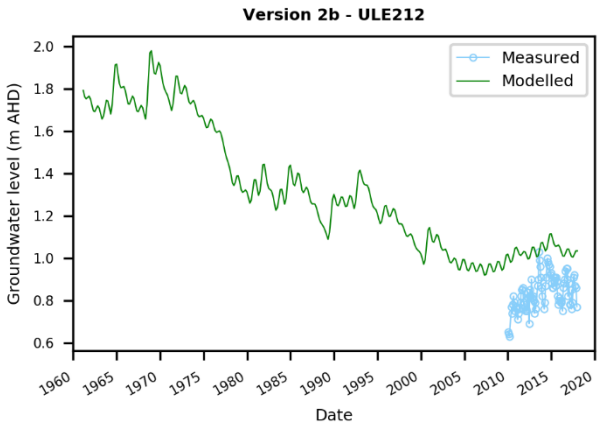

Version 2b - ULE207
Measured
Modelled
Groundwater level (m AHD)
Date

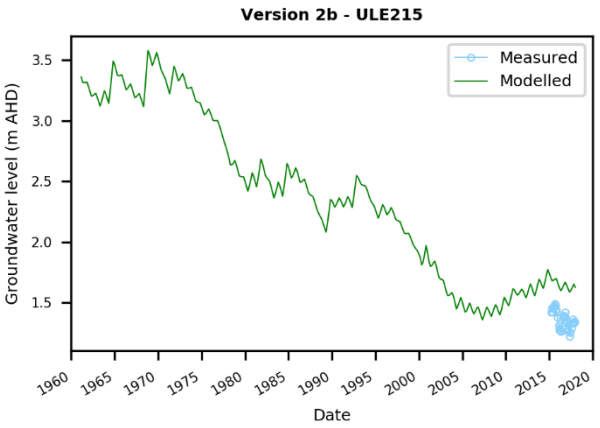

Version 2b - ULE208
Measured
Modelled
Groundwater level (m AHD)
Date


Version 2b - ULE209
Measured
Modelled
Groundwater level (m AHD)
Date

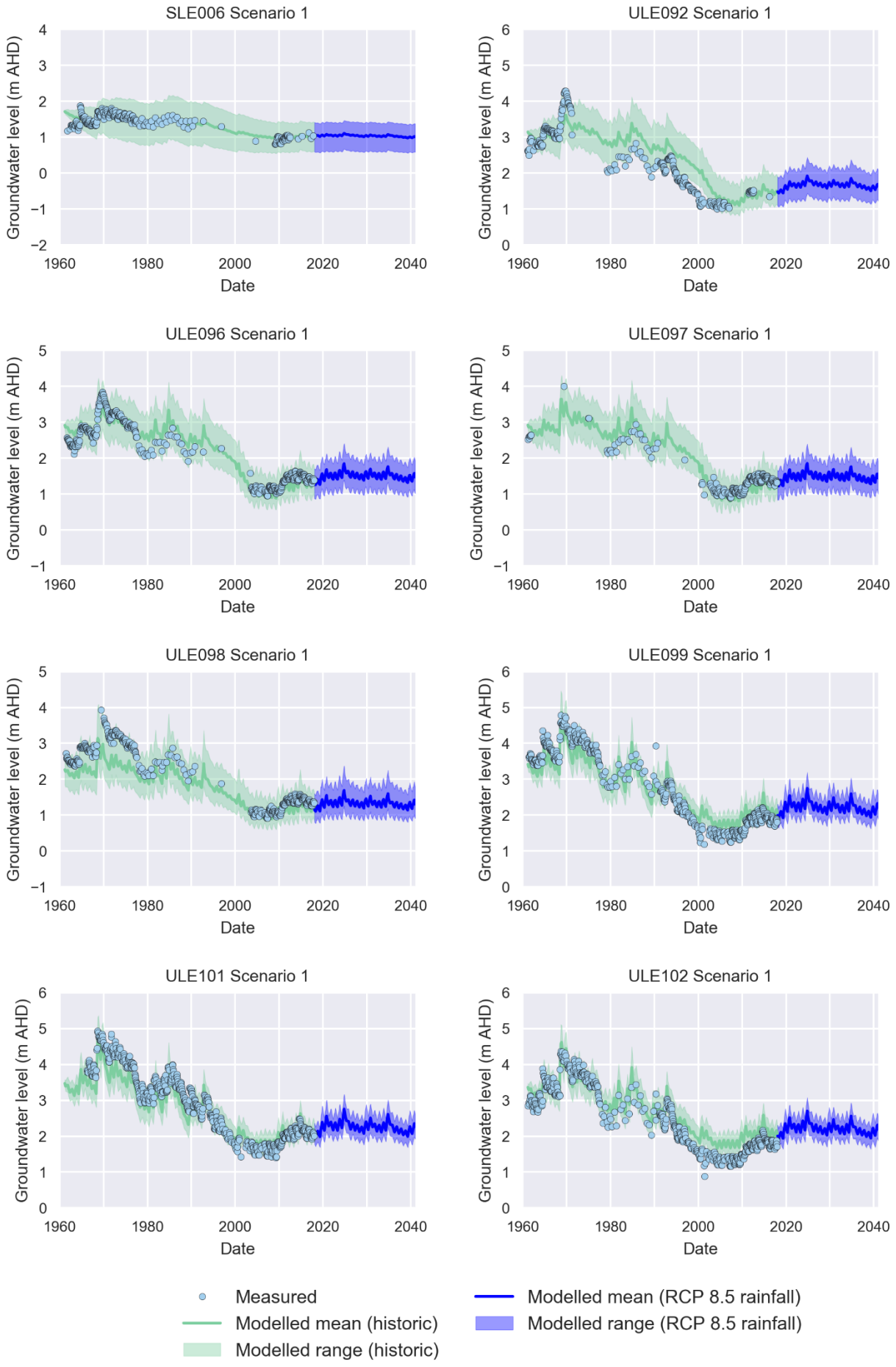

Version 2b - ULE210
Measured
Modelled
Groundwater level (m AHD)
Date

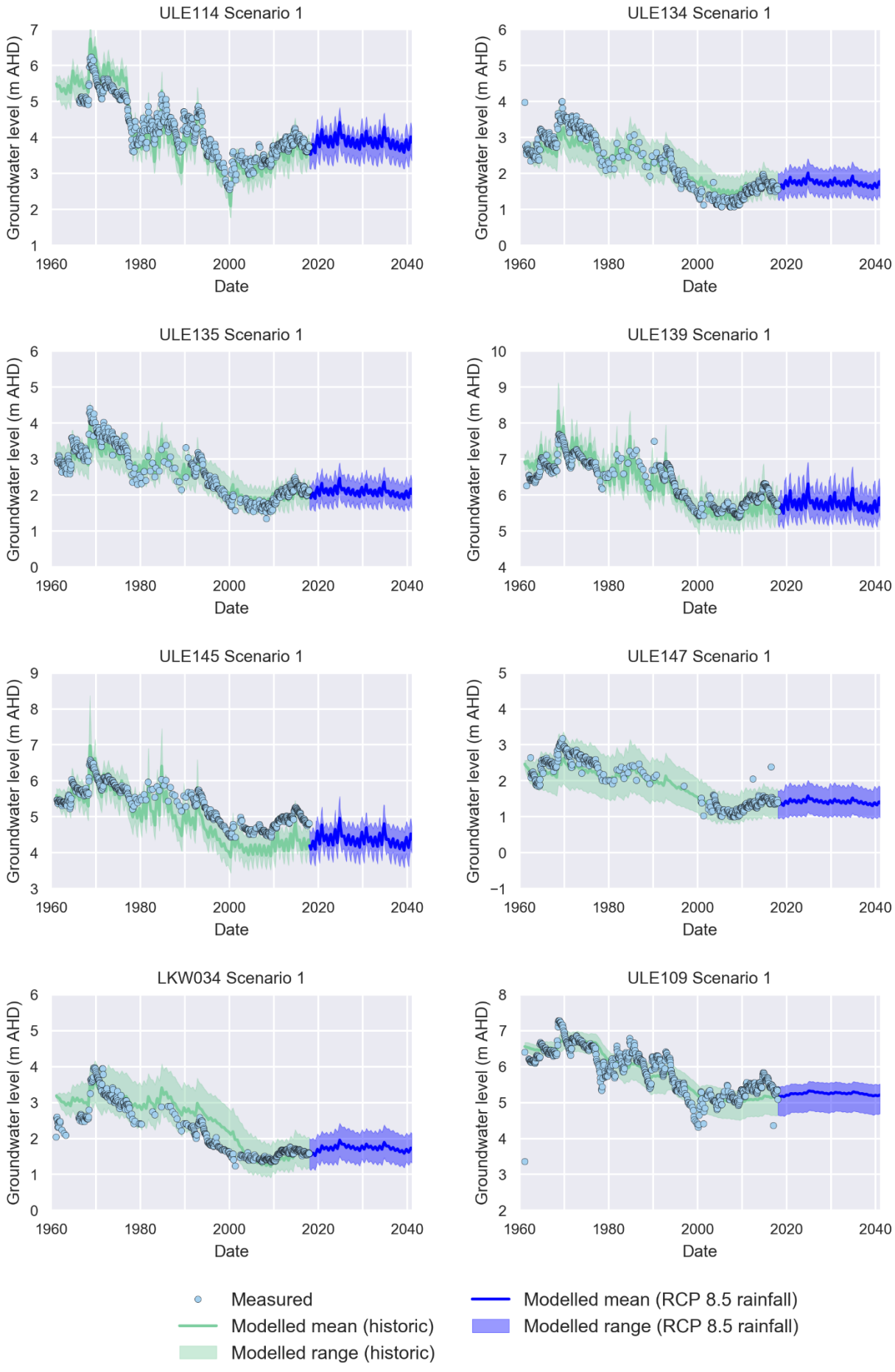

Version 2b - ULE211
Measured
Modelled
Groundwater level (m AHD)
Date

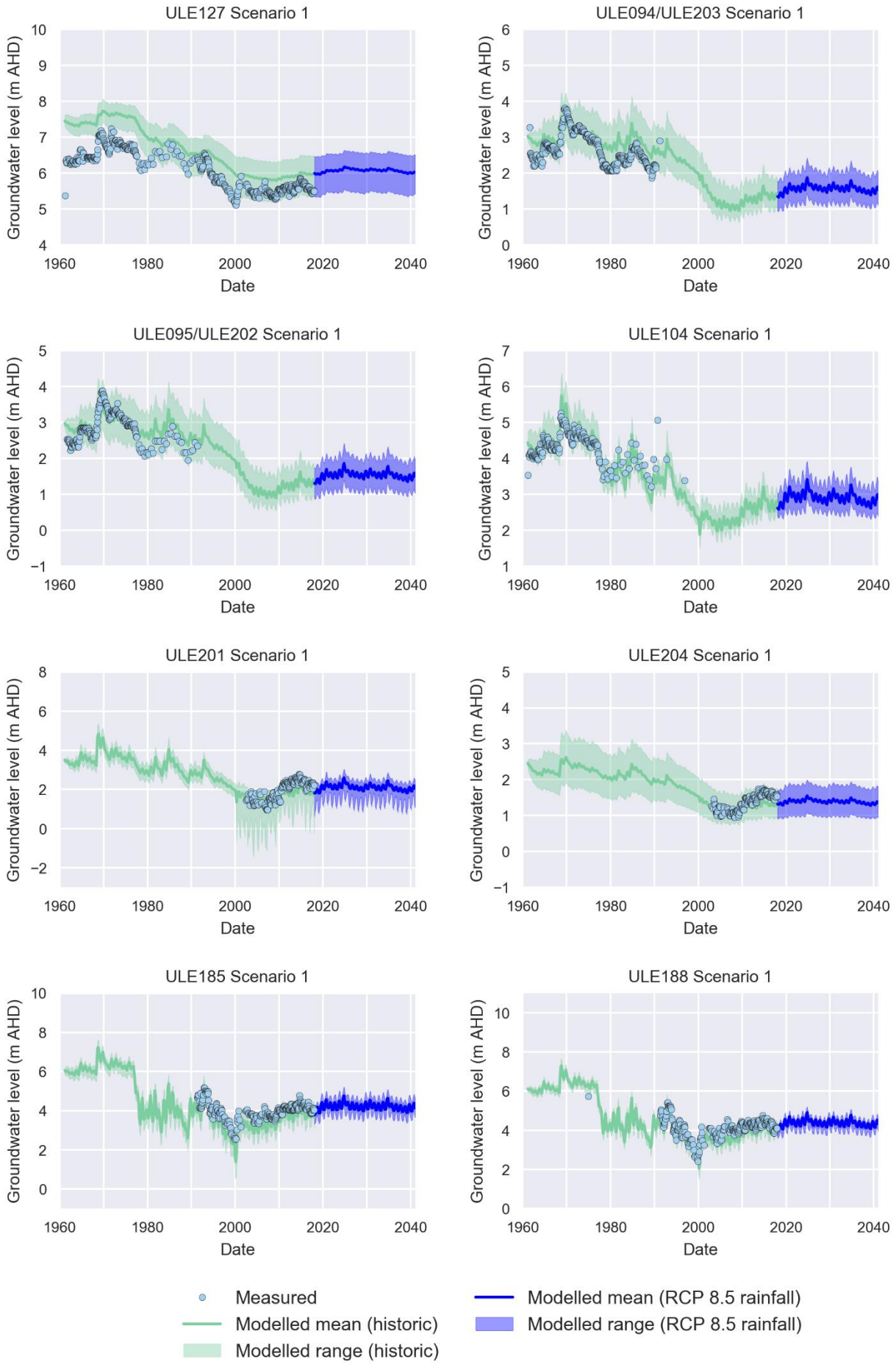

Version 2b - ULE212
Measured
Modelled
Groundwater level (m AHD)
Date

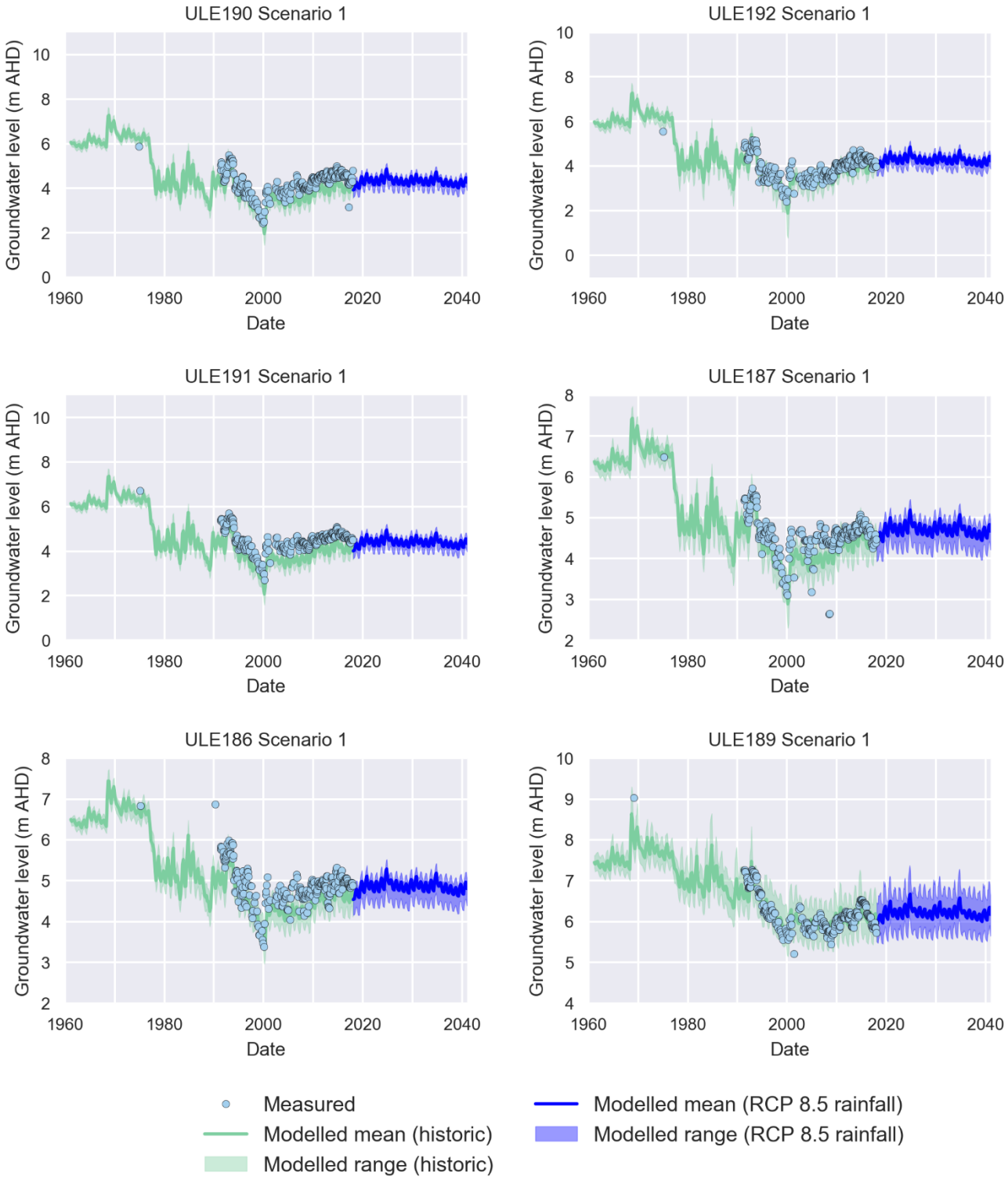

Version 2b - ULE215
Measured
Modelled
Groundwater level (m AHD)
Date

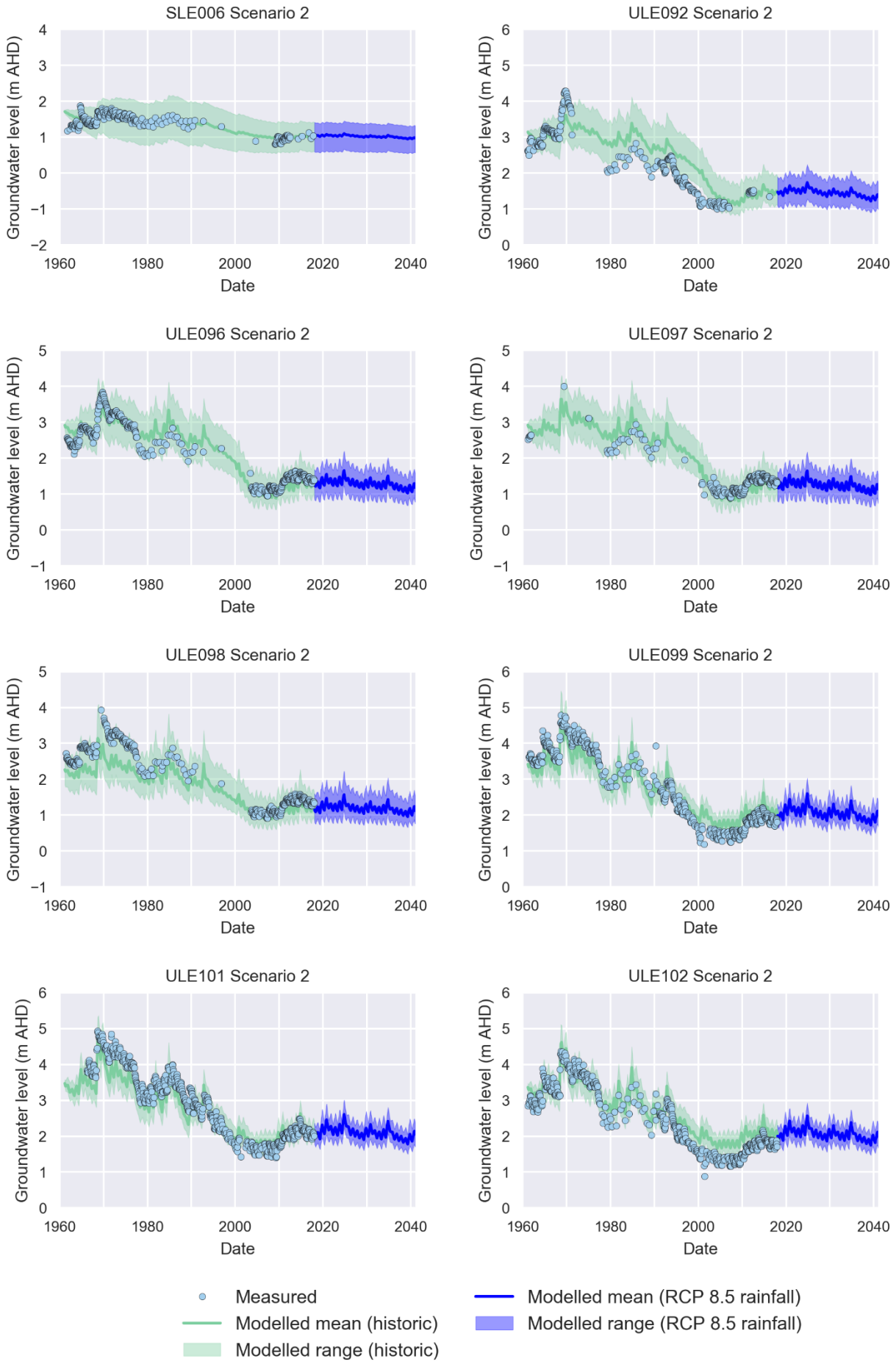
D. Scenario hydrographs

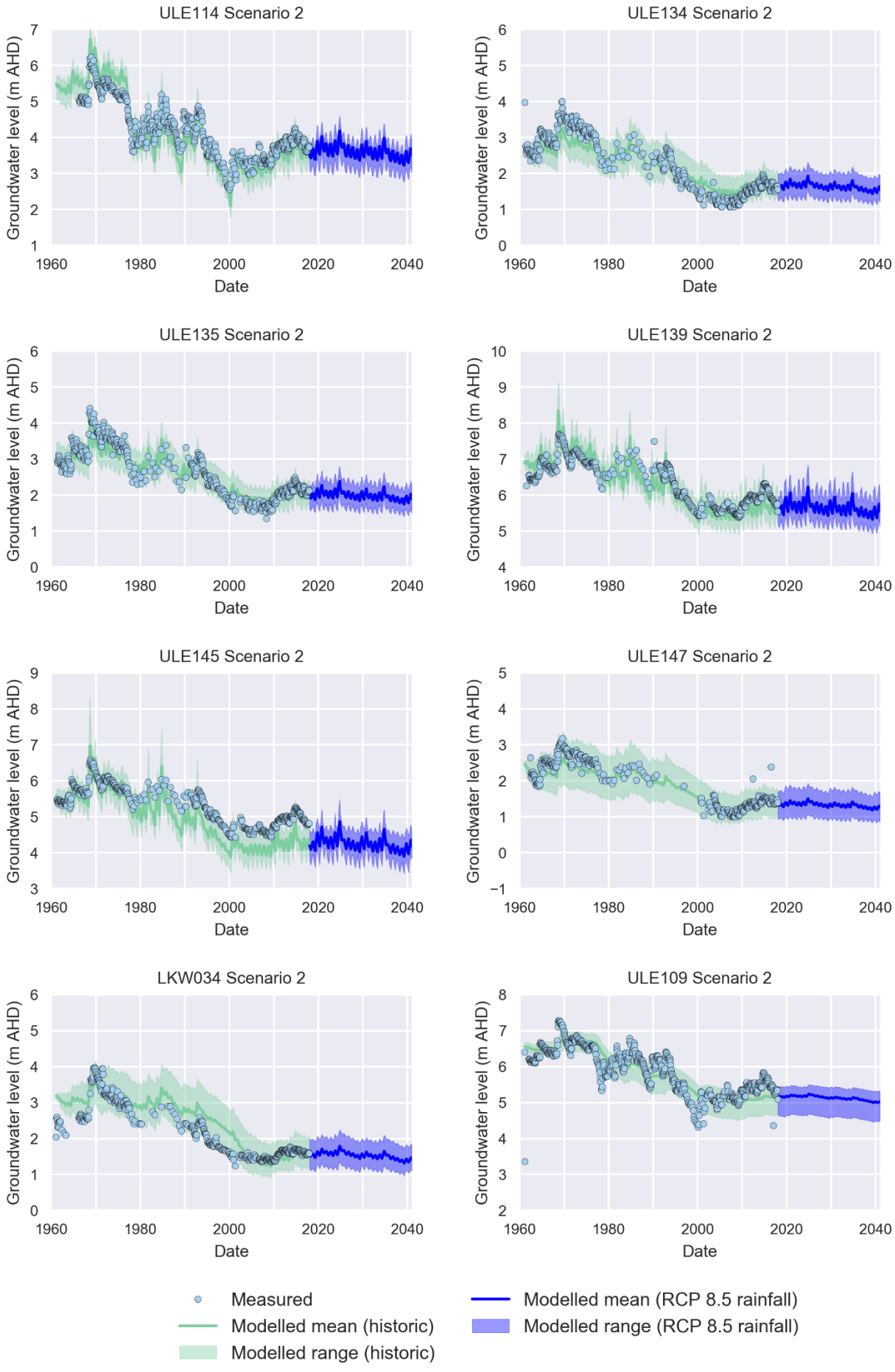

SLE006 Scenario 1
ULE092 Scenario 1
ULE096 Scenario 1
ULE097 Scenario 1
ULE098 Scenario 1
ULE099 Scenario 1
ULE101 Scenario 1
ULE102 Scenario 1
Groundwater level (m AHD)
Date
Measured
Modelled mean (historic)
Modelled range (historic)
Modelled mean (RCP 8.5 rainfall)
Modelled range (RCP 8.5 rainfall)

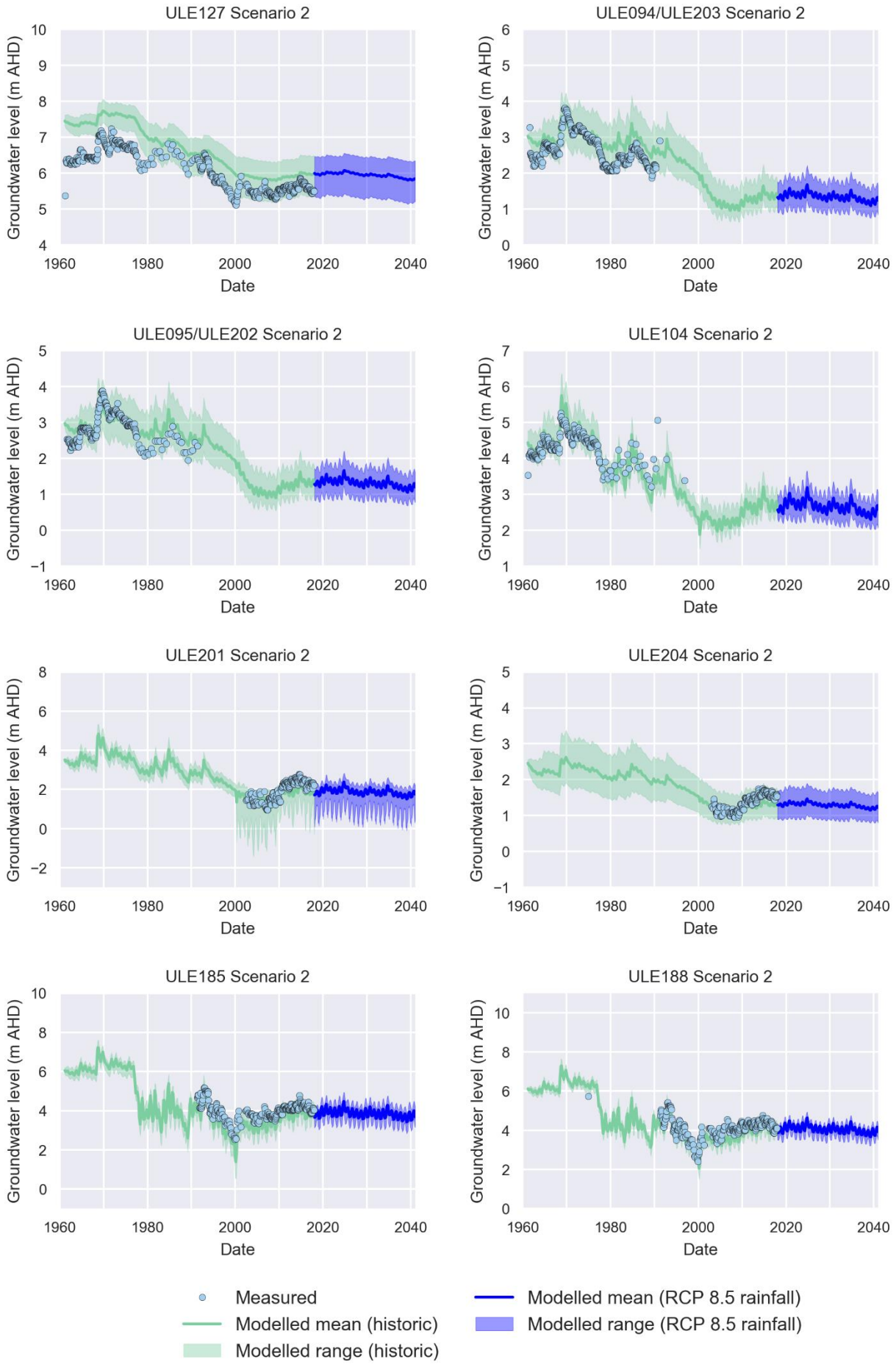

ULE114 Scenario 1
ULE134 Scenario 1
ULE135 Scenario 1
ULE139 Scenario 1
ULE145 Scenario 1
ULE147 Scenario 1
LKW034 Scenario 1
ULE109 Scenario 1
Groundwater level (m AHD)
Date
Measured
Modelled mean (historic)
Modelled range (historic)
Modelled mean (RCP 8.5 rainfall)
Modelled range (RCP 8.5 rainfall)

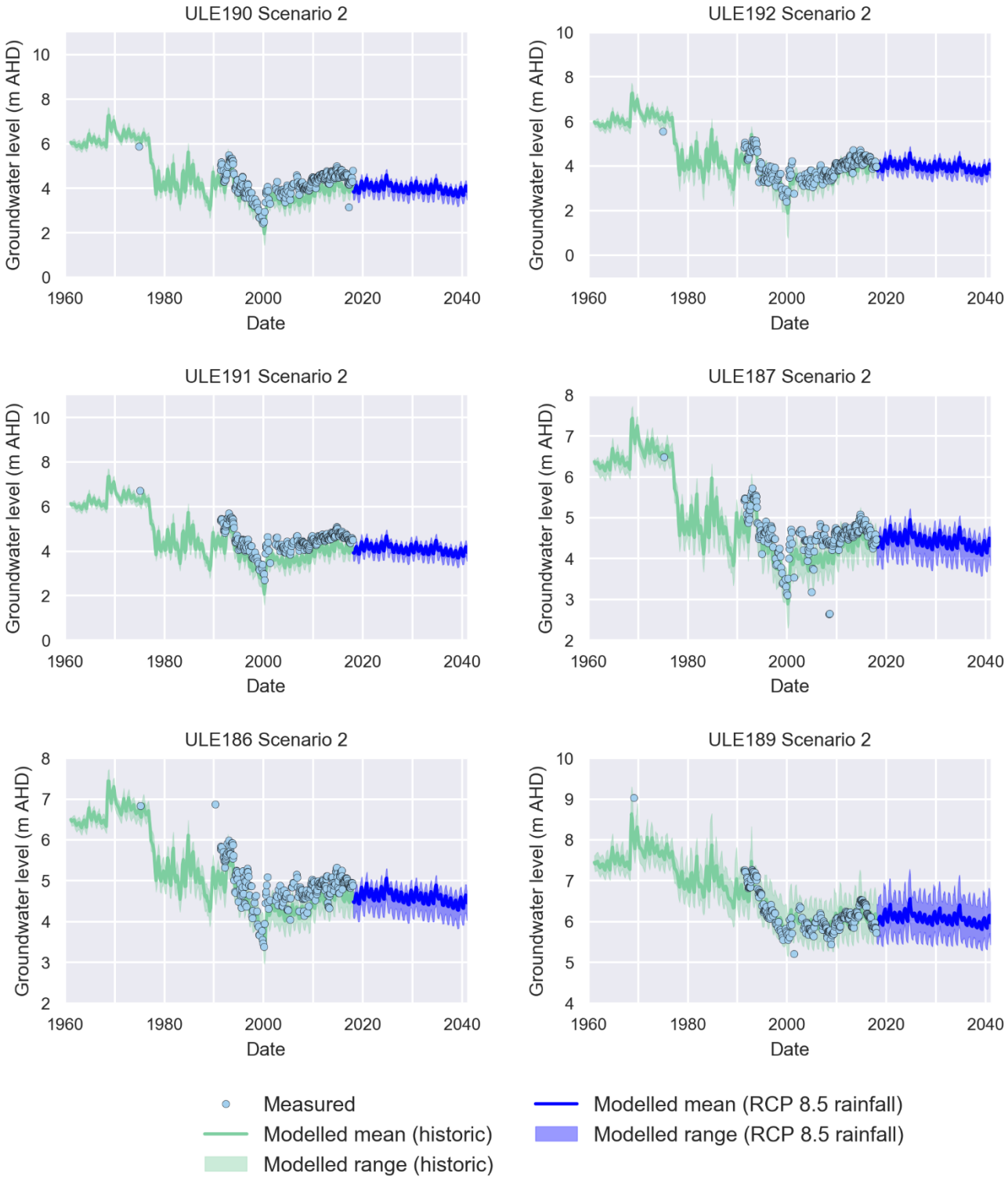

ULE127 Scenario 1
ULE094/ULE203 Scenario 1
ULE095/ULE202 Scenario 1
ULE104 Scenario 1
ULE201 Scenario 1
ULE204 Scenario 1
ULE185 Scenario 1
ULE188 Scenario 1
Groundwater level (m AHD)
Date
Measured
Modelled mean (historic)
Modelled range (historic)
Modelled mean (RCP 8.5 rainfall)
Modelled range (RCP 8.5 rainfall)

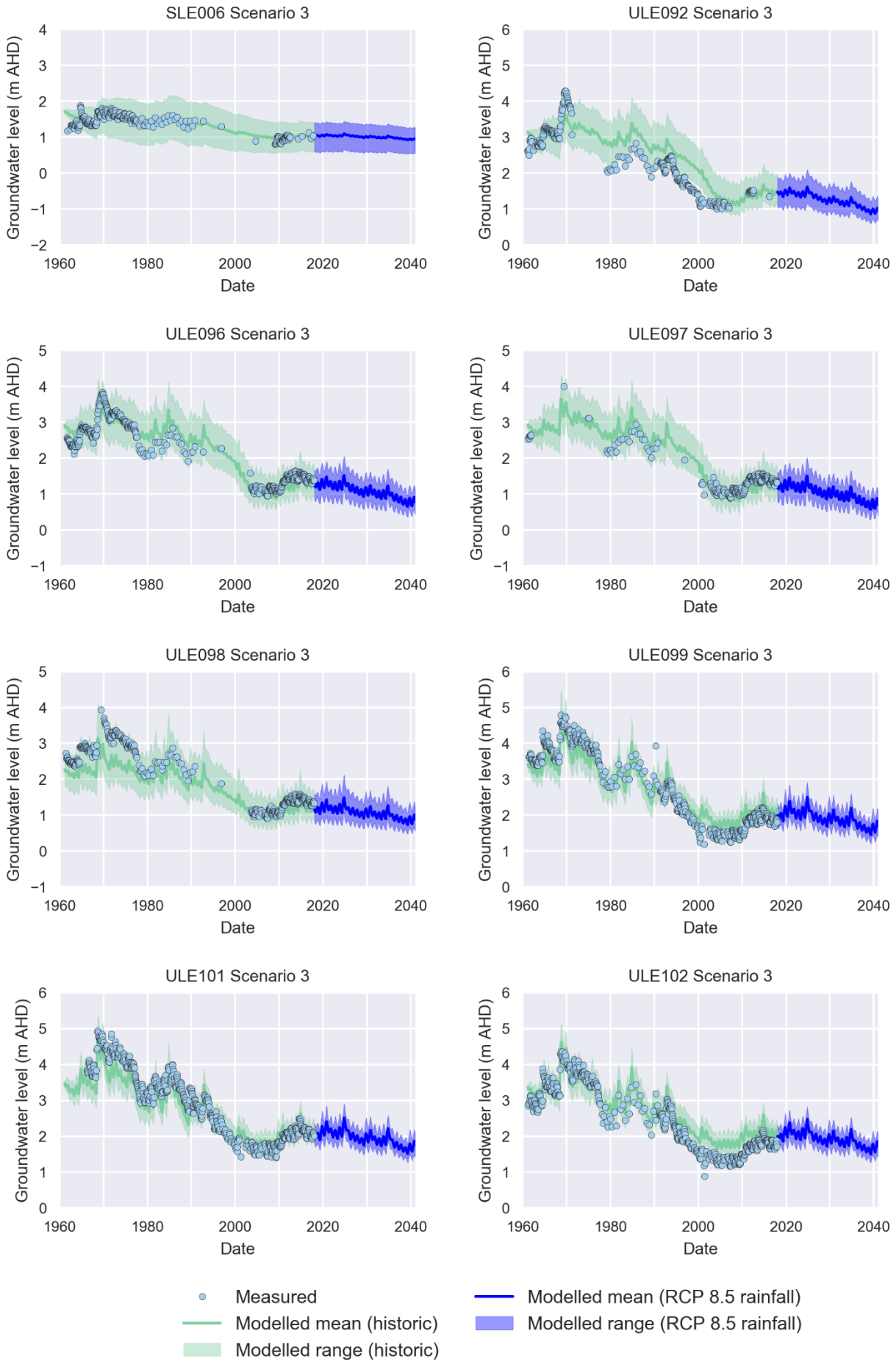

ULE190 Scenario 1
ULE192 Scenario 1
ULE191 Scenario 1
ULE187 Scenario 1
ULE186 Scenario 1
ULE189 Scenario 1
Groundwater level (m AHD)
Date
1960
1980
2000
2020
2040
Measured
Modelled mean (historic)
Modelled range (historic)
Modelled mean (RCP 8.5 rainfall)
Modelled range (RCP 8.5 rainfall)

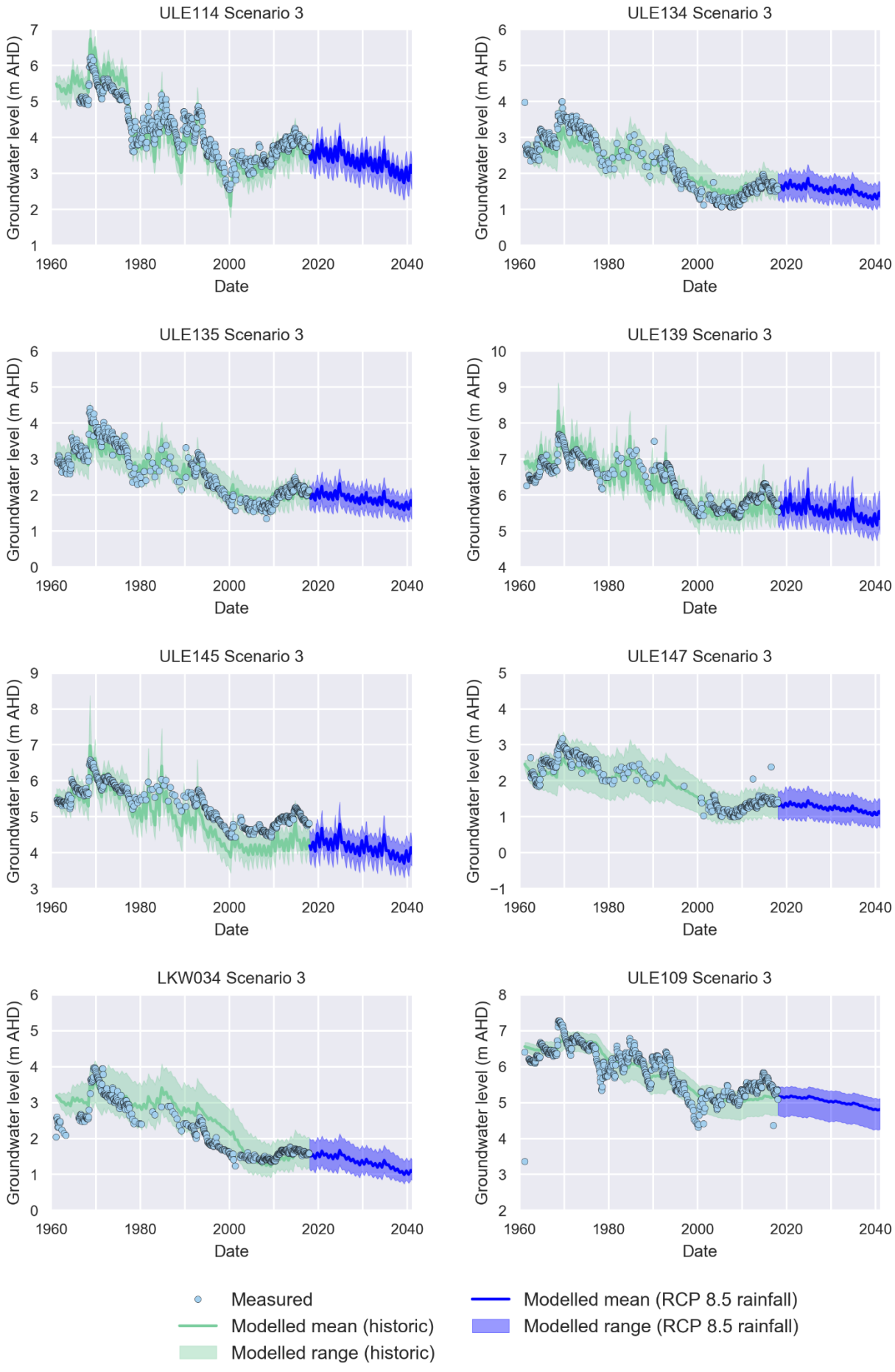

SLE006 Scenario 2
ULE092 Scenario 2
ULE096 Scenario 2
ULE097 Scenario 2
ULE098 Scenario 2
ULE099 Scenario 2
ULE101 Scenario 2
ULE102 Scenario 2
Groundwater level (m AHD)
Date
Measured
Modelled mean (historic)
Modelled range (historic)
Modelled mean (RCP 8.5 rainfall)
Modelled range (RCP 8.5 rainfall)

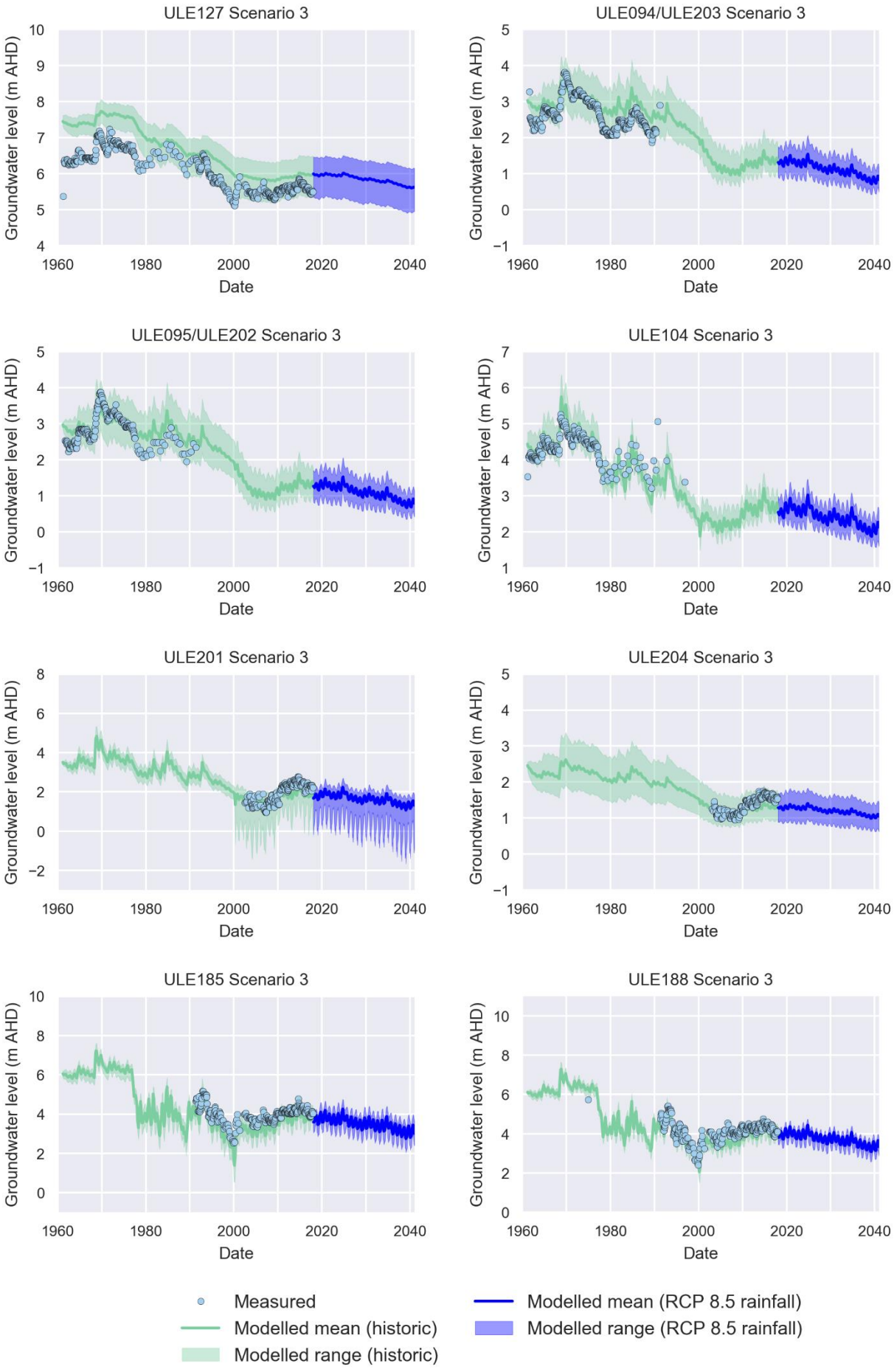

ULE114 Scenario 2
ULE134 Scenario 2
ULE135 Scenario 2
ULE139 Scenario 2
ULE145 Scenario 2
ULE147 Scenario 2
LKW034 Scenario 2
ULE109 Scenario 2
Groundwater level (m AHD)
Date
Measured
Modelled mean (historic)
Modelled range (historic)
Modelled mean (RCP 8.5 rainfall)
Modelled range (RCP 8.5 rainfall)

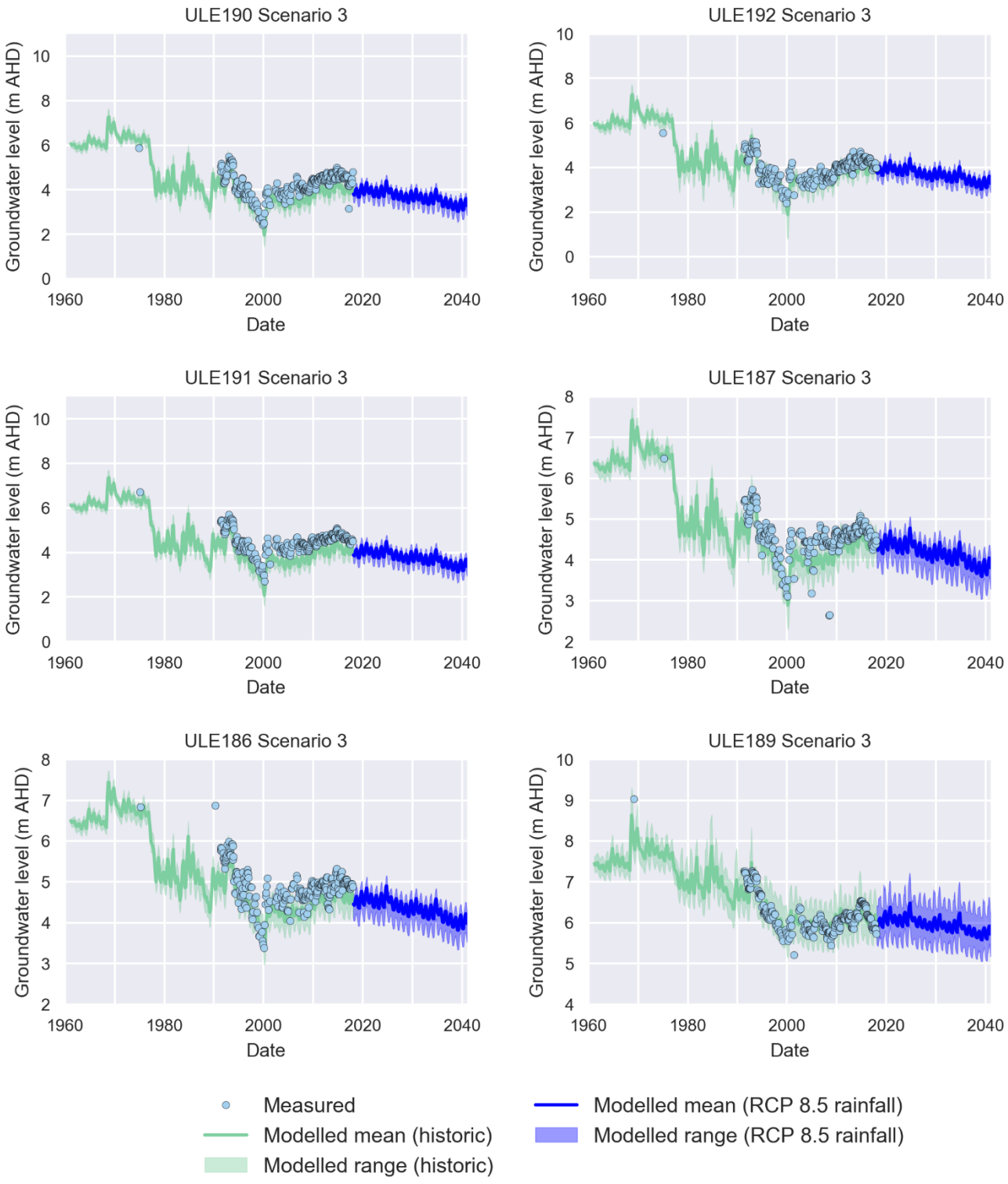

ULE127 Scenario 2
ULE094/ULE203 Scenario 2
ULE095/ULE202 Scenario 2
ULE104 Scenario 2
ULE201 Scenario 2
ULE204 Scenario 2
ULE185 Scenario 2
ULE188 Scenario 2
Groundwater level (m AHD)
Date
Measured
Modelled mean (historic)
Modelled range (historic)
Modelled mean (RCP 8.5 rainfall)
Modelled range (RCP 8.5 rainfall)


ULE190 Scenario 2
ULE192 Scenario 2
ULE191 Scenario 2
ULE187 Scenario 2
ULE186 Scenario 2
ULE189 Scenario 2
Groundwater level (m AHD)
Date
1960
1980
2000
2020
2040
Measured
Modelled mean (historic)
Modelled range (historic)
Modelled mean (RCP 8.5 rainfall)
Modelled range (RCP 8.5 rainfall)


SLE006 Scenario 3
ULE092 Scenario 3
ULE096 Scenario 3
ULE097 Scenario 3
ULE098 Scenario 3
ULE099 Scenario 3
ULE101 Scenario 3
ULE102 Scenario 3
Groundwater level (m AHD)
Date
Measured
Modelled mean (historic)
Modelled range (historic)
Modelled mean (RCP 8.5 rainfall)
Modelled range (RCP 8.5 rainfall)


ULE114 Scenario 3
ULE134 Scenario 3
ULE135 Scenario 3
ULE139 Scenario 3
ULE145 Scenario 3
ULE147 Scenario 3
LKW034 Scenario 3
ULE109 Scenario 3
Groundwater level (m AHD)
Date
Measured
Modelled mean (historic)
Modelled range (historic)
Modelled mean (RCP 8.5 rainfall)
Modelled range (RCP 8.5 rainfall)


ULE127 Scenario 3
ULE094/ULE203 Scenario 3
ULE095/ULE202 Scenario 3
ULE104 Scenario 3
ULE201 Scenario 3
ULE204 Scenario 3
ULE185 Scenario 3
ULE188 Scenario 3
Groundwater level (m AHD)
Date
Measured
Modelled mean (historic)
Modelled range (historic)
Modelled mean (RCP 8.5 rainfall)
Modelled range (RCP 8.5 rainfall)


ULE190 Scenario 3
ULE192 Scenario 3
ULE191 Scenario 3
ULE187 Scenario 3
ULE186 Scenario 3
ULE189 Scenario 3
Groundwater level (m AHD)
Date
1960
1980
2000
2020
2040
Measured
Modelled mean (historic)
Modelled range (historic)
Modelled mean (RCP 8.5 rainfall)
Modelled range (RCP 8.5 rainfall)

10 References

Alcoe D (2009). Evaluating Approaches to Sustainable Groundwater Use: A Case Study of Uley South Lens, Southern Eyre Peninsula, South Australia, Honours Thesis, Flinders University of South Australia.

Allison GB, Stone WJ & Hughes MW (1985). Recharge in karst and dune elements of a semi-arid landscape as indicated by natural isotopes and chloride, Journal of Hydrology 76, pp1–25.

Baalousha HM (2016). The potential of using beach wells for reverse osmosis desalination in Qatar, Modeling Earth Systems and Environment, 2 (97), doi.org/10.1007/s40808-016-0151-5

Badaruddin S (2017). An assessment of transient seawater intrusion processes: physical experiments and numerical modelling, PhD Thesis, Flinders University of South Australia.

Bakker M, Schaars F, Hughes JD, Langevin CD & Dausman AM (2013). Documentation of the Seawater Intrusion (SWI2) Package for MODFLOW, U.S. Geological Survey Techniques and Methods, book 6, chap. A46, U.S. Geological Survey, Reston, Virginia.

Barnett SR (1978). Eyre Peninsula Groundwater Study – Uley South Basin Progress Report (unpublished), Government of South Australia, Department of Mines and Energy, Adelaide.

Barnett B, Townley LR, Post V, Evans RE, Hunt RJ, Peeters L, Richardson S, Werner AD, Knapton A & Boronkay A (2012). Australian groundwater modelling guidelines, Australian Government, Canberra. http://webarchive.nla.gov.au/gov/20160615064846/http://archive.nwc.gov.au/library/waterlines/82

Bestland E (2010). Geology of the Sea Cliffs along Uley South, Eyre Peninsula, Report to the Eyre Peninsula Natural Resource Management Board, Flinders University, South Australia.

BoM (2017). Bureau of Meteorology website, http://www.bom.gov.au Website accessed November 2017

Bourman RP, Murray-Wallace CV & Harvey N (2016). Coastal Landscapes of South Australia, University of Adelaide Press, Adelaide.

Bresciani E, Ordens CM, Werner AD, Batelaan O, Guan H, Post VEA (2014). Spatial variability of chloride deposition in a vegetated coastal area: Implications for groundwater recharge estimation, Journal of Hydrology, 519, pp 1177-1191.

Burnett WC, Aggarwal PK, Aureli A, Bokuniewicz H, Cable JE, Charette MA, Kontar E, Krupa S, Kulkarni KM, Loveless A, Moore WS, Oberdorfer JA, Oliveira J, Ozyurt N, Povinec P, Privitera AMG, Rajar R, Ramessure RT, Scholten J, Stieglitz T, Taniguchi M & Turner JV (2006). Quantifying submarine groundwater discharge in the coastal zone via multiple methods, Science of the Total Environment, 367, pp498-543.

Charles SP & Fu G (2015a). Statistically Downscaled Projections for South Australia, Goyder Institute for Water Research Technical Report Series No. 15/1, Adelaide, South Australia.

Charles SP & Fu G (2015b). SA Climate Ready Climate Projections for South Australia – Eyre Peninsula, Goyder Institute for Water Research fact sheet, Adelaide, South Australia.

Crosbie RS, Davies P, Harrington N & Lamontagne S (2015). Ground truthing groundwater-recharge estimates derived from remotely sensed evapotranspiration: a case in South Australia, Hydrogeology Journal 23: 335–350.

Dausman AM, Langevin C, Bakker M & Schaars F (2010). A comparison between SWI and SEAWAT – the importance of dispersion, inversion and vertical anisotropy, SWIM21 – 21st Salt Water Intrusion Meeting conference proceedings, pp 271-274, Azores Portugal.

Davis AC, Cahill K, Hatch M & Munday T (2012). Aquifer characterization in the Uley South Basin, South Australia, using NMR: Final Report, CSIRO: Water for a Healthy Country National Research Flagship Technical Report (EP-31-01-12-14).

De Marsily G (1986). Quantitative Hydrogeology, Academic Press Inc., Florida.

Department for Environment and Water (2018a). Southern Basins PWA Uley South 2017 Groundwater level and salinity status report, Government of South Australia, Department for Environment and Water.

Department for Environment and Water (2018b). Eyre Peninsula Water Demand and Supply Statement, Government of South Australia, Department for Environment and Water.

Doherty J (2007). Use of PEST and Some of its Utilities in Model Calibration and Predictive Error Variance Analysis:- A Roadmap, Watermark Numerical Computing, Brisbane.

Doherty J (2010). PEST Model Independent Parameter Estimation, Watermark Numerical Computing, Brisbane.

EPNRMB (Eyre Peninsula Natural Resource Management Board) (2016). Water Allocation Plan for the Southern Basins and Musgrave Prescribed Wells Areas, Government of South Australia, Department of Environment, Water and Natural Resources.

Evans SL (1997). Estimating Long Term Recharge to Thin, Unconfined Carbonate Aquifers Using Conventional and Environmental Isotope Techniques: Eyre Peninsula, South Australia, Masters Thesis, Flinders University of South Australia.

Ferre TA (2017). Revisiting the Relationship Between Data, Models, and Decision-Making, Groundwater 55 (5), pp604–614.

Fiore AR, Voronis LM & Wieben CM (2018). Hydrogeology of, simulation of groundwater flow in, and potential effects of sea-level rise on the Kirkwood-Cohansey aquifer system in the vicinity of Edwin B. Forsythe National Wildlife Refuge, New Jersey, U.S. Geological Survey Scientific Investigations Report 2017–5135, doi.org/10.3133/sir20175135

Fitzpatrick A, Cahill K, Munday T & Berens V (2009). Informing the hydrogeology of Coffin Bay, South Australia, through the constrained inversion of TEMPEST AEM data, CSIRO: Water for a Healthy Country National Research Flagship CSIRO Report Number: P2009/300, Australia.

Geoscience Australia (2017). Australian Bathymetry and Topography Grid, June 2009, https://ecat.ga.gov.au/geonetwork/srv/eng/search#!a05f7892-fae9-7506-e044-00144fdd4fa6 website accessed 6 December 2017.

Green G, Gibbs M, Alcoe D & Wood C (2012). Impacts of Climate Change on Water Resources Phase 3 Volume 2 Eyre Peninsula Natural Resources Management Region, DFW 2012/04, Government of South Australia, Department for Water, Adelaide.

Guerschman JP, Van Dijk AIJM, Mattersdorf G, Beringer J, Hutley LB, Leuning R, Pipunic RC & Sherman BS (2009). Scaling of potential evapotranspiration with MODIS data reproduces flux observations and catchment water balance observations across Australia, Journal of Hydrology 369: 107–119.

Hall JAS, Maschmedt DJ & Billing NB (2009). The Soils of Southern South Australia, The South Australian Land and Soil Book Series Volume 1, Geological Survey of South Australia, Bulletin 56, Volume 1, Government of South Australia, Department of Water, Land and Biodiversity Conservation, Adelaide.

Harbaugh, AW (2005). MODFLOW-2005, The U.S. Geological Survey Modular Ground-Water Model – the Ground-Water Flow Process. USGS Techniques and Methods 6-A16. Reston, Virginia.

Harrington N, Evans S & Zulfic D (2006). Uley Basin Groundwater Modelling Project Volume 1: Project Overview and Conceptual Model Development, DWLBC 2006/01, Government of South Australia, Department of Water, Land and Biodiversity Conservation, Adelaide.

Hayes P & Nicol C (2017). Uncertainty by Design: Sufficient model simplification to make predictive uncertainty analysis tractable, in Middlemis et al. (2019) Groundwater modelling uncertainty – implications for decision making. Summary report of the national groundwater modelling uncertainty workshop, 10 July 2017, Sydney, Australia. Flinders University, National Centre for Groundwater Research and Training, Australia. http://groundwater.com.au/news_items/groundwater-modelling-uncertainty

Healy RW & Cook PG (2002). Using groundwater levels to estimate recharge, Hydrogeology Journal, 10 (1), pp 91-109.

Huang Z, Przeslawski R, Kool J, Li J, Bouchet P & Nichol S (2013). Australian Marine Environmental Data Descriptions and Metadata, Record 2013/21, Geoscience Australia, Canberra.

Hughes JD & White JT (2016). Hydrologic Conditions in Urban Miami-Dade County, Florida, and the Effect of Groundwater Pumpage and Increased Sea Level on Canal Leakage and Regional Groundwater Flow, Scientific Investigations Report 2014-5162, U.S. Geological Survey, Reston, Virginia.

Hutson JL (2005). Leaching Estimation and Chemistry Model: a process-based model of water and solute movement, transformations, plant uptake and chemical reactions in the unsaturated zone. Model description and user's guide, New York State College of Agriculture and Life Sciences, Cornell University, Ithaca, NY

James–Smith JM & Brown KG (2002). A groundwater flow model of the Quaternary Limestone aquifer in the Uley South lens, Eyre Peninsula, South Australia, Report DWR 2002/001, Government of South Australia, Department for Water Resources, Adelaide.

JPL (2017). Jet Propulsion Laboratory – ASTER Global Digital Elevation Map Announcement, https://asterweb.jpl.nasa.gov/gdem.asp website accessed 3 November 2017.

Kamps P, Nienhuis P, van den Heuvel D & de Joode H (2016). Monitoring Well Optimization for Surveying the Fresh/Saline Groundwater Interface in the Amsterdam Water Supply Dunes, 24th Salt Water Intrusion Meeting and the 4th Asia–Pacific Coastal Aquifer Management Meeting, 4–8 July 2016, Cairns, Australia, pp96–99.

Knowling MJ, Werner AD & Herckenrath D (2015). Quantifying climate and pumping contributions to aquifer depletion using a highly parameterized groundwater model: Uley South Basin (South Australia), Journal of Hydrology, 523, pp515-530.

Kok A, Auken E, Groen M, Ribeiro J & Schaars F (2010). Using ground based geophysics and airborne transient electromagnetic measurements (SkyTEM) to map salinity distribution and calibrate a groundwater model for the island of Terschelling – The Netherlands, SWIM21 – 21st Salt Water Intrusion Meeting conference proceedings, pp 121-124, Azores Portugal.

Kruseman GP & de Ridder NA (1990). Analysis and Evaluation of Pumping Test Data Second Edition (Completely Revised), International Institute for Land Reclamation and Improvement, Wageningen.

Langevin CD, Thorne DT, Dausman AM, Sukop MC & Guo W (2008). SEAWAT Version 4: A Computer Program for Simulation of Multi-Species Solute and Heat Transport, U.S. Geological Survey Techniques and Methods Book 6, Chapter A22, U.S. Geological Survey, Reston, Virginia.

Luedeling E, Oord AL, Kiteme B, Ogalleh S, Malesu M, Shepherd KD & Leeuw JD (2015). Fresh groundwater for Wajir – ex-ante assessment of uncertain benefits for multiple stakeholders in a water supply project in Northern Kenya, Frontiers in Environmental Science, 3 (16), doi: 10.3389/fenvs.2015.00016

Magarey P & Slater S (2011). South East Town Water Supplies – Geranium, Bordertown and Penola, DFW 2011/24, Government of South Australia, Department for Water, Adelaide.

Middlemis H, Merrick N, Ross J, and Rozlapa K. (2001). Groundwater Flow Modelling Guideline, prepared for Murray–Darling Basin Commission by Aquaterra, January 2001. Murray–Darling Basin Authority, Canberra. www.mdba.gov.au/sites/default/files/archived/mdbc-GW-reports/2175_GW_flow_modelling_guideline.pdf

Middlemis H, Walker G, Peeters L, Richardson S, Hayes P & Moore C (2019). Groundwater modelling uncertainty – implications for decision making. Summary report for the National Groundwater Modelling Uncertainty Workshop, 10 July 2017, Sydney, Australia. Flinders University, National Centre for Groundwater Research and Training, Australia.

Miller KL, Berg SJ, Davison JH, Sudicky EA and Forsyth PA (2018). Efficient uncertainty quantification in fully-integrated surface and subsurface hydrologic simulations, Advances in Water Resources 111, pp381–394.

Morton WH & Steel TM (1968). Eyre Peninsula Groundwater Study Uley South Basin Progress Report No. 1 – Aquifer Evaluation, Report Book 66/49, DM.718/66, Government of South Australia, Department of Mines, Adelaide.

Morton WH & Steel TM (1970). Evaluation of Aquifers in the Uley South Groundwater Basin, Mineral Resources Review South Australia, 128, pp 33-48.

NRC (2013). Eyre Peninsula Water Supply Final Report, Eighty Fifth Report of the Natural Resources Committee "Under the Lens", Natural Resources Committee, Parliament of South Australia, Adelaide.

Ordens CM (2014). Recharge to a semi-arid, heterogeneous coastal aquifer: Uley South Basin, South Australia, PhD thesis, Flinders University, South Australia.

Ordens CM, Post VEA, Werner AD, Huston JL (2014). Influence of model conceptualization on one-dimensional recharge quantification: Uley South, South Australia, Hydrogeology Journal 22, pp795-805.

Ordens CM, Werner AD, Post VEA, Hutson JL, Simmons CT & Irvine BM (2012). Groundwater recharge to a sedimentary aquifer in the topographically closed Uley South Basin, South Australia, Hydrogeology Journal 20 (1), pp 61–72.

Painter JAC (1968). Eyre Peninsula Groundwater Study Consolidated Report No. 1 Summary of Available Data – October 1968, DM.1651/68, Government of South Australia, Department of Mines, Adelaide.

Panday S, Langevin CD, Niswonger RG, Ibaraki M & Hughes JD (2013). MODFLOW–USG Version 1: An Unstructured Grid Version of MODLFOW for Simulating Groundwater Flow and Tightly Coupled Processes Using a Control Volume Finite-Difference Formulation, Techniques and Methods, book 6, chap. A45, U.S. Geological Survey, Reston, Virginia.

Panday S, Rumbaugh J, Hutchison WR, Schorr S (2017). Numerical Model Report: Lower Rio Grande Valley Groundwater Transport Model, GSI Environmental accessed via the Texas Water Development Board (https://www.twdb.texas.gov/groundwater/models/research/lrgv_t/LRGV_Draft_Numerical_Model_Report.pdf, accessed May 2018)

Post VEA, Houben GJ & van Engelen J (2018). What is the Ghijben-Herzberg principle and who formulated it? Hydrogeology Journal, doi 10.1007/s10040-018-1796-0

Rau GC, Acworth RI, Halloran LJS, Timms WA & Cuthbert MO (2018). Quantifying compressible groundwater storage by combining cross-hole seismic surveys and head response to atmospheric tides, Journal of Geophysical Research: Earth Surface 123 (8): 1910–1930.

Rotzoll K, Izuka SK, Nishikawa T, Fienen MN & El-Kadi AI (2016). Quantifying effects of humans and climate on groundwater resources of Hawaii through sharp-interface modelling, American Geophysical Union Fall General Assembly, San Francisco, 12-16 December 2016, poster H23E-1594.

Rumbaugh JO & Rumbaugh DB (2017). Guide to Using Groundwater Vistas Version 7, Environmental Simulations, Inc., Leesport, Pennsylvania.

Seidel A (2008). Seawater Intrusion on the Southern Eyre Peninsula, South Australia: A First-Order Assessment, Honours Thesis, Flinders University of South Australia.

Shalev E, Lazar A, Wollman S, Kington S, Yechieli Y & Gvirtzman H (2009). Biased Monitoring of Fresh Water–Salt Water Mixing in Coastal Aquifers, Ground Water 47 (1), pp49–56

Shepherd RG (1980). Uley South Groundwater Basin Computer Model, DM No 114/69, Eng No 76/24, Report Book No 80/25, Government of South Australia, Department of Mines and Energy, Adelaide.

Sibenaler XP (1976). Eyre Peninsula Groundwater Survey Uley South Basin Progress Report No. 4 – Aquifer Evaluation, Report Book No. 76/30, Government of South Australia, Department of Mines, Adelaide.

Solomon DK, Cook PG & Plummer LN (2006). Models of groundwater age and residence time, In: Use of Chlorofluorocarbons in Hydrology A Guidebook Ch 6 (eds International Atomic Energy Agency), pp 73-88, IAEA, Vienna

Somaratne N (2019). Assessing Aquifer Stress Index (ASI) Using Rating Method and Analytic Hierarchy Process for a Coastal Unconfined Aquifer, Environment and Natural Resources Research, 9 (1) pp35-53.

Somaratne N & Ashman G (2018). Analysis of Saline Intrusion into a Coastal Aquifer: A Case History of Legacy Issues and Challenges to Water Security, Environment and Natural Resources Research, 8 (2), pp16-32, doi 10.5539/enrr.v8n2p16

Somaratne N, Ashman G, Irvine M, Mann S (2018). Geophysical Input to Improve the Conceptual Model of the Hydrogeological Framework of a Coastal Karstic Aquifer: Uley South Basin, South Australia. Geosciences 8 (7), doi 10.3390/geosciences8070226

South Australian Water Corporation (2008). Meeting Future Demand – SA Water's Long Term Plan for Eyre Region, South Australian Water Corporation, Adelaide.

Stewart S (2013). Additional Science Support for the Eyre Peninsula Water Allocation Plan, DEWNR Technical Report 2013/19, Government of South Australia, Department for Environment, Water and Natural Resources, Adelaide.

Swaffer B (2014). Trees and groundwater in the water–limited Eyre Peninsula: an ecohydrological perspective, PhD Thesis, Flinders University of South Australia.

Swaffer B (2017). Southern Basins PWA Water Balance Evaluating the impact of evapotranspiration on groundwater recharge, SA Water report.

Swaffer BA, Holland KL, Doody TM, Li C & Hutson J (2014). Water use strategies of two co-occurring tree species in a semi-arid karst environment, Hydrological Processes, 28, pp 2003-2017.

Tonkin M & Doherty J (2009). Calibration-constrained Monte Carlo analysis of highly parameterized models using subspace techniques, Water Resources Research 45, doi:10.1029/2007WR006678

United States Geological Survey (2017). United States Geological Survey - Shuttle Radar Tomography Mission (SRTM) 1 Arc-Second Global, https://lta.cr.usgs.gov/SRTM1Arc website accessed 2 November 2017.

Wagenet RJ & Hutson JL (1989). LEACHM: Leaching Estimation and Chemistry Model – A process based model of water and solute movement, transformations, plant uptake, and chemical reactions in the unsaturated zone, Cornell University, New York.

Walter DA, McCobb TD, Masterson JP & Fienen MN (2016). Potential effects of sea-level rise on the depth to saturated sediments of the Sagamore and Monomoy flow lenses on Cape Cod, Massachusetts, U.S. Geological Survey Scientific Investigations Report 2016–5058, doi.org/10.3133/sir20165058

Ward J, Werner A & Howe B (2009). Saltwater Intrusion in Southern Eyre Peninsula, Report developed through the Eyre Peninsula Groundwater, Allocation and Planning Project.

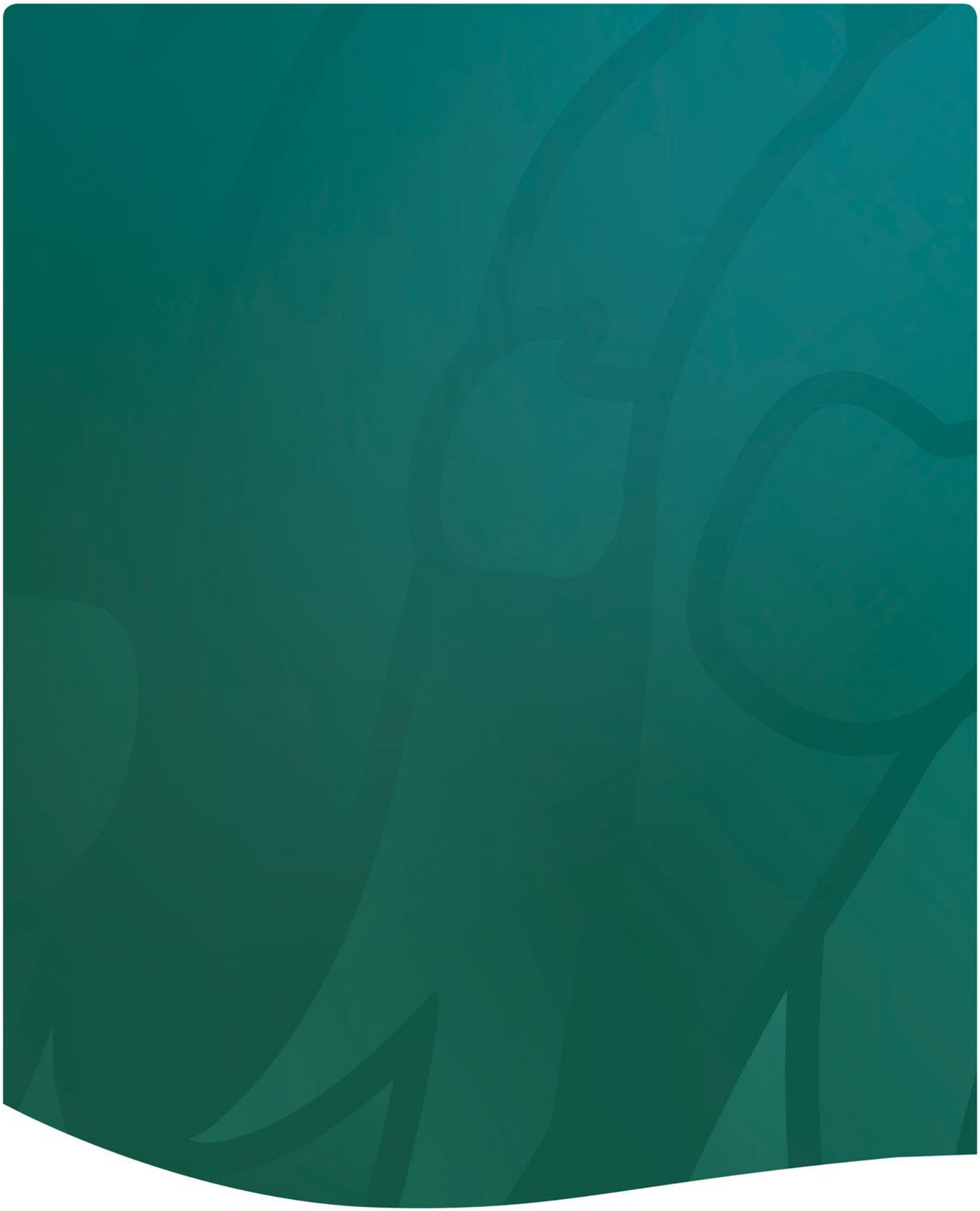
Watkins N, Dang L, Evans S, Telfer A, Burnell R (2015). Uley South Monitoring and Production Bores Pump Testing Analysis, Australian Water and Environment consultant report to SA Water.

Werner A (2010). A Groundwater Flow Model of Uley South Basin, South Australia, Flinders University South Australia.

Werner A and Dang LD (2013). Three-Dimensional Seawater Intrusion Modelling of Uley South Basin, South Australia, In: Groundwater in the Coastal Zones of Asia-Pacific (eds C Wetzelhuetter), pp177-204, Springer, Dordrecht, Netherlands.

Ye M, Pohlmann KF, Chapman JB, Pohll GM & Reeves DM (2010). A Model-Averaging Method for Assessing Groundwater Conceptual Model Uncertainty, Ground Water 48(5), pp 716–728.

Zulfic D, Harrington N & Evans S (2007). Uley Basin Groundwater Modelling Project Volume 2: Groundwater Flow Model, DWLBC 2007/04, Government of South Australia, Department of Water, Land and Biodiversity Conservation, Adelaide.



Government
of South Australia

Department for
Environment and Water